Modelling inherited kidney diseases with kidney organoids derived by directed differentiation of patient induced pluripotent stem cells

Dr Thomas A Forbes MBBS FRACP

ORCHID ID: 0000-0001-6635-8855

December 2019

Department of Paediatrics, The University of Melbourne

Kidney Regeneration Group, Murdoch Children's Research Institute

Submitted in total fulfilment of the requirements of the degree of

Doctor of Philosophy: Medicine, Dentistry and Health Sciences

Abstract

Genetic kidney diseases are a heterogeneous group of disorders with varying phenotypes dependent on the affected nephron segment. Next generation sequencing has increased our appreciation of the breadth of gene variants associated with these diseases. It has also identified large numbers of variants of unknown significance (VUS), which require functional genomic validation. There is an unmet need for novel therapies for genetic kidney diseases as most invariably progress to dialysis or transplantation without any form of targeted treatment.

Laboratory based research of genetic kidney disease requires the recapitulation of a disease phenotype in animal and/or *in vitro* cellular disease models. Interspecies variation in anatomy, physiology and gene function limits the translation of animal models to human disease and clinical care. Classical two dimensional cell cultures lack the complexity and intercellular cross-talk of *in vivo* three dimensional tissue. Kidney organoids are three dimensional, miniature, multicellular, human, *in vitro* micro-tissues, offering distinct disease modelling advantages over other models. Furthermore, kidney organoids can be regenerated from induced pluripotent stem cells (iPSC) reprogrammed from patients with genetic kidney disease, potentially providing outcomes with personalised clinical relevance. As a novel platform, the capabilities and limitations of kidney organoids as disease models are not well understood. By differentiating and characterising kidney organoids from the iPSC of patients with inherited kidney diseases, this thesis aims to explore the application of kidney organoids to disease modelling.

As proof of concept, kidney organoids were first generated from iPSC reprogrammed from a patient with compound heterozygous variants in *IFT140*, an already validated nephronophthisis (NPHP) genotype. An isogenic control was generated by precision CRISPR-Cas9 gene editing. In this project, differential primary ciliary morphology within organoid tubules and transcriptional profiling of organoid epithelium validated the ability of the organoids to model genetic disease.

Attempts were then made to validate novel, candidate variants for other pedigrees with unresolved trio whole exome sequencing. In a proband with clinically suspected NPHP, *DNAH5* was selected as a candidate gene, despite previously association with a motile ciliary phenotype. In this project, kidney organoids were unable to validate the patient

variant as pathogenic. In addition, a number of lessons were learned regarding the necessary variant curation process prior to making a commitment to modelling with kidney organoids.

In the final chapter, kidney organoids validated a novel genotype for the glomerular disease steroid resistant nephrotic syndrome, via international collaboration with the laboratory of Prof Friedhelm Hildebrandt. Glomeruli within kidney organoids differentiated from iPSC expressing a patient-derived, homozygous variant in *NOS1AP*, displayed aberrant development, increased podocyte apoptosis and reduced expression of PAR polarity proteins.

Together these projects demonstrate the strengths and challenges of using kidney organoids as models of inherited renal disease. Kidney organoids stand to complement animal and 2D unicellular disease models rather than replace them. We proposed that patient-derived kidney organoids are best placed to model paediatric onset kidney diseases with the future potential of providing personalised therapeutic screening.

Declaration

I declare this thesis comprises only my original work towards the Doctor of Philosophy except where indicated in the preface.

Due acknowledgement has been made in the text to all other material used.

The thesis is fewer than the maximum word limit in length, exclusive of tables, maps, bibliographies and appendices.

Signed: Dr Thomas A Forbes Date:25 March 2020

Preface

Publication Status of Data Chapters and Contribution of Co-authors

Chapter 3: Published by American Journal of Human Genetics on 26th April 2018.

Dr Thomas Forbes led differentiation experiments, post-fixation analyses and wrote the manuscript. Dr Peter Trnka, Dr Chirag Patel and Assoc Prof Andrew Mallett recruited and phenotyped the patient. Assoc Prof Bruce Bennetts, Ms Gladys Ho, Ms Katherine Holman, Dr Cas Simons, Assoc Prof Andrew Mallett and Ms Joanna Crawford performed whole exome sequencing, analysis and Sanger sequencing of the patient-derived DNA. Dr Sara Howden generated and gene corrected iPSC clones. Dr Kynan Lawlor wrote post-immunofluorescent analysis scripts. Mr Sean Wilson assisted with protein assays. Dr Belinda Phipson and Dr Jovana Maksimovic assisted with bioinformatics analyses. Assoc Prof Alicia Oshlack supervised bioinformatics analyses. Prof Melissa Little, Assoc Prof Cathy Quinlan and Dr Lorna Hale supervised all experiments and manuscript revisions.

Chapter 4: Unpublished material not submitted for publication.

Dr Thomas Forbes led variant curation, differentiation experiments, HUREC cultures, post-fixation analyses and compiled all data. Dr Sara Howden generated and gene corrected iPSC clones. Dr Kynan Lawlor wrote post-immunofluorescent analysis scripts. Prof Melissa Little and Assoc Prof Cathy Quinlan supervised all experiments and manuscript revisions.

Chapter 5: Unpublished material submitted for publication.

Dr Thomas Forbes performed all differentiations, post-fixation analyses, wrote post-immunofluorescence analysis scripts and compiled all data. Dr Kynan Lawlor assisted with bioinformatics analysis. Ms Michelle Scurr assisted with sectioning and immunohistochemistry. Dr Friedhelm Hildebrandt, Dr Amar Majmundar and Dr Florian Buerger assisted with histology analysis. Prof Sara Ellis, Mr Cameron Skinner, Ms Judy Borg and Ms Hanadi Hoblos from the Centre for Advanced Histology and Microscopy, Peter McCallum Cancer Centre, Melbourne, prepared transmission electron microscopy grids and assisted with imaging. Ms Bronwyn

Christiansen, Department of Anatomical Pathology, Royal Children's Hospital, Melbourne, performed PAS stains. Prof Melissa Little supervised all experiments and manuscript revisions.

Funding Acknowledgements

I am grateful for the stipend support provided by the National Health and Medical Research Council Post Graduate Scholarship (GNT1114409) and RACP Jacquot NHMRC Award for Excellence administered by the Royal Australasian College of Physicians, the Australian and New Zealand Society of Nephrology and the Don and Lorraine Jacquot Estate.

Aspects of this thesis were funded by the National Health and Medical Research Council of Australia (NHMRC) (GNT1098654), Kidney Health Australia, the Royal Brisbane and Women's Hospital Foundation, the Royal Children's Hospital Foundation, and the Murdoch Children's Research Institute. The Murdoch Children's Research Institute is supported by the Victorian Government's Operational Infrastructure Support Program.

Acknowledgements

I wish to acknowledge the entire Kidney Development, Disease and Regeneration team, dynamic as it has been over the last 4 years. This includes (in no particular order): Minoru Takasato, Pei Er, Irene Ghobrial, Lorna Hale, Shahnaz Khan, Alex Combes, Sara Howden, Jess Vanslambrouck, Siebe Spijker, Alison Graham, Michelle Scurr, Louise Wardrop, Sean Wilson, Lakshi Starks, Joanne Soo, Pamela Karaith, Penny McDonald, Gemma Martinez, Ker Sin Tan, Santhosh Kumar, Aude Dorison, Andrew Mallett, Belinda Phipson, Alicia Oshlack, Andrew Lonsdale and Linda Cox. I walked into this PhD without having ever picked up a pipette. You have been tremendously patient with me as I learned the ropes, and supportive of my progression as a scientist. It means so much to me to be able to get out of bed in the morning with enthusiasm for the people I see and the work that I do. I am so excited for the opportunities we approach together in future. Within this group I highlight Kynan Lawlor, one of the most selfless, relaxed and highly efficient colleagues I've ever worked with in medicine or science. Kynan spent a great deal of time working with me to optimise some complex post-immunofluorescent analyses, many of which didn't work, but this never phased him. There remains so much for me to learn from him.

Outside of the Kidney Regeneration Group sincere thanks to the generosity of my MCRI colleagues and collaborators from other groups including Cas Simons, Sue White, Matt Burton, Eleanor Jones, Paul Lau, Maelle Le Moing, Stefanie Eggars, Peter Houweling, Chrystal Tiong and Jovana Maksimovic.

I am incredibly grateful to Prof Friedhelm Hildebrandt for the opportunity to collaborate on the *NOS1AP* project. When I first started my PhD I read so much of his work I recall joking to my colleagues about how impossibly but incredibly prestigious it would be to work with him. Thank you also to Amar Majmundar and Florian Buerger for their assistance with this project. To have been welcomed so warmly into this cooperative and industrious group of collaborators is my privilege.

Thank you to all my clinical colleagues for their support and understanding over the last four years of frequent distraction and obsession with this PhD.

Thank you to my Thesis Advisory Committee Shireen Lamande, David Elliot and Joshua Kausman who provided regular boosts of support and endorsement along the way.

My supervisors Prof Melissa Little and Assoc Prof Cathy Quinlan have been a constant source of empathy, support and encouragement throughout this process, including the many challenges that arose outside of the professional environment.

I'm so lucky and grateful to have the most wonderful family. Thank you to Mum, Dad, Lucy and Fergus, Marian and Kethly, and David and Liz for being so understanding, and tolerant of my ridiculous workload over the last four years and for all your interest, love and support over this time.

To my children Penny and Cate, I don't expect you'll ever read beyond this page but in the hope that one day you might at least read this paragraph, know that I love you both more than anything in the world. With quite genuine sincerity, I could not have endured the lows of this PhD without your cuddles and love, and I thought of you at every high. You are such considerate and smart kids. I am so proud of you, and will always be.

To my wife Beth. You know more than anyone how this career redirection has pushed me to (and sometimes beyond) my limit. I simply would not have completed this without you. Well beyond looking after the kids and managing our lives whilst I spent hours in the lab, ward and office, you have been and will continue to be my inspiration in work, love and life. I love that every challenge we face together brings us closer, and that we've never been wary of looking for the next challenge. Thank you for holding me together.

Table of Contents

List of Figures

Chapter 2

Chapter 3

Chapter 4

Chapter 5

List of Tables

Chapter 2

Chapter 3

Chapter 4

Abbreviations

ADPKD	autosomal dominant polycystic kidney disease
AKT	serine, threonine kinase (aka protein kinase B)
ARPKD	autosomal recessive polycystic kidney disease
BBS	Bardet Biedl syndrome
BFP	blue fluorescent protein
CAKUT	congenital abnormalities of the kidney and urinary tract
CD	collecting duct
CM	cap mesenchyme
CKD	chronic kidney disease
CLS	ciliary localisation sequence
CNS	congenital nephrotic syndrome
DCT	distal convoluted tubule
DGE	differential gene expression
DNAH5	dynein heavy chain 5, axonemal
Dvl	Dishevelled *(Wnt signalling component)*
EB	embryoid bodies
EM	electron microscopy
ER	endoplasmic reticulum
ESKD	end stage kidney disease
FSGS	focal segmental glomerulosclerosis
GC	gene corrected
GSK3β	glycogen synthase kinase 3 beta
GBM	glomerular basement membrane
GFR	glomerular filtration rate
HUREC	human urine derived renal epithelial cells
ICM	inner cell mass
IFT	intraflagellar transport
IFT140	intraflagellar transport protein 140 homolog
IHC	immunohistochemistry
IM	intermediate mesoderm
iPSC	induced pluripotent stem cells
JATD	Jeune asphyxiating thoracic dystrophy
LoH	loop of Henle
LTL	*Lotus tetragonolobus* lectin
MACS	magnetic activated cell sorting
MFI	mean fluorescent intensity
MM	metanephric mesenchyme
MSS	Mainzer Saldino syndrome
NOS1AP	nitric oxide synthase associated protein 1
NPHP	nephronophthisis
NPHP-RC	nephronophthisis and related ciliopathies
NS	nephrotic syndrome
PAR	partitioning defective protein
PBMC	peripheral blood mononuclear cells
PBS	phosphate buffered saline
PC2	polycystin 2 (gene product of *PKD2*)

PI3K	phosphoinositide 3 kinase
PPS	posterior primitive streak
Ptc	Patched *(Shh signalling component)*
PCT	proximal convoluted tubule
PS	primitive streak
PT	patient
RP	retinitis pigmentosa
RPE	retinal pigment epithelium
Shh	Sonic hedgehog
SLS	Senior Løken syndrome
Smo	Smoothened *(Shh signalling component)*
SRNS	steroid resistant nephrotic syndrome
SSNS	steroid sensitive nephrotic syndrome
SYNPO	synaptopodin
UB	ureteric bud
UE	ureteric epithelium
VUS	variant of unknown significance
Wnt	Wingless-related integration site

Chapter 1 Introduction

1.1 The health and economic burden of genetic kidney disease

The natural history of many, if not most, inherited kidney disease entails a slow but inexorable decline in kidney function towards end stage kidney disease (ESKD) and the eventual requirement of renal replacement therapy. Dialysis and transplantation are capable of extending the lives of these patients for many years, however this is usually with compromised health and quality of life. These treatments are also expensive with the estimated health service expenditure between $AUD53,000 and $AUD101,000 per patient per year of dialysis (AIHW, 2012) and approximately $AUD110,000 per patient over the first three years following transplantation.(Cass A, 2010) The treatment of chronic kidney disease (CKD) is projected to consume 1.7% of total government health expenditure in Australia reflecting a cost of over $12-13 billion annually by the year 2020.(AIHW, 2014)

Over the last decade, there has been a considerable expansion in the identification of genes responsible for CKD, spurred by advances in Next Generation Sequencing technology.(Renkema et al., 2014, Halbritter et al., 2013, Gee et al., 2014b, Mallett et al., 2017) Approximately 10-20% of adults and 47% of children with CKD in Australia have a genetic aetiology to their disease.(Mallett et al., 2014, Fletcher et al., 2013) There is

therefore a pressing need to improve the understanding of the pathogenesis of inherited kidney disease in order to develop targeted treatments that can reduce this morbidity and expenditure.

1.2 Induced pluripotent stem cells and kidney organoids

In 2007, the laboratory of Shinya Yamanaka published a protocol for the reprogramming of human skin fibroblasts into induced pluripotent stem cells (iPSC) using a straightforward viral vector transfection.(Takahashi et al., 2007) Under the right culture conditions, human iPSC are theoretically capable of differentiation to any cell type within the human body. As such, the discovery of iPSC has given rise to a new branch of science and medicine called *Regenerative Medicine*, whereby iPSC can be reprogrammed from patient-derived somatic cells and then differentiated to a target cell type or tissue of interest, providing a protocol is known.(Hariharan et al., 2015, Cherry and Daley, 2013, Singh et al., 2015)

An iPSC-derived, regenerated tissue which resembles the primary organ is called an *organoid*. The last decade has seen a wave of protocols published for the derivation of various organoids including but not limited to blood cells(Zhang, 2013, Yang et al., 2017, Sweeney et al., 2016), neurons(Lancaster et al., 2013), retina(Parfitt et al., 2016, Reichman et al., 2017), cardiomyocytes(Giacomelli et al., 2017) and hepatocytes(Hannan et al., 2013). Concurrently, about five years ago, multiple laboratories published protocols for the directed differentiation of iPSC to kidney organoid.(Morizane et al., 2015, Takasato et al., 2015, Mae et al., 2013, Taguchi et al., 2014, Lam et al., 2014b, Imberti et al., 2015) Almost all protocols use *in vitro* growth factors to recapitulate what is understood about *in vivo* kidney development from the study of animal models.

The long term aspiration of regenerative medicine involves the creation of patient-specific cells and tissues as transplantable therapies for the treatment of organ injury and failure. However, a more immediately translatable application of regenerated organoids is in disease modelling, which describes the *in vitro* culture of patient-iPSC-derived organoids to study the mechanisms of disease and to conduct personalised therapeutic screening.

Currently, targeted therapies to modify the primary mechanism of inherited kidney diseases are few and almost ubiquitously developed using non-human research models (eg. mouse, zebrafish, etc). The timely translation of these discoveries to human patients in a clinically relevant context is limited by interspecies variability in organ development, gene expression and physiological function. The extent to which these regenerated kidneys can faithfully reproduce a kidney disease *in vitro* is incompletely illustrated in the current literature and is likely to vary based on many factors including the disease mechanism, the age of onset, the genetic contribution to disease and the organoid's representation of the primary cell type affected by the disease. This thesis aims to examine the capabilities and limitations of kidney organoids as living, *in vitro* functional genomic models by examining kidney organoids differentiated from the iPSC of patients with genetic kidney diseases.

1.3 Hypothesis and Aims

This thesis will address the hypothesis that iPSC-derived kidney organoids represent a novel and valid disease modelling platform for inherited renal diseases and have the potential to validate novel genomic variants discovered by next generation sequencing and advance the understanding of disease pathogenesis. To this end, the aims of this thesis are:

i. To demonstrate the ability of patient-iPSC-derived kidney organoids to faithfully model both glomerular and tubular inherited kidney diseases.
ii. To characterise the disease phenotype of iPSC kidney organoids derived from a patient with a previously validated pathogenic genetic variant.
iii. To validate the disease phenotype of a novel, candidate renal disease genotype in kidney organoids.

Chapter 2 Background

2.1 Preface

This chapter begins by providing a summary of the functional unit of the kidney: the nephron. The nephron is anatomically divided into segments with specific and differential functions determined by the cell types present within them.(Figure 2.1) An understanding of the nephron segments is important to comprehend the wide variety of disease phenotypes that can arise in genetic kidney disease.(Table 2.1) This understanding is also critical to be able to appraise the end product of iPSC-to-kidney differentiation protocols, the kidney organoid.

The projects presented in this thesis (Chapters 3-5) focus on two specific, paediatric, inherited kidney diseases: nephronophthisis (pronounced *nef – ron – of – thee – sis,* NPHP) and steroid resistant nephrotic syndrome (SRNS). Therefore a detailed discussion of the current clinical management and molecular understanding of both NPHP and SRNS is presented in Section 0 and 2.4.

This chapter then moves on to introduce kidney organoid differentiation protocols in Section 2.5. As these protocols are based heavily on our understanding of *in vivo* kidney development, a detailed description of mammalian kidney development is provided. The various published kidney organoid differentiation protocols are then compared and contrasted. Finally, examples of kidney organoids used for inherited disease modelling purposes is presented.

2.2 Inherited Kidney Disease

The functional unit of the kidney is the *nephron*. Normal mammalian kidney development gives rise to a pair of kidneys possessing a total of between 200,000 and 2.7 million nephrons.(Hoy et al., 2003, Hughson et al., 2003) The nephron is segmented into 6 major segments: the renal corpuscle, the proximal convoluted tubule (PCT), the descending limb of the loop of Henle (LoH), the ascending limb of the LoH, the distal convoluted tubule (DCT) and the collecting duct (CD). The appropriate distribution and function of a wide variety of cell types within sequential nephron segments results in the meticulous regulation of serum biochemistry, acid-base balance, total body water content, excretion of nitrogenous waste and hormonal responses. This section describes the function of each nephron segment from proximal to distal, and briefly summarises the genetic phenotype characteristic for diseases of each segment. An overview of the wide spectrum of inherited kidney diseases is presented in Table 2.1.

2.2.1 Glomerulus

Each nephron is perfused by an afferent arteriole which supplies the *glomerulus*, a bundle of fenestrated capillaries supported structurally by mesangial cells and covered by a visceral epithelial layer of *podocytes*.(Figure 2.1) Podocytes are highly specialised cells which anatomically interact via interdigitating foot processes bridged by slit diaphragms of specialised proteins, including nephrin, podocin and kirrel.(Reiser and Altintas, 2016, Grahammer et al., 2013) More than a simple proteinaceous sieve, the slit diaphragm is recognised to function as a specialised cell junction, capable of chemical and mechanosensory signalling to podocytes and thereby mediating cytoskeletal dynamics, and essential podocyte functions.(Grahammer et al., 2013) Together the podocytes and the glomerular endothelium produce a glomerular basement membrane (GBM) which sits between them, composed of type IV collagens, laminins and other matrix elements with

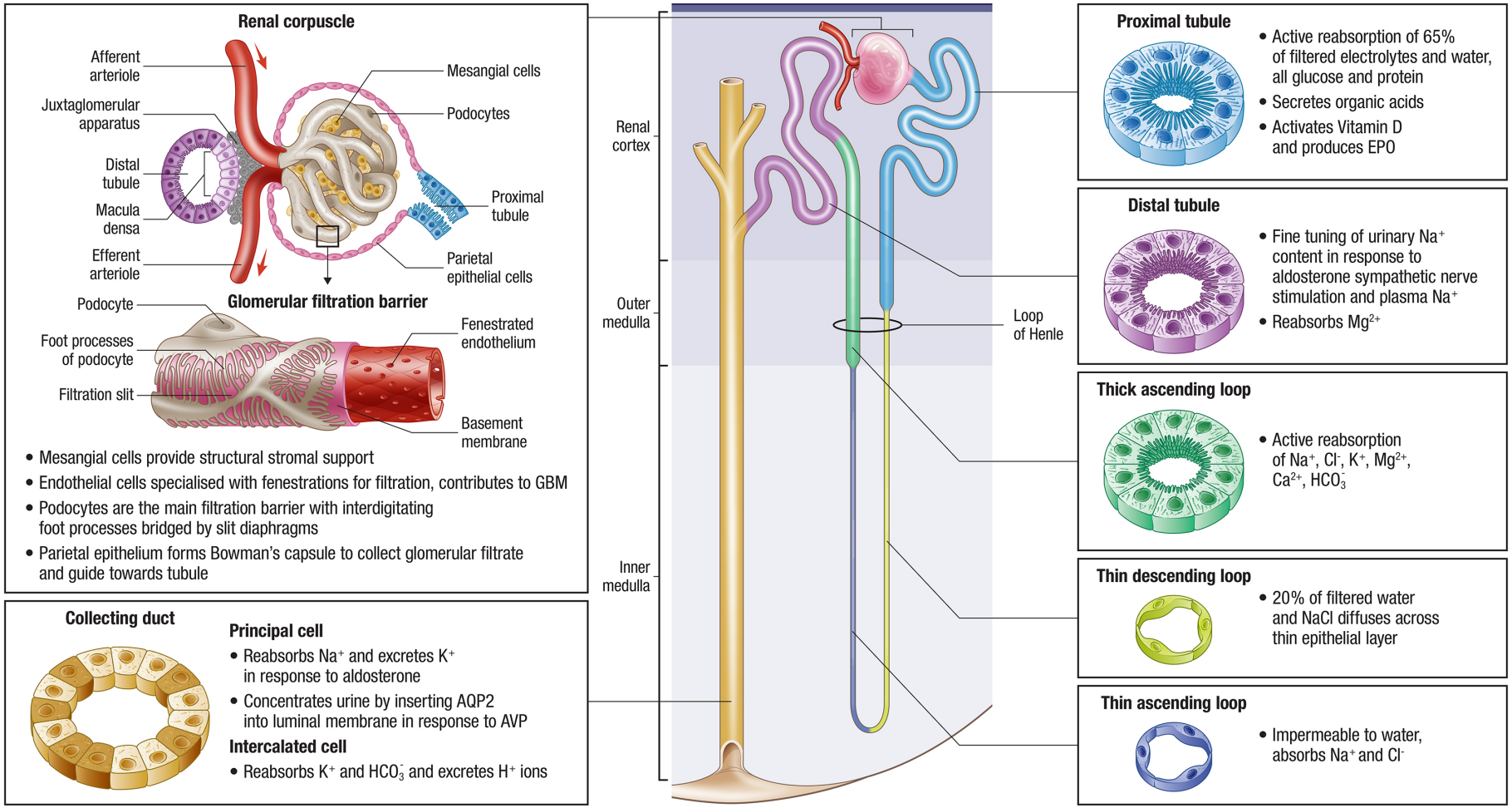

Figure 2.1 The nephron

A single nephron illustrating the complex anatomy and architecture of the different segments and cell types, and a description of their varied, specialised functions. GBM: glomerular basement membrane, AQP2: aquaporin 2, AVP: arginine vasopressin, EPO, erythropoietin. (Reprinted by permission from Springer Nature: Little MH et al, Recapitulating Development to Generate Kidney Organoids Culture In: Organ Regeneration Based on Developmental Biology, Ed. Takashi Springer, Singapore, Copyright 2017)

which both cell types interact for normal function.(Byron et al., 2014, Abrahamson, 2012) The endothelium, the GBM and podocyte slit diaphragm together form the glomerular filtration barrier.(Arif and Nihalani, 2013) Blood entering the glomerular capillaries is filtered by hydrostatic pressures through this barrier, retaining cells and high molecular weight proteins in the healthy state by virtue of size and negative charge selectivity of the barrier.(Fissell and Miner, 2018) This filtrate is collected by Bowman's capsule which is lined by flat, parietal epithelial cells(Shankland et al., 2014) and feeds the filtrate into a single, unidirectional tubule which passes the filtrate through multiple segments, processing the filtrate into urine.

Inherited disease involving the glomerulus can present with haematuria and/or proteinuria (Table 2.1) resulting from disruption of the glomerular filtration barrier and/or effacement of the podocyte foot processes. This can result from defects in the proteins making up the GBM (eg. Alport Syndrome), (Lemmink et al., 1994, Mochizuki et al., 1994) glomerular deposition of abnormal proteins (eg. Fibronectin glomerulopathy)(Castelletti et al., 2008) or defects in the homeostasis of the podocytes (eg. steroid resistant nephrotic syndrome)(Joshi et al., 2013, Lovric et al., 2016, Preston et al., 2019).(Table 2.1) Genetic forms of steroid resistant nephrotic syndrome (SRNS) represent the second most common cause of CKD in children.(Fletcher et al., 2013, 2014) A detailed discussion of SRNS is presented in Section 2.4. Additionally, inherited diseases of systemic complement regulation can lead to thrombotic micro-angiopathy within glomerular capillaries which can cause acute disturbances in the kidneys excretory function.(Aguilar, 2016)

2.2.2 Proximal Tubule

The PCT is lined by cuboidal epithelium possessing a long brush border to maximise the apical cell surface area interacting with the early glomerular filtrate (Figure 2.1) and which avidly binds *Lotus tetragonolobus* lectin (LTL).(Schulte and Spicer, 1983, Hennigar et al., 1985) The role of the PCT is to reabsorb (or reclaim) the bulk of solutes and water from the early glomerular filtrate. This includes 30-50% of filtered potassium, 60-70% of filtered water, sodium, chloride and bicarbonate and 90-100% of filtered glucose, amino acids, low molecular weight protein and phosphate.(Curthoys and Moe, 2014) This is enabled by the establishment of a sodium concentration gradient established by basolateral expression of Na-K-ATPase pump and a series of apical Na-cotransporters

which exploit this gradient.(Curthoys and Moe, 2014) Water absorption occurs through aquaporin 1(AQP1). Limited protein reabsorption from the urinary filtrate occurs via endocytosis after binding to megalin and cubulin proteins expressed on the luminal surface of PCT cells.(Nielsen et al., 2016)

A critical function of the PCT is the stringent maintenance of acid-base balance. In response to acidosis, the PCT maximises its bicarbonate reabsorption and increases its glutamine uptake to metabolise α-ketoglutarate and ammonia.(Hamm et al., 2015) The former can be metabolised by the liver to regenerate bicarbonate and the latter increases acid secretion from intercalated cells in the DCT/CD.(Hamm et al., 2015)

As a consequence of its high re-absorptive capacity and metabolic activity, the PCT is exposed to high levels of filtered drugs and is the major site of nephron injury due to nephrotoxic agents.(Soo et al., 2018) PCT cells also play key endocrine roles in homeostasis, for example, erythropoietin production, activation of vitamin D precursors, production of renin.(Lacombe et al., 1991, Nykjaer et al., 1999, Moe et al., 1993)

Inherited diseases of the PCT may either present as a specific transport defect or a global failure of the reabsorptive capacity of the PCT, eponymously labelled *Renal Fanconi syndrome*. Renal Fanconi syndrome is recognised by the presence of glucose, low molecular weight protein and excess sodium, potassium, phosphate, and other electrolytes in a dilute urine.Table 2.1

2.2.3 Loop of Henle

The LoH extends from the PCT down into the medulla, performing a hairpin turn before ascending to transition into the DCT.(Figure 2.1) It contains three segments, the thin descending limb, the thin ascending limb and the thick ascending limb. The descending limb is highly permeable to water and impermeable to solutes. Therefore, as the loop descends into the hyperosmolar medullary interstitium, the urinary filtrate becomes hyperosmolar.(Hall, 2016, Kokko, 1970) In contrast, the ascending limb is impermeable to water but relatively permeable to ions, which passively diffuse across the squamous membrane down a concentration gradient.(Hall, 2016)

In the thick ascending limb, as in the PCT, active solute transport is driven by a basolateral Na/K/ATPase pump which drives sodium out of the cell and potassium into the cell creating concentration gradients for both across the apical membrane.(Greger, 1985) NKCC2 symporters (gene *SLC12A1*) utilise these gradients to reabsorb 20% of filtered solute in this segment. A basolateral chloride channel Cl-CKb (gene *CLCKNB*) allows systemic chloride reabsorption across the basolateral membrane and critically requires the Barttin subunit (gene *BSND*) for its function.(Estevez et al., 2001) A positive electrochemical gradient is created in the tubular lumen by apical potassium escape from epithelial cells through the ROMK channel (gene *KCNJ1*). This gradient drives paracellular reabsorption of divalent cations (Ca^{2+} and Mg^{2+}) via the Claudin 16 paracellular channel.(Greger, 1985)

Together the differing permeabilities of the descending and ascending limbs of the LoH generate a countercurrent multiplier system which creates an osmolality gradient within the renal interstitium which is highest in the medulla.(Sands and Layton, 2009, de Rouffignac, 1972) This is maintained by blood flow through the *vasa recta*, a capillary network which is a direct extension of the efferent glomerular arteriole for the same glomerulus. This maintenance of a hyperosmolar medullary interstitium is critical to the function of aquaporin channels in the medullary CD, which permit passive water reabsorption across an osmolar gradient during periods of dehydration.

The dominant disease phenotype of the LoH is Bartter Syndrome which represents a failure of the powerful sodium reabsorption mechanism in the thick ascending limb. Multiple dyselectrolytaemias develop due to the reliance of many secondary electrolyte reabsorption mechanisms on this inward sodium current. Bartter Syndrome can present antenatally with polyhydramnios or postnatally with failure to thrive, polyuria and urinary salt wasting.(Table 2.1)

2.2.4 Distal Convoluted Tubule and Collecting Duct

The DCT receives a relatively dilute filtrate following the active solute reabsorption in the preceding tubular segments. The early part of the DCT makes contact with the glomerulus from the same nephron to form the juxtaglomerular apparatus (JGA).(Guyton et al., 1964, Perlewitz et al., 2012) Cells of the JGA sense the composition of the filtrate

and feedback via control on glomerular filtration pressure.(Perlewitz et al., 2012)(Figure 2.1) For example, in response to high filtrate osmolality (reflecting a dehydrated state) the JGA secretes renin, which stimulates a cascade of arteriolar vasoconstrictors (angiotensin I & angiotensin II).(Friis et al., 2013, Thatcher, 2017) This increases systemic vasomotor tone to maintain tissue perfusion and decreases renal blood flow whilst maintaining GFR until such time as the low circulating volume falls below a threshold for adequate renal blood flow, at which point kidney function declines.(Thatcher, 2017) The DCT is impermeable to water and participates in active ion solute reabsorption, increasingly diluting the urinary filtrate before its entry into the CD.(Hall, 2016) The thiazide sensitive, apical NCCT symporter (gene *SLC12A3*) transports sodium and chloride into the DCT epithelial cell which is moved across the basolateral membrane by chloride channel CLCNKB and the Na-K-ATPase pump. Magnesium and calcium reabsorption in this segment is passive across the apical membrane (TRPM6 and TRPV5 respectively) and by sodium exchange across the basolateral membrane (unknown and NCX respectively).

The DCT and CD both contain *principal* and *intercalated epithelial cells*.(Chen et al., 2017)(Figure 2.1) Principal cells express ENaC and ROMK which reabsorb sodium and secrete potassium respectively in response to aldosterone.(Pearce et al., 2015, Pearce et al., 2016) Additionally, principal cells regulate serum osmolality by the movement of aquaporin 2 channels into and out of the apical membrane in response to arginine vasopressin (AVP).(Pearce et al., 2015, Pearce et al., 2016) AVP is released by the posterior pituitary in response to increased serum osmolality which is detected by osmoreceptors in the hypothalamus. The effect of AVP binding to the principle cell receptors is to insert aquaporin 2 (AQP2) channels into the apical membrane, permitting increased free water movement by osmosis, from the relatively hypo-osmolar urinary filtrate to the relatively hyperosmolar medullary interstitium. These processes are critical to the maintenance of sodium and water balance, and thus systemic blood pressure. Once thought to play a focal role in maintenance of acid base balance with a high capacity for secretion of hydrogen ions, recent characterisation of intercalated cells has revealed three intercalated cell types with a broader repertoire of metabolic functions.(Rao et al., 2019, Roy et al., 2015) These cells display differential apicobasal expression of H+-ATPase, Pendrin and *SLC4A9*, display transdifferentiation between subtypes and perform

Disease Name	Inheritance	Genes	Phenotype	OMIM Phenotype Ref
Glomerular Disease				
Steroid Resistant Nephrotic Syndrome	See (Table 2.4), includes syndromic SRNS.			
Alport Syndrome/Thin GBM Membrane Nephropathy	XL, AR, AD	*COL4A5, COL4A3, COL4A4, MYH9*	Recurrent visible haematuria, proteinuria, sensorineural hearing loss, retinal flecks, ESRD.	301050, 203780, 615573, 153640
Fabry's Disease	XL	*GLA*	Proteinuria, neuropathy, neuropathic pain, acroparasthesias, cardiomyopathy, cardiac ischaemia, arrhythmia, hyperhidrosis, angiokeratomas, cerebrovascular disease.	301500
Fibronectin Glomerulopathy	AD	*FN1*	Glomerular deposit disease: haemoproteinuria, renal tubular acidosis, ESRD	135600
Thrombotic thrombocytopenic purpura	AR	*ADAMTS13*	Fever, thrombocytopenia, anaemia, neurological deficits, seizures, acute kidney injury.	604134
Atypical haemolytic uraemic syndrome (aHUS)	AR, AD	*C3, CD46, CFB, CFH, CFHR1, CFHR3, CFHR4, CFI, DGKE, THBD*	Haemolytic anaemia, thrombocytopenia, acute kidney injury, haemoproteinuria, ESRD.	235400, 612922, 612923, 612924, 612925, 612926, 615008
Familial amyloidosis	AD	*FGA, LYZ, APOA1, B2M*	Haemoproteinuria, hypertension, hepatosplenomegaly, glaucoma, polyneuropathy, variable extra-renal amyloidosis, ESRD.	105200
Proximal Tubule				
Renal glycosuria	AD	*SLC5A2*	Benign glycosuria with normoglycaemia	233100
Hereditary renal hyperuricaemia	AR	*SLC22A1 SLC2A9*	Uric acid nephrolithiasis, exercise induced acute kidney injury.	220150 612076
Cystinuria	AR, AD	*CLD3A1 SLC7A9*	Increased urine cystine, recurrent cystine nephrolithiasis.	220100
Proximal renal tubular acidosis	AR	*SLC4A4*	Acidosis, hypokalaemia, metabolic bone disease from chronic acidosis.	604278
Dicarboxylic aminoaciduria	AR	*SLC1A1*	Asymptomatic, elevated urine aspartate, ketotic hypoglycaemia, nephrolithiasis, neurological/developmental anomalies.	222730
Hypophosphataemic Rickets	XL, AR, AD	*PHEX, FGF23, ENPP1, DMP1*	Hyperphosphaturia, growth delay, osteomalacia, rickets, fractures, nephrocalcinosis.	307800, 193100, 613312, 241521
Fanconi-Bickel Syndrome	AR	*SLC2A2*	Glycogen storage disease type XI, renal Fanconi syndrome.	227810
Primary renal Fanconi Syndrome Type 1-4	AD, AR	*GATM, SLC34A1, EHHADH, HNF4A*	Renal Fanconi Syndrome (HNF4A: neonatal hyperinsulinaemia, macrosomia, maturity onset diabetes in the young – MODY)	134600, 613388, 616026

(1 of 4)

Disease Name	Inheritance	Genes	Phenotype	OMIM Phenotype Ref
Lowe Syndrome	XL	*OCRL*	Renal Fanconi Syndrome	309000
Dent's Disease	XL	*CLCN5, OCRL*	Low molecular weight proteinuria, nephrocalcinosis, progressive CKD.	300009, 300555
Nephropathic Cystinuria	AR	*CTNS*	Renal Fanconi Syndrome, ocular crystals, growth impairment, hypergonadotrophic hypogonadism, weakness, hypohydrosis, hypothyroidism, neurological problems.	219800
Isolated Proteinuria	AR	*CUBN*	Isolated benign proteinuria, megaloblastic anaemia (Vit B12 deficiency).	261100
Loop of Henle				
Bartter Syndrome	AR	*SLC12A1, KCNJ1, CLCNKA, CLCNKB, BSND*	Hyponatraemia, hypokalaemia, metabolic alkalosis, hypocalcaemia, hypomagnesaemia, polyuria, failure to thrive, arrhythmia.	601678, 241200, 607364, 613090, 602522
Distal Tubule				
Gitelman Syndrome	AR	*SLC12A3, CLCNKB*	Hypokalaemia, hypomagnesaemia, metabolic alkalosis, salt craving, arrhythmia.	263800
Hereditary hypomagnesaemia	AR	*TRPM6, CLDN16, EGF, CLDN!9*	Hypomagnesaemia, variable hypocalaemia, hypercalciuria, myokymia/hypokalaemia.	602014, 248250, 611718, 248190
	AD	*FXYD2, CNNM2, KCNA1*		154020, 613882, 160120
Familial hypocalciuric hypercalcaemia	AR/AD	*CASR*	Hypocalciuria, hypercalaemia, hyper/hypomagnesaemia, chrondrocalcinosis, pancreatitis.	601199
Gordon Syndrome	AD	*WNK1,WNK4, KLHL3, CUL3*	Pseudohypoaldosteronism hypertension, hyperkalaemia, acidosis.	614491, 614492, 614495, 614496
EAST (SeSAME) Syndrome	AR	*KCNJ10*	Seizures, sensorineural hearing loss, ataxia, intellectual disability, hypokalaemia, alkalosis, hyponatraemia, hypomagnesaemia.	612780
ADTKD-UMOD	AD	*UMOD*	Bland urine sediment, hyperuricaemia, hypouricosuria, gout, medullary echogenicity, CKD, ESRD.	174000
ADTKD-REN	AD	*REN*	Childhood onset EPO-responsive anaemia, hyperuricaemia, gout, hypotension, CKD, ESRD.	613092
ADTKD-MUC1	AD	*MUC1*	Adult onset CKD between 30-60 years. Bland urine sediment. Medullary cyst kidney disease.	174000

Disease Name	Inheritance	Genes	Phenotype	OMIM Phenotype Ref
Collecting Duct				
Liddle Syndrome	AD	*SCNN1G, SCNN1B*	Salt sensitive hypertension, hypokalaemia, metabolic alkalosis, low renin and aldosteronism.	177200
Distal renal tubular acidosis	AR, AD	*ATPV0A4; SLC4A1, ATPV1B1*	Isolated distal renal tubular acidosis, +/- haemolytic anaemia or progressive sensorineural hearing loss, nephrocalcinosis.	602722, 611590, 267300
Pseudohypoaldosteronism Type 1	AR	*SCNN1A, SCNN1G, SCNN1B*	Salt wasting, hyperkalaemia, acidosis, high aldosterone levels.	177735, 264350
Nephrogenic Diabetes Insipidus	XL, AD, AR	*AVPR2, AQP2*	Profound polyuria, polydipsia and hypernatraemia.	304800, 125800
Nephrogenic SIADH	XL	*AVPR2*	Hyponatraemia, hypo-osmolality, free-water excess.	300539
Pantubular/Non-Segment Specific				
ADPKD	AD	*PKD1, PKD2 DNAJB11*	Adult onset ESRD, mitral valve prolapse, intracranial aneurysm and subarachnoid haemorrhage, hypertension, hepatic cysts.	173900, 613095, 618061
ARPKD	AR	*PKHD1, DZIP1L*	Fusiform dilation of collecting ducts causing antenatal to adult ESRD. Pulmonary hypoplasia. Hypertension. Biliary ductal plate malformation, congenital hepatic fibrosis, recurrent cholangitis.	263200, 617610
Nephronophthisis and related ciliopathies	See Table 2.2 and Figure 2.2.			
Congenital Abnormalities of the Kidney and Urinary Tract (CAKUT)				
Renal Cysts and Diabetes Syndrome	AD	*HNF1B*	Varied renal phenotype, bicornate uterus, hypomagnesaemia, gout, maturity onset diabetes in the young (MODY).	137920
Renal hypoplasia or aplasia	AR	*RET, PAX2, UPK3A, GRIB1L, ITGA8, FGF20,*	Highly variable from antenatal oliguria and Potter's sequence to benign, non-syndromic single kidney.	191830, 615721, 617805
Renal coloboma syndrome	AD	*PAX2*	Renal hypodysplasia, vesicoureteric reflux, colobomas.	120330
Branchio-oto-renal syndrome	AD	*EYA1, SIX1, SIX5*	Renal hypodysplasia, ear anomalies and sensorineural hearing loss, branchial fistulae.	113650, 610896
Hypoparathyroidism, deafness and renal disease syndrome.	AD	*GATA3*	Renal hypo/dysplasia, sensorineural hearing loss, hypoparathyroidism.	146255

Disease Name	Inheritance	Genes	Phenotype	OMIM Phenotype Ref
Kallmann syndrome	XL, AR	*KAL1, FGFR1*	Hypogonadotrophic hypogonadism, anosmia, cleft palate, sensorineural hearing loss, renal agenesis.	308700, 147950
Non-syndromic CAKUT	AD	*ROBO2, SOX17, TNXB, KMT2D, ETV4, SALL1, TBX18, DSTYK*	VUR, UPJO, VUJO, variable.	610878, 613674, 143400, 610805
Fraser Syndrome	AR	*FRAS1, FREM2*	Crypophthalmos, syndactyly, CAKUT, ambiguous genitalia, laryngeal/tracheal abnormalities.	219000
16p11.2 Deletion Syndrome	AD	*TBX6*	Central nervous system anomalies, autism, obesity, head and neck anomalies, growth defects, limb defects, kidney agenesis, VUR.	611913
Trichorhinophalangeal syndrome	AD	*TRPS1*	Sparse scalp hair, bulbous nasal tip, long flat philtrum, thin upper vermillion border, protruding ears, skeletal abnormalities, cone shaped phalangeal epiphyses, hip malformations.	190350
Multicystic Dysplastic Kidney	AD	*SRGAP1, NRIP1*	Ureterocele, Horseshoe kidney.	618270
Urofacial Syndrome	AR	*HPSE2*	Dysmorphic bladders, hydroureteronephrosis, VUR, hypertension, ESRD	236730
Simpson-Golabi-Behmel syndrome	XL	*GPC3, OFD1*	Gigantism, enlarged dysplastic kidneys	312870
Townes Brock syndrome	AD	*SALL1*	Imperforate anus, dysplastic ears, thumb malformations, hearing loss, congenital heart disease, CAKUT.	107480

Table 2.1 Monogenic causes of kidney disease

AD – autosomal dominant, AR – autosomal recessive, ADPKD, autosomal dominant polycystic kidney disease, ARPKD, autosomal recessive polycystic kidney disease, ADTKD – autosomal dominant polycystic kidney disease, CKD – chronic kidney disease, EAST – Epilepsy, Ataxia, sensorineural hearing loss and tubulopathy, ESRD – end-stage renal disease, GBM – glomerular basement membrane, XL – X linked, CAKUT – congenital abnormality of the kidney and urinary tract, VUR, vesicoureteric reflux, UPJO – uretopelvic junction obstruction, VUJO – vesicoureteric junction obstruction. Adapted and updated from (Devuyst et al., 2014, van der Ven et al., 2018)

(4 of 4)

functions including acid secretion, bicarbonate secretion, regulation of sodium, chloride, potassium and calcium handling and most recently a role in the innate immune system of the collecting duct.(Rao et al., 2019, Roy et al., 2015)

Inherited disorders of the DCT/CD reflect the gain or loss of function of salt or acid handling transporters or regulators.(Table 2.1) Gitelman syndrome is the classical salt wasting phenotype for the DCT, classically presenting with hypokalaemia and hypomagnesaemia.(Riveira-Munoz et al., 2007, De Jong et al., 2002, Sabath et al., 2004) Disturbances in free water balance can result from gain or loss of function of AQP2 channels. Other rarer presentations are characterised by hypertension or salt wasting, potassium and acid-base disturbances given this segment is the terminal target of the renin-angiotensin-aldosterone axis.(Gordon, 1986, Pujo et al., 2007, Chang et al., 1996, O'Shaughnessy, 2015) Autosomal recessive polycystic kidney disease (ARPKD) is characterised by fusiform dilation of the collecting ducts and not infrequently presents with neonatal oligo-anuria and pulmonary hypoplasia with a high mortality, but can also present with a milder phenotype later in life.

2.2.5 Non-Segment Specific Inherited Kidney Disease

A number of genetic kidney disorders produce non-segment specific disease.(Table 2.1) For example, autosomal dominant polycystic kidney disease (ADPKD) is the most common, lethal monogenic worldwide with estimated incidence of between 1 in 500-1000.(Iglesias et al., 1983, Mallett et al., 2014, Baert, 1978, Lu et al., 1999) Both major gene products responsible for ADPKD (PKD1 and PKD2) localise to the primary cilium and are therefore labelled 'ciliopathies'. Since the discovery of the link between the primary cilium and polycystic kidney disease, NPHP has been established as another ciliopathy with a large and heterogeneous range of genetic variants and distinct syndromic associations. NPHP is one of the diseases modelled in this thesis and is discussed in detail in the next section. Other monogenic diseases can pre-dispose to metabolic crystal formation within the kidney leading to nephrolithiasis or nephrocalcinosis.(Devuyst et al., 2014, Daga et al., 2018)

Congenital abnormalities of the kidney and urinary tract (CAKUT) represent the most common cause of CKD in children.(Vivante and Hildebrandt, 2016, Fletcher et al., 2013)

This includes multicystic dysplastic kidney, renal agenesis, renal hypodysplasia, horseshoe kidney, duplex kidney and obstructive uropathies such as posterior urethral valves and pelviurethral junction obstruction, among others.(Verbitsky et al., 2019, van der Ven et al., 2018)

Whilst the representation of CAKUT in paediatric CKD is so high, one of the largest whole exome sequencing studies identified a monogenic cause in only 14% of pedigrees, although the unsolved rates were much lower in syndromic and reportedly consanguineous families. However, monogenic phenotype associations are far more variable than for other forms of inherited kidney disease, even within individuals of the same family with the same primary genomic variants. Further research has examined a more substantial database of almost 3000 patients and over 22,000 control subjects, establishing the role of large copy number variations in CAKUT.(Verbitsky et al., 2019)

Now that the general structure, function and genetic disease spectrum of the nephron have been summarised, this chapter will discuss the genetic and molecular basis underpinning NPHP and SRNS in more detail. NPHP is a progressive, fibrocystic, renal tubular ciliopathy which represents one of most common causes of end-stage renal disease in the first three decades of life.(Hildebrandt, 2016, Hildebrandt et al., 2011, Wolf, 2015) SRNS is the second most common cause of progressive CKD in children.(Fletcher et al., 2013, 2014) Both NPHP and SRNS almost invariably progress to ESRD and no targeted therapies exist to mitigate this outcome. Thus, there is an unmet need for novel disease modelling approaches for these diseases.

2.3 Nephronophthisis

NPHP is an autosomal recessive genetic renal disease and a common cause of ESRD in children and young adults.(Hildebrandt and Zhou, 2007) The word nephronophthisis is derived from the Greek words *nephros* meaning ‘kidney’ and *phthisis* meaning ‘wasting’. Patients with NPHP are phenotypically classified according the age at which they progress to ESRD. The most common type is juvenile NPHP which progresses to ESRD by a median age of 13 years.(Hildebrandt et al., 1992) Infantile NPHP has a median ESRD onset at 1 year of age (Gagnadoux et al., 1989), and adolescent NPHP 19 years of age.(Omran et al., 2000a) NPHP initially presents with symptoms of tubular dysfunction,

including growth failure, polyuria, polydipsia and secondary nocturnal enuresis due to impaired urinary concentrating ability. Symptoms and complications of CKD follow.(Hildebrandt and Zhou, 2007) Renal ultrasound may show normal or reduced kidney size and generally demonstrates increased echogenicity, reduced corticomedullary differentiation and variable cyst development.(Vester et al., 2010)

NPHP can present as an isolated disorder of the kidneys or, in 10-20% of cases, as part of a multisystem disease known as a ciliopathy (or nephronophthisis related ciliopathy syndrome – NPNP-RC).(Braun and Hildebrandt, 2016) Eponymous syndromes have been classified according to the spectrum of organ involvement however the sheer volume of genes discovered and the phenotypic variability observed within these syndromes is rendering these eponyms somewhat redundant. New phenotypes are also being described for known genes.(Devlin and Sayer, 2019)

Retinal disease is a common association with ciliopathies occurring in around 10-15% of cases (Wolf, 2015, Hildebrandt, 2016) because the light-sensing outer-segment of the retinal photoreceptor is connected to the main body of the cell by a primary cilium and relies on this cilium for the delivery of rhodopsins for vision.(Nemet et al., 2015, Taub and Liu, 2016) Considerable genetic and phenotypic variability occurs within these clinical syndromes. All NPHP-RC syndromes can variably include NPHP in their phenotypic spectrum. Meckel Gruber syndrome shares a number of genes with other syndromic ciliopathies and likely reflects the most severe end of the phenotypic spectrum associated with truncating variants, whilst hypomorphic alleles of the same genes present with milder phenotypes.(Hildebrandt et al., 2011)

On renal biopsy NPHP is histologically characterised by (i) tubular dilatation and atrophy, (ii) thickening, thinning and disintegration of the tubular basement membrane, (iii) tubulointerstitial and periglomerular fibrosis with or without a lymphocytic cellular infiltrate and (iv) the development of *ex vacuo* cysts.(Waldherr et al., 1982) Despite often being classified as a cystic kidney disease, the development of cysts in NPHP is variable in both timing and anatomical location within the kidneys.(Hildebrandt et al., 1992, Slaats et al., 2016) The renal medulla and corticomedullary junction is the classical site of cyst development but many patients will not develop cysts at all. Cyst often develop late in

Eponymous Syndrome	**Phenotype (*Major Features)***	**Genes Described**
Senior Løken Syndrome (OMIM 266900)	*NPHP, retinitis pigmentosa,* hepatic fibrosis	*NPHP1, NPHP4, IQCB1, CEP290, SDCCAG8, WDR19, TRAF31P1*
Cogan Syndrome (OMIM 257550)	NPHP, *oculomotor apraxia*	*NPHP1*
Mainzer-Saldino Syndrome (OMIM 266920)	*NPHP, retinitis pigmentosa, cone shaped phalyngeal epiphyses, flattened femoral epiphyses*, hepatic fibrosis, short ribs, small thorax, short stature, broad femoral neck, postaxial polydactyly	*IFT140*
Jeune Asphyxiating Thoracic Dystrophy (OMIM 208500)	*NPHP, short ribs, small thorax, pulmonary hypoplasia, respiratory insufficiency, short limbs,* liver and pancreatic cysts, retinitis pigmentosa, postaxial polydactyly	*15q13, IFT80, DYNC2H1, TTC21B, IFT144, NEK1, IFT121, WDR60, IFT140, IFT172, WDR34, CEP120, KIAA0586, DYNC2LI1, IFT52, TCTEX1D2, IFT43, IFT81, INTU, IFT27*
Cranioectodermal Dysplasia (OMIM 218330)	*NPHP, short ribs, small thorax, pulmonary hypoplasia, polydactyly, brachydactyly,* hepatic fibrosis, dolichocephaly, facial dysmorphism, microdontia, nail dysplasia, retinitis pigmentosa	*IFT122, IFT121, IFT43, IFT14F*
Oral-facial-digital Syndrome (OMIM 311200)	*Cleft lip, abnormal dentition, facial dysmorphisms, polydactyly, brachydactyly,* cystic renal dysplasia, retinitis pigmentosa, congenital heart disease	*OFD1, DDX59, SCLT1, C2CD3, TMEM231, TCTN3, C5ORF42, OFIP, NPHP1*
Joubert Syndrome (OMIM 213300)	*NPHP, retinitis pigmentosa, hypoplasia of the cerebellar vermis (molar tooth sign)* intellectual disability, ataxia, oculomotor apraxia, occipito meningocele, meningomyelocele	>60 genes associated including, but not limited to: *INPP5E, TMEM216, AHI1, NPHP1, CEP290, TMEM67, RPGRIP1L, ARL13B, CC2D2A, OFD1, TTC21B, TCTN1, TMEM237, TCTN3, ZNF423, KIF7, ARL3*
Alström Syndrome (OMIM 203800)	*NPHP, CAKUT, retinitis pigmentosa, sensorineural hearing loss, hepatic fibrosis, dilated cardiomyopathy, obesity, type 2 diabetes*	*ALMS1*
Bardet Biedl Syndrome (OMIM 209900)	*Cystic renal dysplasia, retinitis pigmentosa, intellectual disability, polydactyly, brachydactyly, obesity,* congenital heart disease, liver fibrosis, hypogonadism, sensorineural hearing loss	*BBS1, BBS2, ARL6, BBS4, BBS5, MKKS, BBS6, TTC8, PTHB1, BBS10, TRIM32, BBS12, MKS1, WDPCP, LZTFL1, IFT27, NPHP6, CEP19*
Meckel Gruber Syndrome (OMIM 249000)	*Posterior encephalocele, polydactyly, cystic kidney dysplasia, hepatic fibrosis,* pre-axial polydactyly, Dandy-Walker malformation, cardiac malformations,	*MKS1, TMEM216, TMEM67, CEP290, RPGRIP1L, CC2D2A, NPHP3, TCTN2, B9D1 B9D2, KIF14, TMEM107, CEP55, TXNDC15*

Table 2.2 Ciliopathy syndromes

This tables summarises the key features associated with NPHP-RC syndromes and the genes that are associated with them. Major features are presented in italic font but inter-individual phenotypic variability is high between subjects. Note that some genes are associated with multiple syndromes indicating a continuum of allelic severity (eg. *CEP290* in all of Senior Løken Syndrome, Joubert Syndrome and the most fulminant phenotype Meckel Gruber Syndrome). OMIM numbers are listed for the first described genotype for each phenotype. (adapted from (Braun and Hildebrandt, 2016, Devlin and Sayer, 2019, Wolf, 2015))

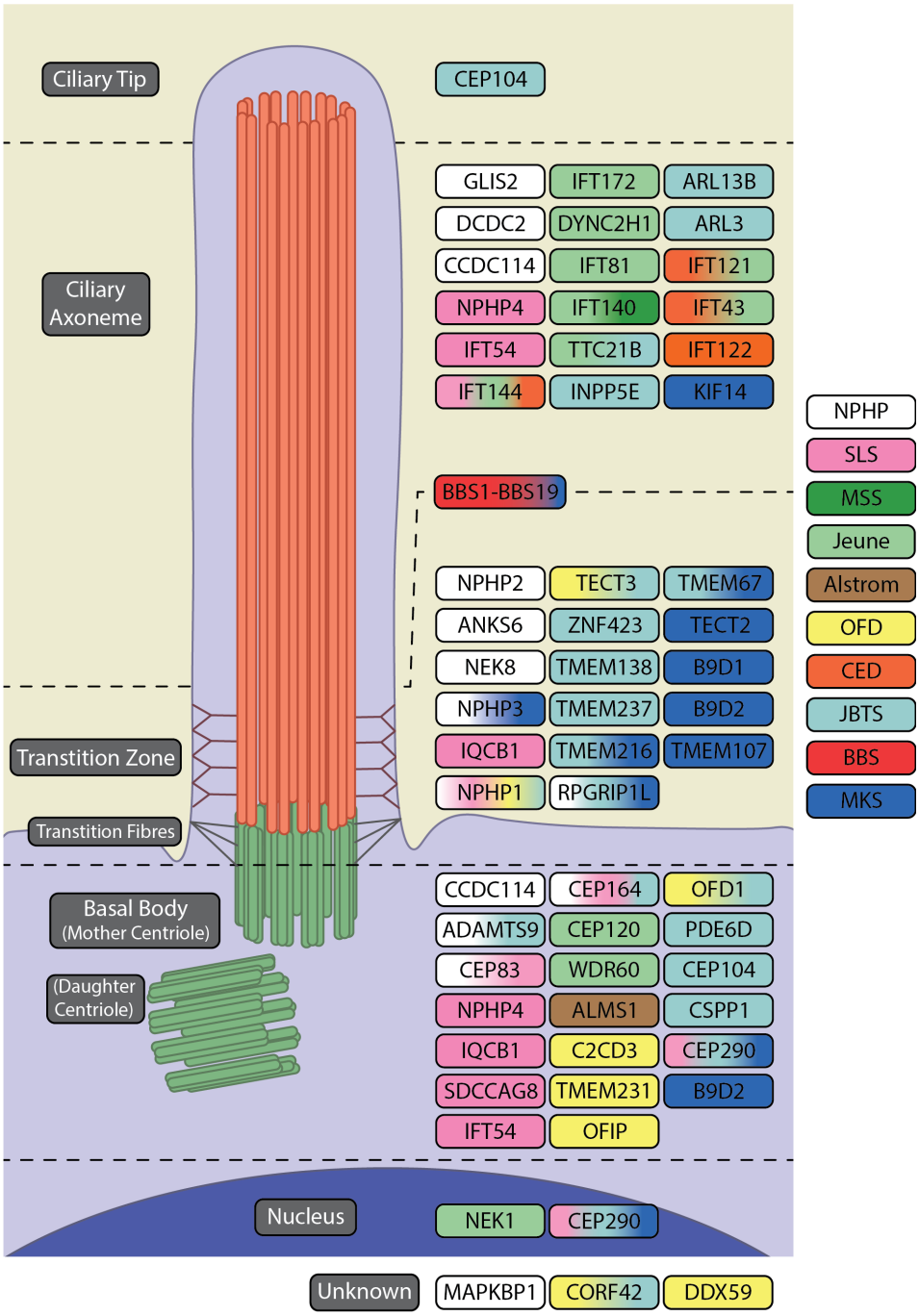

Figure 2.2 Ciliary localisation and syndromic associations of gene products associated with NPHP-RC Genes associated with NPHP-RC are grouped according to their proposed ciliary localisation and shaded according to their syndromic associations. The intention of this figure is to highlight the vast phenotypic variability within NPHP and the emerging redundancy of eponymous syndromes. There are some interesting observations, however, such as the absence of a Jeune Syndrome phenotype and the dominance of Meckel Gruber Syndrome within the genes localised to the Transition Zone. Only those NPHP-RC genes inclusive of a kidney phenotype are listed. NPHP – isolated nephronophthisis; SLS – Senior Løken Syndrome; MSS – Mainzer Saldino Syndrome; OFD – Oral-Facial-Digital Syndrome; CED – Cranio-Ecto-Dermal Syndrome; JBTS – Joubert Syndrome; BBS – Bardet Biedl Syndrome; MKS – Meckel Gruber Syndrome. (Compiled from (Braun and Hildebrandt, 2016, Devlin and Sayer, 2019, Wolf, 2015))

the course of disease and there exists hypothesis that tubulointerstitial fibrosis is the primary, and potentially more important, disease process.(Slaats et al., 2016)

The natural history of NPHP is progression to ESRD requiring dialysis or transplantation. NPHP represents the most common genetic cause of ESRD in children and young adults under 30 years of age.(Braun and Hildebrandt, 2016, Hildebrandt, 1999, Hildebrandt et al., 2011) If diagnosed early, treatment of the secondary physiological effects of CKD (eg. hypertension, proteinuria, acidosis, bone disease) can theoretically slow the rate of progression. As the number of genes associated with NPHP-RC increases, it is becoming evident that there is a spectrum of molecular mechanisms underlying disease for which a universal treatment is unlikely to be applicable.(Srivastava et al., 2017a) As mentioned above, there also remains debate as to whether the most appropriate target of therapy should be epithelial dysfunction or the interstitial fibrosis.(Slaats et al., 2016) For these reasons there is not currently a clinically available treatment targeting the progression of the primary disease process.

2.3.1 The Primary Cilium

There are currently over 70 genes reported in the literature which have been associated with NPHP-RC(Braun and Hildebrandt, 2016, Devlin and Sayer, 2019).(Table 2.2,Figure 2.2) The common link between all NPHP-RC genes is their co-localisation with the primary cilium (illustrated in Figure 2.2) and centrosome.

Cilia are hair-like projections of the cell cytoplasm that extend into the surrounding extracellular space. They are highly conserved cellular organelles across evolution, between species and organs.(Nigg and Raff, 2009) Cilia are categorised into three types: motile, non-motile (also known as '*primary' cilia*) and nodal. All cilia possess an *axoneme*, a cytoskeletal backbone of nine microtubule pairs arranged in a cylinder.(Figure 2.2 and 2.3) Motile cilia are structurally distinguished by the presence of an additional pair of central microtubules connected to the outer microtubules by radial spokes, and inner and outer dynein arms which connect outer microtubules and enable the synchronised beating of sheets of motile cilia across the apical surface of a cell and tissue.(Lindemann and Lesich, 2010)(Figure 2.3) Motile cilia are present on the epithelium of airways, cerebrospinal fluid spaces, fallopian tubes and spermatozoa.

Motile cilia enable mucociliary clearance of airway secretions, movement of ova along the fallopian tube, propagation of spermatozoa and flow of CSF through the brain. During development, nodal cilia on the surface of the embryonic node beat with a unique twirling motion, generating a morphogen gradient that determines left-right axis patterning of the embryo.(Okada et al., 1999, Nonaka et al., 2002) Structurally, nodal cilia resemble primary cilia but with inner and outer dynein arms.(Horani and Ferkol, 2018)(Figure 2.3)

The first human disease linked to the human cilium was Kartagener's syndrome (OMIM #244400), discovered in 1976 upon the recognition of the absence of the linking dynein arms in the tails of immotile sperm from infertile men.(Afzelius, 1976) Kartagener's syndrome is also called primary ciliary dyskinesia (PCD), a somewhat confusing nomenclature where the adjective *primary* is used to describe the genetic (rather than acquired or 'secondary') nature of the condition and bears no reference to the primary (non-motile) cilium. PCD is an autosomal recessive condition presenting with infertility, chronic suppurative lung disease (due to impaired mucociliary clearance) and dextrocardia due to the impaired establishment of the morphogen gradient at the embryonic node during development.(Dasgupta and Amack, 2016, Nonaka et al., 2002) A large number of genetic variants have been associated with primary ciliary dyskinesia, and none of the existing reports describe a renal phenotype.(Horani and Ferkol, 2018)

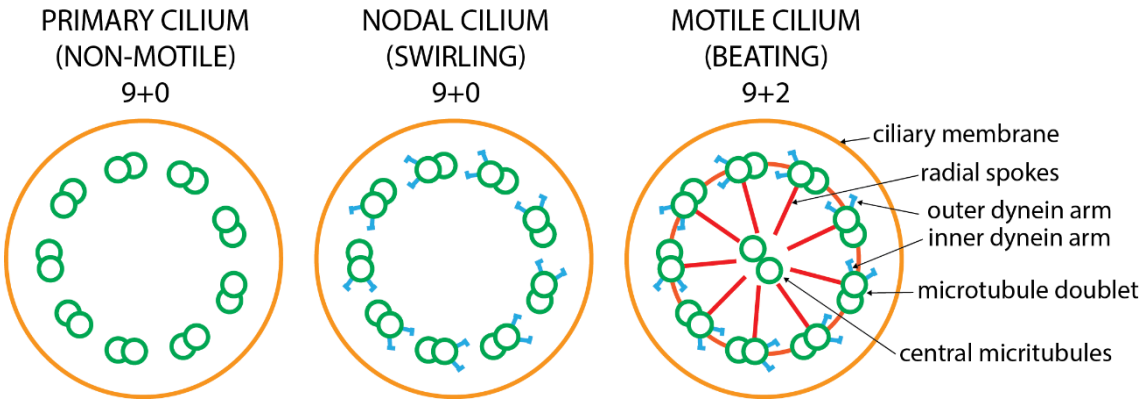

Figure 2.3 Structural differences between ciliary subtypes
Schema of the cross sectional axonemal structure of the three different types of cilium.

Rather than performing the dynamic functions of cell propagation or movement of extracellular material along an epithelium, the *primary cilium* is involved in sampling the extracellular environment and communicating with the main body of the cell to regulate

proliferation, cell relationships and polarity.(Spasic and Jacobs, 2017, Brown and Witman, 2014, Basten and Giles, 2013) The primary cilium is also implicated in cell division as it is deconstructed prior to mitosis and reconstructed by both daughter cells following cytokinesis.(Basten and Giles, 2013, Pan et al., 2013) The observation of multisystem developmental anomalies in human patients and animal models with poorly functioning cilia strongly advocate the role of the cilium in development.

The *basal body* is the anchor of the cilium within the cell and describes the mother centriole once it has attached to the cell membrane following mitosis. This attachment is mediated by nine *transition fibres* which extend from the distal (C-terminal) end of each microtubule triplet of the basal body to the base of the ciliary membrane, marking the proximal border of the *transition zone*. The proteome of the primary cilium is unique to any other part of the cell.(Ishikawa et al., 2012)

2.3.2 The Molecular Basis of Nephronophthisis is Incompletely Understood

With the arguable exception of Bardet Biedl Syndrome, there is significant heterogeneity in the phenotypic expression and established molecular function between the genotypes identified in affected families.(Braun and Hildebrandt, 2016, Hildebrandt, 2016, Hurd and Hildebrandt, 2011) Whilst a convergent or unifying pathway responsible for the similar histological and renal phenotypes is not characterised, some of the more established genotype-specific pathways implicated are discussed below.

Maintenance of Cell-Cell and Cell-Matrix Adhesions

NPHP1 (OMIM #607100; Chromosome 2q13) was the first described gene variant in NPHP by positional cloning and is implicated in 20-25% of all NPHP disease. (Hildebrandt, 2016) Recessive *NPHP1* variants most often produce a juvenile phenotype and roughly 85% of NPHP1 patients carrying deletions with missense variants accounting for the rest.(Otto et al., 2000, Saunier et al., 2000, Hildebrandt and Otto, 2005)

In an attempt to unify one or more common pathways within this expanding list of gene products, Sang et al. (2011) used a localisation and affinity purification (LAP) tag attached to 9 known NPHP proteins in a variety of immortalised cell cultures and determined interacting proteins by mass spectrometry. They mapped a network of

protein-protein interactions and characterised three core '*NPHPomes'*.(Sang et al., 2011) A complex of NPHP1, NPHP4 and RPGRIP1L localised to basolateral cell-cell junctions and the basal body, interacting with a separate complex including NPHP2 and NPHP3.(Sang et al., 2011) This recent, agnostic approach supports work published prior to the discovery of nephronophthisis as a ciliopathy. Before it was localised to the transition zone of the primary cilium (Fliegauf et al., 2006), NPHP1 co-immunoprecipitated with cell-cell and cell-matrix adhesions proteins in polarised IMCD3 and MDCK renal epithelial cell lines.(Benzing et al., 2001, Donaldson et al., 2000, Donaldson et al., 2002) An interaction with cell-cell junction protein and p130Cas substrate Ack1 has been characterised further emphasising a role of NPHP1 in maintaining cell-cell junctions.(Eley et al., 2008) This study also found immunofluorescent expression of NPHP1 was limited to the collecting duct in mouse kidney tissue and correlated this with the impaired concentrating ability often seen clinically.(Eley et al., 2008) Beyond this, the precise function of NPHP1 remains unknown. Interactions between NPHP1 and NPHP2,(Otto et al., 2003) NPHP3(Olbrich et al., 2003) and NPHP4(Mollet et al., 2002) have been characterised via co-immunoprecipitation and immunofluorescence.

Canonical Wnt signalling pathways and non-canonical Wnt-mediated Planar Cell Polarity (PCP).

NPHP2 (OMIM #602088) and *NPHP3* (OMIM #608002) are two NPHP genes with evidence to suggest abnormalities in canonical Wingless-related integration site (Wnt) signalling. *NPHP2* was the first gene characterised for the infantile phenotype of NPHP.(Haider et al., 1998, Otto et al., 2003) Pathogenic variants in *NPHP3* have since been identified in a cohort of patients with infantile histology in China and Europe.(Sun et al., 2016, Tory et al., 2009) Infantile NPHP is phenotypically distinguished by the atypical features of enlarged kidneys, cortical cystic changes and preservation of tubulointerstitial membrane morphology.(Tory et al., 2009) *Situs inversus* is also a feature of infantile NPHP phenotypes suggesting a role for nephrocystins in the nodal cilia during determination of left-right axis patterning, earning the name inversin for the gene product of *NPHP2*.(Simons et al., 2005) However, there exists further phenotypic variability as both *NPHP2* and *NPHP3* variants have been described in patients with juvenile and adolescent onset NPHP respectively.(Olbrich et al., 2003, Omran et al., 2000a) This

phenotypic variability has been hypothesised to be due to allelic severity with truncating variants more likely to give rise to infantile disease and non-truncating variants adolescent disease. Another hypothesis is the oligogenic, disease modifying contribution of heterozygous variants in other NPHP genes to a heterozygous or homozygous *NPHP3* gene status.(Tory et al., 2009, Hoefele et al., 2007, Devlin and Sayer, 2019)

Wnt signalling pathways are highly conserved developmental pathways across species and have also been implicated in the development of cystic kidney diseases other than NPHP.(Lancaster and Gleeson, 2010, Kim et al., 1999, MacDonald et al., 2009, Fischer et al., 2006, Schnell and Carroll, 2014) Canonical Wnt signalling begins with the binding of a Wnt ligand to a Frizzled receptor, recruiting LRP5/6 to activate Dishevelled (Dvl) which goes on to inhibit the ß-catenin destruction complex. This complex of proteins includes glycogen synthase kinase 3ß (GSK3ß), axin, adenomatous polyposis coli, protein phosphatase 2A and casein kinase 1-alpha which together ubiquitinate ß-catenin targeting it for proteosomic degradation.(MacDonald et al., 2009) When the ß-catenin destruction complex is inhibited, an accumulation of cytosolic ß-catenin enters the nucleus where it activates TCF transcription factors and subsequently genes involved in developmental signalling and proliferation.(Lancaster and Gleeson, 2010) There are numerous non-canonical pathways downstream of Wnt ligand-receptor binding but the planar cell polarity (PCP) pathway is most implicated in cystic kidney disease.(Fischer et al., 2006, Schnell and Carroll, 2014) Much less is characterised regarding non-canonical Wnt signalling which deviates from the canonical pathway at the level of Dvl and therefore operates independently of ß-catenin. Membrane bound Dvl interacts with Wnt-ligand-bound Frizzled and then activates Ras homolog gene family member A (RhoA) and/or Ras-related C3 botulinum toxin 1 (Rac1). These compounds then activate Rho kinase and c-Jun N-terminal kinase which leads to transcription of genes involved in planar cell polarity and cytoskeletal rearrangement.(Lancaster and Gleeson, 2010) The primary cilium has been implicated in directing the response from the ligand-bound Frizzled receptor towards either pathway but the precise mechanism for this remains incompletely understood.

Due to the observation of cystic renal phenotypes in both Wnt gain-of-function and Wnt loss-of-function mouse models, it is likely that Wnt-signalling in the kidney requires a

precise balance for normal development and homeostasis.(Saadi-Kheddouci et al., 2001, Marose et al., 2008, Lancaster and Gleeson, 2010) This has been demonstrated in *PKD1* mediated ADPKD. The C-terminus of polycystin 1 (the *PKD1* gene product) has been demonstrated in separate studies to play a role in both inhibition and activation of canonical Wnt signalling (Kim et al., 1999) and animal models with gain or loss of polycystin 1 both develop cystic renal disease.(Lantinga-van Leeuwen et al., 2004, Thivierge et al., 2006)

NPHP2/Inversin has been demonstrated to inhibit canonical Wnt signalling by forming a complex with Dvl targeting it for degradation and thereby releasing the beta-catenin destruction complex from Dvl inhibition.(Simons et al., 2005) In HEK293T cells transfected to overexpress either or both of *NPHP2* and *NPHP3* demonstrated either protein could independently inhibit canonical Wnt signalling quantified by *TCF*/*LEF-1* dependant luciferase reporter activity.(Bergmann et al., 2008) Decreased canonical Wnt signalling has also been reported in an *Ahi1* knockout mouse, an animal model for classical Joubert Syndrome including a classical NPHP renal phenotype.(Lancaster et al., 2009) Furthermore co-immunoprecipitation and yeast two-hybrid cDNA library screening identified and characterised an interaction between *Glis2* and ß-catenin and also demonstrated that *Glis2* acts as a repressor of TCF mediated transcriptional activation, as well as that of its own target gene *CCND1*.(Kim et al., 2007)

Unlike cytosolic Dvl, membrane bound Dvl (implicated in non-canonical Wnt signalling) appears immune to inversin mediated degradation and thus, inversin performs the role of a ‘switch’ between the two Wnt pathways.(Simons et al., 2005) A similar mechanism has been established for *NPHP3*.(Bergmann et al., 2008) Other ciliopathy genes have been associated with the non-canonical pathway including BBS proteins, HNF1ß, and OFD1, supporting a role for Wnt signalling in ciliopathy pathogenesis.(Lancaster and Gleeson, 2010)

Exactly how the balance between canonical and non-canonical Wnt signalling might lead to cystic kidney disease is not known. Defective orientation of tubular cell mitosis has been postulated to play a role with the observation of disturbed mitotic angles observed in *HNF1ß* mutant mice and *Pck* rats (*Pkhd1* mutant orthologue).(Fischer et al., 2006) As

described in subsequent sections on mammalian kidney development, multiple Wnt ligands play an important role in kidney development.(see Section 2.5.2) Over the course of nephron development, a shift from canonical to non-canonical dominant signalling is essential and disruption in this balance may give rise to developmental renal anomalies such as NPHP.(Park et al., 2007) Indeed, this may explain why *NPHP2/Inversin* and *NPHP3* variants (with their links to early Wnt-signal regulation) give rise to much earlier disease than other genotypes.

The primary cilium is involved in hedgehog signalling, which is dysfunctional in NPHP

Another of the Sang et al NPHPomes was a complex of co-purifying proteins including MKS1, MKS6 and TCTN2, found to localise to the base of the cilium and also interact with AHI1/Jouberin.(Sang et al., 2011) MKS1 has been hypothesised to affect abnormal hedgehog signalling in the developmental patterning of the limb and brain in the *krc* mouse.(Weatherbee et al., 2009) *Tctn2-/-* mice demonstrated severely abnormal phenotype consistent with abnormal hedgehog signalling (fully penetrant neural tube defects, exencephaly, polydactyly, microphthalmia and cleft palate), reduced transcription of hedgehog target genes *Ptc1* and *Gli1* and also increased amounts of unprocessed Gli3 protein, all consistent with reduced hedgehog responsiveness. It is possible that the MKS1 NPHPome is an important contributor to hedgehog pathway signalling. (Sang et al., 2011) In separate work *GLIS2* is established as an NPHP genotype and recapitulates a classical NPHP histology in 4 week old mutant mouse model.(Attanasio et al., 2007) Upregulated gene pathways in *Glis2* mutant mice include epithelial to mesenchymal transition, apoptosis, fibrosis, cell cycle inhibition as well as a role for Glis2 to act in a feed forward loop on Gli1 transcription targets (eg. *Bmp4*, *Pax2*, *Sall1*, *Ccnd1* and *N-myc*).(Attanasio et al., 2007)

The evidence for dysfunctional hedgehog signalling in Joubert Syndrome is conflicting, with animals demonstrating abnormal hedgehog signalling phenotype on a molecular level (Hynes et al., 2014, Damerla et al., 2015) but often incomplete JBTS phenotypes including normal dorsoventral patterning of the neural tube, a developmental process believed to rely heavily on intact hedgehog signalling.(Damerla et al., 2015, Abdelhamed et al., 2013, Hynes et al., 2014) It is possible that this variability in molecular and developmental hedgehog signalling phenotype between reports is due to variability in the

severity of disruption to the signalling pathway, tissue specific effects of different genes or technical difficulties in measuring hedgehog signalling activity in research models.

Another reason for this variability could be interspecies differences in hedgehog signal transduction. Mouse studies suggest that Gli2 is the principle transcription activator whilst Gli3 the principle transcription repressor whilst both proteins are capable of both functions.(Matise et al., 1998, Litingtung and Chiang, 2000) Whilst Gli1is essential for normal Hh signalling in zebrafish(Karlstrom et al., 2003), it has no repressor function in mammals and contributes only modestly to Gli2 mediated transcriptional activation.(Park et al., 2000) In amphioxus, alternatively spliced isoforms of the one *Ci* (*Gli* ortholog) gene act as repressors or activators.(Shimeld et al., 2007) Finally in mammals, post-translational proteolysis of multiple *Gli* genes is controlled by phosphorylation of the C-terminal to determine repressor or activator function.(Briscoe and Therond, 2013) Whilst existing animal ciliopathy models strongly suggest disturbances in hedgehog signalling play a role in disease, high interspecies variation in hedgehog signalling transduction would suggest ongoing research is best performed in a human cellular functional genomic model.

DNA Damage Response Pathways and Cell Cycle Arrest

The third complex identified in the Sang et al (2011) report illustrated that CEP290 is required to recruit NPHP5 to the centrosome prior to cell division. The cilium is deconstructed prior to mitosis, at which point the basal body of the cilium becomes the mother centrosome.(Basten and Giles, 2013, Pan et al., 2013) It is therefore highly likely that mutant basal body proteins could disrupt the mitotic process. In one report, *Cep290* mutant mice demonstrated supra-numerary centrioles, increased DNA replication stress and DNA damage, a phenotype that was rescued by CDK inhibitors.(Slaats et al., 2015) Other human NPHP genotypes implicated in increasing DNA damage response include *CEP164*(Sivasubramaniam et al., 2008), *ZNF423*(Chaki et al., 2012), *OFD1, SDCCAG8*(Otto et al., 2010) and *NEK8*(Choi et al., 2013a). CDK5 inhibitors have also been demonstrated to successfully retard histological disease progression in a *NEK8* mutant mouse model.(Husson et al., 2016) and represent a promising targeted therapy not only in the NPHP literature but also in ADPKD.(Bukanov et al., 2012, Bukanov et al., 2006, Moreno et al., 2008, Booij et al., 2017)

2.3.3 Intraflagellar Transport

There is no mechanism for protein synthesis within the cilium so all proteins must be manufactured in the cell cytoplasm and transported into the cilium. The transition zone represents the most proximal zone of the cilium. It is distinguished by bifid proteins (called Y-links) which extend from the midpoint of the axonemal microtubular doublets to the ciliary membrane.(Figure 2.3) Here they attach to beads giving the appearance of multiple studded necklaces around the base of the cilium (the *ciliary necklace*).(Fisch and Dupuis-Williams, 2011) The term '*ciliary gate'* refers to the transition fibres and transition zone. This label refers to the function of the ciliary gate as a regulator of protein entry to (and exit from) the ciliary cytoplasm. The transition fibres are also important in the recruitment of the necessary proteins to the distal centriole to initiate and promote ciliogenesis.(Garcia-Gonzalo and Reiter, 2016) The protein subunits from which the transition fibres and Y-links of the ciliary gate are composed are well represented in lists of gene products associated with ciliopathy syndromes.(Garcia-Gonzalo and Reiter, 2016, Hildebrandt, 2016)(Figure 2.2)

There are multiple mechanisms for the entry of cilia-targeted proteins to the ciliary space. Membrane bound or transmembrane proteins are targeted to the cilium via transport of vesicles direct from the Golgi apparatus.(Nachury et al., 2010) It is also likely that specific amino acid motifs (called ciliary localisation sequences – CLS) identify proteins for ciliary localisation.(Bloodgood, 2000, Garcia-Gonzalo and Reiter, 2012) These CLS interact with intraflagellar transport (IFT) and Bardet Biedl Syndrome (BBS) proteins at the junction of the transition fibres and ciliary membrane and facilitate transition of these proteins across the ciliary gate by mechanisms that are not clearly characterised.(Vieira et al., 2006, Hou et al., 2007, Qin et al., 2011)

Because the basal body lumen is obstructed with electron dense, centrin-2 containing structures, the only path for soluble proteins into the cilium is across the transition fibres.(Fisch and Dupuis-Williams, 2011) There are multiple described mechanisms by which proteins can make this transition. IFT protein levels have been observed to swell beneath the *Chlamydomonas* flagellum at the transition fibres before a controlled release or 'avalanching' into the ciliary space.(Ludington et al., 2013) This may be mediated by a phosphorylation dependent, Ras-related nuclear (Ran-GTP) protein gradient capable of

sensing flagellar length and therefore self-regulating the availability of construction machinery.(Ludington et al., 2013, Dishinger et al., 2010) Perhaps the most important mechanism of soluble protein transfer into the ciliary cytoplasm is, as for membrane bound proteins, the ability to interact with IFT proteins, IFT motors, BBSome proteins and other proteins such as importin-2.(Garcia-Gonzalo and Reiter, 2012, Dishinger et al., 2010, Hou et al., 2007) Many of the above-described mechanisms illustrate similarities between ciliary and nuclear protein targeting.(Verhey et al., 2011) Indeed, nucleoporins have been found to localise at the ciliary base (Kee et al., 2012) and kinesin motors have been observed shuttling transcription factors between ciliary and nuclear compartments.(Chennathukuzhi et al., 2003, Morris et al., 2004, Dishinger et al., 2010) Exactly how this translates to disease mechanism is yet to be elucidated but it is clear that ciliary protein importation is a complex and highly regulated process which is partly dependent on IFT proteins.

Kinesin protein multimers ascend the ciliary axoneme driving anterograde IFT whilst dynein protein complexes descend the cilium driving retrograde IFT.

Once across the transition fibres a system of IFT moves proteins up and down the cilium alone the axoneme. Transport of proteins from the base to the tip is called anterograde IFT and the transport of proteins in the reverse direction is called retrograde IFT.(Kozminski et al., 1993, Rosenbaum and Witman, 2002) Anterograde IFT is performed by a kinesin-II motor made of three protein subunits (KIF3A, KIF3B and KAP) whilst retrograde IFT is performed by a more complex dynein motor composed of eight protein subunits.(Kozminski et al., 1995, Pazour et al., 1999) These motors interact with the ciliary axoneme and with IFT protein complexes (which in turn interact with IFT *cargo* proteins and the BBSome) to form IFT *trains*.(Rosenbaum and Witman, 2002) Anterograde and retrograde motors have been demonstrated to associate with the B- and A- tubules of the microtubule doublets respectively which prevents collision of motors moving in different directions.(Stepanek and Pigino, 2016)

The function and dysfunction of the heterotrimetic kinesin-II was first demonstrated using a temperature controlled *fla-10* mutant (orthologue to human *KIF3A*) *Chlamydomonas* model.(Kozminski et al., 1995) When the temperature was raised to restrict *fla-10* expression, cessation of IFT was observed and the flagellum started to

shorten.(Kozminski et al., 1995) This indicates that not only is anterograde IFT required for ciliary construction, but also for maintenance of the mature cilium. *Kif3a* knockout mouse models have since demonstrated absence or severe shorting of poorly motile cilia at the embryonic node. (Marszalek et al., 1999, Takeda et al., 1999) The phenotype of these mice included *situs inversus*, abnormal mesodermal patterning and embryonic lethality.(Marszalek et al., 1999, Takeda et al., 1999)

Retrograde IFT is driven by a cytoplasmic dynein 2 multimer motor and mutations in subunits of this motor give rise to a classical ciliary morphology of shortened cilia with bulbous tips.(Pazour et al., 1999, Collet et al., 1998, Signor et al., 1999, Wicks et al., 2000, May et al., 2005) The expanded ciliary tip represents the accumulation of retrograde IFT cargo unable to descend the cilium. The shortened cilium is thought to arise from the unavailability of anterograde IFT machinery held up in the ciliary tip, which would otherwise be recycled for ciliary maintenance.(Pazour et al., 1999) The recycling of IFT components is evidenced by the observation of ongoing IFT despite the arrest of cellular protein synthesis by aminoglycoside toxicity.(Iomini et al., 2001)

IFT proteins are separated into IFT-A and IFT-B groups.

Both anterograde and retrograde motors interact with ciliary proteins via bridging IFT proteins.(Rosenbaum and Witman, 2002, Lechtreck, 2015, Taschner and Lorentzen, 2016)(Table 2.3) IFT proteins are rich in tetratricopeptide repeats, WD40 domains, and coiled-coil domains which are all well characterised protein-protein interaction domains.(Taschner et al., 2012) Whilst many of the protein-protein interactions have been identified in yeast two hybrid analyses and similar protein-protein association experiments, many of the interactions between IFT proteins have since been demonstrated to require the interaction of cargo with the assembled IFT complex.(Taschner et al., 2016)

IFT proteins rely on protein components of the transition fibres for appropriate localisation in the cilium both during ciliogenesis and in the ciliary maintenance state. For example, in RPE cell monolayers, *Cep164* siRNA treatment was associated with reduced localisation of IFT88 at the transition zone of the cilium without a reduction in the amount of *IFT88* expression.(Schmidt et al., 2012) In a separate report, *CCDC41* knockdown reduced IFT20 localisation to the basal body and reduced docking of ciliary

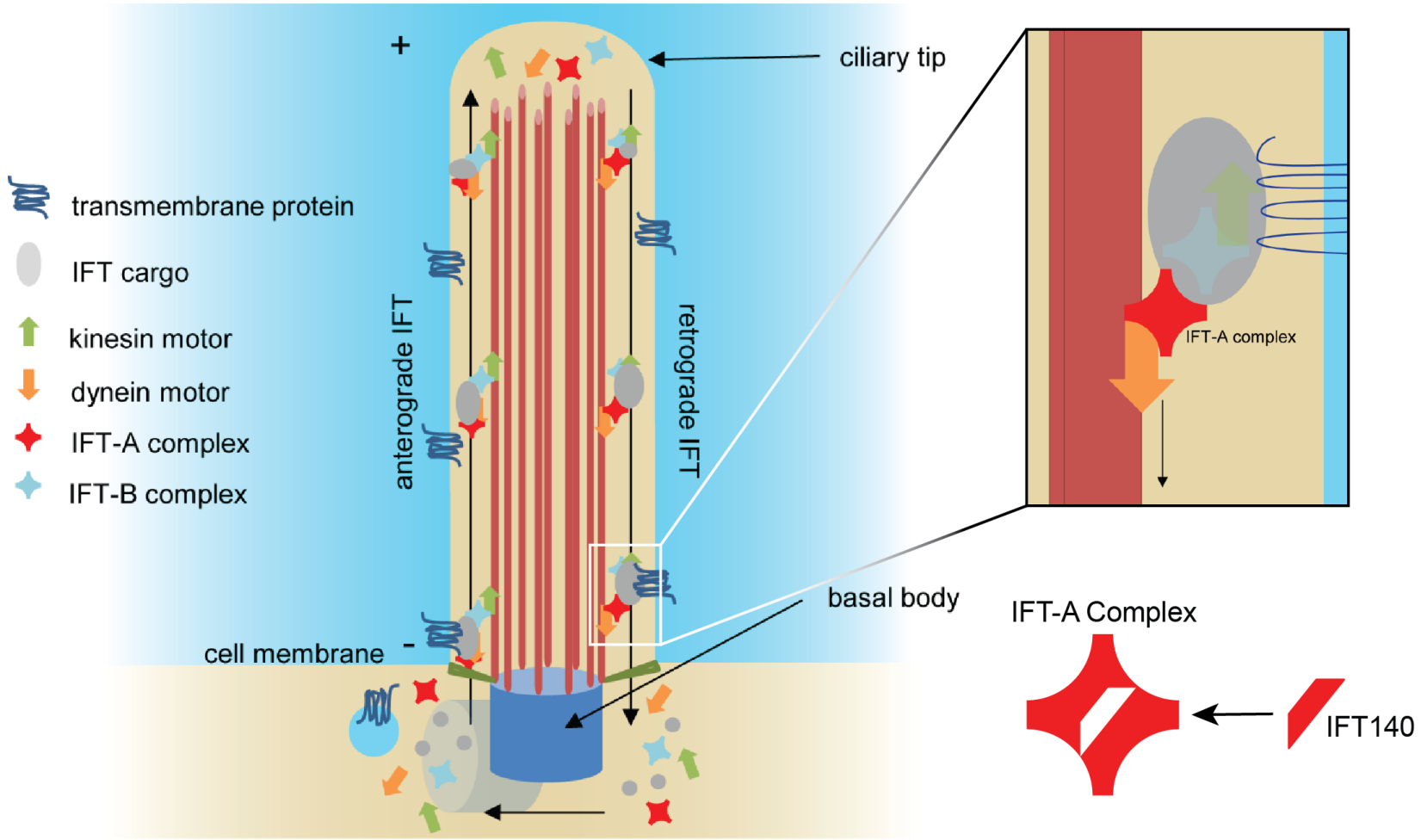

Figure 2.4 The role of IFT140 in the primary cilium
The primary cilium is a hair-like projection from the apical surface of the renal epithelial cell. With no internal protein manufacturing equipment, the cilium imports proteins from the main body of the cell and transports them up and down the cilium using intraflagellar transport (IFT). IFT140 Forms a core component of the IFT-A complex which binds IFT cargo to the dynein motor which descends the ciliary axoneme, returning its cargo the base of the cilium for export into the main cell cytoplasm.

vesicles.(Joo et al., 2013) In mouse embryonic fibroblasts treated with *C2cd3* siRNA recruitment of IFT88 and IFT52 to the basal body was reduced.(Ye et al., 2014) Finally, extrapolating from a *C. elegans* model, transition protein FBF1 is believed to interact with the IFT-B complex of assembled IFT proteins to mediate ciliary import.(Wei et al., 2013)

IFT-B proteins link IFT cargo to kinesin motors in anterograde IFT.

There are 16 proteins within the IFT-B complex which are further grouped into a *core* subunit (IFT-B1: IFT88,81,74,70,56,52,46,27,25 and 22) and a *peripheral* subunit (IFT-B2: IFT172,80,57,54,38 and 20). (Table 2.3) Members of the IFT-B1 complex are defined by strong hydrophobic bonds that resist dissociation at saline concentrations greater than 2 molar.(Taschner et al., 2014) Whilst peripheral IFT-B2 proteins dissociate from the IFT-B complex at a lower salinity (reflecting weaker associations), they are capable of independently forming their own complex in the absence of IFT-B1 proteins.(Taschner et al., 2016) The two subcomplexes interact at IFT88/52 and IFT38/57.(Taschner et al., 2016)

Mutations in IFT-B proteins demonstrate absent or very short cilia, similar to the severe ciliogenesis defects seen in kinesin-II mutants. An *IFT88* mutant *C. reinthardii* model demonstrated absent flagella and the mouse and human homologue gene was identified to be *Tg737*, for which a mouse model demonstrates early onset polycystic kidney disease (Pazour et al., 2000) potentially implicating IFT dysfunction as a cause of PKD. An *IFT172* knockout *Tetrahymena* demonstrated a similar ciliary morphology however the introduction of a partially truncated rescue construct developed short cilia with accumulation of IFT88 at the ciliary tip, implicating IFT172 in the rearrangement of retrograde IFT particles in the transition between anterograde and retrograde IFT.(Tsao and Gorovsky, 2008) All of *IFT52*(Richey and Qin, 2012), *IFT46*(Hou et al., 2007) and *IFT74*(Brown et al., 2015) null mutants also demonstrate severely impaired ciliogenesis in *C. reinthardii* models.

Other specific functions of IFT-B proteins include the following.[Reviewed in(Taschner and Lorentzen, 2016)]

- IFT25 and IFT27 are essential in the export of Sonic hedgehog (Shh) signalling mediators from the cilium and produce defects in signalling in mouse models. These proteins may also assist in the export of BBSome proteins which accumulate in the ciliary space in knockout mutants. Variants in *IFT27* have been identified in patients with BBS.
- IFT20 localises to the Golgi apparatus and is thought to associate with ciliary membrane bound proteins, targeting them for ciliary localisation. The precise mechanism for this is not identified.
- Transport of tubulin heterodimers for ciliogenesis and maintenance via an IFT81/74 binding site and an IFT54 binding site.

IFT-A proteins participate in retrograde IFT.

The IFT-A proteins are smaller in number with three proteins forming a *core* subcomplex (IFT140, IFT144 and IFT122, Table 3).(Mukhopadhyay et al., 2010, Behal et al., 2012) The core proteins maintain their association in the presence of a mutant *non-core* protein (IFT139, IFT121 and IFT43, Table 3).(Mukhopadhyay et al., 2010, Behal et al., 2012) Mutations in core IFT-A proteins don't disrupt the other core proteins, however, they can destabilise and deplete the non-core proteins from the IFT-A complex.(Behal et al., 2012)

In mouse germline knockout models of IFT-A genes *IFT44*, *IFT140*, *IFT139*, *IFT122* and *IFT121* result in embryonic lethality or neonatal death with profound defects in skeletal, ophthalmic, craniofacial and neurological development.(Tran et al., 2008, Cortellino et al., 2009, Liem et al., 2012, Mill et al., 2011, Miller et al., 2013, Yuan and Yang, 2015) No mouse model of *IFT43* has been published but variants in all IFT-A genes (including *IFT43*) have been described in patients with skeletal ciliopathies.(Perrault et al., 2012, Schmidts et al., 2013, Bredrup et al., 2011, Walczak-Sztulpa et al., 2010, Davis et al., 2011, Smith et al., 2016, Arts et al., 2011) *Chlamydomonas* temperature-sensitive *IFT144*, *IFT139* and *IFT121* mutants demonstrate shortened cilia with a bulbous tip (Iomini et al., 2001, Blacque et al., 2006, Piperno et al., 1998), similar to dynein 2 mutant models. (Pazour et al., 1999, Collet et al., 1998, Signor et al., 1999, Wicks et al., 2000, May et al., 2005) IFT-A mutant *Chlamydomonas* models also demonstrate reduced retrograde transport velocities.(Piperno et al., 1998) Collectively these observations demonstrate the indispensable nature of IFT-A proteins for retrograde IFT.

The IFT-A complex has been strongly implicated in Sonic hedgehog (Shh) signalling (Liu et al., 2005, Huangfu et al., 2003, Jonassen et al., 2012). With Shh ligand unbound, the Patched (Ptc) receptor inhibits activity of Smoothened (Smo) G-protein coupled receptors in and around the ciliary membrane.(Stone et al., 1996) Binding of the Shh ligand releases this inhibition and allows Smo to become phosphorylated and migrate into the cilium whilst Ptc and other Shh repressors leave the cilium and peri-ciliary membrane.(Briscoe and Therond, 2013) Activated Smo inhibits C-terminal phosphorylation the Gli family of zinc finger proteins (Gli1, Gli2 and Gli3) by protein kinase A, GSK3ß and casein kinase 1 within the cilium. Phosphorylation of Gli proteins results in partial proteolytic degradation and the shortened proteins are translocated to the nucleus where they act as transcriptional repressors of Shh targets.(Briscoe and Therond, 2013) Smo-related inhibition of this phosphorylation allows the transcription factors to migrate to the nucleus free from to proteolytic breakdown where they act as transcriptional activators for the same gene targets.(Briscoe and Therond, 2013) Gene targets have been identified using chromatin immunoprecipitation and include components of the Shh pathway itself (eg. *Ptc* and the *Gli* gene family) and genes involved in developmental patterning in a tissue specific manner.(Vokes et al., 2007, Vokes et al., 2008)

IFT-A Core	**IFT-A Non-Core**	**IFT-B1 (Core)**	**IFT-B2 (Periph)**
IFT144	IFT139	IFT88	IFT172
IFT140	IFT121	IFT81	IFT80
IFT122	IFT43	IFT74	IFT57
		IFT70	IFT54
		IFT56	IFT38
		IFT52	IFT20
		IFT46	
		IFT27	
		IFT25	
		IFT22	

Table 2.3 Intraflagellar transport proteins classified according to subcomplex
(adapted from (Taschner and Lorentzen, 2016))

Many IFT-A mutants exhibit activation of the Shh pathway in the absence of ligand binding to Ptc(Tran et al., 2008, Qin et al., 2011, Liem et al., 2012, Jonassen et al., 2012, Miller et al., 2013) but some models, along with the Dynein-2 motor mutant have documented reduced Shh signalling.(Liem et al., 2012, Ocbina et al., 2011, Cortellino et al., 2009) Mouse models with reduced signalling are observed to have more severe

problems with ciliogenesis and this is postulated as the reason for reduced Shh signalling. However, at least one dynein-2 (DYNC2H1) mutant mouse model manifests the same ciliary morphology as IFT-A mutants but with *reduced* Shh signalling suggesting that defective retrograde IFT is probably not the only mechanism moderating Shh pathways within cilia.(Ocbina et al., 2011) A role has been established for IFT144 proteins in the ciliary import of Smo, Arl13b and adenylyl cyclase III which is required for the phosphorylation of Gli gene products to target them for proteolytic degradation to repressor isoforms.(Liem et al., 2012)

Another potential mechanism of Shh dysfunction was discovered by tandem affinity purification and immunofluorescence suggesting the core IFT-A complex (potentially IFT122) is responsible for the ciliary import of Tubby like protein 3 (TULP3)(Mukhopadhyay et al., 2010, Qin et al., 2011) The same group demonstrated TULP3 is responsible for ciliary import of G protein coupled receptors, including Gpr161 but *not* including Smo. Gpr161 was then shown to be a negative regulator of Shh signalling by findings of increased expression of Shh transcriptional targets *Ptc* and *Gli1* as well as a ventralised neural tube in a *Gpr161* mutant.(Mukhopadhyay et al., 2010, Mukhopadhyay et al., 2013) Further study of the this model identified (i) that Shh over-activation was Smo independent, (ii) that treatment with Shh ligands lead to ciliary exportation of Gpr161 and most importantly (iii) that basal activity of Gpr161 leads to increased cyclic AMP levels (Mukhopadhyay et al., 2013) which is one of the closest molecular links between IFT-A dysfunction and polycystic kidney disease reported in the literature.(Pazour et al., 2000)

Collectively, this research suggests a role beyond retrograde IFT for IFT-A proteins, namely ciliary importation of proteins. Furthermore, a *C. elegans* model in which hypomorphic mutations in *IFT144* or *BBS1* that disrupted their interaction, led to decreased ciliary import of multiple BBSome proteins and the absence of any anterograde movement of the BBSome.(Wei et al., 2012) IFT assembly at the ciliary base was normal, however accumulation of IFT machinery at the ciliary tip was hypothesised to be due to the absence of the BBSome to moderate this transition.(Wei et al., 2012) This not only suggests that IFT proteins are assembled outside the cilia but also that defective retrograde IFT might occur indirectly due to reduced importation of accessory components to IFT,

rather than the more simplistic failure of cargo proteins to associate with the IFT-A complex.

The precise details of interactions between IFT-A proteins and the mechanisms by which mutations in these proteins might disturb Shh signalling are uncharacterised.

Pathogenic variants in IFT140 are associated with NPHP related ciliopathies.

Case reports and series of patients with variants in *IFT140* have established a phenotypic association with Mainzer-Saldino Syndrome (MSS), Jeune Asphyxiating Thoracic Dystrophy (JATD) and non-syndromic retinal dystrophy.(Perrault et al., 2012, Schmidts et al., 2013, Xu et al., 2015) Expanding the phenotypic spectrum further, recent case of Opitz Trigonocephaly C Syndrome has been reported with biallelic *IFT140* variants.(Pena-Padilla et al., 2016) In patients with Jeune syndrome, biallelic *IFT140* variant genotype confers a more severe renal and retinal phenotype, and a more favourable skeletal phenotype compared to other genes.(Schmidts et al., 2013) This is consistent with the finding that IFT140 is most heavily expressed in the developing retina and kidney during murine foetal development.(Schmidts et al., 2013)

IFT140 is a 1462 amino acid protein with 31 exons. It possesses five WD40 repeat domains and nine tetratricopeptide repeats typical of IFT proteins and indicative of involvement in IFT protein multimers and extensive protein-protein interactions.(Taschner and Lorentzen, 2016) Within the IFT-A core complex, *Chlamydomonas,* yeast two-hybrid and co-expression/pulldown techniques suggest IFT140 interacts directly with IFT144 and IFT122.(Behal et al., 2012)

The spectrum of *IFT140* variants includes non-truncating missense variants, and rare truncating variants including splice site, frameshift and non-sense variants.(Schmidts et al., 2013) All reported non-consanguineous cases carry compound heterozygous variants.(Perrault et al., 2012, Schmidts et al., 2013) In the Perrault et al (2012) cohort, variants associated with MSS were located at the N-terminus of the protein, whereas variants associated with JATD were move evenly distributed throughout the whole gene. The most severe published *IFT140* phenotype describes an infant with a missense donor splice variant at exon 24 *in trans* with a 17 bp deletion in exon 1, presenting with a

combined MSS and Opitz trigonocephaly C syndrome.(Pena-Padilla et al., 2016) This infant survived 31 days. No patient has been reported with two truncating variants indicating that some protein function is required for survival of the embryo.

An *IFT140* mutant mouse model, the *Cauli* mouse, was identified by comprehensive, phenotype driven ENU mutagenesis screening and carries homozygous missense mutations in exon 19 at position 2564 (T to A) affecting a change from isoleucine to lysine at amino acid position 855.(Miller et al., 2013) Cilia morphology reflected abnormal retrograde IFT (shortened cilia with bulbous tip) without *any* ciliary IFT140 expression.(Miller et al., 2013) Numerous, profound, skeletal developmental defects dominated the phenotype accompanied by spina bifida, exencephaly, digital abnormalities, cardiac anomalies and embryonic lethality.(Miller et al., 2013) No renal phenotype was observed but may have developed if the embryos had survived longer. Why a missense mutation resulted in such a severe phenotype is not known.

To overcome the difficulty posed by early embryonic lethality in studying renal manifestations of *IFT140* mutation, a HoxB7-Cre driven selective knockout was engineered by Jonassen et al (2012), which produced a selective deletion of *IFT140* in the CD and manifest cystic changes in this segment by post-natal day 5. This model demonstrated increased mitotic index in cystic collecting ducts, no IFT140 association with the mitotic spindle during mitosis and preserved mitotic spindle orientation in the CD.(Jonassen et al., 2012)

Immunohistochemical analysis of limb buds in the *Cauli* mouse demonstrated ectopic Sonic hedgehog expression in the anterior limb bud margin.(Miller et al., 2013) The HoxB7-Cre driven null mutant model demonstrated increased expression of non-canonical Wnt and Sonic hedgehog signalling pathways as well as increased Hippo and complement activity following the onset of cystic disease, hypothesising that this pathway activity was a secondary effect attempting to constrain hyperproliferation rather than a primary consequence of ciliary dysfunction.(Jonassen et al., 2012)

In *Drosophila* flies carrying mutations in the orthologue for *IFT140* (called *rempA* or reduced mechanoreceptor A), cilia adopt a defective retrograde IFT morphology

(shortened with bulbous tip) and failure to localise TRPV4 to the cilium, whereas a dynein mutant displayed mislocalisation of TRPV4 within the cilia.(Lee et al., 2008) Once again, this advocates a role for IFT140 in importation of ciliary proteins across the ciliary gate.

Patient-derived, FLAG-tagged *IFT140* variants have also been expressed in transfected RPE cell lines and demonstrated loss of basal body localisation, however wild type IFT140 localisation in fibroblasts from two patients was consistent with control along the ciliary axoneme.(Perrault et al., 2012) Ciliary number was reduced in mutant fibroblasts and mutant cilia demonstrated accumulation of IFT-B components at the bulbous tip characteristic of defective retrograde transport.(Perrault et al., 2012)

In summary, *IFT140* variants have been associated with nephronophthisis related ciliopathies, particularly skeletal ciliopathies. The precise functional genomic characterisation of this protein is in its early stages and has relied primarily on non-human models which have suggested roles in retrograde IFT and import of specific ciliary proteins.

2.4 Steroid Resistant Nephrotic Syndrome

Nephrotic syndrome (NS) describes the clinical sequence of profound proteinuria sufficient to lead to hypoproteinaemia. This is a potentially life-threatening condition as the proteins lost in the urine support immune function and prevent spontaneous thrombosis, leaving patients vulnerable to sepsis and blood clots.(Kerlin et al., 2014, McIntyre and Craig, 1998) The loss of plasma oncotic pressure reduces interstitial fluid reabsorption in the micro-circulation leading to tissue oedema.

In children with NS over 80-90% have a systemic, circulating aetiology with no suspected intrinsic renal component.(Noone et al., 2018, Greenbaum et al., 2012, Sinha et al., 2015, Teeninga et al., 2013, Yoshikawa et al., 2015) These patients experience relapsing and remitting episodes of proteinuria with eventual, spontaneous resolution of the primary disease stimulus. Based on the frequent response to immunosuppression, it is believed that this idiopathic stimulus is produced by the immune system.(Franke et al., 2019, Greenbaum et al., 2012, Noone et al., 2018) The first line immunosuppressive therapy is corticosteroids which gives rise to the diagnostic sub-category of steroid resistant nephrotic syndrome (SRNS) for those who don’t respond within 4-6 weeks.

Steroid resistant nephrotic syndrome (SRNS) is the second most common cause of progressive CKD in children (Fletcher et al., 2013, NAPRTCS, 2014) and invariably leads to the need for dialysis or kidney transplantation.(D'Agati et al., 2011) The most common histological lesion in SRNS is focal segmental glomerulosclerosis (FSGS), although patients presenting in infancy may demonstrate diffuse mesangial sclerosis or collapsing glomerulopathy.(Hildebrandt and Heeringa, 2009, Sadowski et al., 2015) At an electron microscopic level, NS is characterised by morphological effacement of interdigitating podocyte foot processes. In the healthy state, these foot processes are bridged by a network of proteins called the slit diaphragm.(Noone et al., 2018, Fissell and Miner, 2018, Arif and Nihalani, 2013) In active NS this structure is lost along with the size and charge selectivity of the glomerular filtration barrier, allowing negatively charged proteins to be filtered into the urine.

Whilst SRNS patients may still have a non-genetic, systemic circulating aetiology, up to 45% of patients under 25 years of age with SRNS carry a genetic variant associated with their disease.(Sadowski et al., 2015, Warejko et al., 2018) At present there are over 60 genes associated with SRNS in adults and children

The earlier the onset of disease, the more likely a genetic aetiology. In genetic disease, the pathogenesis is intrinsic to the podocytes with most known gene products contributing to essential developmental or homeostatic podocyte pathways.(Löwik et al., 2009, Ashraf et al., 2018, Lovric et al., 2016, Warejko et al., 2018, Machuca et al., 2009) Genetic forms of SRNS are less likely to respond to second and third line immunosuppressive treatments and therefore these patients are usually selected for genetic screening.(Giglio et al., 2015, Ruf et al., 2004, Hinkes et al., 2007) Targeted therapy exists for only a few and progression to end-stage kidney disease is inevitable. Disease recurrence is not seen following kidney transplantation.

2.4.1 Molecular Biology of SRNS

Podocytes wrap themselves around glomerular capillaries using primary and secondary foot processes to form a three-dimensional layer of interdigitating cells.(Figure 2.1) The primary processes are supported by a microtubular cytoskeleton and the secondary interdigitating foot processes are supported by an actin cytoskeleton.(Welsh and Saleem,

2011) This morphology serves to maximise the surface area for cell-cell and cell-matrix adhesion, given the podocytes must withstand the force of glomerular filtration emanating from the capillaries.(Schell and Huber, 2017, Lennon et al., 2014) Like any blood vessel, glomerular capillaries are dynamic structures which can expand and retract in response to intravascular hydrostatic forces. In order to accommodate changes in the glomerular capillary surface area, podocytes must be able to readily remodel their cytoskeleton and adhesion. This is especially prudent in the setting of recovery from glomerular injury where *in vivo* live imaging has demonstrated podocytes increase their motility.(Hackl et al., 2013) The effacement of foot processes seen in NS represents a loss of cytoskeletal organisation. As more and more SRNS associated genes are discovered, a more granular understanding of the heterogeneous molecular basis underlying SRNS is evolving and centring around regulation of the actin cytoskeleton. A list of genes associated with SRNS is provided in Table 2.4.

The slit diaphragm is anchored to and regulates the actin cytoskeleton

Slit diaphragm proteins nephrin and podocin were the first discovered mutated gene products giving rise to SRNS.(Kestila et al., 1998, Boute et al., 2000) Nephrin (encoded by *NPHS1*), is a transmembrane protein with a large extracellular region containing eight IgG-like domains. Nephrin is the backbone of the slit diaphragm, coordinating recruitment of other slit diaphragm associated proteins both extra- and intra-cellularly.(Saleem et al., 2002, Schwarz et al., 2001, Sellin et al., 2003) Podocin (encoded by *NPHS2*) extends from sturdy lipid rafts in the podocyte membrane to bind and stabilise the slit diaphragm via nephrin.(Huber et al., 2003b) Initially slit diaphragm protein complexes were believed to perform a purely structural role as a filtration barrier, however, they have subsequently been characterised as a specialised cell-cell junction which communicates with polarity complexes (Hartleben et al., 2008, Scott et al., 2012, Ebarasi et al., 2015) and regulates the actin cytoskeleton.

A series of proteins that assemble intracellularly around the nephrin-podocin complex are encoded by SRNS-associated genes including *CD2AP*, *TRPC6*, *PLCE1, MAGI2* and *PODXL*.(Huber et al., 2003a, Winn et al., 2005, Hinkes et al., 2006, Barua et al., 2014a, Reiser et al., 2005, Lehtonen et al., 2005) CD2AP binds the nephrin-

Gene	Inh	OMIM	Histology	Phenotype Notes	Reference
Slit Diaphragm and Associated Components					
NPHS1	AR	602716	FSGS	CNS, SRNS (Infancy); Critical slit diaphragm protein.	(Kestila et al., 1998)
NPHS2	AR	604766	FSGS	CNS, SRNS (Adult/Child); Anchors slit diaphragm to cell membrane.	(Boute et al., 2000)
PLCE1	AR	608414	DMS, FSGS	CNS, SRNS (Infancy); Reports of response to immunosuppression.	(Hinkes et al., 2006)
CRB2	AR	609720	FSGS	SRNS; Modulates apico-basal polarity regulation.	(Ebarasi et al., 2015)
CD2AP	AD/AR	609825	FSGS	SRNS; Modulates PI3K to modulate PI3K/AKT signalling. Links nephrin to actin cytoskeleton via anillin.	(Huber et al., 2003a)
TRPC6	AD	603652	FSGS	SRNS (Adult); Calcium channel modulated by podocin and DAG.	(Winn et al., 2005)
Actin Binding Proteins					
ACTN4	AD	604638	FSGS	SRNS (Adult); Mutant protein increased affinity for F-actin.	(Kaplan et al., 2000)
ANLN	AD	616027	FSGS	SRNS (Adult); Links actin and CD2AP.	(Gbadegesin et al., 2014)
MYH9	AD	160775	FSGS	SRNS; Risk gene for FSGS, especially in African-Americans. Cataracts, macrothrombocytopenia, ID, SNHL	(Kopp et al., 2008)
MYO1E	AR	601479	FSGS	SRNS; Prevents calmodulin binding, thickened GBM on biopsy.	(Mele et al., 2011)
TTC21B	AR	612014	FSGS/IFTA	Combined NPHP/FSGS (Adolescent/Adult); Cerebral aneurysm in 2 patients, SNHL, primary biliary cirrhosis all reported in single cases.	(Huynh Cong et al., 2014)
RHO/RAC/CDC42 Actin Regulation					
ARHGAP24	AD	610586	FSGS	SRNS (Adult); RhoA-activated Rac1 GTPase-activating protein.	(Akilesh et al., 2011)
ARHGDIA	AR	601925	FSGS	CNS/SRNS; Seizures, cortical blindness. Reduced interaction with RAC1/CDC42. May respond to eplererone.	(Gee et al., 2013)
CDK20	AR	610076	MPGN	SSNS (one case 2.5 years old)	(Ashraf et al., 2018)
DLC1	AR	604258	FSGS	SSNS/SRNS (Child/Adult); glomerulonephritis, seizures, cerebral atrophy, retinal angiopathy, hypermetropia.	(Ashraf et al., 2018)
FAT1	AR	600976	FSGS	SRNS Neurological phenotype, tubular ectasia, haematuria.	(Gee et al., 2016)
INF2	AD	610982	FSGS	SRNS (Adult); Charcot Marie Tooth Type E: Chronic peripheral and sensory motor neuropathy. Diaphanous inhibitory domain.	(Brown et al., 2010)
ITSN1	AR	602442	FSGS	SSNS/SRNS. Child. Cases described with partial response to immunosuppression. GEF for CDC42 GTPases.	(Ashraf et al., 2018)
ITSN2	AR	604464	MCD/MPGN		(Ashraf et al., 2018)
KANK1	AR	607704	FSGS	SRNS. Interaction with ARHGDIA, which regulates RHO GTPases. Haematuria.	(Gee et al., 2015)
KANK2	AR	614610			
KANK4	AR	614612			
TNS2	AR	607717	DMS, FSGS	SSNS, SDNS (Child).	(Ashraf et al., 2018)
MAGI2	AR	606382	FSGS	CNS, SSNS (Child); Hydrocephalus. Binds nephrin. Some cases steroid, cyclosporine responsive.	(Ashraf et al., 2018)

Gene	Inh	OMIM	Histology	Phenotype Notes	Reference
Nuclear Proteins					
E2F3	AD	600427	FSGS	Proteinuria, ID. Disrupts VEGF levels during renal development.	(Izu et al., 2011)
LMNA	AD	150330	FSGS	SRNS; familial partial lipodystrophy. Mechanism uncharacterised.	(Thong et al., 2013)
LMX1B	AD	602575	FSGS	SRNS; Nail patella syndrome: dysplasia of nails, patella, elbows. Cataracts.	(Boyer et al., 2013)
NUP93	AR	614351	FSGS	SRNS (Child: *NUP107*) Variants disrupt nuclear pore complex assembly.	(Braun et al., 2016)
NUP107	AR	607617	FSGS		(Miyake et al., 2015)
NUP205	AR	614352	FSGS		(Braun et al., 2016)
NXF5	XLR	300318	FSGS	Proteinuria, progressive heart block. Single pedigree.	(Esposito et al., 2013)
PAX2	AD	167409	FSGS	SRNS; Wide phenotypic spectrum: haploinsufficiency, adult onset FSGS.	(Barua et al., 2014b)
SMARCAL1	AR	606622	FSGS	SRNS; Schimke Immuno-osseous Dysplasia. T cell immunodeficiency, short stature, cerebral infarcts, ID, spondyloepiphyseal dysplasia.	(Boerkoel et al., 2002)
WDR73	AR	616144	DMS, FSGS	SRNS (Adult); Galloway-Mowat Syndrome: post-natal microcephaly, severe ID.	(Colin et al., 2014)
WT1	AD	607102	DMS, FSGS	SRNS; Denys-Drash DSD, urogenital abnormalities, nephroblastoma. Frasier Syndrome: gonadoblastoma, male pseudohermaphroditism.	(Mendelsohn et al., 1982)
XPO5	AR	607845	FSGS	SRNS; Variants disrupt nuclear pore complex assembly.	(Braun et al., 2016)
Mitochondrial/CoQ10 Biosynthesis					
ADCK4	AR	615567	FSGS	SRNS; Reduced CoQ10 biosynthesis (interaction with COQ6). Responsive to CoQ10 supplementation.	(Ashraf et al., 2013)
COQ2	AR	609825	CG	SRNS; Encephalopathy: progressive, epilepsy. Present in infancy. Biopsy shows dysmorphic mitochondria. Responsive to CoQ10 therapy.	(Diomedi-Camassei et al., 2007, Starr et al., 2018)
COQ6	AR	614647	DMS, FSGS	SRNS; Enzyme of CoQ10 biosynthetic pathway. SNHL. May be responsive to CoQ10 supplementation.	(Heeringa et al., 2011)
PDSS2	AR	610564	FSGS	SRNS; Leigh syndrome: hypotonia, ataxia, SNHL, poor growth.	(Lopez et al., 2006)
MTTL1	Mit	590050	FSGS	SRNS; mtDNA A3242G $tRNA^{Leu(UUR)}$ gene variant. Broad, variable phenotype: MELAS, GH deficiency, diabetes.	(Yorifuji et al., 1996)
Collagens/Integrins/Laminins/Other GBM associated proteins					
COL4A3	AR/AD	120070	FSGS	SRNS; Alport Syndrome: progressive SNHL, retinal flecks, recurrent macroscopic haematuria.	(Lemmink et al., 1994, Mochizuki et al., 1994, Barker et al., 1990)
COL4A4	AR/AD	120131			
COL4A5	XL*	303630			
ITGA3	AR	605025	FSGS	SRNS; Neurological, interstitial lung disease, mild EB.	(Has et al., 2012)
ITGB4	AR	147557	FSGS	SRNS; EB. Pyloric atresia.(Single case)	(Kambham et al., 2000)
LAMA5	AR/AD	601033	FSGS	SSNS; SRNS; Non-syndromic. Variable response to IS.	(Braun et al., 2019)
LAMB2	AR	150325	DMS, FSGS	SRNS: Pierson Syndrome: neurological abnormalities, microcoria	(Zenker et al., 2004)

Gene	Inh	OMIM	Histology	Phenotype Notes	Reference
Lysosomal Proteins					
OCRL	XL	300535	FSGS	Lowe Syndrome; Dent's Disease; SRNS	(Attree et al., 1992)
SCARB2	AR	602257	FSGS	Action myoclonus renal failure syndrome, ataxia, tremor.	(Berkovic et al., 2008)
Cytosolic/Membrane Proteins					
APOL1	Biallelic	603743	FSGS	Risk gene for FSGS, especially in African Americans.	(Genovese et al., 2010)
ALG1	AR	605907	FSGS	Congenital disorder of glycosylation type IK	(Kranz et al., 2004)
PMM2	AR	601785	CG,DMS	CNS; Congenital disorder of glycosylation type I (one case)	(van der Knaap et al., 1996)
CFH	AR	134370	FSGS	SRNS; aHUS. Rarely isolated proteinuria. Drusen. Susceptibility to meningococcaemia.	(Dragon-Durey et al., 2004)
DGKE	AR	601440	FSGS	Proteinuria, aHUS doesn't respond to eculizumab	(Sadowski et al., 2015)
EMP2	AR	602334	FSGS	SSNS/SRNS (Child). Mutants increased CAVEOLIN-1 and reduce cell proliferation.	(Gee et al., 2014a)
PODXL	AD	602632	FSGS	SRNS (Adult); Mechanism unclear.	(Barua et al., 2014a)
PTPRO	AR	600579	FSGS	SRNS (Child); Mechanism unknown.	(Ozaltin et al., 2011)
SGPL1	AR	603729	FSGS	SRNS; ER enzyme involved in sphingolipid metabolism. Icthyosis, adrenal insufficiency.	(Lovric et al., 2017)
ZMPSTE24	AR	275210	FSGS	Manibuloacral dysplasia: mandibular and clavicular hypoplasia, cutaneous atrophy, lipodystrophy, acro-oestolysis.	(Agarwal et al., 2006)
Phenocopies					
CLCN5	XLR	300008	-	Dent Disease. Low molecular weight heparin and hypercalciuria.	(Lloyd et al., 1996)
CTNS	AR	606272	-	Cystinosis. Renal Fanconi syndrome. Failure to thrive.	(Town et al., 1998)
CUBN	AR	602997	-	Reduced proximal tubular protein reuptake. B12 deficiency.	(Ovunc et al., 2011)
FN1	AD	135600	-	Fibronectin 1 glomerulopathy.	(Castelletti et al., 2008)
GLA	XL	300644	-	Fabry Disease	(Bernstein et al., 1989)
LRP2	AR	600073	-	Megalin. Reduced proximal tubular protein reuptake.	(Kantarci et al., 2007)

Table 2.4 Genotypes associated with SRNS

Adapted from (Preston et al., 2019) and (Lovric et al., 2016). AD: autosomal dominant, AR: autosomal recessive, XLR: X-linked recessive, XL*: X linked with affected carriers observed, Mit: mitochondrial inheritance, FSGS: focal segmental glomerulosclerosis, CG: collapsing glomerulopathy, DMS: diffuse mesangial sclerosis, ER: endoplasmic reticulum, IFTA: interstitial fibrosis and tubular atrophy, MCD: minimal change disease, SSNS: steroid sensitive nephrotic syndrome, SDNS: steroid dependent nephrotic syndrome, SRNS: steroid resistant nephrotic syndrome, CNS: congenital nephrotic syndrome, SNHL: sensorineural hearing loss, PI3K: phosphoinositol 3 kinase, DAG: diacylglycerol, GH: growth hormone, MELAS: mitochondrial encephalopathy, lactic acidosis, stroke-like episodes, ID: intellectual disability, , DSD: disorder or sexual development, MPGN: membranoproliferative glomerulonephritis, EB: epidermolysis bullosa, IS: immunosuppression. (3 of 3)

podocin complex to the actin cytoskeleton via ANLN. (Schwarz et al., 2001, Gbadegesin et al., 2014) CD2AP recruits actin capping protein and cortactin which are involved in the formation of new actin structures at the cell periphery, enabling cell migration.(Zhao et al., 2013) Phosphorylated tyrosine residues in the cytoplasmic tail of nephrin recruit NCK1/2 proteins(Verma et al., 2006) and in combination CD2AP, activate the PI3K/AKT pathway. In addition to promotion of cell survival, the PI3K/AKT pathway activates CFL1, which also plays a role in actin remodelling during podocyte recovery from injury.(Garg et al., 2010, Huber et al., 2003a, Cooper et al., 2018) The FYN kinase responsible for phosphorylating cytoplasmic nephrin also phosphorylates tyrosine residues on TRPC6, opening the ion channel to calcium influx.(Hisatsune et al., 2004, Reiser et al., 2005) Furthermore, wild type podocin can attenuate TRPC6 calcium influx in the setting of membrane stretch (Anderson et al., 2013), suggesting the ability of the slit diaphragm to respond to the mechanosensory cues in the intercellular junction and respond with calcium influx and actin remodelling.(Greka and Mundel, 2012, Jiang et al., 2011) PLCE1 is also a slit diaphragm associated protein with a demonstrable role in podocyte calcium balance. PLCE1 binds to the nephron-podocin intracellular complex indirectly via IQGAP1. PLCE1 hydrolyses phospholipids from the cell membrane to form inositol-1,4,5-triphosphate (IP3), which triggers calcium release from the endoplasmic reticulum(Berridge, 2016), and diacylglycerol (DAG), which opens TRPC6 to extracellular calcium influx.(Anderson et al., 2013)

Thus the podocyte slit diaphragm represents much more than a mechanical barrier to urinary protein loss, rather a complex symphony of inter-dependant protein interactions balancing multiple cellular processes to dynamically regulate one of the most intricate cellular morphologies seen in nature.

Rho/Rac/Cdc42 GTPase Regulation of Actin Cytoskeleton

Rho/Rac/Cdc42 GTPases are a highly conserved group of proteins within the Ras superfamily which collectively play a major role in the regulation of actin dynamics.(Heasman and Ridley, 2008) Consequently the Rho GTPase pathways are strong candidate pathways for dysregulation in SRNS. For example podocyte specific *Cdc42* knockout mouse models develop foot process effacement and proteinuria consistent with an SRNS phenotype.(Huang et al., 2016, Scott et al., 2012)

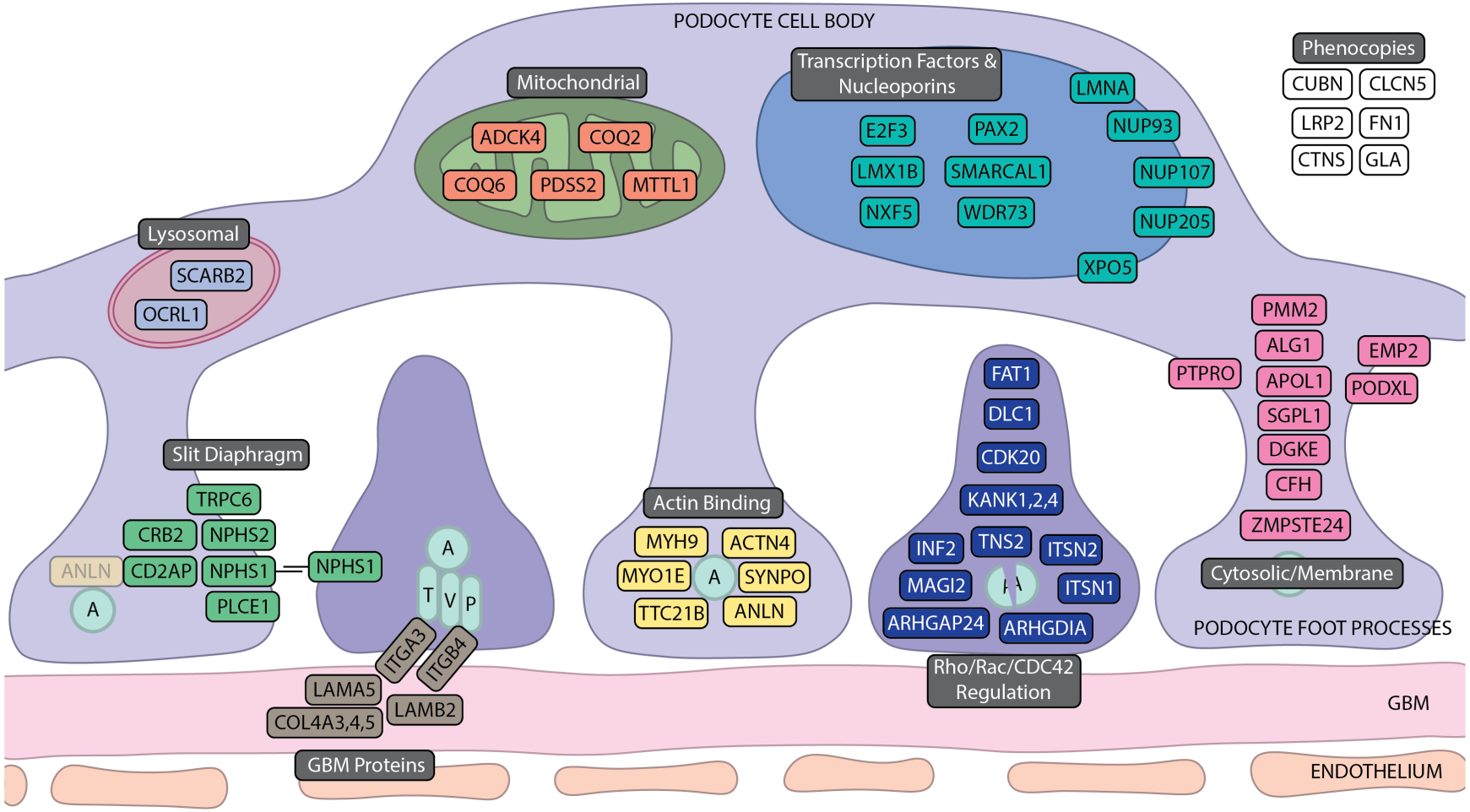

Figure 2.5 Schematic of known SRNS genes illustrated by functional association within the glomerular filtration barrier
Genes are displayed in groups determined by common function of their protein products including: Slit diaphragm proteins (green), glomerular basement membrane (GBM) proteins (brown), actin binding proteins (yellow), Rho/Rac/CDC42 GTPase regulators (navy), lysosomal proteins (pale blue), mitochondrial gene products (orange), transcription factors and nucleoporins (aqua) and other cytosolic/membrane proteins (pink). Phenocopies are pictured top right in white. A: actin, T:talin, V:vinculin, P : paxillin. Adapted and updated from (Lovric et al., 2016, Preston et al., 2019)

These GTPases switch from an inactive GDP-bound state and an active GTP-bound state affected by guanine nucleotide exchange factors (GEFs). Active GTPases can then exert their function until they are either (i) inactivated by GTPase activating proteins (GAPs), (ii) sequestered by guanine nucleotide dissociation inhibitors (RhoGDIs), or (iii) undergo ubiquination induced degradation.(Jaiswal et al., 2013, Murali and Rajalingam, 2014) Variants in a number of genes associated with SRNS have been established to disturb the regulation of these GTPases and thus the regulation of actin dynamics.(Lovric et al., 2016, Preston et al., 2019)(Table 2.4, Figure 2.5)

For example, wild type ARHGDIA forms a complex with RAC1 and CDC42 reducing their activation and GTPase activity.(Gee et al., 2013) Expression of SRNS patient-derived *ARHGDIA* variants in cultured podocytes demonstrated uncontrolled activation of RAC1 and CDC42 activity and increased podocyte migration which improved with RAC1 inhibitor treatment.(Gee et al., 2013) Similar results were found by another group modelling *ARHGAP24* knockdown podocytes after identifying a family with a dominant variant in this gene.(Akilesh et al., 2011) Variants in *KANK1, 2* and *4* have also been identified in patients with SRNS.(Gee et al., 2015) In rat glomeruli and cultured human podocytes, KANK2 interacts with ARHGDIA.(Gee et al., 2015) However, knockdown of KANK2 in cultured podocytes *increased* RhoA GTPase activity and reduced podocyte motility, indicating a mechanism independent of ARHGDIA.(Gee et al., 2015) A series of six rare, novel, SRNS genes (*ITSN1, ITSN2, MAGI2, TSN2, DLC1* and *CDK20*) characterised across 17 unrelated pedigrees affected by steroid sensitive NS (SSNS) and SRNS was recently published by Ashraf and colleagues (2018). In this report, variants in *ITSN1* and *ITSN2* expressed in HEK293 cells or human podocytes demonstrated reduced CDC42 activation compared to wild type vectors. (Ashraf et al., 2018) Podocyte cultures were examined for filopodia extension as an assay of CDC42 associated actin dynamics and were noted to be absent in *ITSN1/2* mutant transfected cultures.(Ashraf et al., 2018, McGavin et al., 2001) The same report demonstrated interaction between MAGI2, TSN2, DLC1 and CDK20 in the GAP regulation of Rho/Rac/CDC42 GTPases.(Ashraf et al., 2018) Using overexpression and knockdown studies for all four genes in various cell cultures, they demonstrated a disturbance in and GTPase activity and podocyte migration rate.(Ashraf et al., 2018)

Dominant variants in *ACTN4* are associated with adult onset FSGS.(Kaplan et al., 2000) *ACTN4* encodes an actin cross linking protein, α-ACTININ 4 which bundles actin fibres and links the actin cytoskeleton to integrins and vinculin.(Akchurin and Reidy, 2015, Weins et al., 2005) Mutant proteins appear to have increased affinity for actin, over-stabilising the cytoskeleton and preventing remodelling and sprouting of actin projections.(Kaplan et al., 2000, Weins et al., 2005, Michaud et al., 2006) Another actin binding protein associated with childhood onset SRNS is MYO1E, a non-muscle myosin.(Mele et al., 2011) These ATPase driven, actin-dependent myosin motors possess actin, calmodulin and cargo binding sites, playing a role in actin reorganisation, intracellular transport and cell signalling.(Krendel et al., 2009, Bi et al., 2013)

Interactions with the Glomerular Basement Membrane

A series of variants in genes encoding laminins and integrins have been linked to SRNS (Kambham et al., 2000, Has et al., 2012, Braun et al., 2019, Zenker et al., 2004), advocating that interaction with the GBM is critical for normal podocyte function. Laminin-521 is the dominant laminin heterotrimer in the mature GBM, composed of α5β2γ1 proteins, and possesses protein interaction domains with many GBM components.(Chew and Lennon, 2018) The LG domain of the LAMA5 (encoding laminin α5) subunit binds to α3β1 integrin and dystroglycan expressed on the apical surface of the podocyte.(Chew and Lennon, 2018) Integrin α3β1 then forms part of adhesion complexes which interact with the actin cytoskeleton, demonstrating that sound adhesion of the podocyte to the GBM also contributes to actin dynamics.(Akchurin and Reidy, 2015) Recessive variants in both *LAMA5* and *LAMB2* (encoding the α5 and β2 subunits) have been described in patient with SRNS.(Braun et al., 2019, Hasselbacher et al., 2006) Studies of *Lamb2-/-* knockout mice have noted proteinuria prior to the development of GBM or podocyte abnormalities, raising the possibility of disease mechanisms extrinsic to the glomerular filtration barrier.(Jarad et al., 2006) No functional modelling of hypomorphic LAMB2 or LAMA5 alleles is published. GBM collagen components COL4A3, COL4A4 and COL4A5 are associated with Alport syndrome and also frequently manifest with proteinuria and FSGS on a histological level.(Zhu et al., 2018, Zhang et al., 2019, Papazachariou et al., 2017, Deltas et al., 2015) The precise molecular mechanism by which collagen deficiencies in the GBM disturb podocyte biology are not well understood but an impairment in podocyte-matrix adhesion seems likely.

Other Genotypes and Proposed Pathways

A series of pathogenic variants in genes encoding proteins involved in coenzyme Q10 (CoQ10) biosynthesis have been described, including *MTTL1*, *PDSS2*, *COQ2*, *COQ6* and *ADCK4*.(Yorifuji et al., 1996, Lopez et al., 2006, Heeringa et al., 2011, Diomedi-Camassei et al., 2007, Starr et al., 2018, Ashraf et al., 2013) CoQ10 is a mitochondrial free-radical scavenger of toxic reactive oxygen species and a cofactor in mitochondrial ATP generation by the respiratory chain enzymes. Knockdown of *COQ6* in human podocytes and zebrafish led to increased apoptosis, rescued by CoQ10 supplementation, supporting a direct toxicity effect.(Heeringa et al., 2011) However *ADCK4* knockdown in podocytes led to impaired migration, an assay well validated in other classes of SRNS genotypes.(Ashraf et al., 2013) Actin polymerisation requires ATP so it is possible mitochondrial SRNS gene variants retard actin remodelling by ATP deficiency.

Other rare variants in genes coding proteins associated with lysosomes, transcription factors, nucleoporins and other cytosolic or membrane pathways have been described which are summarised in Figure 2.5 and Table 2.4. For a number of these genes a genotype-phenotype association has been established on grounds of segregation alone (Ozaltin et al., 2011, Thong et al., 2013, Agarwal et al., 2006, Esposito et al., 2013) without a direct molecular link to regulation of actin dynamics. Others have recapitulated foot process effacement and proteinuria in mutant mouse models.(Braun et al., 2019)

As more genes and their mechanisms are discovered, interactions between the various groups of proteins and pathways are becoming evident. For example ANLN binds CD2AP and may play a role in facilitating signal transduction from the slit diaphragm to the actin cytoskeleton.(Schwarz et al., 2001, Gbadegesin et al., 2014) Another example is IQGAP1 which was found by immunoprecipitation to interact with many slit diaphragm components including nephrin, podocin, MAGI1, CD2AP, NCK1/2, podocalyxin, ACTN4(Rigothier et al., 2012, Lehtonen et al., 2005) and PLCE1. (Hinkes et al., 2006) IQGAP proteins share a number of functions with non-muscle myosins including calcium/calmodulin binding and signalling and regulation of the actin cytoskeleton by interaction with Rac and CDC42 GTPases.(Briggs and Sacks, 2003, Lehtonen et al., 2005, Mateer et al., 2003) Further examples include actin binding protein

MYO1E interaction with cell junction protein ZO1 (Bi et al., 2013) and interaction between ACTN4 and membrane integrins.(Dandapani et al., 2007)

It is important to acknowledge that nephrotic range proteinuria is not solely the manifestation of glomerular disease and a number of genetic causes of proteinuria can act as phenocopies. (Figure 2.5 and Table 2.4)

Genotype Phenotype Correlation

Like many genetic diseases, SRNS is usually phenotypically categorised by the age of onset of proteinuria. Congenital nephrotic syndrome (CNS) has classically described the syndrome of profound neonatal proteinuria and rapid progression to ESRD due to variants in *NPHS1*, one of the first SRNS genes discovered with two specific alleles highly prevalent in Finland (hence the term 'Finnish Type CNS').(Kestila et al., 1998) The definition of CNS now broadly applies to children diagnosed under the age of three months. Up to 85% of patients under 3 months of age are due to variants in *NPHS1*, *NPHS2*, *WT1* and *LAMB2*.(Hinkes et al., 2007) Variants in *PLCE1, ARHGDIA, MAGI2 and COQ2* have also been demonstrated to contribute significantly to disease burden in this age group.(McCarthy et al., 2013, Sadowski et al., 2015, Gee et al., 2013, Ashraf et al., 2018, Starr et al., 2018)

Beyond this age group, genotype-phenotype association becomes more variable. The age of onset of proteinuria is unsurprisingly governed by both the disturbance of the variant on the protein function, and the dispensability of the protein in the normal homeostasis of podocytes. In older infants and young children, variants in *NPHS2* are most common.(Bierzynska et al., 2017, Santin et al., 2011) Hypomorphic variants in *NPHS1* are described in both children and adults.(Philippe et al., 2008, Santin et al., 2009) The same phenomenon is observed in *LAMB2* variants where highly deleterious variants give rise to Pierson syndrome whereas missense variants manifest as isolated nephrotic syndrome.(Hasselbacher et al., 2006)

Dominant genotypes are generally more likely to cause adult onset phenotypes, whereas recessive phenotypes have higher representation in paediatric disease. Dominant and recessive phenotypes have been proposed within the same genotype. *CD2AP* related

disease has been described in both heterozygous carriers (Gigante et al., 2011) and one infant with SRNS.(Lowik et al., 2007) Whilst autosomal dominant variants in *LAMA5* were first associated with SRNS,(Chatterjee et al., 2013, Gast et al., 2016) subsequent identification of multiple autosomal recessive carriers and lack of phenotype in heterozygous mice (Miner and Li, 2000) have suggested a recessive mode of inheritance.(Braun et al., 2019) Despite the classical X-linked inheritance of *COL4A5* variants and recessive inheritance pattern of *COL4A3* and *COL4A4* variants, the persistence of microscopic haematuria in individuals with heterozygous carriage of any of these genes reflected a dominant phenotype.(Savige et al., 2019) Once termed 'benign familial haematuria' a proportion of these patients will develop a more fulminant phenotype.(Fallerini et al., 2014, Fallerini et al., 2017)

Treatments of SNRS are limited

Whilst non-genetic forms of nephrotic syndrome can be effectively treated with immunosuppressive therapy, this is broadly understood to be ineffective for genetic forms of SRNS.(Ruf et al., 2004, Hinkes et al., 2007, Giglio et al., 2015) This is especially true of congenital (<3 months old) and infantile (<12 months old) onset SRNS, which illustrates the important role for genetic testing in establishing those patients where immunosuppressive treatment represents risk without benefit.(Hinkes et al., 2007) In contrast, *PLCE1, EMP2* and *LAMA5* variants have documented cases of steroid sensitivity.(Gee et al., 2014a, Braun et al., 2019, Hinkes et al., 2006) Additionally, select patients with *WT1, PLCE1* and *LAMA5* variants have demonstrated remission with cyclosporine.(Braun et al., 2019, Hinkes et al., 2006, Gellermann et al., 2010) A number of recently discovered variants have demonstrated partial to complete response to various immunosuppressive therapies.(Ashraf et al., 2018, Gee et al., 2014a) Calcineurin inhibitors have been well characterised for their immunosuppressive effect on T cells, but they are also able to effect a stabilisation of the actin cytoskeleton through improved control of Rho GTPase pathway, a feature that may well benefit patients with genetic variants that produce with Rho GTPase disturbances.(Faul et al., 2008) Variants in *CDK20, DLC1, ITSN2, ITSN2, EMP2, TNS2 and MAGI2* are reported to display corticosteroid sensitivity.(Gee et al., 2014a, Braun et al., 2019, Ashraf et al., 2018) This challenges the previously held dogma that steroid sensitive nephrotic syndrome patients are unlikely to benefit from genetic testing, a conundrum that remains unresolved for

many clinical centres, given the higher frequency of SSNS and the expense of genomic sequencing.

For patients with variants in genes involved in the synthesis of CoQ10, supplementation with CoQ10 has been associated with improvement in proteinuria.(Heeringa et al., 2011, Ashraf et al., 2013, Diomedi-Camassei et al., 2007, Starr et al., 2018) Whilst it has not been demonstrated to improve proteinuria, supplementation of vitamin B12 in patients with *CUBN* variants is recommended, as this gene product is involved in the intestinal absorption of this nutrient and deficiency can give rise to serious haematological and neurological sequelae.(Ovunc et al., 2011)

New treatments for nephrotic syndrome are being described in pre-clinical research models. For example, a report by Zhou et al (2017) links increased TRPC5 translocation to the podocyte cell membrane to FSGS disease progression in ATIG transgenic rats. They go on to identify a selective TRPC5 inhibitor AC1903 which improved proteinuria and podocyte loss.(Zhou et al., 2017) Because membrane TRPC5 translocation is upregulated by activated Rac-1, genotypes implicated in dysregulation of the Rho/Rac/Cdc42 GTPase pathway may stand to benefit from this therapy. In another example, 2D podocyte cultures expressing patient-derived podocin variants treated with endoplasmic reticulum (ER) chaperones have improved delivery of ER-retained podocin to the cell membrane.(Ohashi et al., 2003, Roselli et al., 2004) Indeed, allelic variants within a number of genotypes have demonstrated ER retention and activation of the unfolded protein response, with the potential to respond to this brand of chaperone treatment.(Cybulsky et al., 2009, Liu et al., 2001, Chen et al., 2013, He et al., 2011)

Gee et al (2013) treated *Arghria*$^{-/-}$ morpholino knockdown zebrafish with Rac1 inhibitors and a repurposed mineralocorticoid antagonist eplenerone based on the observation of increased Rac1 and mineralocorticoid receptor dependent signalling. They observed a 16-23% reduction in oedema suggesting eplenerone may be a candidate therapy of partial benefit for this genotype.(Gee et al., 2013)

Like many inherited kidney diseases, NPHP and SRNS are both genetic conditions without any targeted therapies in clinical use, but with a number of preliminary therapies

which have been established using animal models. Human kidney organoids represent an opportunity to use a 3D, human, renal, cellular platform for the expedited validation and personalised therapeutic screening of novel therapeutic compounds such as these.

2.5 The directed differentiation of pluripotent stem cells to kidney organoids

2.5.1 Induced pluripotent stem cells (iPSC) can be reprogrammed from somatic cells.

The discovery that skin mature fibroblasts could be reprogrammed to a pluripotent state by the forced, transient expression of key pluripotency genes has revolutionised the field of stem cell research.(Takahashi et al., 2007) Prior to this, stem cell research was performed in murine ESCs or in human ESCs (hESC) obtained from unused human embryos, which became an ethically contentious issue.(McLaren, 2001) iPSC are capable of rapid and extensive self-renewal under appropriate culture conditions. They are also theoretically capable of differentiation to any cell type in the body. Indeed, following injection of stem cells into immunodeficient mice, the formation of a teratoma containing tissues derived from all three germ layers is considered a gold standard assay of pluripotency.(Hentze et al., 2009) The ability to reprogram iPSC from an individual patient's own somatic cells is therefore an approach which overcomes these ethical challenges and opens the door to the field of personalised research and regenerative medicine through directed differentiation of iPSC to various cell types and organoids.

Organoids are small, self-organising, *in vitro* micro-tissues derived from stem cells, which resemble the cell types and structure of the *in vivo* organ.(Lancaster and Knoblich, 2014) The common principle of organoid differentiation protocols is to accurately reproduce the signalling cues that would be experienced by the cell during the development of the *in vivo* organ. Various organoid protocols have established success using this approach, including brain(Lancaster et al., 2013), heart(Giacomelli et al., 2017), liver(Wu et al., 2019a), stomach and intestine(McCracken et al., 2014, Spence et al., 2011)

As outlined above, the kidney contains over 25 different specialised cell types arranged in a complex tissue architecture, performing a variety of highly coordinated functions. Additionally, the nephron is uniquely derived from two different embryologic progenitors. For these reasons the *in vitro* differentiation of kidney from iPSC represents

significant challenges. A number of differentiation protocols have been published for the directed differentiation of kidney organoids,(Morizane et al., 2015, Takasato et al., 2014, Takasato et al., 2015, Taguchi et al., 2014, Freedman et al., 2015) all following the premise of recapitulating in vivo kidney development, much of which has been learned from the study of animals.

During embryogenesis, a continuous sequence of anatomical structures develop under the influence of growth factor signals (also known as morphogens). Each individual cell will experience a varying magnitude and duration of exposure to various morphogens based on their anatomical location as the embryo develops, altering that cell's gene expression and consequently driving its eventual cell fate. Research characterising these developmental pathways has been conducted primarily on non-human animal models and more recently using mouse embryonic and hESC and iPSC models. The following sections detail what is known about mammalian kidney developmental and how this has informed the successful differentiation protocol for kidney organoids.

2.5.2 Development of the Mammalian Kidney

All cells making up the mature organs in mammals derive from the *inner cell mass* (ICM), a collection of pluripotent stem cells capable of infinite self-renewal and differentiation into any mature somatic cell. The path to kidney involves cell progression from ICM through posterior *primitive streak* (PS) and *intermediate mesoderm* (IM). The anterior IM gives rise to the *nephric duct,* from which the *ureteric bud* (UB) develops. The posterior IM gives rise to the *metanephric mesenchyme* (MM), the nephron progenitor cell population. The UB invades the MM and undergoes repetitive bifurcation (called branching morphogenesis) to form the tree-like collecting duct structure of the kidney. The MM condenses to form a *cap mesenchyme* (CM) around each tip of the expanding ureteric tree. Reciprocal signalling interactions between the UB and CM drive and synchronise (i) the dichotomous branching of the ureteric tree, (ii) the expansion and maintenance of the CM and (iii) the differentiation of CM cells into *renal vesicles*, which go on to form elongating nephron structures patterned by morphogen gradients within the kidney.(Lindstrom et al., 2014, Takasato and Little, 2015, Little et al., 2016, Little and McMahon, 2012, Costantini and Kopan, 2010) The ureteric tree expands from the centre

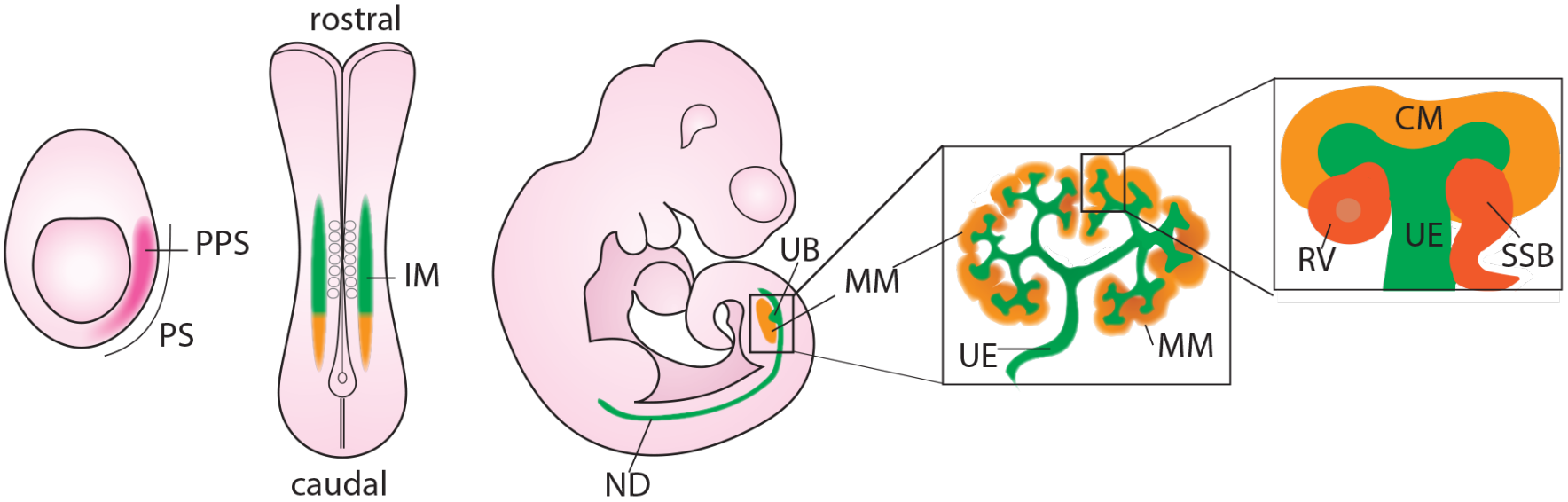

Figure 2.6 Development of the mammalian kidney
Schematic diagram detailing the development of the mammalian kidney starting from the posterior primitive streak (PPS) of the gastrulating embryo, from which the mesoderm arises. The intermediate mesoderm (IM) arises between lateral plate and paraxial mesoderm. The IM patterns into anterior (green) and posterior (orange) intermediate mesoderm. The anterior IM gives rise to the nephric duct (ND) which extends along the embryo. The metanephric mesenchyme (MM) forms near the tail bud and the ureteric bud invaginates the MM from the ND at its distal end. The UB forms a dichotomous branching tree of ureteric epithelium (UE) within the MM. Kidney development is controlled by reciprocal signalling between the UE and cap mesenchyme (CM) and Wnt signals from the tips of the ureteric tree promote differentiation of the CM to renal vesicles (RV) which develop into comma shaped bodies and then S shaped bodies (SSB) on their way to develop into nephrons.
. (Reprinted by permission from Springer Nature: Little MH et al, Recapitulating Development to Generate Kidney Organoids Culture In: Organ Regeneration Based on Developmental Biology, Ed. Takashi Springer,Singapore, Copyright 2017)

of the developing organ, pushing the uncommitted CM to the periphery and giving rise to the *nephrogenic zone*. By 36 weeks of human gestation (and shortly after birth in mouse) all nephron progenitor cells are committed to nephron formation and the nephron progenitor pool is extinguished.(Hinchliffe et al., 1991, Ryan et al., 2018) Therefore, in humans, no further nephron units can be generated to replace those diseased or damaged during post-natal life. Individual nephron endowment varies between 0.2 and 2.7 x 10^6 nephrons per person and is positively correlated with birth weight and gestational age.(Keller et al., 2003, Hughson et al., 2003, Hoy et al., 2003, McNamara et al., 2008)

Posterior primitive streak develops and patterns by the influence of opposing BMP/Nodal morphogen gradients and Wnt signals.

Cells that give rise to the mature kidney arise from the primitive streak (PS), which develops on day 15 of human embryo development as a proliferation and ingression of cells from the epiblast into the dorsal midline of the caudal end of the embryonic disc, undergoing epithelial to mesenchymal transition (EMT). The specification of the PS to form on the posterior aspect of the epiblast occurs via expression of Nodal antagonists *Cer1* and *Lefty1* from the distal visceral endoderm and production of Wnt3 antagonist Dkk1 from the anterior visceral endoderm.(Yamamoto et al., 2004) Both Nodal mutant (Conlon et al., 1994) and Wnt3 mutant mouse embryos (Barrow et al., 2007) fail to develop PS. Formation of the PS both heralds the beginning of gastrulation (the formation of a trilaminar embryonic disc: endoderm, mesoderm and ectoderm) and defines the left-right, dorsal-ventral and cranio-caudal axes of the embryo.

Opposing gradients of BMP and Nodal/Activin signalling pattern the PS such that anterior structures (exposed to dominant Nodal/Activin signalling) give rise to definitive endoderm (alimentary canal, liver, pancreas, lungs, urinary bladder) whereas more posterior structures experience increasingly dominant BMP4 signalling resulting in mesodermal fate (kidneys, lower urinary tract, gonad musculoskeletal system, heart, blood, spleen).(Robb and Tam, 2004, Tam and Loebel, 2007, Sumi et al., 2008, Nostro et al., 2008) BMP4 signalling is strongest in the posterior PS as it is produced by the proximal embryonic ectoderm. It drives Wnt/ß-catenin signalling via *Wnt3* expression which leads to the co-expression of posterior PS markers *Mixl1*, *Brachyury* (*T*) and *Kdr*.(Ben-Haim et al., 2006) *Bmp4*$^{-/-}$ null mice and BMP receptor mutant mice fail to form

posterior PS or its derivatives indicating BMP4 is essential for mesodermal development.(Winnier et al., 1995, Beppu et al., 2000) Additionally, brief treatment of hESC cultures with BMP4 alone is sufficient to derive mesodermal structures. (Zhang et al., 2008)

The anterior primitive streak produces BMP4 antagonist (*Noggin*) allowing dominance of Nodal signalling which, in concert with Wnt/ß-catenin signalling, leads to comparatively higher *Mixl1* expression in the anterior IM, expressing *Sox17*, *Eomes* and *Foxa2*.(Funa et al., 2015, Sumi et al., 2008) Both Nodal/Activin and BMP signalling pathways act on a *Mixl1* promoter by generating different complexes of phosphorylated Smad proteins and FoxH transcription factors.(Hart et al., 2005, Attisano and Wrana, 2002, Massague et al., 2005, Funa et al., 2015) Whilst complete Nodal knockout leads to failure of the PS to form(Conlon et al., 1994), progressive attenuation of nodal signalling leads to a proportional loss of the more anteriorly derived mesodermal structures within the primitive streak (eg. axial and paraxial mesoderm) supporting the phenomenon of graded exposure to Nodal determining anterior mesodermal and definitive endodermal fate.(Vincent et al., 2003)

Patterning of the intermediate mesoderm by intermediate BMP4/Nodal gradients and FGF signalling

Patterning of the mesoderm also occurs along a mediolateral plane according to growth factor gradients. IM is characterised by co-expression of *Osr1*, *Lhx1* and *Pax2/8* in animal and hESC models.(James et al., 2006, Bouchard et al., 2002, Tsang et al., 2000) *BMP4* signalling remains strongest dorsolaterally, and is countered by its antagonist Noggin produced by the axial and paraxial mesoderm and spinal cord.(Wijgerde et al., 2005) The IM arises between the *BMP4* dominant lateral plate mesoderm and the *Noggin* dominant paraxial mesoderm under the added influence of FGF9 expression observed in the paraxial and IM.(Colvin et al., 1999, James and Schultheiss, 2003, Takasato et al., 2014) The paraxial mesoderm also produces Nodal inhibitor *Cer1* which tempers Nodal signalling along this axis, without which, the IM is noted to expand.(Fleming et al., 2013)

The nephric duct arises in the anterior mesoderm due to Pax2/8 and LHX1 Transcription

The nephric duct (also known as the Wolffian, pronephric or mesonephric duct) arises by mesenchymal-to-epithelial transition from the anterior aspect of the IM, and can be identified by co-expression of *Pax2*, *Lhx1*, *Ret*, *Gata3* and *Hoxb7* among others.(Little and McMahon, 2012) *Lhx1* null mice exhibit reduced *Pax2* expression, disrupted IM differentiation and underdeveloped nephric duct structures(Tsang et al., 2000) with another study finding absence of kidney and gonads.(Shawlot and Behringer, 1995) Expression of *Pax2* or *Pax8* transcriptional regulators has been demonstrated in mouse models to be essential for nephric duct development (Bouchard et al., 2002) and a promotor of *Gata3* expression.(Grote et al., 2006) *Gata3* is a transcription factor expressed widely in the developing genitourinary tract (GUDMAP), *Gata3* null mice demonstrate abnormal nephric duct development and caudal extension.(Grote et al., 2006)

Removal of the BMP4 producing surface ectoderm from chick embryos hampered nephric duct development and nephrogenesis which was rescued by preimplanting BMP4 coated beads suggesting BMP4 remains active and important within the anterior IM for nephric duct development.(Obara-Ishihara et al., 1999) The absence of nephric ducts in retinaldehyde dehydrogenase null mice suggests retinoic acid production from medial mesodermal structures is also important in nephric duct development.(Niederreither et al., 1999)

In human kidney development, two pairs of primitive, transient excretory organs arise from interaction between the nephric duct and nephric cord mesenchyme: the pronephos and mesonephros.(Ranghini and Dressler, 2015) Around the 5th week of human gestation, the MM interacts with UB to form the definitive kidney (the metanephros), after which the pronephros and mesonephros degenerate along with the associated regions of the nephric ducts.(Takasato and Little, 2015)

Induction of the metanephros by reciprocal signalling between the ureteric bud and metanephric mesenchyme

Hox11 gene family expression within the posterior IM has been demonstrated to define MM from the more anterior mesonephric structure by transcribing proteins which form

complexes with *Pax2* and *Eya1*, driving expression of glial-derived neurotropic factor (*Gdnf*) and *Six2* within the MM.(Gong et al., 2007, Mugford et al., 2008)

The formation of the metanephros is initiated by the response of the nephric duct to *Gdnf* produced by the MM, which binds to the *Ret/Gfrα1* receptor on nephric duct cells. In response to the Gdnf signal, cells expressing higher levels of *RET/GFRα1* receptor concentrate at the site of the eventual outgrowth of the UB towards the Gdnf signal.(Chi et al., 2009, Costantini and Kopan, 2010) Gdnf/Ret signalling also upregulates *RET/GFRα1* receptor expression creating a positive feedback cascade of *Ret* receptor expression and UB cell proliferation towards the Gdnf source.(Pepicelli et al., 1997) It also increases *Wnt11* expression which serves to upregulate *Gdnf* expression from within the MM and maintain the CM during kidney development.(Majumdar et al., 2003) Other downstream signals and targets of Gdnf/Ret signalling include Erk/Mapk and Pi3k/Akt signalling pathways which influence cell proliferation, migration and ultimately contribute to a bifurcating pattern of branching morphogenesis of the UB within the MM. (reviewed in (Costantini and Kopan, 2010, Little and McMahon, 2012)) Thus, Ret+ ureteric tip cells ultimately give rise to the entire ureteric tree. Indeed, variants in *GDNF/RET/GFRα1* are found in human patients with renal agenesis or CAKUT(Chatterjee et al., 2012, Davis et al., 2014) and complete loss of *Gdnf*, *Ret* or *Gfrα1* expression in mice leads to foetal death from renal agenesis.(Jain, 2009)

Nephrogenesis is initiated within CM by Wnt signals from the UB

The MM condenses around the tips of the branching ureteric tree forming the CM. The CM represents the nephron progenitor cell population of the developing kidney giving rise to all epithelial segments of the nephron from glomerulus to early CD. The tightly regulated reciprocal signalling between the CM and ureteric tree results in expansion of the *nephrogenic zone* outwards from the original nucleus of the metanephros confining nephrogenesis to the surface of the developing organ. As the nephrogenic zone moves radially outwards, it leaves behind nephrons which undergo further patterning and development.

CM cells move dynamically within the cap in response to signals from the ureteric tip which support self-renewal and expansion of the nephron progenitor population.(Lawlor

et al., 2019) The CM population are specified by expression of *Six2* and *Cited1*.(Boyle et al., 2008, Kobayashi et al., 2008) *Six2*+*Cited1*+ cells represent the committed but undifferentiated nephron progenitor population and are maintained and expanded by low levels of canonical Wnt9b, BMP7 and FGF9/20 signalling from the ureteric tip.(Karner et al., 2011, Barak et al., 2012, Muthukrishnan et al., 2015) Whilst Wnt9b is a key signal for cells expressing low levels of *Six2* to initiate nephrogenesis, Wnt9b/ß-catenin signalling in the areas of CM expressing higher levels of *Six2* promotes its maintenance.(Karner et al., 2011) Attenuated FGF9 or FGF20 signalling leads to premature differentiation of the cap mesenchyme and loss of FGF20 altogether leads to renal agenesis in mice and humans.(Barak et al., 2012) Downstream signalling pathways of BMP7 and FGF9 interact to maintain cell cycle progression in nephron progenitor cells.(Muthukrishnan et al., 2015) Increased Wnt9b canonical signalling from the underside of the tip promotes Wnt4 expression which acts to induce subsequent differentiation of renal vesicles by mesenchymal to epithelial transition (MET).(Tanigawa et al., 2011, Burn et al., 2011, Carroll et al., 2005) Of note, and of particular relevance to our kidney organoid protocol, pharmacological treatment of isolated mouse kidney mesenchyme to GSK3β inhibitors have been demonstrated to initiate nephrogenesis.(Kuure et al., 2007) *Foxd1*+ stroma in the nephrogenic zone, through expression of *Fat4*, also plays an active role both in the preventing excessive expansion of the CM and contributing to the signal that induces CM commitment to nephrogenesis.(Das et al., 2013, Bagherie-Lachidan et al., 2015, Mao et al., 2015)

Patterning of the nephron by canonical Wnt signal gradient

The renal vesicle is an epithelial structure which becomes polarised, develops a lumen, invades the distal end of the ureteric tip (forming a connecting segment) and subsequently elongates away from it.(Bard et al., 2001, Georgas et al., 2009) A differential proximal-distal expression pattern becomes evident within the pretubular aggregate, persisting in the renal vesicle and throughout the ongoing development of the 'comma shape' and 'S-shape' body.(Mugford et al., 2009, Brunskill et al., 2008, Georgas et al., 2009, Saxen and Sariola, 1987) This observation implies the continued role of the ureteric tip in patterning the nephron beyond the initiation of nephrogenesis. The glomerulus and distal tubule juxtapose and the tubular loop between them extends almost clonally into the medulla from an *Lgr5*+ cell cluster within the medial S-shaped body.(Barker et al., 2012)

Patterning of the nephron continues via a Wnt signalling gradient, strongest at the ureteric tip and progressively decreasing towards the glomerulus.(Kopan et al., 2007, Georgas et al., 2009, Lindstrom et al., 2015) The effect of canonical Wnt signalling on the developing nephron has been demonstrated by experiments exposing embryonic kidney organ cultures of a mouse expressing GFP-tagged beta-catenin to GSK3ß antagonists and canonical Wnt antagonists.(Lindstrom et al., 2015) These experiments elegantly demonstrate higher Wnt signalling gives rise to increased distal tubular structures and inhibition of Wnt signalling more proximal structures.(Lindstrom et al., 2015)

The other signalling pathway well characterised in patterning the proximal nephron is the Notch pathway, with Notch2$^{-/-}$ null mutants generating no proximal tubules or glomeruli and Notch overexpression blocking glomerular expression.(Cheng et al., 2007, Boyle et al., 2011) Inhibition of Notch in the Lindstrom et al study found increased Wnt/ß-catenin signalling and associated loss of proximal cell types. This phenotype was rescued by inhibition of ß-catenin signalling suggesting that the role of Notch pathways in nephron patterning may be to antagonise ß-catenin signalling.(Lindstrom et al., 2015) This study also found that ß-catenin signalling was downregulated in the medial segments of the nephron (which give rise to the elongating loop of Henle).(Lindstrom et al., 2015)

Uncharacterised aspect of the molecular biology determining nephrogenesis and nephron patterning remains are likely to be illuminated by technological advances such as single cell RNA sequencing. Preliminary reports would suggest regionalised segregation and interactive signalling between stromal, ureteric and developing nephron structures.(Thiagarajan et al., 2011, Magella et al., 2018, Combes et al., 2019a, Combes et al., 2019b, Rutledge et al., 2017, Lee et al., 2015)

Cessation of nephrogenesis potential in humans before birth

In mice nephrogenesis continues for a few days into post-natal life, with a gradual reduction in nephron progenitor numbers occurring with each division of the ureteric tree.(Lindstrom et al., 2018a, Combes et al., 2014) In humans nephrogenesis continues until around 36 weeks of gestation (Hinchliffe et al., 1991) at which point a surge of nephrogenesis extinguishes the CM.(Hartman et al., 2007, Rumballe et al., 2011) As a

result, no nephron progenitor population remains to generate new nephrons in the post-natal human that may be lost to disease, injury or aging.

2.5.3 Directed differentiation of iPSC to kidney organoid.

A number of groups have published approaches for the directed differentiation of embryonic or induced pluripotent stem cells to a renal end point, be that a specific kidney cell type or multicellular kidney organoid.(Mae et al., 2013, Mae et al., 2018, Taguchi et al., 2014, Taguchi and Nishinakamura, 2017, Lam et al., 2014b, Takasato et al., 2014, Takasato et al., 2016, Takasato et al., 2015, Freedman et al., 2015, Morizane et al., 2015, Imberti et al., 2015, Araoka et al., 2014, Przepiorski et al., 2018) All *in vitro* protocols share a common approach of mimicking the *in vivo* pathway of kidney development from ICM through PPS to IM, MM and putative nephron.

Early protocols were performed starting with either monolayers of stem cells cultured in 2D or embryoid bodies (EB). Kidney regeneration approaches using EB as a start point took their cue from published organoid protocols for blood, pancreas, optic cup, brain and intestinal tract differentiation.(Ng et al., 2005, Micallef et al., 2007, Lancaster et al., 2013, McCracken et al., 2014, Eiraku et al., 2011) Comparable kidney specific end points have been achieved with both strategies, indicating neither is superior.(Wu et al., 2018b)

Canonical Wnt signalling is sufficient to differentiate iPSC to posterior primitive streak.

Most protocols have utilised a small molecule GSK3β inhibitor CHIR99021 to induce canonical Wnt signalling and pattern iPSC to PPS, assessed by co-expression *MIXL1* (a PS marker) and *T* (more specific to PPS) and reduced expression of *SOX17* (anterior PS).(Lam et al., 2014a, Takasato et al., 2014, Takasato et al., 2016, Takasato et al., 2015, Freedman et al., 2015, Przepiorski et al., 2018) As already discussed, GSK3β forms part of the β-catenin degradation complex and its inhibition allows for increasing cytosolic β-catenin and subsequent canonical Wnt signalling. Whilst the dose and duration of CHIR99021 varies between protocols, this is most likely a product of the inherent variability of necessary culture conditions between different iPSC lines used by different laboratories. Many groups have incorporated Activin A and BMP4 into their protocols, in an attempt to better specify and pattern PPS.(Taguchi et al., 2014, Araoka et al., 2014, Mae et al., 2013) This is not an unreasonable approach given the role of Nodal signalling

in PPS development and the opposing gradients of BMP4 and Nodal signalling establishing its anteroposterior patterning (described in Section 2.5.2). Indeed using a *MIXL1-GFP* reporter and qPCR for *T* and *SOX17* expression, Takasato et al described that co-treatment with high BMP4 (30ng/mL) and low Activin A (10ng/mL) or 7uM CHIR99021 were equally capable of differentiating PPS.(Takasato et al., 2014) Finally, Morizane added Noggin (a BMP4 antagonist) to CHIR99021 PPS induction to reduce expression of *FOXF1* (lateral plate mesoderm) in their PPS culture.(Morizane et al., 2015)

Induction of the intermediate mesoderm by FGF9 signalling.

Attempting to recapitulate the many multidimensional morphogen gradients in the increasingly complex embryo has yielded variety of published approaches for progressing kidney organoid cultures from PPS to IM. Freedman et al (2015) add no further growth factors and simply cultured a monolayer of cells in Roswell Park Memorial Institute (RPMI1640) basal media with B27 supplement. Areas of the culture that start to develop tubular structures are then dissected from the primary culture and cultured further.(Freedman et al., 2015) Whilst it is likely that this method gives rise to significantly more off-target differentiation in the primary monolayer, it has proven a remarkably straightforward and reproducible approach. At the other end of the spectrum, Taguchi et al (2014) describe an intricate protocol informed by a meticulous *in vivo* lineage tracing approach in mice. This protocol patterns iPSC to a posteriorised nascent mesoderm with CHIR99021 and BMP4 and then IM with by addition of retinoic acid and Activin A.(Taguchi et al., 2014)

Both Morizane et al (2015) and Takasato et al (2015) give consideration to the *in vivo* timing of cellular migration from the PS, and how this temporally determined exposure to its morphogen signalling affects mesodermal patterning along the anteroposterior axis. Cells migrating earlier will encounter greater FGF9 and RA signalling and form the anterior IM and subsequently UB structures. Cells migrating later will not move as far caudally and therefore experience more Wnt signalling that FGF9 or RA signalling, fating posterior IM and subsequent MM progenitors. Having screened a large number of candidate growth factors (including FGF9 up to a concentration of 100ng/mL), Morizane et al (2015) targeted posterior IM by treating with Activin A to arrive at

Author, Year	Culture Method	Derivation of Intermediate Mesoderm (IM) via Posterior Primitive Streak (PPS)	Derivation of Metanephric Mesenchyme (MM) and/or Ureteric Bud (UB)	Endpoints and markers by immunofluorescence						Notes
				Glom	PCT	DT	CD	Endo	Stroma	
Mae et al. 2013	Monolayer	*PPS:* 3 days CHIR99021 + Activin A *IM:* 8 days CHIR99021 + BMP7	*MM*: 7 days CHIR99021, BMP7	+	+					Generated an OSR1-GFP reporter line to enable high throughput growth factors screening for IM induction.
Taguchi et al, 2014	Embryoid Body	*Epiblast:* 2 days Activin A *PPS:* 2 days CHIR99021, BMP4 *Posterior nascent mesoderm:* 4 days CHIR99021, BMP4 *Posterior IM:* 2 days Activin A, BMP4, CHIR99021, RA	*MM:* 3 days CHIR99021, FGF9	+	+	+				MM was derived under fully defined conditions but culture of organoid end points was by culture with dorsal spinal cord.
Lam et al, 2014	Monolayer	*PPS:* 2 days CHIR99021 *IM:* 4 days FGF2 + RA	*MM:* 3 days FGF9 + Activin A		+					IM differentiated into LTL+, N-cadherin+ PCT cells with removal of FGF2 and RA and 1 day CHIR99021.
Takasato et al, 2014	Monolayer	*PS:* 2 days CHIR99021 *IM:* 4 days FGF9 + Heparin	*MM and UB:* 6 days FGF9 + Heparin then 6 days no growth factors.	+	+	+	+			Early podocytes colocalising WT1+ and synaptopodin+ with PCR evidence for upregulation of podocyte genes.
Araoka et al, 2014	Monolayer	*PPS:* 2 days CHIR99021 + Activin A *IM:* 4 days AM580 or TTNPB	*MM and UB:* 8 days Wnt3a + BMP7	+	+		+?			Also found CHIR99021 alone can give rise to PPS. TTNPB protocol was utilised for the differentiation of end point cultures.
Imberti et al, 2015	Monolayer	*PPS/IM:* 6 days RA + PI3K inh + RhoA inh + 2 days activin A	*MM:* FGF2 + BMP7 + GDNF	+	+					Integration of human renal progenitors into cisplatin injured mouse nephrons was observed.
Morizane et al, 2015	Monolayer then 3D	*Late PS:* 4 days CHIR99021 ± noggin *Posterior IM:* 3 days activin A	*MM:* 2 days FGF9 *Self-organising nephrons:* 2 days FGF9 + CHIR99021 then 3 days FGF9 then no growth factors.	+	+	+			*	3D culture performed by replating cells on day 10 to ultra-low-attachment, round bottom 96-well plates and in suspension culture.
Freedman et al, 2015	Spheroid	*Epiblast spheroid:* 2 days sandwiched between Matrigel in mTeSR1 medium *Mesoderm:* 1.5days CHIR99021	*Self-organising nephrons:* 12 days B27 supplement	+	+	+		+		Generated epiblast spheroids in Matrigel sandwich culture, prior to differentiation. CD31+/vWF+ endothelium also present.
Takasato et al, 2015	Monolayer then 3D	*PPS:* 4 days CHIR99021 *Ant and Post IM:* 3d FGF9 + Heparin	*Organoid:* 1 hour CHIR99021, then 5 days FGF9 + Heparin, then 7 days no growth factors.	+	+	+	+	+	+	First report of endothelial progenitors (CD31+, SOX17+) with lumen formation, observed invading glomeruli.

Table 2.5 Fully defined protocols for the *in vitro* directed differentiation of human iPSC to nephron fate
IM – intermediate mesoderm; PPS – posterior primitive streak; RA – retinoic acid; Glom – glomerular structures; PCT – proximal convoluted tubule; DT – distal tubule; CD – collecting duct; Endo – endothelium, *personal communication . (Reprinted by permission from Springer Nature: Little MH et al, Recapitulating Development to Generate Kidney Organoids Culture In: Organ Regeneration Based on Developmental Biology, Ed. Takashi Springer,Singapore, Copyright 2017)

WT1+/*HOXD11*+/*PAX2*-/*LHX1*- cell population. Takasato et al (2014a) titrated FGF9 with and without Noggin or BMP4 with the goal of achieving a balance of anterior and posterior IM, arriving at a treatment of FGF9 alone at 200ng/mL for 3 days for the iPSC line tested. The addition of heparin is required as FGF9 is a heparin dependent ligand for FGF receptors.(Hecht et al., 1995) This gave rise to a *PAX2*+/*LHX1*+/*OSR1*+ culture with lowest expression of *TBX6* (paraxial mesoderm) and *FOXF1*.(Takasato et al., 2014) Importantly from a disease modelling perspective, the Takasato protocol illustrates the potential to engineer the relative exposures to CHIR99021 and FGF9 during the monolayer cultures to pattern the regenerated nephrons to more proximal (eg. glomerular structures) or more distal (eg. distal tubular) structures, based on the disease being studied. (Takasato et al., 2015)

3D culture permits self-organisation of nephrons from differentiated cells.

Whilst the spontaneous development of nephron structures has been demonstrated in 2D cultures the field has unquestionably moved in the direction of 3D cultures. Having initially optimised a protocol in 2D (Takasato et al., 2014), Takasato et al (2015) adapted embryonic kidney reaggregation protocols,(Weiss and Taylor, 1960, Unbekandt and Davies, 2010, Saxen and Lehtonen, 1987) dissociating the monolayer culture and reaggregating cells in centrifuged pellets on a transwell membrane.(Figure 2.7) These cultures were given a 'pulse' of CHIR99021 for 1 hour as a canonical Wnt stimulus to induce nephrogenesis.(Takasato et al., 2015) They were then treated with FGF9 for a further 5 days followed by withdrawal of all growth factors. (Takasato et al., 2015) Cells within these aggregates self-organised into nephrons representing 4 major segments including NPHS1+ glomeruli, LTL+ proximal tubule, ECAD+ distal tubule and ECAD+/GATA3+ late distal tubule/collecting duct structures.(Takasato et al., 2015)(Figure 2.7) A similar principle of providing a nephrogenic Wnt stimulus was employed by Taguchi et al (2014) co-culturing their MM cultures with mouse embryonic spinal cords. However this may be a dispensable step given the number of protocols successfully differentiating kidney organoids without a nephrogenic Wnt source. (Freedman et al., 2015, Morizane et al., 2015, Przepiorski et al., 2018) Morizane et al deferred dissociation until day 9 when cells had reached MM identity and reaggregated cells by moving the culture to low attachment 96 well U bottom plates.

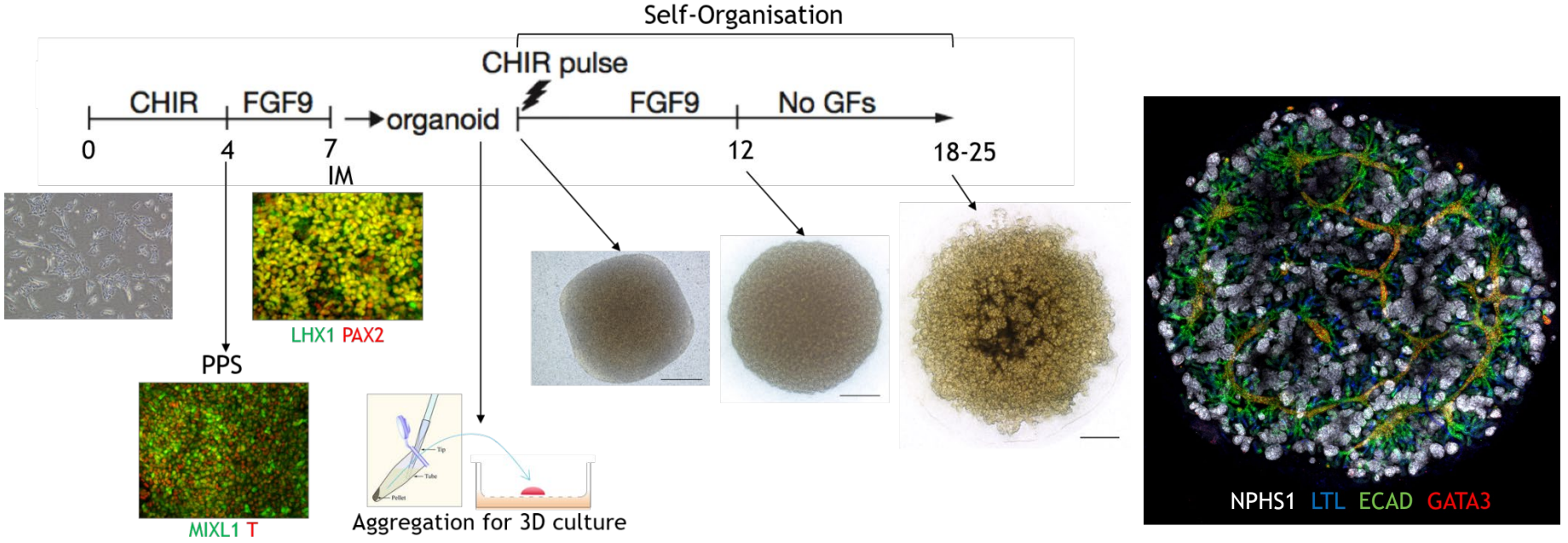

Figure 2.7 Schematic depiction of the Takasato et al (2015) iPSC kidney organoid differentiation protocol used throughout this thesis
iPSC cells are plated on Matrigel one day prior (D-1) to differentiation in Essential 8. On D0 cells commence culture in basal media treated with CHIR99021 for between 3 and 5 days before switching to FGF9 and its required cofactor heparin. Each individual cell line requires optimisation to establish the correct protocol to guide the cells through posterior primitive streak and intermediate mesodermal fates. On D7 the cell monolayer is dissociated and re-aggregated by centrifugation into pellets which are then cultured on a transwell air-liquid interface. Nephrogenic stimulus is provided by a 1 hour treatment (a 'pulse') of CHIR99021 before continuing FGF9 treatment for 5 days and then withdrawing all growth factors. Cells self-organise into nephron structures as validated by immunofluorescence for NPHS1 (glomeruli, white), LTL (proximal tubule, blue), ECAD (distal tubule, green) and ECAD/GATA3 (collecting duct, green and red) Scale bars 500 um.

These organoids demonstrated glomeruli, proximal tubules and ECAD+ distal tubular structures but lacked a GATA3 positive cell population. Single cell RNA sequencing of these protocols has demonstrated a similar spectrum of cell types, including vascular progenitors (CD31+/KDR+/PECAM+), pericytes (PDGFRA+) multiple separable clusters of stroma (MEIS1+), and 10-20% of cells representing off-target cell types.(Wu et al., 2018b, Combes et al., 2019b, Subramanian et al., 2019, Phipson et al., 2019)

An increased yield of kidney organoid tissue has been published by two groups utilising suspended culture approaches.(Kumar et al., 2019, Przepiorski et al., 2018) Kumar et al adapted the Takasato et al protocol (2015) into a swirler culture in a 5cm diameter low attachment culture dish, demonstrating an equivalent end product but with 4x greater cell yield.(Kumar et al., 2019) Przepiorski et al (2018) published a similar protocol starting with EB culture and moving to a larger spinner flask. This report substituted Knockout Serum Replacement (KOSR) for expensive recombinant human FGF representing significant cost savings without appreciably altering the quality of the cells derived, but with a higher frequency of spheroids lacking kidney structures.(Przepiorski et al., 2018) The reason why KOSR acted as a reasonable substitute for recombinant FGF2/9 is not clear.

Culture of ureteric epithelium

One controversy pertaining to the Takasato et al (2015) organoid has been whether the ECAD+/GATA3+ segments genuinely represent a derivative of the UB or, rather an MM derived connecting segment, the region connecting the nephron to the ureteric tree. Contiguous networks of ECAD+/GATA3+ epithelium are noted in these cultures connecting multiple nephrons.(Little and Combes, 2019, Higgins et al., 2018)(Figure 2.7) *SIX2* lineage tracing suggests that GATA3+ cells do not derive from a *SIX2*+ MM precursor.(Howden et al., 2019) Finally transplantation of organoids under the murine renal capsule gives rise to tubular maturation and the EM appearance of principle and intercalated cells of CD.(van den Berg et al., 2018) However, the morphogenesis of these ECAD+/GATA3+ segments is not reminiscent of dichotomous UB branching seen *in vivo*. Additionally, neither bulk RNA nor single cell profiling of kidneys has not identified a cluster of cells expressing ureteric tip markers such as *WNT9B* or *RET*.(Wu et al., 2018b, Combes et al., 2019b, Subramanian et al., 2019, Phipson et al., 2019) It has recently been

established that GATA3 is expressed in the murine connecting segment which is derived from the MM.(Lindstrom et al., 2018c, Georgas et al., 2009, Combes et al., 2019a) This raises the question of which markers are specific for ureteric epithelium (UE) without expression in late distal tubule or the connecting segment. Indeed, a number of traditionally used markers for UE/CD have been demonstrated to be expressed in connecting segment in mice using single cell RNA sequencing.(Combes et al., 2019a) This includes markers such as *Apq2*, *Krt8*, *Krt18* and even *Hoxb7* which has long been utilised as a Cre-driver for flox knockout mouse in mouse collecting duct.

In an attempt to differentiate UB, Xia et al patterned iPSC monolayers to a *T*+ PPS using BMP4 and FGF2 for two days, followed by RA, Activin A and BMP2 for another two days to induce an OSR1+/LHX1+/PAX2+/PAX8+/GATA3+ anterior IM.(Xia et al., 2013) Two days after removal of growth factors cells displayed escalating expression of *HOXB7*, *RET*, *GFRA1* and *GDNF* by qPCR with low expression of CM markers *SIX2*, *CITED1* and *SALL1*.(Xia et al., 2013) These cells integrated into aggregate cultures with dissociated mouse kidney to form chimeric ureteric bud structures positive for CK8 and displaying *in vivo* ureteric tip like morphology complete with non-chimeric SIX2+ CM.(Xia et al., 2013) This protocol was replicated in iPSC from patients with ADPKD without demonstration of any disease specific phenotype.(Xia et al., 2013)

Two further reports have since been published describing precise, stepwise protocols, based on an eloquent understanding of mouse nephric duct and UB development, under the premise that to derive true UE requires a separate protocol to that for MM.(Mae et al., 2018, Taguchi and Nishinakamura, 2017) Both used combinations of Activin A, BMP4, CHIR99021, TGFβ inhibitors, RA analogues and FGF8 to pattern to anterior IM.(Mae et al., 2018, Taguchi and Nishinakamura, 2017) From this point Taguchi et al (2017) purified their culture by flow cytometry for CXCR4+/KIT+ nephric duct progenitors and were able to induce stunning branching morphology using GDNF. Furthermore, aggregate co-culture with mouse ESC derived nephron progenitors and primary mouse fetal kidney stroma established successful culture of a ‘higher order kidney’ complete with *SIX2*+ nephron progenitors and forming nephrons attached to a branching central backbone of ureteric epithelium.(Taguchi and Nishinakamura, 2017) Regrettably, they were unable to recapitulate the protocol using human iPSC. Mae et al (2018) achieved a

greater induction efficiency (~70%) and morphology reminiscent of *in vivo* dichotomous branching GATA3+ ureteric tip with RET+ tips and CK19+ stalks following treatment with GDNF.(Mae et al., 2018)

Thus a number of protocols, all varying in their growth factor treatments and 3D culture strategy broadly appear to arrive at similar end points. This might suggest that self-organisation plays a major role in the final cell fate specifications once guided in the correct direction. An alternative interpretation would be that the high degree of flexibility of these protocols explains the somewhat rudimentary nature of the model in its current form.

Presently, from a disease modelling perspective, a balance needs to be established between precise, highly engineered protocols such as those published by Taguchi et al (2014, 2017) and Mae et al (2018) and the practicality and transferability of the more simplistic Morizane et al (2015) and Takasato et al (2015) protocols. Whilst the latter may derive less mature or precise end products, their simplicity is attractive in the circumstance where multiple iPSC lines will require protocol optimisation. As it was developed within our laboratory and gives rise to more nephron segments than other published protocols, the Takasato et al (2015) protocol will be utilised exclusively throughout this thesis.(Figure 2.7)

Ultimately a protocol will suffice if the model is able to reflect a disease phenotype that is faithful to that seen *in vivo*, is reproducible and can be performed in a timely enough manner to guide a personalised therapeutic management.

2.6 Renal Disease Modelling using Kidney Organoids

2.6.1 Strengths and limitations of iPSC-derived kidney organoids as a disease model.

The opportunity to study complex, multicellular, *in vitro* kidney tissues regenerated from a patient's own cells offers clear advantages to existing disease modelling platforms. However, organoids also have limitations and stand to complement, rather than replace, animal models and 2D cell cultures.

2D vs 3D culture

A clear benefit of organoids as accurate models of *in vivo* kidneys lies in the ability to culture cell types in 3D. This permits physiological cell-cell and cell-ECM interactions more faithful to the *in vivo* circumstance.(Pampaloni et al., 2007) This was acknowledged even prior to the development of organoids. For example, the gene expression profile of melanoma cells in spheroid culture was observed to be closer to primary melanoma tissue than those cultured in 2D.(Ghosh et al., 2005) In another example, human immortalised proximal tubular epithelial cells cultured in a 3D printed tubular lumen exhibit superior cuboidal morphology, brush border density, megalin expression and albumin uptake than in 2D culture even prior to perfusion flow.(Homan et al., 2016) Using an iPSC line expressing a blue fluorescent protein (BFP) inserted at the start codon of the endogenous *MAFB* locus, expression of this key podocyte gene was able to be assayed in real time culture.(Hale et al., 2018) Glomeruli sieved from kidney organoids maintained *MAFB-BFP* expression for up to 4 days in suspension culture, however as soon as they were allowed to settle, *BFP* expression vanished from both the glomeruli and the 2D podocyte monolayer than emanated from them, suggesting rapid dedifferentiation.(Hale et al., 2018) Furthermore, bulk RNA sequencing of isolated organoid glomeruli demonstrated superior expression of numerous key podocyte genes compared to 2D immortalised podocytes.(Hale et al., 2018) This work also demonstrated improved maturation of ECM within 3D glomeruli, with evidence of collagen and laminin switching.(Hale et al., 2018)

The self-organisation of cells into complex tissue structures in kidney organoids provides a perspective on tissue function not seen in 2D cell culture. An example is the podocalyxin knockout organoid published by Freedman et al (2015) where glomeruli formed in the absence of podocalyxin but seemed unable to establish an organised and polarised internal glomerular structure.

Another benefit of 3D organoids is the ability to culture multicellular structures. Whilst not fully characterised, cell-cell crosstalk between different populations is likely to play a role in cell behaviour, disease and development.(Pampaloni et al., 2007) A developmental example is the regulation of the CM expansion by *Foxd1*+ stroma in the nephrogenic zone which is co-dependant on *Fat4* expression from the stroma and *Six2* expression from the CM.(Das et al., 2013, Bagherie-Lachidan et al., 2015, Mao et al.,

2015) In NPHP, most research has focused heavily on epithelial dysfunction, however interstitial fibrosis is a key histological feature of this disease that many consider a primary aspect of disease rather than a secondary consequence of epithelial damage and dysfunction.(Slaats et al., 2016, Wynn and Ramalingam, 2012) Additionally, cell microenvironment has been demonstrated to play a key role in cystogenesis of organoid models of ADPKD, with cysts increasing in size when removed from adherent culture.(Czerniecki et al., 2018) Whilst much of the cell-cell cross talk in kidney development and disease is between stromal and epithelial cells, the characterisation of renal stroma in human fetal kidney is in evolution and the ability for kidney organoids to accurately replicate this is also uncharacterised.(Lindstrom et al., 2018a, Little and Combes, 2019) Furthermore, single cell RNA sequencing analysis of kidney organoids has established that they contain a significant component of off-target cell types.(Wu et al., 2018b, Subramanian et al., 2019, Combes et al., 2019b) Characterisation, optimisation and reproducibility of the stromal component of organoids will be critical before any meaningful research can be performed examining 'fibrosis' of the organoids as a readout of disease.

Multicellular, *in vitro* culture in three dimensions is not without its disadvantages. Cell culture in 2D is less faithful to the *in vivo* cell context, it is straightforward, cheap and represents minimal technical variability. Whilst the simplicity of 2D cell culture may limit its *in vivo* relevance, the generation of pure unicellular RNA or protein lysates takes seconds to minutes permitting the testing of multiple conditions. In contrast, the isolation of a single cell type from a complex, multicellular organoids requires extended dissociation and technical protocols which take hours to complete. This limits the number of conditions that can be executed simultaneously and introduces technical artefact and variation arising during dissociation and purification.

Renal disease is best studied in renal cellular models

Patient-derived cells, usually skin fibroblasts, have been utilised for decades as surrogate functional genomic models for other less obtainable primary tissues. In the ciliopathy field, there has been a long held assumption that primary cilia (an almost ubiquitous cellular organelle) maintained the same structure and function in all cells.(Wheatley, 1995) However, recent studies have demonstrated subtle differences in the physiology of

cilia in different cells. For example, a study examining *Kif17* (encoding homodimeric kinesin II motor) homozygous mutant zebrafish found morphological differences only in olfactory cilia.(Zhao et al., 2012) In contrast, *Kif3b* (encoding heterotrimeric kinesin-II protein) was obligatory for ciliogenesis, except in photoreceptors and some auditory hair cells.(Zhao et al., 2012) In another example, a mouse expressing mutant *Tctn1* (a ciliary transition zone protein) demonstrated abnormal cilia number and appearance at the embryonic node and neural tube but with undisturbed ciliogenesis in the limb bud and perineural mesenchyme.(Garcia-Gonzalo et al., 2011) Most recently in human iPSC modelling patients with *CEP290* variants, tissue specific ciliogenesis defects were identified in iPSC derived optic cups, but not in skin fibroblasts from patients with Leber's congenital amaurosis.(Shimada et al., 2017) In patients with Joubert syndrome, however, both fibroblasts and iPSC derived optic cups were affected.(Shimada et al., 2017) These studies advocate that modelling of renal disease should ideally be performed using renal tissue, and this represents one of the major strengths of kidney organoids as a functional genomic platform.

The advantages of throughput and scale

Another key advantage of iPSC-derived kidney organoids over other models is the capacity to culture infinite quantities of an individual patient's kidney tissue. Combining microwell plates with robotic culture techniques and machine learning, Czerniecki et al (2018) were able to efficiently optimise a culture protocol for three iPSC lines. Whilst the results between replicate wells were somewhat variable, this represents a notable example of the power of automated liquid handling systems and high content analysers in organoid research. As a disease modelling extension of this approach the same group screened cystogenesis in PKD1 knockout kidney organoids treated with eight candidate compounds.(Czerniecki et al., 2018, Cruz et al., 2017) This led to the discovery of increased cystogenesis in response to treatment with a non-muscle myosin II (NMII) inhibitor, and the subsequent testing of a NMII activator as a candidate novel therapy for ADPKD.(Czerniecki et al., 2018, Helms et al., 2019)

In vivo *vs* in vitro *disease modelling*

The murine kidney grows within a physiological, developmental environment with a blood supply and urinary drainage system. Kidney organoids possess vascular progenitors

but *bona fide* blood vessels are not demonstrated to develop within organoids unless they are transplanted into an organism that can vascularise them.(Sharmin et al., 2016, van den Berg et al., 2018, Tanigawa et al., 2018) This has been demonstrated to improve the maturity of the organoids, establish tubular flow and develop the glomerulus for objective assessment of foot process morphology in nephrotic syndrome.(van den Berg et al., 2018, Tanigawa et al., 2018) Theoretically this may also provide the ability to model diseases of the GBM. The act of transplanting an *in vitro* organoid into a mouse, however, regresses a potentially high throughput platform into a more cumbersome, low throughput platform with more limited disease modelling utility, essentially trading higher quality for lower quantity. Accordingly, efforts have been made at *in vitro* vascularisation utilising flow. In a specialised microfluidic culture device, kidney organoids were exposed to fluid flow sheer stress, which increased both the vasculature and the transcriptional maturity of the organoid.(Homan et al., 2019) The addition of VEGF increased the volume of blood vessels but reduced the average proximity of the vessels to the epithelial structures, concluding that relying on the endogenous VEGF production from organoid glomeruli was more ideal.(Homan et al., 2019) Whilst glomerular vasculature was observed by EM, the development of a glomerular filtration barrier remained primitive.(Homan et al., 2019) Additionally, there was no convincing evidence of perfusability of the vessels formed.(Homan et al., 2019) A suite of complex bioengineering vascularisation techniques exist to overcome this challenge, including sacrificial inks and microfluidic chips among others.(Grebenyuk and Ranga, 2019) This will remain a critical hurdle for the field to overcome given the importance of the endothelial-podocyte interaction in the modelling of glomerular disease.

Mouse vs human disease models

Animal disease models offer many benefits that organoids cannot fulfil. Firstly, the mouse kidney belongs to a fully functioning organism, allowing interrogation of non-renal phenotype and the study of systemic diseases that are recognised to extrinsically damage the kidneys. Secondly, organoids exhibit technical variation in differentiation end-point including degree of off-target cell populations and nephron patterning, between individual experiments.(Phipson et al., 2019), whilst a naturally developed animal kidney will broadly arrive at the same end-point for any given time.

For the most part, modelling of human derived genotypes in mice gives rise to a similar phenotypic representation.(Hofmeister et al., 2017) However, significant differences in development, anatomy, physiology, gene-ortholog representation and environment limit the direct translation of findings in animal models to clinical practice. To begin with, mouse kidneys are unipapillate and develop much faster (~1 week) than human kidneys (~30 weeks) which are multipapillate.(Little, 2015) Human nephrons demonstrate a capacity to develop away from the branching ureteric tip and insert into other nephrons, usually in the cortex, a process called arcading not seen in mice.(Zhai et al., 2006) Nephrogenesis ceases in humans prior to term gestation but continues in mice until 1-3 days post-natal age.(Hartman et al., 2007, Hinchliffe et al., 1991) These phenomena suggests fundamental differences between the species in the behaviour and relationship between the CM and the ureteric tree.

Transcriptional and anatomical differences in kidney development highlight examples where translation between the species may be limited.(Lindstrom et al., 2018a, Lindstrom et al., 2018b, Lindstrom et al., 2018c) For example, there appears to be a functional redundancy between *SIX1* and *SIX2* within the maintenance of human CM, whereas *Six1* is downregulated in mouse CM and *Six2* is essential for maintenance of the murine CM.(O'Brien et al., 2016) Autosomal dominant *SIX1* variants have a recognised association with branchio-oto-renal (BOR) syndrome in humans and *SIX2* variants have an association with CAKUT. The differential expression profiles of these genes in CM between mouse and human and the lack of functional redundancy between the two genes in mouse has created some confusion with regards to the clinical pathogenicity of *SIX2* variants in human kidney disease.(Combes et al., 2018, Weber et al., 2008, Faguer et al., 2012, Hwang et al., 2014) Multiple attempts to model ARPKD in mice have failed to emulate an early onset polycystic kidney disease, rather an early onset liver disease and variably penetrant polycystic kidney disease manifesting around 3-6 months.(Bakeberg et al., 2011, Woollard et al., 2007, Moser et al., 2005, Williams et al., 2008) The reason for this is not understood but it is likely to involve differential splicing given the gene is so large and transcribes a large number of isoforms.(Ward et al., 2002, Menezes et al., 2004, Nagasawa et al., 2002, Boddu et al., 2014) Another example is autosomal dominant *HNF1B* variants, a common cause of a spectrum of CAKUT in humans(Decramer et al., 2007, Heidet et al., 2010, Clissold et al., 2015), but which only displays a renal phenotype

in mice when homozygote deletions are introduced.(Desgrange et al., 2017, Massa et al., 2013) These examples where mice seem unable to accurately portray a well established human phenotype make human kidney organoids an attractive model for research.

In *Haao*$^{+/-}$ and *Kynu*$^{+/-}$ mice engineered to model cardiac, vertebral and renal congenital defects thought to be due to antenatal nicotinamide adenine dinucleotide (NAD) deficiency, no phenotype was observed in offspring due to differences in niacin metabolism between mouse and human and a high niacin content of the mouse feed.(Shi et al., 2017) However, offspring of *Haao* and *Kynu* null mice demonstrated universal fetal mortality, which was effectively rescued by progressive niacin supplementation.(Shi et al., 2017) This represents a fascinating example of how differential interspecies gene-environment interactions can confound functional genomic modelling.

Further to representing a human genotype, iPSC derived from patients with inherited kidney disease can model a patient specific genotype, inclusive of the gene of interest and any other previously unrecognised genetic variants which might also be contributing to the phenotype. Where no variant has been identified, an iPSC derived organoid will contain the correct genetic variant responsible for disease and potentially allow its identification, though no such examples of this retrospective approach have been published.

Whole organoid expression profiling most closely correlates to trimester 1-2 human fetal kidney (Takasato et al., 2015) and maturation effectively arrests following the withdrawal of growth factors.(Phipson et al., 2019) As such, organoids are likely best placed to model renal diseases with an onset of phenotype in childhood, or even antenatally. Whilst a number of adult onset diseases have been modelled in organoids(Dvela-Levitt et al., 2019, Cruz et al., 2017), whether this immaturity will affect or confound the findings of these reports remains unknown. Mouse models, by comparison provide the opportunity to study disease phenotype after much longer periods and with continuing physiological development and subsequent aging of the kidneys and disease.

Ethical considerations

Finally, iSPC reprogramming obviates the ethically controversial need to obtain hESC from discarded, IVF-conceived, human embryos.(Zheng, 2016, Zacharias et al., 2011) However, the use of iPSC cells in research brings with it a new set of ethical considerations. It is essential that when a patient is recruited for iPSC based tissue culture research, that consent processes exist to fully inform that patient of the confidentiality and control they retain over their cells and the information generated by iPSC research, which would be analogous to that they maintain over their clinical medical records.(Lowenthal et al., 2012, Aalto-Setälä et al., 2009) All such research must be overseen by relevant regulatory and ethical review committees.(Lowenthal et al., 2012) Researchers are advised to discuss with donors: (i) the types of experiments their cells and differentiated tissues could be used for (eg. xenotransplantation); (ii) any intention to genetically modify their cells or share cells with other researchers; and (iii) large scale genome sequencing of cells which may discover clinically relevant incidental genomic diagnoses.(Aalto-Setälä et al., 2009, Mallett et al., 2015, Lowenthal et al., 2012) Any clinical human transplantation or reproductive research would require a separate and specific regulatory and ethics committee review and donor consent process.(Aalto-Setälä et al., 2009)

Each class of functional genomic model inclusive of animal models, organoid models and 2D cellular models, possess a distinctive set of advantages and limitations. Kidney organoids offer a middle ground between animal and 2D cell models, with unique advantages being their high throughput potential and expression of a human (potentially patient specific) genome in 3D, and the major drawback being their immaturity and variability. In future a well-considered approach to functional genomic disease modelling will exploit the strengths of each in combination.

2.6.2 Existing literature describing iPSC-derived renal genetic disease models.

At the time this PhD commenced, there were no published examples of iPSC derived kidney organoids used for disease modelling. Since this time the field has made considerable progress and a number of examples have been published.

Prior to the publication of the three landmark protocols for iPSC derived kidney regeneration (Morizane et al., 2015, Takasato et al., 2015, Freedman et al., 2015) the first use of iPSC for functional genomic modelling characterised undifferentiated iPSC derived from 3 patients with ADPKD-*PKD1* and 2 patients with ARPKD as well as patient-iPSC-derived embryoid bodies and hepatoblasts.(Freedman et al., 2013) Pursuing the hypothesis that polycystin 1 is necessary for the ciliary localisation of polycystin 2 (PC2, gene product of *PKD2*), this study found a 75% reduction in the immunofluorescent PC2 expression of $PKD1^{+/-}$ heterozygous iPSC cilia (as well as differentiated embryoid bodies and hepatoblasts) when compared to controls.(Freedman et al., 2013) They also demonstrated the capacity to rescue PC2 expression with transfection of wild type *PKD1* vectors in *PKD1* knockout IMCD3 cells.(Freedman et al., 2013) In addition to being one of the first demonstrations of a personalised, patient-specific brand of scientific research, the significance of this study was that reduced ciliary PC2 localisation had only previously been demonstrated in kidney epithelium of established human ADPKD cysts(Nauli et al., 2006, Xu et al., 2007), and thus the same findings described in a range of patient-derived cell types suggested that reduced ciliary PC2 localisation was a product of the constitutional heterozygous *PKD1* variant and not due to an acquired 'second hit' or other secondary factor. Without a morphological readout or molecular link to ADPKD, this study could not extend these findings mechanistically to PKD cystogenesis.

In subsequent publications featuring iPSC-derived regenerated kidney tissue, this group would need to engineer a homozygous $PKD1^{-/-}$ knockout iPSC line using CRISPR/Cas9 to be able to achieve *in vitro* cystogenesis.(Freedman et al., 2015) Large, epithelial, ballooning cystic structures arose from 6% of $PKD1^{-/-}$ organoid tubules, compared to 0% of control cultures.(Freedman et al., 2015) The same authors increased the efficiency of cystogenesis from both $PKD1^{-/-}$ and $PKD2^{-/-}$ knockout kidney organoids in suspension culture.(Cruz et al., 2017) Cysts were noted to be hyperproliferative by immunofluorescence for phosphohistone H3 compared to controls. Cysts were dissected from the tubular remnant and the two were compared transcriptionally by microarray analysis, suggesting increased MYC and mTOR activity in the cyst.(Cruz et al., 2017) Comparison to control organoids would have been more appropriate. Most recently, in an impressive demonstration of the potential for high throughput screening using their $PKD1^{-/-}$ kidney organoid cyst assay, this group screened eight factors thought to modulate

the cell to microenvironment interaction in a 96 well plate.(Czerniecki et al., 2018) The identification of increased cyst swelling during treatment with blebbistatin, a non-muscle myosin II B (NMIIB) inhibitor, has led to the hypothesis of NMIIB activators as potential novel treatment for ADPKD-*PKD1*.(Czerniecki et al., 2018, Helms et al., 2019)

Whilst an impressive body of work, there remain some limitations. For example, the conservation of renal epithelial cell identity in these extended cultures was determined by LTL and ECAD positive immunofluorescence, without any more granular analysis of their transcriptional data or more specific immunofluorescence for markers of renal epithelial identity.(Cruz et al., 2017, Czerniecki et al., 2018) Another limitation is the described inability to translate the protocol to an ARPKD patient-derived iPSC line, as the use of CRISPR engineered *PKD1*$^{-/-}$ and *PKD2*$^{-/-}$ homozygous iPSC do not specifically illustrate the *bona fide* genotype of ADPKD and will not allow for personalised therapeutic screening should this compound eventually reach clinical application.

Whilst not strictly iPSC derived, a comprehensive characterisation of primary kidney and urine derived renal epithelial 'tubuloids' was published from Hans Clevers laboratory this year including a number of disease modelling applications.(Schutgens et al., 2019) They demonstrated the infection of in vitro tubules with BK virus and the subsequent treatment of this infection with cidofivir, establishing a model for post-transplant BK virus nephropathy that may be useful for testing novel therapeutics.(Schutgens et al., 2019) Secondly, they modelled Wilm's tumour by culturing tubuloids established from nephrectomy specimens alongside those established from healthy kidney tissue from the same specimen, demonstrating typical triphasic histology in culture and establishing a tumour-specific, increased expression of *SIX2,* a recognised driver of nephroblastoma. (Schutgens et al., 2019) Finally, they extended their primary intestinal organoid forskolin swelling assay as a model of cystic fibrosis severity to urine derived tubuloids, observing a complex, overfolded morphology of CF patient tubuloids compared to control, and establishing a pathologically diminished swelling response to forskolin treatment (as seen in primary intestinal CF organoids) which improved with pre-treatment of a CFTR potentiator.(Schutgens et al., 2019)

Oculocerebrorenal Syndrome (eponymously known as Lowe Syndrome) is an X-linked monogenic disorder caused by pathogenic variants in *OCRL* which produces inositol-5-phosphatase.(Recker et al., 2015) In one of the first attempts at patient-iPSC-derived renal disease modelling, Hsieh et al (2018) reprogrammed patient fibroblasts to iPSC and differentiated them to 'kidney lineage' cells using 4 days of CHIR99021 followed by 12 days of bFGF and withdrawal of growth factors for a further 9 days. A kidney lineage differentiation end point was characterised by positive immunofluorescence for PAX2, N-cadherin and cadherin-16.(Hsieh et al., 2018) These cells demonstrated reduced rates of ciliogenesis (consistent with previous non-renal cellular modelling in Lowe Syndrome) and retention of SIX2 away from the nucleus in the Golgi apparatus, rescued with lithium treatment.(Hsieh et al., 2018) Additionally, the authors concluded by counting the relative proportions of SIX2+ and CK8+ cells within the monolayer, that OCRL variants patterned mesoderm in favor of ductal structures (CK8+).(Hsieh et al., 2018) This study was limited by the lack of adequate characterisation of the mesodermal cell populations derived, the use of non-isogenic control iPSC lines and use of G-banded karyotyping for quality control of derived iPSC, introducing the possibility that the unexpected phenotypes observed may have been due to unrecognised variants in other genes. The differences in SIX2 and CK8 cellular proportions could well be explained by technical variation in the execution of differentiation or idiosyncratic iPSC line specific factors – a phenomenon now well acknowledged by the field. The conclusions were therefore somewhat speculative without much resolution linking inositol-5-phosphatase to the cellular phenotype identified.

Associate Professor Alan Davidson's laboratory has published two projects examining inherited kidney disease using their laboratory's simplified bioreactor protocol for organoid generation.(Przepiorski et al., 2018, Hollywood et al., 2019) The first used CRISPR engineered *HNF1B*$^{-/-}$ knockout iPSC and compared their differentiation to the parental isogenic control iPSC clone in an attempt to model renal cysts and diabetes syndrome (RCAD). They document downregulation of key *HNF1B* transcriptional target genes as well as the failure of the proximal and distal tubular segments to develop within the organoids, consistent with human phenotype and mouse models of the disease.(Przepiorski et al., 2018) A separate report focuses on the lysosomal storage disease cystinosis, and establishes an additive repurposed role for mTOR inhibitor

everolimus to the existing standard of care in cysteamine.(Przepiorski et al., 2018) Organoids from both CRISPR/Cas9 engineered *CTNS* knockout iPSC and patient-derived iPSC demonstrated recognised pathologies of (i) enlarged lysosomes accumulating cystine and cysteine and (ii) reduced cellular basal macroautophagy.(Hollywood et al., 2019) Whilst cysteamine effectively resolved the former, everolimus was demonstrated to rescue the latter.(Hollywood et al., 2019) In undifferentiated iPSC combination therapy appeared to provide additive effect but in iPSC derived organoids, combination therapy appeared no more effective than either alone.(Hollywood et al., 2019)

A number of reports have examined the role of organoids in modelling inherited diseases of the glomerulus.(Hale et al., 2018, Tanigawa et al., 2018, Freedman et al., 2015) In organoids differentiated from *podocalyxin* knockout iPSC, glomeruli demonstrated reduced polarised, linear expression of SYNPO and ZO-1, rather adopting a more diffuse and punctate expression pattern.(Freedman et al., 2015) This finding was restricted to the glomerular segment, consistent with an evolving understanding of podocalyxin as a rare genotype associated with SRNS.(Kang et al., 2017, Barua et al., 2014a) Two reports have examined glomeruli of organoids differentiated from the iPSC of patients with congenital nephrotic syndrome due to biallelic variants in *NPHS1*.(Hale et al., 2018, Tanigawa et al., 2018) Both demonstrated loss of nephrin expression in patient organoid glomeruli by immunofluorescence.(Hale et al., 2018, Tanigawa et al., 2018) Hale et al (2018) used non-isogenic iPSC as a control and also documented reduced expression of podocin and CD2AP (but not kirrel) by immunofluorescence of isolated glomeruli. In a separate report, comparison to a gene corrected control demonstrated restoration of nephrin expression and the widening of gaps (implying restoration of a slit diaphragm) between foot processes on transmission EM.(Tanigawa et al., 2018) Together, these reports establish precedent for the modelling of glomerular disease in kidney organoids.

One of the more significant recent demonstrations of the potential power of the organoid platform in drug discovery came from Associate Professor Anna Greka's laboratory at the Broad Institute.(Dvela-Levitt et al., 2019) ADTKD-*MUC1* is ubiquitously caused by frameshift variants in a variable number of tandem repeats region of the *mucin 1* (*MUC1*) gene, and the resultant mutant protein accumulates in the endoplasmic reticulum (ER) in the distal convoluted tubules and activates the unfolded protein response.(Kirby et al.,

2013, Dvela-Levitt et al., 2019) By developing an antibody specific for the frameshift variant gene product (MUC1-fs), this group developed a high throughput screen of a repurposed compound library which was able to detect the preferential clearance of MUC1-fs over the wild type MUC-1 gene product.(Dvela-Levitt et al., 2019) Having narrowed down their library to a single compound of interest, BRD4780, they validated their assay on both genetically engineered mice and kidney organoids differentiated from iPSC of 3 patients with ADTKD-*MUC1*, achieving convincing clearance of the MUC1-fs protein in all cases.(Dvela-Levitt et al., 2019) This novel therapeutic discovery was reported with much greater impact as a result of a demonstrated utility in a regenerated patient-derived human kidney tubule.

2.7 Summary

The human kidney is an anatomically and physiologically complex organ, giving rise to a plethora of distinct inherited disease phenotypes. The functional genomic study of inherited kidney disease using animal and 2D cell culture platforms has increased our theoretical understanding of these diseases. However, these models are limited in their ability to easily translate findings back to human- or patient-specific disease in a clinical context.

A sound understanding of mammalian kidney development, derived largely from the study of mouse models has directly informed the development of protocols for the differentiation of human iPSC derived kidney organoids. Whilst only representative of the immature organ, kidney organoids represent a novel functional genomic platform, capable of complementing the limitations of animal and 2D cell culture models. Most excitingly, iPSC reprogramming from patients with inherited kidney disease offers the opportunity for patient-specific modelling and personalised, *in vitro* therapeutic screening.

A number of kidney organoids have now been published and the field is moving rapidly. A number of groups have modelled adult onset kidney disease, most often using engineered knockout iPSC cells. Our approach has been to model early onset genetic renal diseases using patient reprogrammed iPSC and CRISPR gene edited isogenic control clones. The aims of this thesis are to establish a role for patient-iPSC-derived kidney

organoids in the modelling of both glomerular and tubular disease, initially from known genotypes as proof of concept, and then from novel genotypes. Chapters 3-5 describe three separate projects highlighting the strengths and limitations of iPSC derived kidney organoids as models of inherited kidney disease.

Chapter 3 Patient-iPSC-derived kidney organoids show functional validation of a ciliopathic renal phenotype and reveal underlying pathogenetic mechanisms.

3.1 Preface

At the commencement of this PhD project, kidney organoids were a novel discovery and their potential for disease modelling was hypothesised but yet to be demonstrated. A number of factors were considered in choosing a disease and gene from the patient database for a pilot disease modelling project.

i. In the primary publication of the protocol, kidney organoids had been transcriptionally profiled and compared to a range of human fetal tissues. They most closely resembled first trimester human fetal kidney, followed by second trimester human fetal kidney.(Takasato et al., 2015) Consequently, the model was felt likely to be more faithful to an infantile phenotype than an adult phenotype, and these pedigrees were prioritised.

ii. Understanding that kidney organoids lacked urinary drainage, and due to the poorer genetic understanding of CAKUT than more classical monogenic renal diseases, CAKUT was excluded from consideration.

iii. Disorders of the GBM (eg. Alport Syndrome) were excluded based on the lack of glomerular vasculature and ensuing immaturity of the glomerular basement membrane.

iv. With the intention of executing a research pipeline that included transcriptional profiling of a purified cell population from the organoids, the method of purification was considered, and Magnetic Activated Cell Sorting of EPCAM+ epithelial cells was considered a straightforward and validated method for this, prompting the prioritisation of tubular epithelial diseases.

Incorporating all of these considerations, a proband presenting with retinopathy at 1 year of age and abruptly with advanced NPHP at 5 years of age secondary to compound heterozygous variants in *IFT140* was selected.

The author-accepted version of the manuscript published in the American Journal of Human Genetics is included below.(Forbes et al., 2018)[*] Phenotyping of the proband and all clinical information was provided by Peter Trnka, Chirag Patel and Andrew Mallett. Whole exome and genome sequencing and variant curation was performed by Cas Simons and Bruce Bennett. The simultaneous reprogramming and CRISPR gene correction was performed by Sara Howden.

[*] Thomas A. Forbes,Sara E. Howden,Kynan Lawlor,Belinda Phipson,Jovana Maksimovic,Lorna Hale,Sean Wilson,Catherine Quinlan,Gladys Ho,Katherine Holman,Bruce Bennetts,Joanna Crawford,Peter Trnka,Alicia Oshlack,Chirag Patel,Andrew Mallett,Cas Simons, Melissa H Little. 2018. Patient-iPSC-Derived Kidney Organoids Show Functional Validation of a Ciliopathic Renal Phenotype and Reveal Underlying Pathogenetic Mechanisms. *Am J Human Genet*. 102(5):816-831, https://doi.org/10.1016/j.ajhg.2018.03.014

3.2 Authors Details

Thomas A Forbes[1,2,3], Sara E. Howden[1,2], Kynan Lawlor[1], Belinda Phipson[1,4], Jovana Maksimovic[4], Lorna Hale[1,2], Sean Wilson[1], Catherine Quinlan[1,2,3], Gladys Ho[5], Katherine Holman[5], Bruce Bennetts[5,6,7], Joanna Crawford[8], Peter Trnka[9,10], Alicia Oshlack[1,4], Chirag Patel[11], Andrew Mallett[10,12], Cas Simons[8], Melissa H Little[1,2*]

[1]Kidney Development, Disease and Regeneration Group, Murdoch Children's Research Institute, Parkville, Victoria 3052, Australia.

[2]Department of Paediatrics, University of Melbourne, Parkville, Victoria 3052, Australia.

[3]Department of Nephrology, Royal Children's Hospital, Parkville, Victoria 3052, Australia.

[4]Bioinformatics Group, Murdoch Children's Research Institute, Parkville, Victoria 3052, Australia.

[5]Department of Molecular Genetics, The Children's Hospital at Westmead, Sydney, New South Wales 2145, Australia.

[6]Western Sydney Genetics Program, The Children's Hospital at Westmead, Sydney, New South Wales 2145, Australia.

[7]Discipline of Paediatrics and Child Health, and Discipline of Genetic Medicine, Sydney Medical School, University of Sydney, New South Wales 2000, Australia.

[8]Institute for Molecular Bioscience, University of Queensland, St. Lucia 4072, Queensland, Australia.

[9]Child and Adolescent Renal Service, Lady Cilento Children's Hospital, Brisbane, Queensland 4101, Australia.

[10]Faculty of Medicine, University of Queensland, Brisbane, Queensland, Australia.

[11]Genetic Health Queensland, Royal Brisbane and Women's Hospital, Brisbane, Australia.

[12]Department of Renal Medicine, Royal Brisbane and Women's Hospital, Brisbane, Australia.

3.3 Abstract

Despite the increasing diagnostic rate of genomic sequencing, the genetic basis of more than 50% of heritable kidney disease remains unresolved. Kidney organoids differentiated from patient-derived induced pluripotent stem cells (iPSC) represent a potential, but unvalidated, patient-specific platform for the functional validation of novel gene variants and investigation of underlying pathogenetic mechanisms. In this study, trio whole exome sequencing of a prospectively identified nephronophthisis (NPHP) proband and her parents identified compound heterozygous mutations in *IFT140*, a gene previously associated with NPHP-related ciliopathies. *IFT140* plays a key role in retrograde intraflagellar transport but the precise downstream cellular mechanisms responsible for disease presentation remains unknown. A one-step reprogramming/gene-editing protocol was used to derive both uncorrected patient and isogenic gene-corrected iPSC which were differentiated to kidney organoids. Patient organoid tubules demonstrated shortened, club shaped primary cilia whilst gene-correction rescued this phenotype. Differential expression analysis of epithelial cells isolated from organoids suggested downregulation of apicobasal polarity, cell-cell junction and dynein motor assembly genes in patient epithelial cells. Matrigel cyst cultures confirmed a defect in polarisation in patient versus gene-corrected renal epithelium. As such, this study represents a 'proof of concept' for the use of patient-derived iPSC to model renal disease and illustrates dysfunctional cellular pathways beyond the primary cilium in the setting of *IFT140* mutations, which are established for other NPHP genotypes.(Figure 3.1)

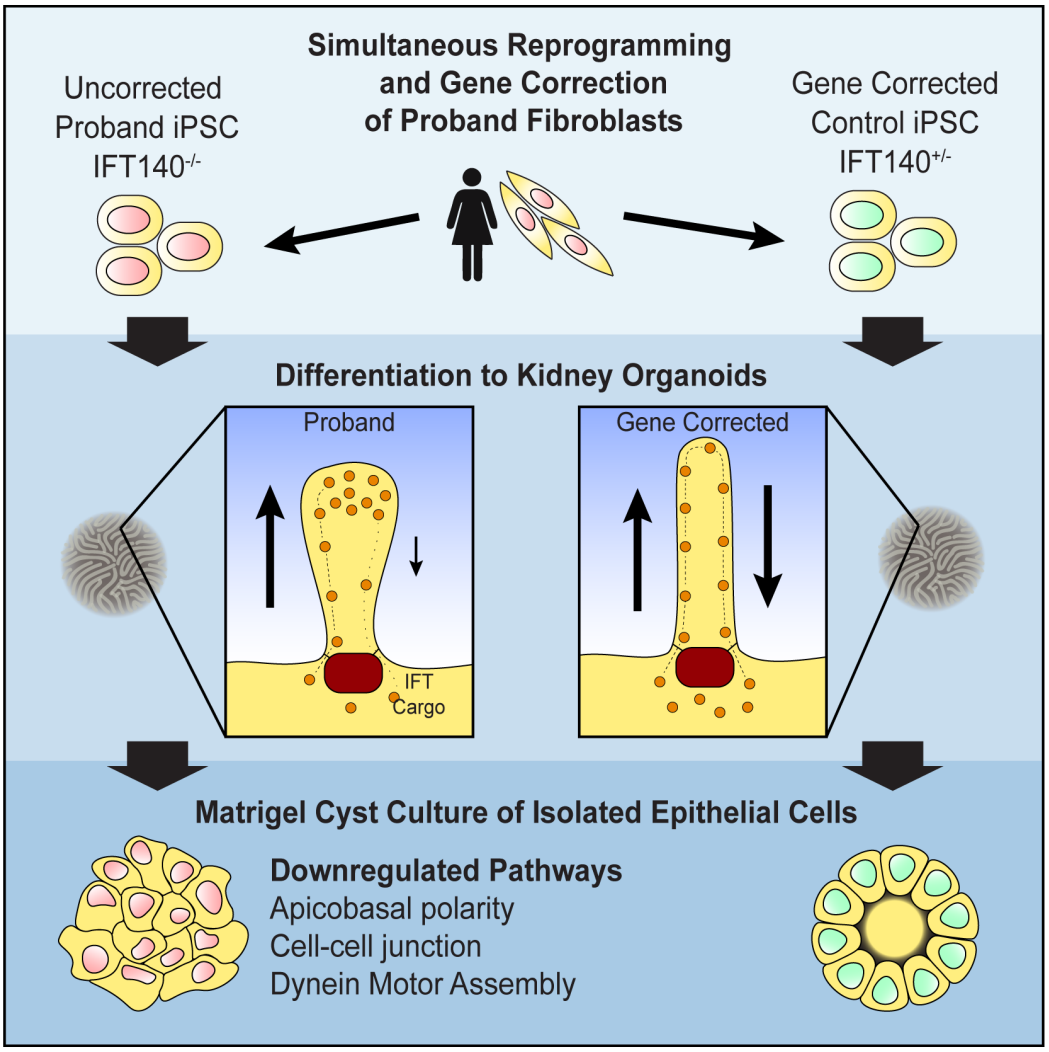

Figure 3.1 Graphical abstract
Summary of experimental approach. First skin fibroblasts obtained from a patient with compound heterozygous variants in *IFT140* were simultaneously reprogrammed to iPSC and gene corrected for one of the pathogenic alleles. Organoids differentiated from these iPSC clones demonstrated clubbed cilia whereas gene corrected cilia demonstrated wild type morphology. Epithelial cyst culture demonstrated impaired lumen formation consistent with RNA profiling from MACS sorted epithelial subfractions.

3.4 Introduction

The kidney is a complex, multicellular organ affected by a wide spectrum of genetic disease, including congenital abnormalities of the kidney and urinary tract, steroid resistant nephrotic syndrome, polycystic kidney disease, tubular electrolyte processing disorders and stone forming nephropathies. Single gene disorders account for up to 10% of adult and 50% of paediatric end-stage kidney disease (ESKD).(Mallett et al., 2014, Fletcher et al., 2013) The ability of next generation sequencing techniques to achieve a genetic diagnosis varies significantly between disease groups.(Otto et al., 2011, Mallett et al., 2017, Halbritter et al., 2013) In addition, the identification of novel gene changes, referred to as variants of unknown significance (VUS) cannot provide a genetic diagnosis without some form of functional evaluation. Modelling of novel VUS has previously been performed in a variety of animal models, including gene knockouts or knockdown in cell lines or model organisms from fly through zebrafish to mouse. However, such animal models are limited by interspecies variation in gene structure and function and an inability to account for the possibility of phenotypic variation arising from patient modifier genes that are not present in the model organism. Patient-derived primary cell lines overcome these limitations, but an *in vitro*, three dimensional, patient-derived renal cellular model is not previously reported.

Recent advances in the directed differentiation of human iPSC towards renal lineages could represent a novel disease modelling platform for functional genomics.(Takasato et al., 2015) The generation of iPSC from patient skin or blood samples is now routine.(Takahashi et al., 2007) Additionally, CRISPR/Cas9-mediated correction of candidate VUS enables the generation of isogenic control iPSC lines, isolating the effect of the VUS within the experimental comparison and removing the confounding influences of genomic variation created by a non-isogenic control. In theory, the comparison of organoids generated from patient and matched gene-corrected iPSC lines should isolate the phenotypic effect of the patient's specific allele. However, kidney organoids currently represent a model of the developing nephron and the demonstration of a disease phenotype within a patient-derived organoid has not previously been demonstrated.

This study explores the utility of kidney organoids as a disease modelling platform in the setting of prospective identification of a paediatric patient with a heritable renal disease. The proband presented with a nephronophthisis related ciliopathy (NPHP-RC) due to compound heterozygous *IFT140* mutations. NPHP is a progressive, fibrocystic renal disease histologically characterised by tubular basement membrane disruption, tubular dilatation and atrophy, interstitial fibrosis and an inevitable decline to ESKD. Whilst rare (estimated prevalence 1 in 50,000-80,000 live births)(Waldherr et al., 1982, Levy and Feingold, 2000), NPHP represents the most common monogenic cause of CKD in the first three decades of life.(Braun and Hildebrandt, 2016) In spite of the discovery of over 40 associated genes, up to 40% of NPHP-RC patients remain undiagnosed following targeted exome sequencing.(Halbritter et al., 2013) Furthermore, the pathogenetic mechanism linking the cilium/centrosome complex to disease phenotype is unresolved. Proposed mechanisms described in the literature vary, including but not limited to disturbances in cell adhesion (Benzing et al., 2001), cell polarity (Donaldson et al., 2002), cytoskeletal function (Bizet et al., 2015, Yasunaga et al., 2015), Wnt signalling (Simons et al., 2005), Hippo signalling (Habbig et al., 2011), centrosomal function (Tammachote et al., 2009) and DNA replication stress (Slaats et al., 2015, Choi et al., 2013a).

A common feature to all genes associated with NPHP-RC is their association with the primary cilium and/or centrosome.(Braun and Hildebrandt, 2016) *IFT140* is a core component of the IFT-A complex which links ciliary maintenance proteins, signalling molecules and transmembrane receptors to the dynein motor complex in order to descend the ciliary axoneme to the basal body, a process known as retrograde intraflagellar transport (IFT).(Stepanek and Pigino, 2016)(Figure 2.4) *IFT140* dysfunction results in a shortened cilium with an accumulation of IFT cargo distending the ciliary tip.(Piperno et al., 1998, Miller et al., 2013)(Figure 3.1) In addition, IFT proteins contribute to the selective importation of targeted proteins into ciliary cytoplasm.(Hirano et al., 2016, Liem et al., 2012, Mukhopadhyay et al., 2010) This includes G-protein coupled receptors important in the negative regulation of hedgehog signalling.(Mukhopadhyay et al., 2013) Beyond these observations, a biological pathway explaining human NPHP disease phenotype is not known.

By demonstrating an established cellular genotype-phenotype correlation within a patient-derived *IFT140* variant kidney organoid, this proof of concept study validates the use of patient-derived kidney organoids for disease modelling and future ratification of novel VUS. Using a simultaneous reprogramming and CRISPR editing protocol (Howden et al., 2015), patient and gene-corrected, isogenic control iPSC were generated from the skin fibroblasts of the patient described above with compound heterozygous *IFT140* mutations. Both iPSC lines were used to generate patient-derived kidney organoids. Within the tubular epithelium of unedited patient organoids, a classical ciliary morphology indicative of retrograde IFT dysfunction was identified. Gene-corrected organoids demonstrated a capacity to resolve this ciliary morphology thereby verifying the genomic variant as disease causing. Additionally, transcriptional profiling and differentiation gene expression analysis using patient-derived and gene-corrected organoids revealed dysfunctional pathogenetic pathways not previously described in *IFT140* mutation but established for other NPHP genes, suggesting this model could clarify the common pathogenetic mechanisms for this heterogenetic rare disease.

3.5 Methods

3.5.1 Genome Sequencing and Analysis

This research was conducted with approval from the human research ethics committees of the Lady Cilento Children's Hospital (HREC/15/QRCH/126), the University of Queensland (MREC Approval 2014000453) and the Royal Brisbane and Women's Hospital (HREC/14/QRBW/34), including research governance approval at all sites. Written informed consent was obtained from the study participant.

Genomic DNA was isolated from peripheral blood using standard techniques. The exome of the proband and each of her parents was captured using the Nextera Rapid Capture Exome kit (Illumina Inc.) then sequenced on an Illumina HiSeq instrument using V4 chemistry (2 × 125nt paired end reads). Read alignment was performed with BWA-mem v0.7.15, variant calling was performed using Real Time Genomics (Hamilton, New Zealand) integrated analysis tool rtgFamily v3.6.2(Cleary et al., 2014) and annotated using SnpEff v4.1k.(Cingolani et al., 2012) In-house custom analysis pipelines were used to filter and prioritize variants for autosomal recessive or de-novo disease-causal variants

based on the clinical pedigree for the family as previously described.(Vanderver et al., 2016) Segregation of the candidate variants was confirmed using Sanger sequencing.

3.5.2 Derivation and correction of patient iPSC

Gene-corrected and uncorrected iPSC lines were generated from patient dermal fibroblasts using a one-step reprogramming/gene-editing protocol as previously described.(Howden et al., 2015, Howden et al., 2016) Fibroblasts were harvested with TrypLE two days after passaging and resuspended in Buffer R at a final concentration of 1 x 10^7 cells/mL. 100 µl of the cell suspension was added to a tube containing reprogramming plasmids (pEP4E02SET2K, pEP4E02SEN2L, pEP4E02SEM2K, pSimple-miR302/367) mRNA encoding SpCas9-Gem, a plasmid encoding a sgRNA that overlaps the patient-specific (c.634G>A) mutation and a repair template plasmid carrying 942 bp (hg38 chr16:1591716-1592658) corresponding to sequence within the *IFT140* gene. The repair template included a 3 bp synonymous change to act as a Cas9-blocking mutation and to facilitate the identification of gene-corrected iPSC clones by allele-specific PCR. Electroporation was performed in a 100 µl tip using the following conditions: 1400 V, 20 ms, 2 pulses. Following electroporation cells were plated on a 6-well Matrigel-coated plate and maintained in fibroblast media until 4 days post-transfection, and then switched to Essential 7 medium (Essential 8 (E8) medium without TGFβ) supplemented with 100 µM sodium butyrate and changed every other day as described previously (Chen et al., 2011). Sodium butyrate was removed from the media after the appearance of the first iPSC colonies at around day 10. Gene-corrected iPSC were identified by allele-specific PCR and confirmed by Sanger sequencing. One gene-corrected clone and one uncorrected iPSC clone were selected and expanded for further analysis. Karyotype was confirmed by Infinium CoreExome-24 DNA microarray (Illumina) and cells tested negative for mycoplasma contamination. Pluripotency of iPSC lines was confirmed by flow cytometry after staining with antibodies to pluripotency markers (EPCAM, CD9, SSEA4).

3.5.3 Cell Culture and Directed Differentiation to Kidney Organoids

Undifferentiated iPSC were maintained in feeder free conditions on hESC qualified Matrigel in E8 media. One day prior to differentiation, iPSC were dissociated from 60-70% confluence with TrypLE (Thermo Fisher) and plated at 3.5 x 10^4 cells per cm^2 in a

6 well plate on hESC qualified Matrigel (BD Biosciences) in 2.5mL E8 media supplemented with Revitacell (Thermo Fisher). The following morning, cells were treated with 8µM CHIR99021 in APEL2 basal media (STEMCELL Technologies) supplemented with 3.5% Protein Free Hybridoma Media 2 (PFHM2) and Antibiotic-Antimycotic (Life Technologies) for 4 days, followed by FGF9 (200ng/mL) and heparin (1µg/mL) for 3 days, changing media every two days. At day 7, cells were dissociated with trypsin 0.05% and 0.25 x 10^6 cells were spun 3 times at 300g in 1.5mL tubes. Using a large bore P200 pipette tip, pellets were transferred to a Transwell 0.4µm pore polyester membrane (CLS3450 Corning). Pellets were cultured over APEL2 + 3.5% PFHM2 + Antibiotic-Antimycotic supplemented with 5µM CHIR 99021 for 1 hour followed by FGF9 (200ng/mL) and heparin (1µg/mL) for 5 days. Transwell culture continued without added growth factors for up to 24 days changing media three times a week.

3.5.4 Immunofluorescence

Organoids were fixed at the desired time-point with 2% paraformaldehyde for 20 mins on ice and washed three times with PBS. Organoids were incubated with 10% donkey serum, 0.3% Triton X/PBS overnight at 4°C. Primary antibodies were incubated for 48 hours in the blocking buffer at 4°C. Following 6 washes with 0.3% Triton X/PBS, secondary antibodies were incubated overnight at 4°C. Where applicable, DAPI staining was applied at 1:1000 for 3 hours. Following 4 washes with PBS, organoids underwent immunofluorescent imaging with a Zeiss LSM 780 confocal microscope. For ciliary length analysis, three images were captured from two separate experiments. 100 cilia per image were measured in ZEN (v2.3, Zeiss) and statistical analyses performed in GraphPad Prism using unpaired t test with Welch's correction for unequal variance.

Spheroid culture assays were fixed and stained according to a previously published protocol.(Giles et al., 2014) Matrigel was dissolved and spheroids fixed with 4% paraformaldehyde at room temperature for 30mins. Spheroids were washed with DPBS with 1mM $CaCl_2$ and 1mM $MgCl_2$ and blocked with a gelatine based permeabilisation buffer (DPBS,1mM $CaCl_2$, 1mM $MgCl_2$, 7mg/mL gelatine and 0.5% Triton X) for 1 hour before overnight incubation with primary antibodies in permeabilization buffer at 4°C. Spheroids were washed four times with permeabilization buffer and incubated with secondary antibodies overnight. Following incubation with FITC-conjugated phalloidin

for 1 hour and DAPI for 10 minutes, spheroids were washed with DPBS with $CaCl_2$ and $MgCl_2$ three times and mounted with Prolong Diamond Antifade Mountant.

Primary antibodies used included: anti-NPHS1 (Bioscientific, AF4263, 1:300), biotinylated Lotus tetragonolobus lectin (LTL) (Vector Laboratories, B-1325, 1:300), anti-CDH1 (BD Biosciences, 610181, 1:300), anti-CDH1 (Cell Signalling Technologies, 3195S, 1:300), anti-GATA3 (R&D Systems, AF2605, 1:300), anti-acetylated tubulin (Sigma Aldrich, T6793, 1:500), anti-IFT140 (Proteintech, 17460-1-AP, 1:100), anti-WDR19 (Proteintech, 13647-1-AP, 1:100), anti-IFT88 (Proteintech, 13967-1-AP, 1:100), anti-EpCAM-AF488 (Biolegend, 324210, 1:300), anti-ZO1 (Life Technologies, 40-2300, 1:200), anti-beta catenin (Sigma Aldrich, C2206, 1:200), Phalloidin-FITC (Sigma-Aldrich, P5282, 1:1000).

Secondary antibodies included: Streptavidin Alexa Fluor 405 conjugate (Life Technologies, S32351, 1:400), Alexa Fluor 488 Donkey anti-mouse IgG (H+L) (Invitrogen, A21202, 1:400), Alexa Fluor 568 Donkey anti-rabbit (H+L) (Invitrogen, A10042, 1:400), Alexa Fluor 647 Donkey anti-sheep (H+L) (Invitrogen, A21448, 1:400), Alexa Fluor 647 Donkey anti-goat IgG (H+L) (Invitrogen, A21447, 1:400), Alexa Fluor 647 Donkey anti-mouse IgG (H+L) (Invitrogen, A31571, 1:400), Alexa Fluor 568 Donkey anti-mouse IgG (H+L) (Invitrogen, A10037, 1:400).

3.5.5 Ciliary Morphology Assessment

Raw confocal images of cilia were median filtered (radius = 2) and segmented using a Fiji script (Schindelin et al., 2012) to implement the watershed, region labelling, and volume filtering (minimum = 200 voxels) functions from the MorpholibJ library.(Legland et al., 2016) Labelled images were processed using a custom Python script to isolate and maximum project labelled regions representing a single cilium and then randomly select a subset of cilia from the combined dataset for scoring. The program generates blinded and unblinded scoring tables referencing a randomised, multi-image tiff file of individual cilia sampled from both genotypes. Image sets were spiked with automatically generated images (solid greyscale circles) to allow the scorer to reference their position within a 1000 image set whilst scoring. Tiff files were manually scored and referenced back to

their genotype using the unblinded table. Proportions were compared using chi-squared contingency tests in GraphPad Prism.

3.5.6 RNA Sequencing

RNA from the epithelial fraction of whole kidney organoids was extracted using Invitrogen PureLink Mini RNA (Invitrogen) extraction kit including treatment with PureLink DNAse Set (Invitrogen), and sequencing libraries prepared using Illumina's TruSeq stranded total RNA protocol with RiboZero rRNA depletion. In total, six samples (three from each iPSC clone) were sequenced using an Illumina NextSeq 500 sequencer at the Translational Genomics Unit, Murdoch Children's Research Institute, Australia. The data was submitted to GEO (GEO accession number: GSE107230). The raw reads were quality and adapter trimmed using trimmomatic v0.35(Bolger et al., 2014) and mapped to the human genome (hg38) using STAR v2.5.2a(Dobin et al., 2013) in the two-pass mapping mode. Reads were summarised over genes using featureCounts(Liao et al., 2014) and GENCODE V20 annotation. Genes that had expression levels of at least one count per million in at least three samples were kept for further analysis. The data was TMM normalised(Robinson and Oshlack, 2010) and voom transformed(Law et al., 2014). Differential gene expression (DGE) was initially identified with robust paired moderated t-tests in the limma R Bioconductor package (Ritchie et al., 2015) applying a false discovery rate cut-off of less than 5%. This identified 1097 down-regulated and 1244 up-regulated genes in the corrected iPSC versus uncorrected iPSC lines. Testing for enrichment of the Broad Institute's Hallmark gene sets (see Web Resources) was performed using CAMERA(Wu and Smyth, 2012). To further refine the list of differentially expressed genes, we removed 570 genes from the DGE analysis that we have previously identified as being highly variable experiment to experiment and are therefore likely to be false positives (Table 3.3), and restricted our focus to significant significantly up- and down-regulated DGE (adjusted $p<0.01$, $n=954$). Gene set enrichment analysis of these 308 genes was performed using the ToppGene Suite(Chen et al., 2009). Downregulated DGE analysis (log fold change <-0.7, $n = 308$) was performed utilising an adjusted p-value cut off of <0.05. Histograms and heatmaps were generated using GraphPad Prism (v7.01). Protein Interactomes were generated using STRING v10.5(Szklarczyk et al., 2015) and nodes were recoloured from GraphPad Prism heatmaps in Adobe Illustrator (Adobe, v2015.2.1).

cDNA was generated from RNA samples using GoScript™ Reverse Transcription Kit (Promega) and qPCR validation of selected differentially expressed genes was performed using SensiFAST SYBR Lo-ROX Kit (BIOLINE) and QuantStudio5 Real-Time PCR System (Thermo-Fisher).

3.5.7 Magnetic Associated Cell Sorting (MACS) and Cyst Culture

Twelve whole organoids were dissociated in 2.0mL TrypLE Select (Thermo Fisher) for 12 minutes and inactivated by dilution with chilled MACS buffer solution (PBS, 2mM EDTA and 0.5% bovine serum albumin). The cell solution was passed sequentially through a 70µm, 40µm and 30µm sieve. Cells were counted, centrifuged at 300g for 5 minutes and resuspended in 300µL of MACS buffer and 100µL of EpCAM+(CD326) Microbeads (Miltenyi Biotech) for 30 minutes. Cells were rinsed with MACS buffer and centrifuged twice before resuspending in 500µL of MACS buffer and passage through an MS MACS column according to the manufacturer's protocol (Miltenyi Biotech). The EpCAM+ fraction was eluted gently from the column in chilled Renal Epithelial Cell Growth Medium 2 (RECGM2, Promocell). 1.0 x 10^6 cells in 100µL of RECGM2 was mixed with 100µL Matrigel GFR (BD Biosciences) and plated immediately into an 8 well chamberslide. Cell/Matrigel suspension was incubated at 37 °C for 30 minutes before the addition of 200 µL RECGM2 supplemented with 1x Revitacell overnight. RECGM2 without Revitacell was refreshed daily until spheroids were visible by bright field microscopy. Following fixation and immunofluorescent staining (as above) spheroids were imaged with a Zeiss LSM 780 confocal microscope. One hundred consecutive spheroids were assessed per condition and proportions were compared statistically in GraphPad Prism (version 7.01) using Fisher's exact test. Cilia per nucleus was manually counted in 10 epithelial cysts imaged at higher resolution in Fiji using Cell Counter plugin. Mean cilia per nucleus expressed as a percentage for each clone were compared with GraphPad Prism (v7.01) using unpaired t test with Welch's correction for unequal variance.

3.5.8 Simple Western Blot

1.0 x 10^6 EPCAM+ cells were centrifuged in cold MACS buffer and then lysed in RIPA buffer with protease inhibitor (1:500) for 15 minutes on ice. Lysates were vortexed for 45 seconds and centrifuged at 13.3g for 10 minutes at 4°C. The supernatant was collected

and diluted 1:5 with 1x Sample Buffer (ProteinSimple). Protein quantification was performed using a 66-440kDa plate in a ProteinSimple Wes Capillary Western Blot analyser according to the manufacturer's instructions.

3.6 Results

3.6.1 Identification of compound heterozygous IFT140 *mutations reclassifies patient phenotype to Mainzer-Saldino Syndrome*

The patient was diagnosed with retinitis pigmentosa (RP) at 1 year of age (Figure 3.2A) and ESKD at 6 years of age, suggesting a phenotype of Senior Løken Syndrome (SLS [OMIM: 266900]). SLS is a NPHP-RC syndrome describing the co-occurrence of retinal and renal ciliopathy. Renal ultrasound identified two kidneys of appropriate size for age displaying increased renal cortical echogenicity and loss of corticomedullary differentiation without any visible cysts. (Figure 3.2B) Renal biopsy was not performed as it was felt unlikely to contribute any diagnostic features beyond those of advanced, end-stage kidney fibrosis. Neither her non-consanguineous parents nor any of her three siblings showed signs of disease and there was no extended family history of renal or other inherited disease (Figure 3.2C).

Trio exome sequencing analysis identified compound heterozygous, single base pair mutations in *IFT140* confirmed by Sanger sequencing to exist *in trans* (NM_014714.3:c.634G>A; p.Gly212Arg; NM_014714.3:c.2176C>G; p.Pro726Ala) (Figure 3.2D). Both sites are highly conserved throughout the vertebrate lineage (Figure 3.2E), and are predicted to be damaging by Polyphen, MutationTaster and CADD. Both mutations have low population allelic frequencies of $4.1x10^{-6}$ and $5.4x10^{-5}$ respectively (Table 3.1). The c.634G>A mutation is located at the -1 position of the splice donor site of exon 6. This mutation has been previously described in patients with Mainzer-Saldino Syndrome (MSS) and Jeune's Asphyxiating Thoracic Dystrophy (JATD) (both SRTD9 [OMIM: 266290]) and validated by expression of FLAG-tagged transcripts in immortalised human retinal pigmented epithelial (RPE) cells, suggesting mislocalisation of the protein away from the primary cilium.(Perrault et al., 2012) The nucleotide c.G634 is totally conserved in all vertebrates and the c.634G>A mutation is predicted to disrupt the activity of the donor splice site.(Desmet et al., 2009) The c.2176C>G mutation has not previously been described.

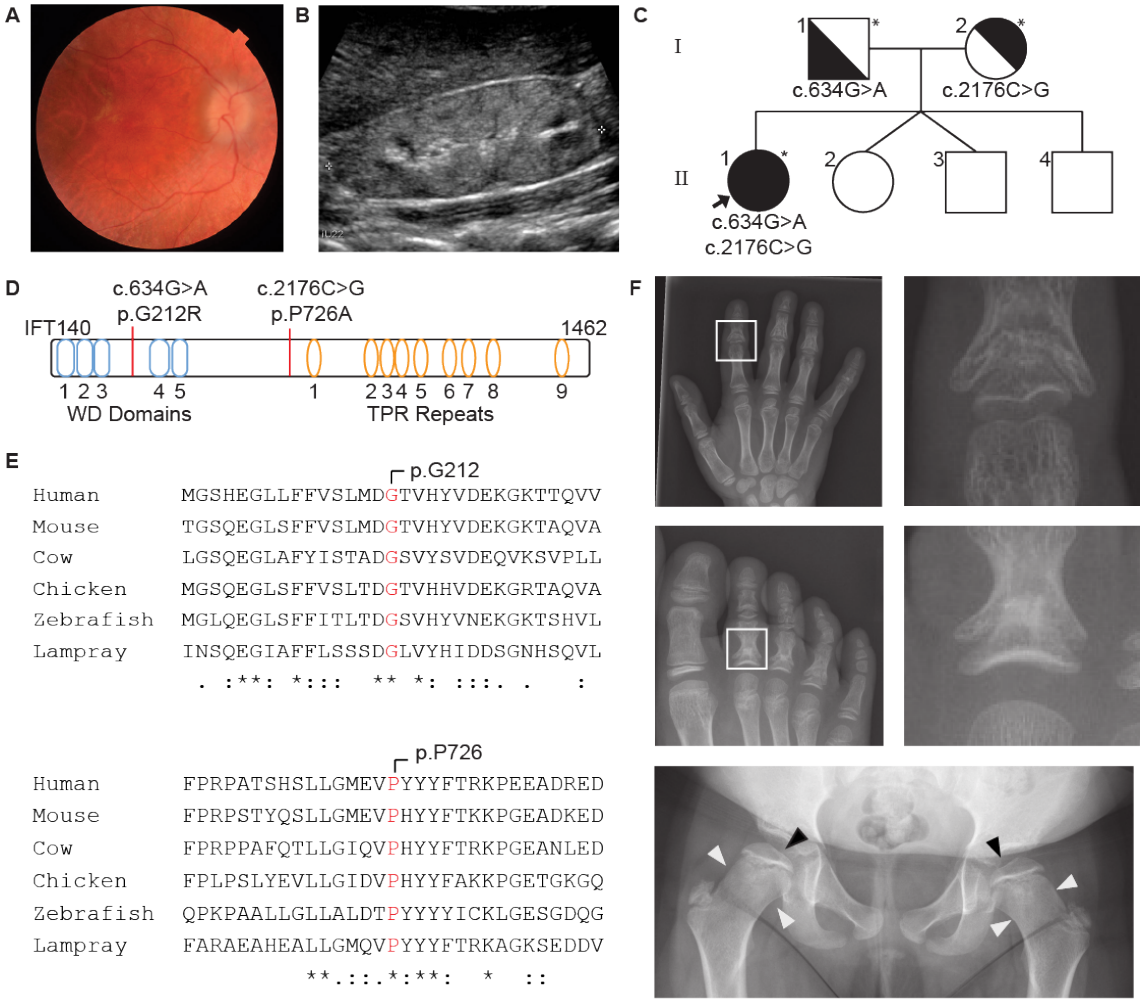

Figure 3.2 Whole exome sequencing (WES) leads to revision of clinical phenotype
(A) Patient retinal photograph demonstrate retinitis pigmentosa and (B) Renal ultrasound demonstrating echogenic kidney with loss of corticomedullary differentiation form the basis of the eponymous diagnosis of Senior Loken Syndrome prior to WES. (C) Trio WES identifies compound heterozygous IFT140 mutations (* indicates sequenced individual.) (D) IFT140 protein structure with mutation loci identified. (E) Conservation of both amino acid loci across vertebrate species. (F) Following identification of *IFT140* mutations skeletal survey found cone-shaped epiphyses in the phalanges of the hand and foot (white boxes), flattened femoral heads (black arrowhead) and widened femoral neck (white arrowheads) consistent with Mainzer-Saldino Syndrome.

	Variant 1	**Variant 2**
Genomic position (hg19)	chr16:1612009 G > C	chr16:1642177 C > T
cDNA	NM_014714.3:c.2176C>G	NM_014714.3:c.634G>A
Predicted effect	p.(Pro726Ala)	p.(Gly212Arg) and/or splicing defect.
dbSNP ID	rs1057518064	rs201188361
Inheritance	Maternal	Paternal
Population frequency[a]	4.1x10-6 (AC=1)	5.4x10-5 (AC=15)
Damage prediction scores: - Polyphen - MutationTaster - CADD	 1.0 1.0 23.9	 0.91 1.0 27.4
Predicted splicing impact[b]	na	Broken WT Donor Site (score: -11.59)
ACMG Classification (evidence codes[c])	Likely Pathogenic (PM2, PM3, PP2, PP3, PP4 and PP5)	Pathogenic (PS1, PS3, PM2, PP2, and PP3)

Table 3.1 Variant curation details for proband

[a] gnomAD database, http://gnomad.broadinstitute.org (Lek et al., 2016)

[b] Human Splicing Finder web service, http://www.umd.be/HSF3/index.html (Desmet et al., 2009)

[c] PS, pathogenic strong; PM, pathogenic moderate; PP, pathogenic supporting (Richards et al., 2015)

Compound heterozygous mutations in *IFT140* have not previously been associated with SLS but are reported as a cause of JATD and MSS which are distinguished by classical skeletal phenotypes.(Perrault et al., 2012, Schmidts et al., 2013, Beals and Weleber, 2007) A subsequent skeletal survey in the patient identified flattened femoral heads with widened necks as well as cone shaped phalangeal epiphyses (Figure 3.2F), revising her phenotype to MSS.

3.6.2 Simultaneous reprogramming and gene-correction of patient fibroblasts

Using a previously described one-step protocol that combines both an episomal-based, reprogramming strategy and CRISPR/Cas9-mediated gene-editing (Howden et al., 2015), clonal uncorrected and gene-corrected iPSC lines were generated within a single experiment (Figure 3.3A). The Cas9 repair template included correction of the c.634G>A mutation as well as an additional synonymous three base pair change to facilitate identification of corrected clones and prevent Cas9-mediated cleavage following successful homology directed repair (Figure 3.3A). Gene-correction was identified in 1 of 44 screened iPSC clones (2.3%). One uncorrected patient (henceforth referred to as 'PT') and the isogenic, gene corrected clone ('GC') were carried forward to further experiments. Pluripotency was confirmed by culture morphology and staining for common pluripotency markers and subsequent flow cytometry. (Figure 3.4A,B)

3.6.3 Gene-correction of iPSC rescues unstable mRNA transcript

The patient-specific mutations were confirmed following Sanger sequencing of PCR amplicons spanning exon 6 or exon 18 of the *IFT140* locus (Figure 3.3C, red arrowhead) whereas loss of the c.634G>A mutation and gain of the synonymous three base pair change was confirmed in gene-corrected iPSCs.

Total RNA was extracted and RT-PCR was performed to amplify *IFT140* transcripts from gene-corrected and uncorrected patient iPSCs, which were then sequenced. This analysis revealed that only the c.2176C>G allele was detectable at the transcriptional level in uncorrected iPSCs (Figure 3.3C). This indicates that the c.634G>A mutation results in defective splicing of exon 6 and the incorrectly spliced transcripts are potentially targeted for degradation. Hence only one allele of the *IFT140* gene is likely to be transcribed and translated. In contrast, transcription from both alleles was detected in gene-corrected

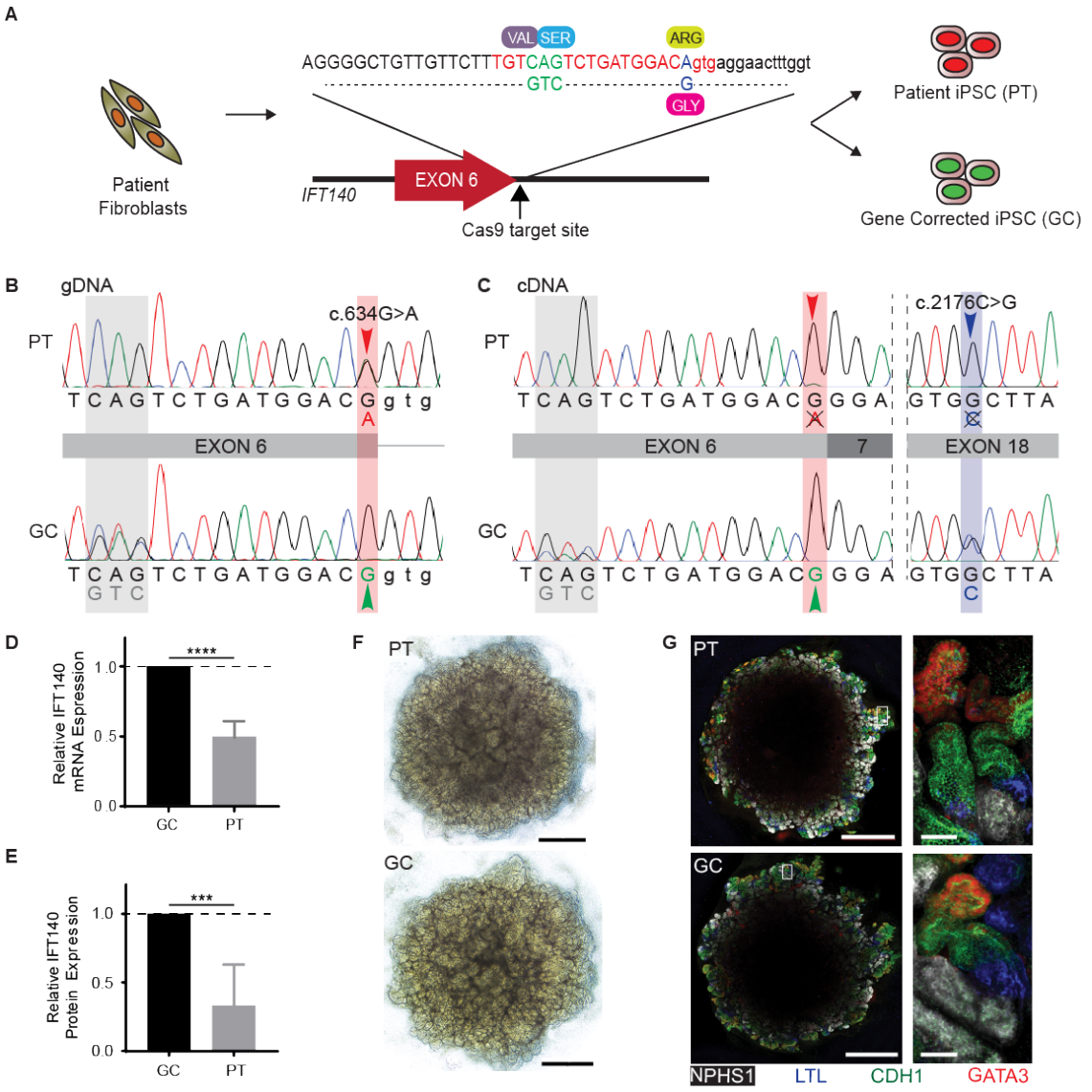

Figure 3.3 Gene-correction, transcript analysis and differentiation to kidney organoid
(A) The gene-correction template for the c.634G>A mutation contains the corrected single base pair (blue) and a synonymous downstream three base pair substitution (green) for ease of identification by Sanger sequencing. Successfully reprogrammed clones are screened for unsuccessful (red nuclei, PT) or successful (green nuclei, GC) gene-correction. (B) DNA sequencing demonstrates the c.634G>A mutation in the PT clone (red arrowhead) and successful correction of this mutation in the GC clone (green arrowhead) as well as the synonymous 3 base pair change in this allele (grey shading). (C) Sanger sequenced RNA (copy DNA) transcripts suggests the mutant allele is not detectable as a stable transcript indicated by a single chromatogram peak at both the c.634G>A locus (red arrowhead) and the c. 2176C>G mutation (blue arrowhead) in the PT clone. The double chromatogram peak at the synonymous 3 base pair substitution (grey) and the c. 2176C>G mutation locus (not gene-corrected; blue) in the GC clone indicates gene-correction has rescued this transcript. (D) qPCR identifies 50% relative mRNA expression in the PT iPSC compared to control. (data represented as mean + 95% confidence interval, p=0.0001) (E) Capillary western blot reveals 43% relative IFT140 protein expression in PT differentiated renal epithelial cells compared to GC. (data represented as mean + 95% confidence interval, p<0.001) (F) Bright field images of kidney organoids on day 25 of culture (day 18 of aggregate culture, scale bar 1mm). (G) Immunofluorescence images of whole organoids demonstrate balanced expression of glomerular precursors (NPHS1; white), proximal tubule, (LTL; blue), distal tubule (CDH1, green) and collecting duct (CDH1/GATA3, green/red). Scale bar 1mm in low magnification and 50um in high magnification images.

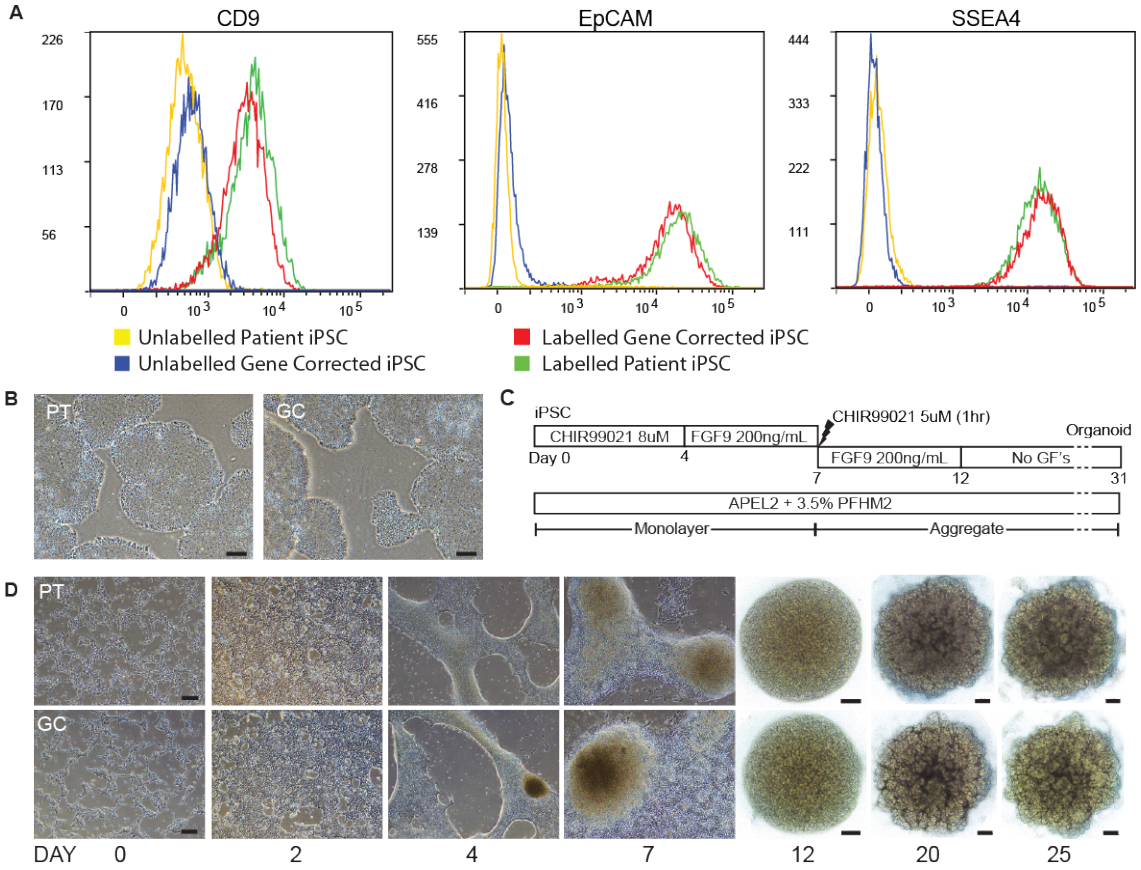

Figure 3.4 Pluripotency of iPSC clones and differentiation to kidney organoids
(A) Pluripotency analysis of PT and GC iPSC clones. (B) Bright field images of PT and GC iPSC clones demonstrating iPSC morphology: tightly packed colonies with shiny edges. Scale bar 200um. (C) Differentiation protocol adapted from Takasato et al.(Takasato et al., 2016) See methods section for details. (D) Bright field mages of differentiation demonstrate epithelial to mesenchymal transition between day zero and day four. Cultures become raised and rugated by day seven and self-organised structures are evident by day twelve, which mature with further culture. Monolayer scale bar 200um. Aggregate scale bar 500um.

iPSCs as evidenced by presence of the synonymous 3 base pair change adjacent to the corrected mutation.(Figure 3.3C) This was also supported by the finding of 53% *IFT140* mRNA and 33% protein expression in the PT clone relative to the GC clone (Figure 3.3D,E).

3.6.4 Kidney organoid tubules demonstrate ciliary morphology consistent with defective retrograde IFT

Multicellular kidney organoids were differentiated from both patient and control iPSC lines (Figure 3.3F) adapting a protocol previously published by Takasato et al (2015) to one which used fully defined, serum and feeder free culture conditions.(Figure 3.4C) Organoids produced from both lines were validated as reaching a renal end-point by the contiguous immunofluorescent expression of nephrin (NPHS1, staining glomerular precursors), *Lotus tetragonolobus* lectin (LTL, staining proximal tubule), cadherin 1 (CDH1, also known as ECAD, staining distal tubule) and co-immunofluorescence for CDH1 and GATA3 (collecting duct) (Figure 3.3G).

Previous *IFT140* null mouse models demonstrated shortened primary cilia with swollen ciliary tips in developing limb buds.(Miller et al., 2013) It should be noted that dual *IFT140* knockout resulted in embryonic lethality.(Miller et al., 2013) Acetylated tubulin and ARL13B stained primary cilia were clearly identified in the tubular epithelium of iPSC-derived kidney organoids by immunofluorescence (Figure 3.5A,D). Automated image processing was used to generate a random series of images of individual cilia from CDH1+ regions of kidney organoids (n = 900 cilia) for blinded scoring (Figure 3.5A). A clubbed morphology similar to that seen in the murine *IFT140* null was evident in the majority of PT cilia (59%; 95%CI 54-63%) whilst a similar majority of GC cilia (60%; 95%CI 56-65%) demonstrated wild type morphology (Figure 3.5B). PT cilia were significantly shorter than GC cilia and the difference between PT and GC mean ciliary length increased with time in aggregate culture (Figure 3.5C). Ciliary IFT140 expression within club shaped cilia in GATA3+ regions of organoid tubules demonstrated increased IFT140 staining of the swollen ciliary axoneme. Other IFT-A and B proteins demonstrated a similar intensification of fluorescence in the ciliary tip consistent with defective retrograde IFT. (Figure 3.5D)

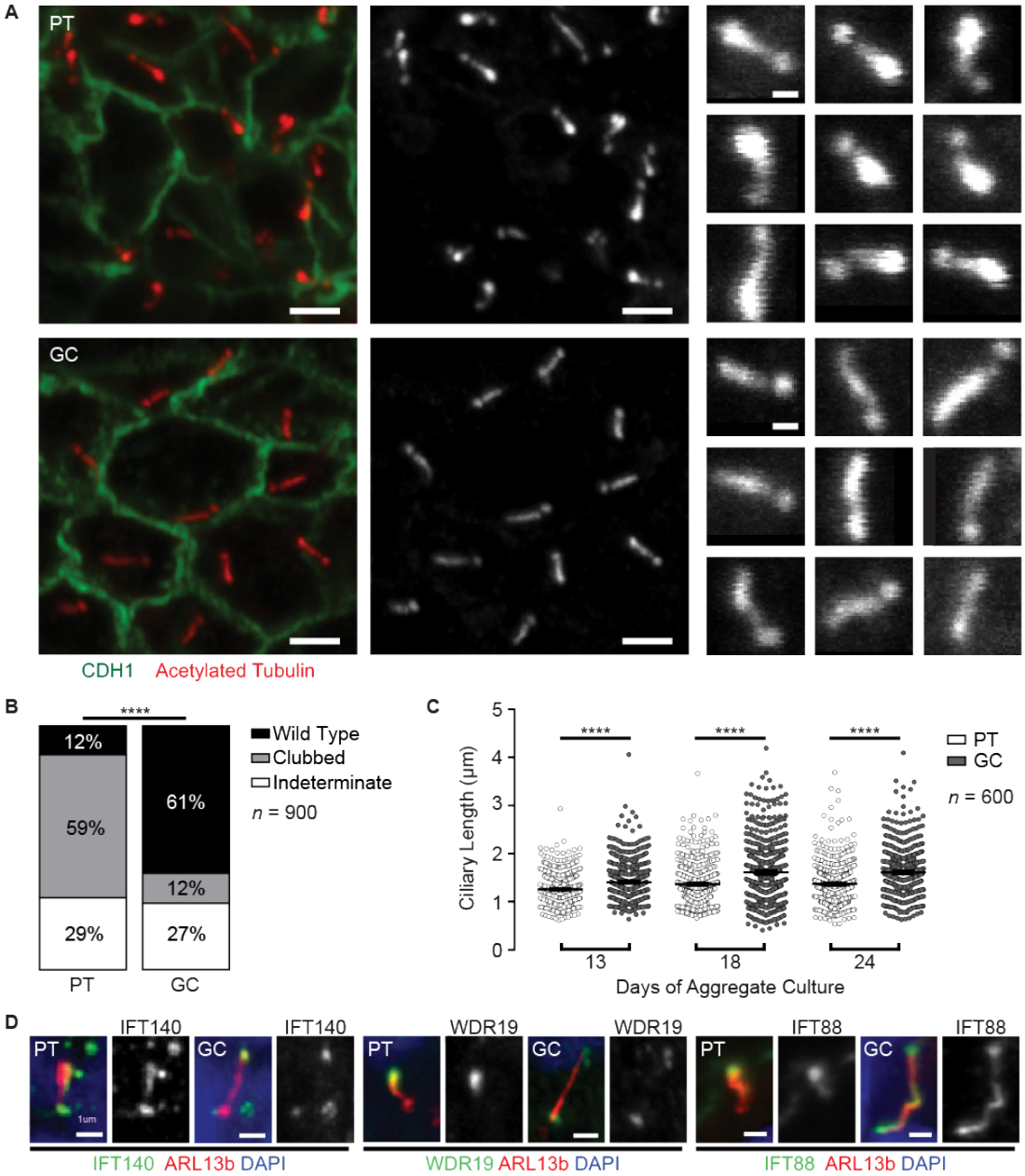

Figure 3.5 Patient organoid tubules demonstrate abnormal cilia which are rescued by gene-correction (A) Cilia of CDH1+ tubular epithelial cells demonstrate classical morphology associated with defective retrograde IFT: short with swollen ciliary tips (left and middle panels, scale bar 2µm). Individual cilia were isolated from these images (right panels, scale bar 500nm) and shuffled for blinded scoring of morphology. (B) Quantitative output of blinded cilia morphology analysis demonstrating predominantly clubbed cilia in PT organoids (59%) and predominant wild-type morphology in gene corrected cilia (61%) (n = 900, p <0.0001, Chi-squared test). (C) PT cilia were shorter than GC cilia at every culture time point, with an increasing difference noted with time in culture (n = 600 cilia per condition, p < 0.0001, Welch's t test, error bars represent mean + 95% confidence interval). (D) IFT components IFT140, WDR19 and IFT88 were all found to accumulate in the PT ciliary tip. Gene corrected organoids displayed wild type distribution (scale bar 1µm).

3.6.5 Transcriptional profiling identifies dysfunctional cellular processes resulting from c.634G>A mutation

The isolated transcriptional effects of the c.634G>A mutation were investigated by comparing bulk RNA sequencing profiles (GEO accession number: GSE107230) of the epithelial (EPCAM+) cell fractions isolated from iPSC-derived kidney organoids by magnetic activated cell sorting (MACS) (Figure 3.7A). Based on co-immunofluorescence analysis, this EPCAM+ fraction included proximal tubule (LTL+) and collecting duct structures (GATA3+) as well as an epithelial structure resembling Bowman's capsule surrounding visceral epithelial cells (Figure 3.6A,B). Validation of EPCAM+ purification by MACS was confirmed by flow cytometry (Figure 3.6C). Replicates clustered appropriately on a principle component analysis with clear separation between PT and GC transcription profiles upon unbiased clustering. (Figure 3.7B,C).

For the purposes of gene enrichment analysis, the primary differential gene expression (DGE) dataset (Table 3.2) was filtered for genes that have previously exhibited high transcriptional variability between repeated differentiation experiments of a human wild-type iPSC cell line (CRL1502, clone C32).(Phipson et al., 2017) This transcriptional 'noise' is batch associated and likely to result from slight variations in relative maturation between individual organoids. Any of the top 1000 most variable genes within the CRL1502 dataset were excluded from further analysis (n = 570,Table 3.3).

Gene enrichment analysis of remaining genes with significant DGE (adjusted p value <0.01, n=954;Table 3.4) returned gene ontology (GO) terms illustrating disturbances in cell adhesion and cytoskeletal interaction pathways (Figure 3.7D). This analysis returned one single human phenotype term 'Vitreoretinal Degeneration' (HP:0000655), consistent with the patient phenotype (Figure 3.8A) and inclusive of *CRB1*, a critical component of the highly conserved Crumbs polarity complex which is strongly associated with RP and Leber's Congenital Amaurosis.(den Hollander et al., 2001) Cell polarity complexes are highly conserved, critical regulators of epithelial polarity modulating asymmetrical cytoskeletal organisation within the cell, and cell junction integrity in order to preserve apicobasal expression of transmembrane receptors and transporters.(Pieczynski and Margolis, 2011) Differential expression of Crumbs complex genes within the primary

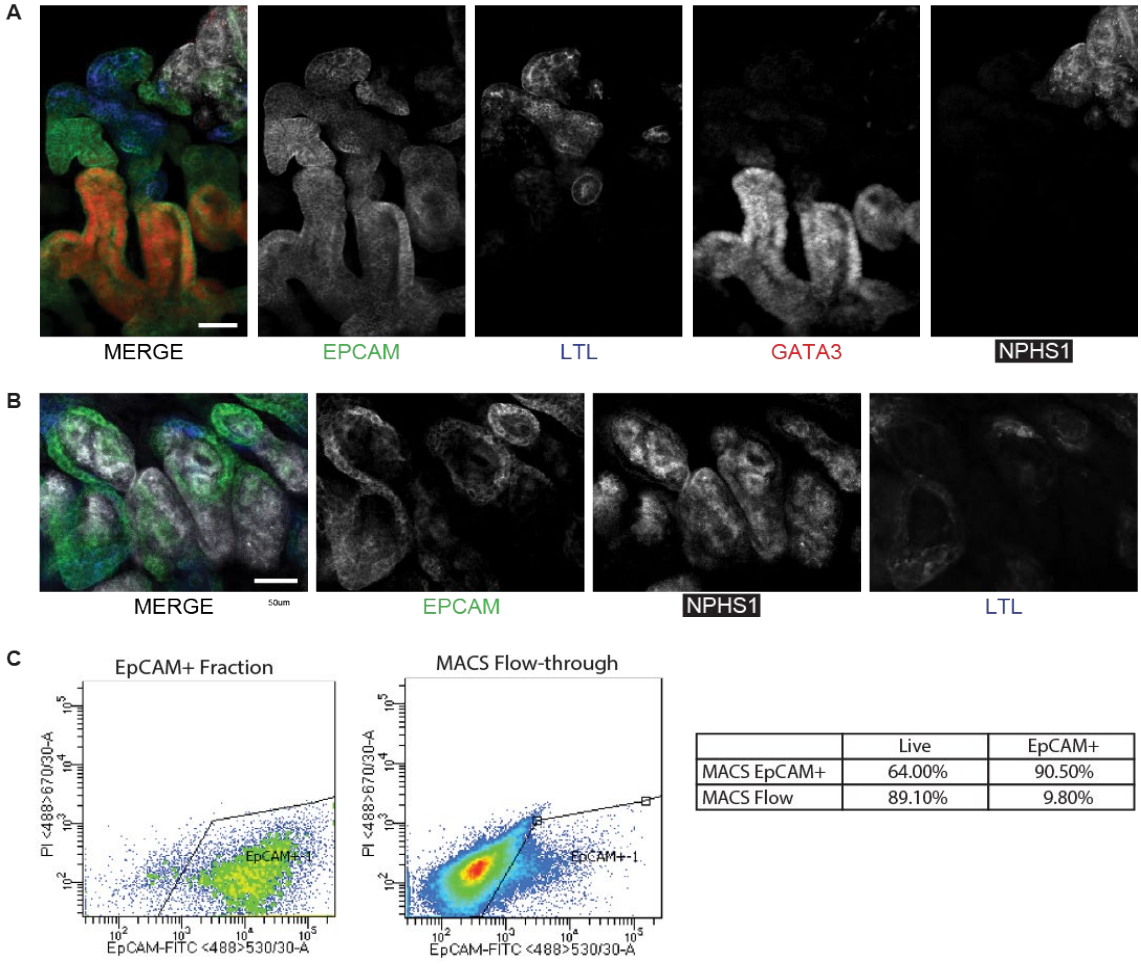

	Live	EpCAM+
MACS EpCAM+	64.00%	90.50%
MACS Flow	89.10%	9.80%

Figure 3.6 Characterisation and validation of EPCAM MACS sorting.
(A) Immunofluorescent validation of the cell populations that represent the EPCAM positive fraction of organoids. EPCAM conjugated with Alexafluor-488 (green) co-immunofluorescence with LTL+ proximal tubule (blue) and GATA3+ collecting duct (red) with a contiguous tubular structure between (distal tubule, reliably CDH1+ in other staining protocols). (Scale bar 50um) (B) NPHS1+ podocytes (white) are EPCAM negative but a rim of EPCAM+ cells surrounding glomerular structures resembles Bowman's capsule. (Scale bar 50um) (C) Flow cytometry of MACS sorted kidney organoids additionally incubated with EPCAM conjugated with Alexafluor-488 antibody demonstrates 64% viability in the eluted cell fraction which is 90.5% EPCAM+.

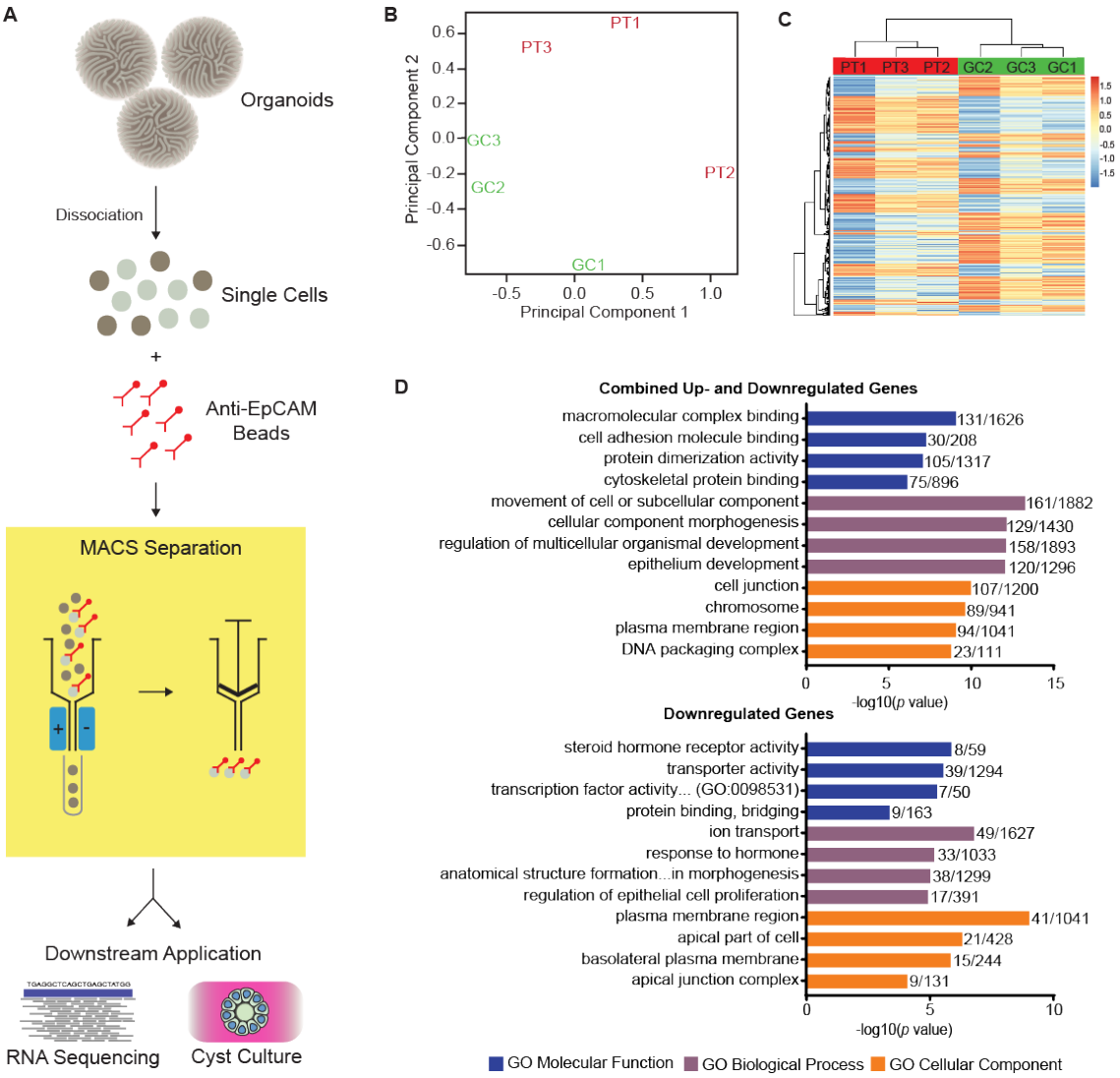

Figure 3.7 RNA sequencing of epithelial sub-fractions of organoids demonstrate dysfunctional cellular processes resulting from *IFT140* mutations

(A) Diagrammatic representation of epithelial magnetic associated cell sorting (MACS) from dissociated organoids. Dissociated organoids were incubated with EPCAM antibody conjugated magnetic beads and passed through a magnetic field, trapping epithelial cells which could be gently eluted for downstream application following removal of the magnetic field. (B) Principal component analysis of primary RNA sequencing data demonstrates clustering of PT and GC replicates. (C) Heatmap demonstrates consistency of gene expression across replicates. (D) Top GO terms output from ToppGene gene list enrichment of *Set 1* (combined up and downregulated genes with significant differential expression adjusted p <0.01; top graph) and *Set 2* (genes with log fold change >0.7 favouring GC and significant differential expression <0.05; bottom graph). Bar represents $-\log_{10}(p \text{ value})$ and adjacent fraction represents number of genes within the data set (numerator) and number of genes within the GO gene list (denominator). Similar GO terms with near-identical DGE representation and GO term have been filtered out to avoid repetition. Blue: GO Molecular Function, Purple: GO Biological Process, Orange: GO Cellular Component.

RNASeq dataset suggested downregulation in PT renal epithelia compared to GC (Figure 3.8B). Transcriptional differences within the associated PAR polarity complex were less consistent between replicates with the exception of *CDC42* which was downregulated in PT (Figure 3.8C). Of interest, animal knockout models of *Cdc42*$^{-/-}$ develop a NPHP-like renal histology and demonstrate loss of photoreceptor cilia.(Choi et al., 2013b) CDC42 was also a central node within a STRING protein interaction network of DGE highlighted within the 'Adherens Junction' term (GO:0005912, Figure 3.9A,B). EGFR was also a downregulated central interacting gene product identified by STRING protein interactome with significant downregulated expression. EGF signalling is strongly associated with the proliferative epithelial phenotype seen in ADPKD cysts and inhibition of this signalling pathway reduces cyst progression in animal models (reviewed in (Harskamp et al., 2016)). The observation of CDK1 (int:CDK1) and CDK2 (int:CKD2) in the top 5 interacting gene products is of interest given increasing evidence of benefit in both animal and cellular nephronophthisis models when treated with CDK-inhibitors.(Booij et al., 2017, Srivastava et al., 2017b, Bukanov et al., 2012, Moreno et al., 2008)

IFT related ciliopathy is often associated with increases in canonical Wnt, Shh and Notch signalling pathways, usually amplified by treatment with a pathway agonist.(Liem et al., 2012, Hynes et al., 2014, Mukhopadhyay et al., 2013) Whilst these pathways did not feature prominently in ToppGene enrichment analysis, all three signalling pathways were upregulated in Hallmark gene list enrichment analyses on the primary dataset before the exclusion of highly variable genes (Figure 3.9D-F). In a murine *IFT140 HoxB7-Cre* knockout model, transcriptional changes in these signalling pathways were not observed until post-natal day 15-20.(Jonassen et al., 2012) The present study, however, demonstrates changes in these pathways consistent with the existing literature, within a model that transcriptionally most closely resembles first trimester human foetal kidney.(Takasato et al., 2015)

Gene enrichment analysis of downregulated DGE reflected disturbances to apical and basolateral plasma membranes, the apical junction complex as well as downregulated transporter activities associated with these cellular membranes (Figure 3.7D). Additional

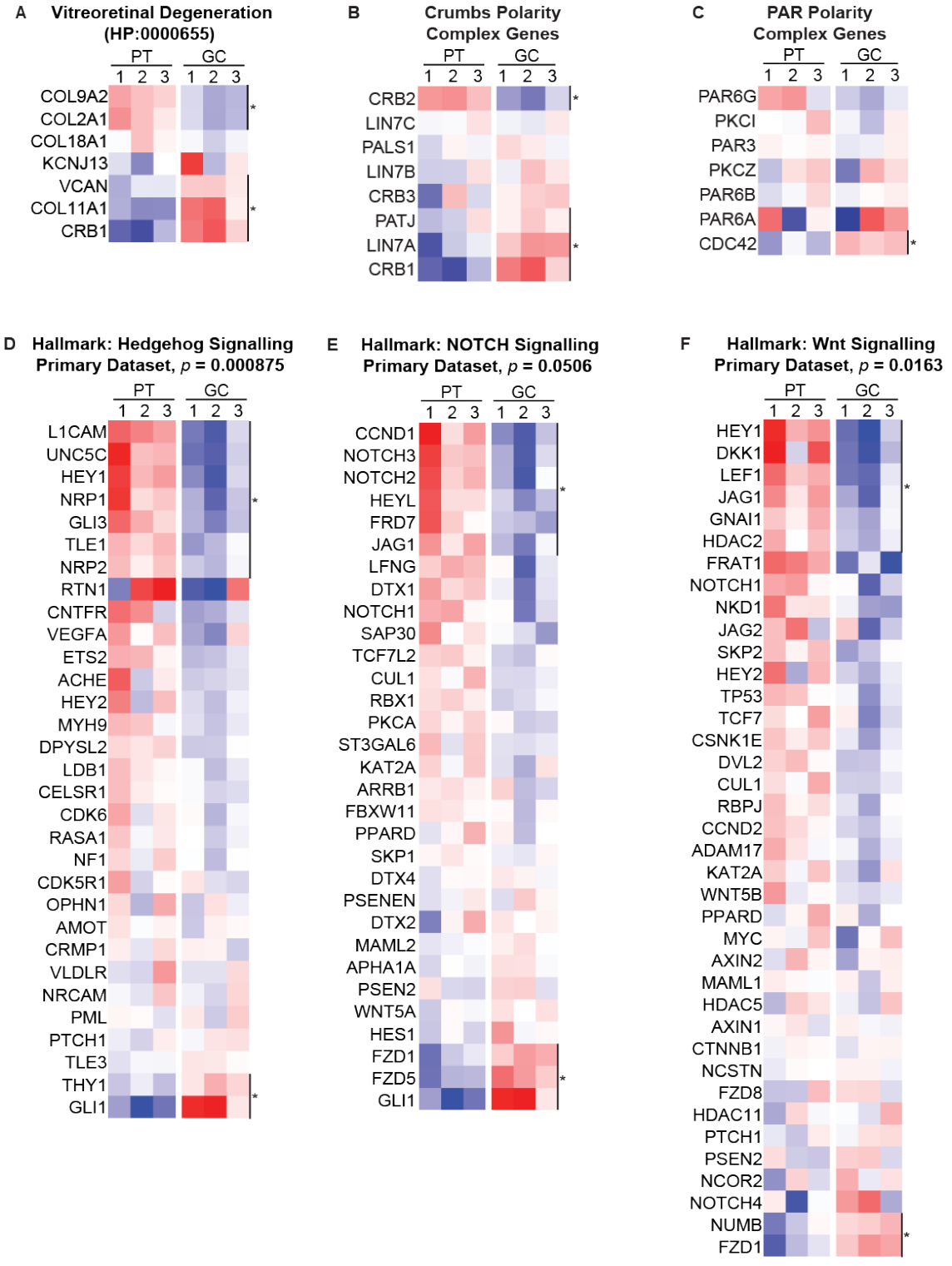

Figure 3.8 Differential expression within polarity and cell signalling pathways
Heatmaps summarising DGE within primary RNASeq dataset (A) Human Phenotype term Vitreoretinal degeneration, (B) Crumbs polarity complex genes, (C) Par Polarity complex genes, (D) Hallmark Hedgehog signalling gene list, (E) Hallmark NOTCH signalling gene list, (F) Hallmark Wnt beta Catenin signalling gene set. Individual genes with significant DGE (i.e. $p < 0.05$) indicated by *.

downregulated GO outputs of interest included 'negative regulation of epithelial cell proliferation' (GO:0050680) and 'axonemal dynein complex assembly' (GO:0070286; Figure 3.9C,D). RNA sequencing of selected differentially expressed genes from these GO terms was validated by qPCR (Figure 3.12).

3.6.6 Impaired spheroid culture in IFT140(-/-) epithelial cells sorted from kidney organoids

The differential expression profiling highlighted downregulation of genes expressed in the apical part of the cell and the cell junction (Figure 3.10A,B). The functional validation of apicobasal polarity defects using three dimensional epithelial spheroid culture has previously been applied in the study of ciliopathies.(Giles et al., 2014) Accordingly, MACS sorted EPCAM+ cells from both PT and GC organoids were subjected to spheroid culture and stained with markers of apical junctions (ZO-1 and CDH1) and apicobasal polarity (acetylated tubulin and beta-catenin) (Figure 3.10C). Consistently fewer PT EPCAM+ cells developed spheroids with polarised epithelium when compared with GC EPCAM+ cells (PT 34.0% [25.4-43.7], GC 53.0% [43.2-62.5]; p =0.01; Figure 3.10D). This confirms the utility of spheroid culture as an assay for evaluation of cellular polarisation using patient-derived renal epithelium and indicates an underlying defect in cell-cell interactions potentially present during human development. Assessment of primary cilia per nucleus was technically challenging in whole 3D organoids but manual counting in cultured cysts was more straightforward. Cilia per nucleus was reduced in PT cysts compared to GC cysts and also demonstrated increased variability (Figure 3.11) (PT 83.7% [74.7-89.3], GC 93.8% [91.1-96.7]; $p < 0.01$).

3.7 Discussion

This study presents the prospective application of patient-originated iPSC derived kidney organoids for functional genomic disease modelling. We demonstrate the utility of an isogenic, gene-corrected control iPSC clone for the functional validation of an isolated, patient-specific gene mutation. The demonstration of such a clear restoration of renal ciliary morphology by gene-correction of a single mutated allele of an autosomal recessive genotype supports the likely efficacy of this approach for validation of novel VUS in future studies. Previous reports of iPSC-based renal disease modelling have relied on the generation of mutations using CRISPR/Cas9-induced non-homologous end joining

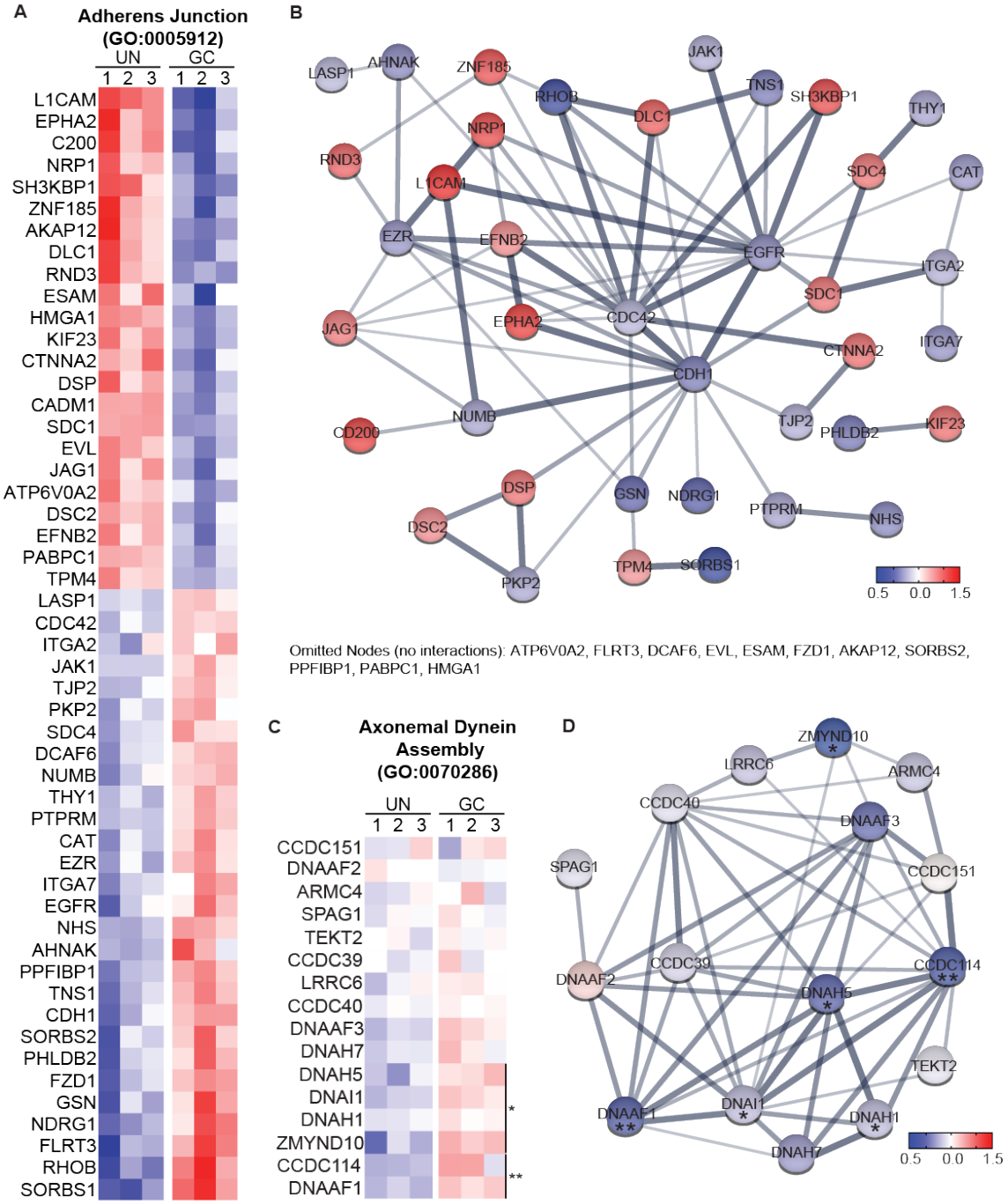

Figure 3.9 Differential expression within adherens junction and axonemal dynein assembly GO terms with STRING protein interactomes
(A) Heatmap demonstrating differential expression of genes from Adherens Junction GO Term (adjusted $p < 0.01$ for all genes). (B) STRING protein interactome of Adherens Junction DGE. Node colours represent average differential expression in of the PT triplicate relative to average of GC triplicate. Thickness of lines indicates strength of data supporting the shared function between the proteins. Protein nodes without interactions have been hidden. (C) Heatmap demonstrating differential expression of genes from Dynein Complex Assembly GO Term (* indicates adjusted $p < 0.05$, ** indicates adjusted $p < 0.01$). (D) STRING protein interactome of Dynein Complex Assembly DGE. Node colours represent average differential expression in of the PT triplicate relative to average of GC triplicate. Thickness of lines indicates strength of data supporting the shared function between the proteins. No omitted nodes.

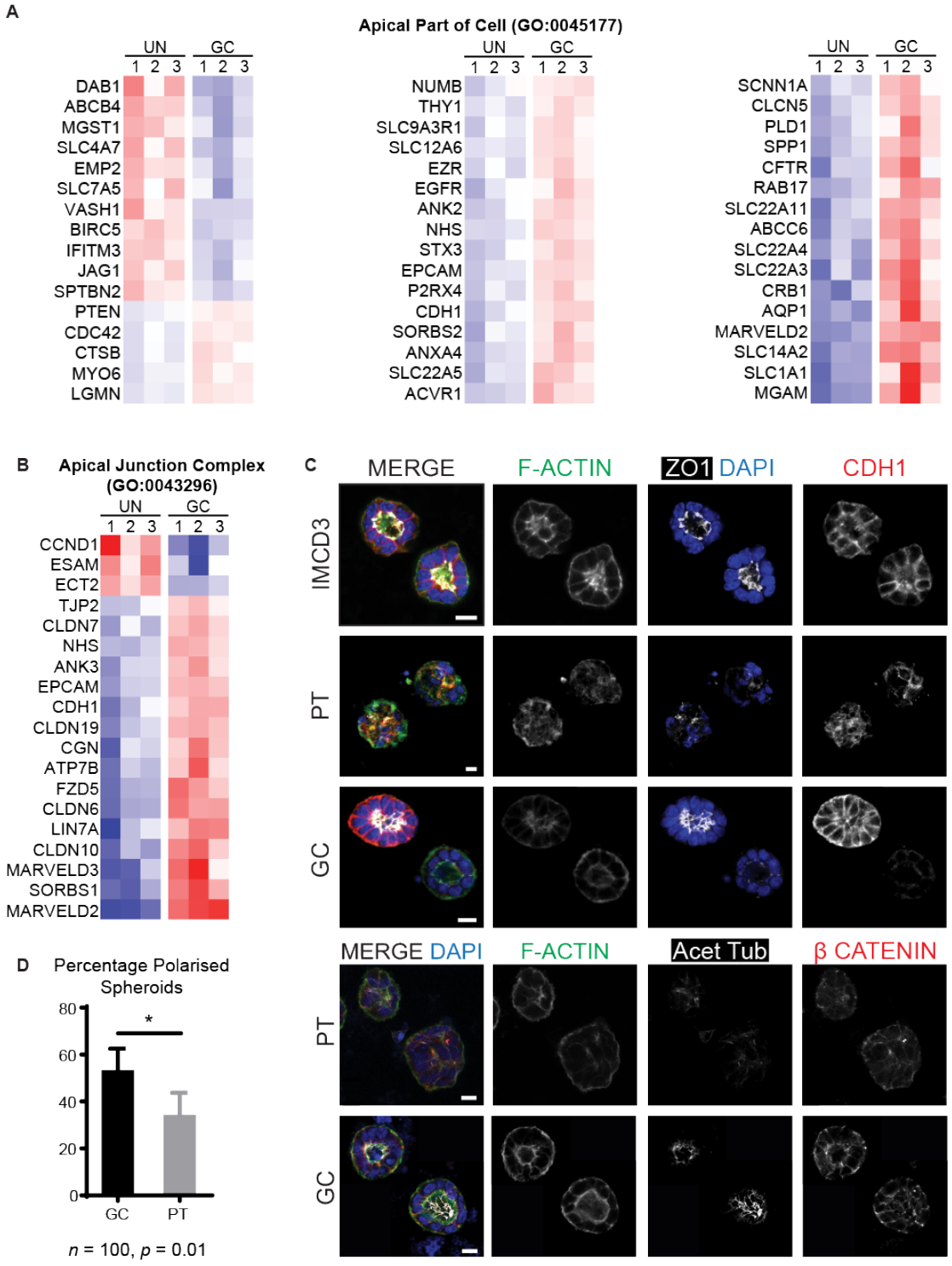

Figure 3.10 Spheroid culture demonstrates functional assay of disturbed apicobasal polarity in patient organoid epithelium
(A,B) Heatmaps demonstrating significant downregulation of components of apical part of the cell and apical cell junction in patient line (red indicates expression above the mean, blue indicates expression below the mean, * signifies adj p <0.01). (C) Immunofluorescent images from spheroid culture of EPCAM+ MACS sorted epithelial cells demonstrating examples of poorly polarised structures (PT), well polarised structures (GC) and reference images from IMCD3 cells. (D) PT EPCAM+ cells were less able to establish polarised spheroids than GC controls. (PT 34.0% [25.4-43.7], GC 53.0% [43.2-62.5]; p =0.01; error bars represent 95% confidence interval).

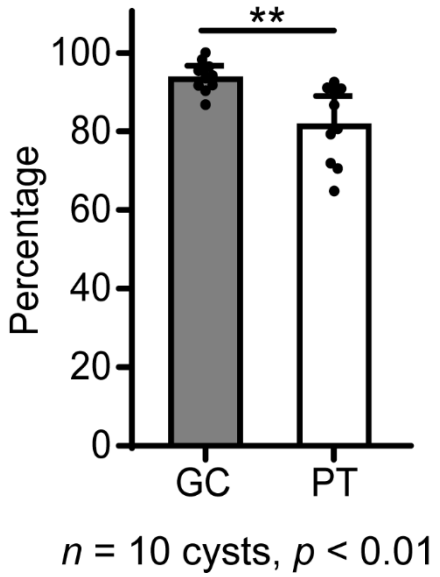

Figure 3.11 Cilia per nucleus measured from epithelial cyst culture
Mean cilia per nucleus counts from cyst culture demonstrate small but significant reduction in ciliation in PT cysts compared to GC cysts (PT 83.7% [74.7-89.3], GC 93.8% [91.1-96.7]; $p < 0.01$; error bars represent 95% confidence interval).

in wildtype human cell lines.(Cruz et al., 2017, Freedman et al., 2015) Patient-iPSC-derived kidney organoids model not only the patient-specific alleles for any candidate variant, but also the genomic background of that patient, allowing for contributions to phenotype from gene modifiers or allowing multigene disorders to be dissected. Importantly, if a modelled candidate VUS proves ultimately non-disease associated, data derived from the study of the patient-derived organoids continues to express the *bona fide* VUS potentially permitting a retrospective diagnosis.

Whilst the functional genomic study of human ciliopathy has previously relied on animal models, immortalised cell-based models or patient-derived fibroblast monolayers, an increasing body of evidence advocates that differences in ciliary biology occur between species(Lu et al., 1999, Wu et al., 2002, Karlstrom et al., 2003, Park et al., 2000, Shimeld et al., 2007, Briscoe and Therond, 2013) and between cell types in the same individual.(Shimada et al., 2017) This emphasises that modelling a human renal disease in a human renal tissue model is essential for the future application to human patients in a clinical setting. Additionally, generation of transgenic models of allelic insufficiency by knockdown with morpholino oligomers, silencing mRNA or gene knockout fails to recapitulate the specific allelic dysfunction for the individual patient. This is especially pertinent for a gene such as *IFT140*, which is frequently characterised by a compound

heterozygous genotype creating a spectrum of gene dysfunction and variable phenotypes as a result of different allelic permutations.(Perrault et al., 2012, Schmidts et al., 2013) Indeed, the c.634G>A allele present in this patient has been previously studied by expression of a FLAG-tagged variant transcript in immortalised RPE cells, suggesting mislocalisation of this variant IFT140 protein.(Perrault et al., 2012) Our results, however, suggest lack of a stable transcript from the c.634G>A allele resulting in a 50% reduction in mRNA and protein consistent with probable mRNA transcript decay. The ability to examine the specific transcriptional consequence of a single base pair mutation against an isogenic control is a novel and unique advantage of this disease modelling approach.

Transcriptional profiling of epithelial cells sorted from patient-derived organoids and gene corrected controls yielded results consistent with the evolving literature on *IFT140* dysfunction. Integral components of dynein motor assembly were found to be downregulated in PT organoid epithelium. This observation supports a growing body of evidence for a novel role of IFT140 (and other IFT-A proteins) in maintaining retrograde IFT activity by ciliary import and assembly of dynein motor components, rather than solely for the linking of ciliary proteins to the dynein motor for axonemal descent.(Blisnick et al., 2014)

The apparent success of our approach is likely critically associated with the use of patient and isogenic corrected lines to reduce genetic variation between test and control. However, acknowledging the variability in gene expression within a regenerative disease modelling platform is essential for the accurate interpretation of disease-associated transcriptional change. Here we apply a novel approach that is based upon an extensive prior evaluation of the source of transcriptional variability between kidney organoids.(Phipson et al., 2017) It is possible that a portion of those genes removed from the analysis did represent genes of relevance to the disease state rather than simple experimental variation. To investigate this further, an isolated gene enrichment analysis of the excluded 570 genes returned GO terms associated with plasma membrane transporter activity and kidney/urogenital system development. Such terms are related to relative maturation of nephrons within organoids, which we have shown does vary, but could also be attributed to the *IFT140* mutations. Importantly, where a gene was

associated with the disease state in our analyses, we have investigated gene changes in all genes for linked GO terms in order to more comprehensively evaluate pathway changes.

Over 40 genes have been identified as related to NPHP and all are linked with the primary cilium/centrosome complex.(Braun and Hildebrandt, 2016) Within this group, a variety of proposed disease mechanisms exist for NPHP gene products but no unifying pathogenetic mechanism is known. Cell junction, apicobasal polarity and cytoskeleton terms featured strongly in our DGE analysis. Whilst these pathways have not previously been described in IFT140 dysfunction, they have been implicated in NPHP pathobiology since the discovery of the first NPHP genes.(Donaldson et al., 2002, Otto et al., 2003, Delous et al., 2009, Yasunaga et al., 2015) A cytoplasmic role for IFT-B protein IFT54 (*NPHP20*) in the negative regulation of microtubule stabilisation by its interaction with MAP4 has recently been described.(Bizet et al., 2015) Affected patients had only mildly disturbed ciliary morphology but an over-stabilised microtubule cytoskeleton and the authors proposed that defective delivery of protein complexes to cell junctions and cell membranes leads to impaired polarity, differentiation and degeneration of the renal tubular epithelium.(Bizet et al., 2015) In another study, *nphp4* knockdown in *Xenopus* epidermis disrupted the subapical actin cytoskeleton impairing communication with ciliary basal bodies and motile cilia function.(Yasunaga et al., 2015) Nephrocystin and nephrocystin 2 also interacts with beta-tubulin.(Otto et al., 2003) In the demonstration of disease mechanisms for IFT140 which are well established for other NPHP genes, we demonstrate how the cumulative examination of further NPHP genotypes using organoid modelling might better illustrate the common and/or distinguishing pathways mediating NPHP disease. Additionally, the ToppGene Human Phenotype output of *Vitreoretinal Degeneration* closely resembled the patient's non-renal phenotype, validating the fidelity of the disease model and differential expression analysis.

Existing research on renal ciliopathies suggests epithelial dysfunction as the cause of disease, (Braun and Hildebrandt, 2016) hence the epithelial component of the organoids were purified and examined. As a multicellular three-dimensional disease model, any segment of the nephron or non-epithelial cell type could be isolated from differentiated tissue using this method depending on the disease in question and the

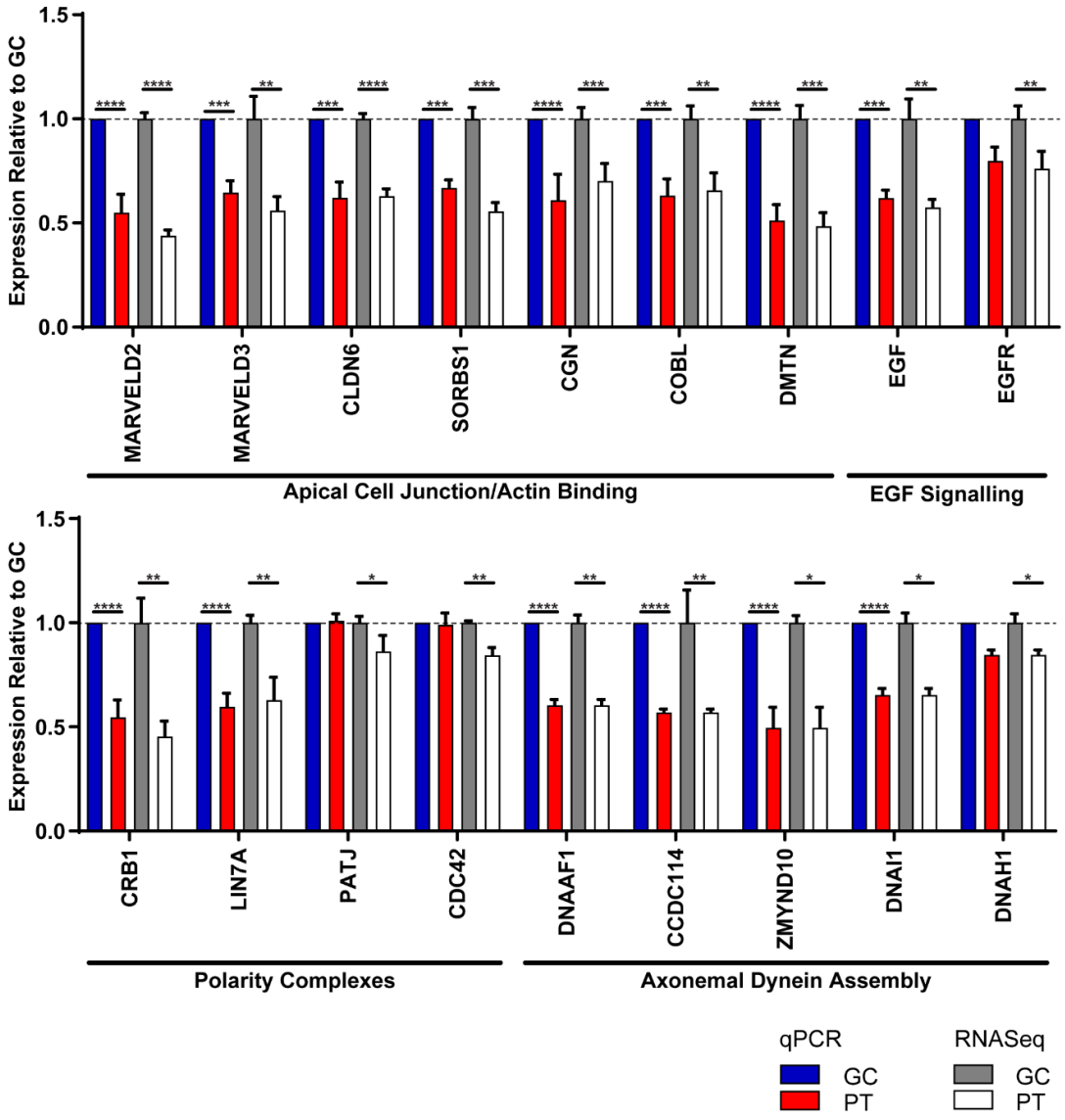

Figure 3.12 Validation of RNA Sequencing by qPCR
Quantitative real-time PCR (qPCR) of selected genes from RNA sequencing dataset. Genes were selected on the basis of adjusted *p* value and magnitude of read counts. For qPCR samples (GC blue; PT red) all PT values are graphed as 2^{-ddCT} and adjusted *p* values calculated by *t* test with Bonferroni-Dunn correction for multiple comparisons. For RNA sequencing samples (GC dark grey, PT light grey), all values were normalised to mean GC count and adjusted *p* values represent those from original bioinformatics analysis. (error bars represent standard error of the mean, * indicates adjusted $p < 0.05$, ** indicates adjusted $p < 0.01$, *** indicates adjusted $p < 0.001$, **** indicates adjusted $p < 0.0001$).

availability of an antibody for a specifying cell surface marker. The ability to fractionate different cell types from the organoids could theoretically illustrate the differential contribution of each cell type to the disease pathobiology. For example, the interstitial expansion seen *in vivo* in NPHP raises the possibility of stromal contribution to disease pathobiology.(Slaats et al., 2016) Whilst a stromal element of the organoid exists(Takasato et al., 2015), it is yet to be sufficiently characterised as renal stroma and as such was not studied in this work.

In this report, the study of a previously validated genotype directed the assays performed (e.g. ciliary number, length and morphology). In any future study of a previously unvalidated VUS, such guidance may not be available and the most appropriate assay may not be obvious. This raises the prospect of false negatives and false positives. The use of isogenic lines and normalisation for highly variable genes will be important to remove false positives. With respect to false negatives in the case of NPHP, a number of cell-line based functional genomic studies in this field have added pathway agonists (e.g. hedgehog modifiers, forskolin) to amplify readouts of dysfunctional molecular pathways(Hynes et al., 2014, Srivastava et al., 2017b, Booij et al., 2017). While this may also be applicable in organoids, it is not known whether such treatments would alter patterning rather than reveal a relevant disease response. Indeed, even using cell lines to model NPHP, it is not known whether this 'stress' pushes the model beyond the boundary of what remains relevant to the original disease or patient. Hence this is not a unique challenge to organoids. What we do demonstrate here is the application of an unbiased quantitative approach to the evaluation of cilia morphology. This approach could be applied to other NPHP models and further development could integrate machine learning to support a fully automated high-throughput assay for the purposes of patient specific compound screening without the need to dissociate the regenerated tissue.

The application of kidney organoids to the *in vitro* modelling of other types of inherited kidney disease raises specific challenges with respect to the disease studied. The transcriptional profile of the organoid derived by our protocol most closely resembles trimester 1 human fetal kidney.(Takasato et al., 2015) This suggests that diseases with antenatal or infantile disease onset (e.g. congenital nephrotic syndrome [OMIM: 256300]; autosomal recessive polycystic kidney disease [OMIM: 606702]) may be more readily

studied, compared to those with adult onset (e.g. autosomal dominant polycystic kidney disease [OMIM: 601313]). Without a patent vasculature, urinary drainage system or urine production, modelling of congenital anomalies of the kidney and urinary tract, or glomerulopathies such as inherited nephrotic syndrome and Alport Syndrome [OMIM: 301050, 203780], is less feasible. Prenatal, and hence low, expression of electrolyte channels and transporters may also limit the modelling of some tubulopathies. However, improving the degree of cellular maturation of the organoid model by refining culture conditions and introducing flow(Homan et al., 2016, Jansen et al., 2015, van den Berg et al., 2018) will likely expand the repertoire of kidney diseases amenable to disease modelling using iPSC derived models.

This study demonstrates that kidney organoids derived from patient iPSC are capable of expressing an inherited developmental renal disease phenotype. Together with CRISPR/Cas9 mediated gene-correction, kidney organoids represent a novel functional genomic platform for the validation of novel genomic variants. This study also demonstrates the study of human renal disease via a patient-derived, three dimensional, *in vitro* model. The fidelity of transcriptional profiling to identify not only established *IFT140* disease mechanisms but also those implicated for other NPHP genes heralds the ability to refine the common cellular pathways in NPHP through the future study of other known and novel genotypes. This study was enabled via coordinated clinical and laboratory research arms able to provide a comprehensive clinical and research genomic service for the rapid identification of novel VUS in a patient-specific disease model. The future applications of kidney organoids as a disease model may include high-throughput personalised therapeutic screening which could feed back to the patient within such a multidisciplinary clinical/experimental team approach.

3.8 Accession Numbers

The accession number for the RNA sequencing primary dataset is:

GEO accession number: GSE107230

3.9 Online Links to Supplementary Datasets

All available via: https://doi.org/10.1016/j.ajhg.2018.03.014

Table 3.2 Primary RNA Sequencing Dataset with Counts per Million and Statistical Significance.
https://ars.els-cdn.com/content/image/1-s2.0-S0002929718301034-mmc2.xlsx

Table 3.3 Genes Excluded from Further Analysis according to Their Recognized Variability between Differentiation Experiments.
https://ars.els-cdn.com/content/image/1-s2.0-S0002929718301034-mmc3.xlsx

Table 3.4 Set 1 Gene List with Counts per Million and Statistical Significance.
https://ars.els-cdn.com/content/image/1-s2.0-S0002929718301034-mmc4.xlsx

Table 3.5 Set 2 Gene List with Counts per Million and Statistical Significance.
https://ars.els-cdn.com/content/image/1-s2.0-S0002929718301034-mmc5.xlsx

Table 3.6 Top 50 Hallmark Terms from Primary Dataset.
https://ars.els-cdn.com/content/image/1-s2.0-S0002929718301034-mmc6.xlsx

Chapter 4 An unsuccessful attempt to validate a novel gene for nephronophthisis using patient-iPSC-derived kidney organoids.

4.1 Introduction

In Chapter 3, we demonstrate the capacity of patient-iPSC-derived kidney organoids to express a compound heterozygote *IFT140* disease phenotype consistent with that seen in previously published *IFT140* mutant models. Having established a set of protocols and assays optimised and validated to examine epithelial dysfunction as a model of NPHP, we then attempted to identify a novel gene for another patient with a genetically undiagnosed infantile NPHP phenotype.

In Australia, the KidGen Renal Genetic Collaborative has established a database of patients who remain undiagnosed following whole exome or genome sequencing. Established in 2016, KidGen is a consortium of nephrologists, geneticists, genetic counsellors and research scientists with a view to forwarding the genetic understanding of kidney disease.(Kidgen, 2017, Mallett et al., 2017) Patients are assessed in dedicated

renal genetics clinics and offered diagnostic targeted exome or genome sequencing where appropriate.(Mallett et al., 2016, Mallett et al., 2017, Jayasinghe et al., 2019) Patients with non-diagnostic sequencing results are referred for research level whole exome or genome sequencing analysis.

In the following chapter, a female proband with an infantile presentation of CKD resembling NPHP is identified carrying a homozygous VUS in *DNAH5*. This patient is prioritised for modelling in iPSC derived kidney organoids with a focus on testing the hypothesis that the *DNAH5* variant is causative of the disease phenotype. DNAH5 is an axonemal dynein heavy chain which contributes to the interlinking outer dynein arm between the microtubule pairs of motile cilia.(Olbrich et al., 2002) Mutations in *DNAH5* are an established cause of Primary Ciliary Dyskinesia Type 3 (PCD3; [OMIM 608644]). As previously mentioned , the term 'primary' in this case is intended to imply a congenital dysfunction of the *motile* cilium (ie. not acquired or secondary) rather than to describe any problem with the primary (ie. non-motile) cilium. Individuals with PCD3 may present with *situs inversus* due to impaired nodal ciliary motility, recurrent respiratory tract infections and chronic suppurative lung disease due to impaired mucociliary clearance of airway sections, and infertility in males due to immotile spermatozoa.(Olbrich et al., 2002, Omran et al., 2000b, Failly et al., 2009, Knowles et al., 2013) PCD3 is not classically associated with any renal phenotype.

This project was ultimately unsuccessful in validating this *DNAH5* variant as causative of kidney disease for this proband using the kidney organoid model, as were our collaborators who modelled the variant in mice. This project highlights the importance of the variant curation process in the selection of appropriate candidate variants to model with kidney organoids and the need for revision of the novel gene validation thresholds for our laboratory moving forward.

4.2 Acknowledgements

In this project, Dr Catherine Quinlan phenotyped the proband, genome sequencing was performed by Dr Cas Simons (MCRI), isolation of peripheral blood mononucleocytes and iPSC reprogramming was performed by the iPSC Core Facility (MCRI, Dr Katerina Vlahos) and gene correction of the iPSC performed by the Gene Editing Core Facility

(MCRI, Dr Sara Howden). Post-immunofluorescent analysis scripts for ciliary morphology and cyst culture analysis were written by Dr Kynan Lawlor.

4.3 Methods

4.3.1 Genome Sequencing and Analysis

Ethics approvals, exome sequencing and analysis pipelines were performed using the same methods described in Chapter 3.5.1.

4.3.2 Reprogramming and Gene Correction of iSPC

In contrast to the simultaneous reprogramming and gene correction protocol described in Chapter 3.5.2, we were unable to sample patient fibroblasts and thus employed a two-step protocol reprogramming iPSC from patient peripheral blood mononuclear cells (PBMC) followed by gene correction of reprogrammed patient iPSC.

Using density gradient centrifugation, PBMC were isolated from a patient blood sample and cultured in erythroid expansion medium (Stem Cell Tech; Cat# 09605 & 02692) for 7 days, with alternate daily media changes. At day 7,500 x 10^3 PBMCs were pelleted and re-suspended in erythroid expansion medium containing Sendai virus (Life Tech; Cat# A167517) with MOIs of 5,5,and 5 (i.e., KOS MOI = 5, hc-Myc MOI = 5, h-Klf4 MOI = 5) and polybrene (4 ug/ml) to final concentration of 500x10^3 cells/ml. Cells were then plate in one well of a 12-well plate and centrifuged at 2000 rpm for 30 minutes at room temperature.

Sendai virus was removed at 24 hours by centrifugation of the cell and virus suspension at 300g for 5 minutes and resuspension in fresh erythroid expansion medium and returning the cells to the original well. Three days following transduction, cells were plated onto irradiated mouse embryonic fibroblasts in 1:1 mix of StemSpan SFEM II (Stem Cell Tech; Cat #09605) and hiPSC media. On day 5 additional human iPSC media was added. On day 7 all media was aspirated and refreshed with human iPSC media, changed daily until colonies were able to be selected (around three weeks post-transduction).

4.3.3 Cell Culture and Directed Differentiation to Kidney Organoids

Undifferentiated iPSC were maintained in feeder free conditions on hESC qualified Matrigel in E8 media (STEMCELL Technologies). The originally published organoid protocol was optimised in APEL media, however this media was withdrawn by its manufacturer and replaced with APEL2. Having experienced some difficulty in reproducing our kidney differentiations in APEL2, the laboratory made a decision to switch to TeSR Essential 6 (E6, STEMCELL Technologies) base media as a fully defined, low-cost media which could be easily made in-house in the context of any future supply difficulties.

One day prior to differentiation, iPSC were dissociated from 60-70% confluence with TrypLE (Thermo Fisher) and plated at 7.5 x 10^4 cells per cm^2 in a 6 well plate coated with hESC qualified Growth Factor Reduced Matrigel (BD Biosciences) in 2.5mL E8 media supplemented with Revitacell (Thermo Fisher). The following morning, cells were treated with 6-8μM CHIR99021 in E6 basal media (STEMCELL Technologies) for 3-5 days, followed by FGF9 (200ng/mL) and heparin (1μg/mL) for 2-4 days, changing media every day. Cell monolayers were dissociated to a single cell suspension using TrypLE Select (Thermo Fisher) on day 7 and resuspended in 5 μL TeSR-E6 media per million cells. Cells were bioprinted as previously described.(Higgins et al., 2018) The dissociated cell suspension was aspirated into a sterilised 100 μL Gastight syringe (Hamilton) with a 21-guage Removable Needle (Hamilton) and loaded onto the NovoGen MMX bioprinter (Organovo) before printing 8 x 4 mm lines of cells onto 0.4 μm polyester membrane 6 well Transwell inserts (CLS3450 Corning Costar). Organoids were cultured over E6 with 5μM CHIR 99021 for 1 hour to induce nephrogenesis. Organoids were then cultured over E6 supplemented with FGF9 (200ng/mL) and heparin (1μg/mL) for five days, followed by all *trans* retinoic acid (2μM) and Antibiotic-Antimycotic (0.5x) for 2-4 days. Transwell culture continued in E6 supplemented with Antibiotic-Antimycotic (0.5x, Invitrogen) and no added growth factors for 11 days changing media three times a week.

4.3.4 Immunofluorescent Analysis

Organoids were fixed in 2% paraformaldehyde for 20 mins on ice and washed with PBS. Whole organoids were cut from the Transwell filter and blocked/permeabilised for at least 3 hours in 10% Donkey serum/0.3% Triton X/PBS. Both primary and secondary

antibodies were incubated overnight at 4 degrees and washed with 0.3% Triton X/PBS. Whole mounts were mounted into MatTek glass bottom dishes and cleared with 90% glycerol. Images were obtained with an Andor Dragonfly Spinning Disk confocal microscope.

4.3.5 Ciliary Analyses

Ciliary length was measured manually from Z stack images in ImageJ (version 1.51n). Image file names were shuffled and blinded. Segmented lines were traced over cilia and measured using the ROI Manager tool and Measure analysis functions. Cilia crossing the boundary of the image (ie. not fully captured in the Z stack) were not included. Proportions were compared using chi-squared contingency tests in GraphPad Prism (version 7.04).

Ciliary morphology was assessed in using a similar protocol to that described in Chapter 3.5.5. Ilastik 1.3.2 (Berg et al., 2019) was used to classify voxels as belonging to cilia or background based on manual annotation of a subset of regions. Classification probability maps were processed using the scikit-image 0.15 python library.(van der Walt et al., 2014).to import each image, perform Gaussian blurring (Sigma : x = 0.8, y= 0.8, z = 0) and assign labels to regions with pixel value greater than 0.6. These regions mainly represented cilia and were processed to generate sets for visual scoring based on the previously described method (Forbes et al., 2018) except that objects with area less than 200 voxels were excluded.

4.3.6 Magnetic Associated Cell Sorting (MACS) and Cyst Culture

MACS and Matrigel cyst culture was performed in an 8 well chamberslide using the same protocol as reported in Chapter 3.5.7. Following fixation and immunofluorescent staining the entire chamberslide well was imaged for both genotypes with an Andor Dragonfly Spinning Disk confocal microscope. Using a protocol analogous to the ciliary morphology protocol, ECAD+ cysts were filtered from these raw images using a Fiji script. 280 ECAD+ structures were isolated from the combined data set and presented as 3-dimensional tiff files with 4 isolated channels. Cysts were shuffled and blinded to genotype for assessment. Each cyst was manually categorised with regards to the apical distribution of ZO-1 and/or F-actin expression (polarised, non-polarised, indeterminate)

Proportions were compared statistically in GraphPad Prism (version 7.01) using Fisher's exact test.

For cysts where the basolateral boundary of the cyst did not cross the border of the isolated image, the outline of a maximum intensity projection of the ECAD signal was manually traced with the polygon selection tool. The perimeter, area and maximum diameter was then calculated using the Measure function of ImageJ. Proportions were compared statistically in GraphPad Prism (version 7.01) using students *t* test and Bonferroni adjusted Type 1 false discovery rate of 1% (ie. $p < 0.01$) for multiple comparisons.

4.3.7 qPCR

cDNA synthesis and qPCR was performed according to the protocol outlined in Chapter 3.5.6.

4.3.8 Isolation and Culture of Human Urine Derived Renal Epithelial Cells

Human urine derived renal epithelial cells (HURECs) were isolated according to a published protocol by Zhou et al.(Zhou et al., 2012) At least 50mL of fresh urine was centrifuged at 400g for 10 minutes at room temperature. The supernatant was aspirated down to 1mL of urine and the pellet resuspended. The cell suspension was then washed in 10mL chilled PBS supplemented with Primocin (Invivogen). The sample was then centrifuged at 200g for 10 mins. The supernatant was aspirated and the pellet resuspended in 1mL primary medium[†] and transferred to a 12 well plate coated with Laminin-521. Another 1mL of primary media was added and cells were cultured overnight at 37°C, 5% CO_2. For the next three days, 1mL of media was added each day (no media was removed). On the fourth day 3mL of media was aspirated with a P1000 and 1mL proliferation media (1:1 RE media[‡]:MC media[§]) was added. Each subsequent day 1mL of media was removed

[†] 100mL primary medium = 45mL high glucose DMEM (Hyclone) + 45mL Ham's F12 (Invitrogen) + 10mL FBS (Interpath Services) + 200µL Primocin (Invivogen) + 700µL combined REGM SingleQuots (Lonza)

[‡] 100mL RE media = 100mL REBM Renal Epithelial Growth Basal Media (Lonza) + 700µL combined REGM SingleQuots (Lonza) – combined and filtered using 0.2µm filter unit.

[§] 100mL MC media = 90mL high glucose DMEM (Hyclone) + 10mL FBS (Interpath Services) + 1mL Glutamax (Invitrogen) + 1mL non-essential amino acids (Invitrogen) + 0.5µg bFGF (Lonza) + 0.5 µg EGF (Peprotech) + 0.5ug PDGF-AB (Peprotech), – combined and filtered using 0.2µm filter unit.

from the well and 1mL fresh proliferation media was added. Once colonies of proliferating epithelial cells were observed, they were dissociated with Trypsin-EDTA 0.05%, inactivated with FDMEM (high glucose DMEM + 10% FBS + 1x Glutamax + 1x NEAA + 1x antibiotic/antimycotic) and replated to a fresh, uncoated well of a 12 well plate in fresh proliferation media. Cells were passaged at 80-90% confluence to 100-150x10^3 cells/well of a 6 well plate.

In preparation for immunofluorescence cells were cultured on sterilised 15mm diameter glass coverslips. In a Class II Biological Safety Cabinet, coverslips were briefly immersed in 80% ethanol and then, held with sterilised pincers, briefly dried in the air flow of the cabinet before immersing in DPBS. Three coverslips were transferred to each well of a 6 well plate and dissociated cells were seeded over the top and allowed to culture to confluence before in-well fixation.

4.4 Results

4.4.1 A case of genetically unresolved infantile nephronophthisis.

The proband (RG1005.213) was born premature at 32 weeks gestation. Her mother had undergone amniocentesis and chromosomal microarray at 20 weeks gestation because of echogenic bowel and consanguineous parentage.(Figure 4.1A) This demonstrated no genomic imbalances but long continuous stretches of homozygosity. Later in the pregnancy RG1005.213 was found to have oligohydramnios and was born with contractures and pulmonary hypoplasia but with a normal urine output and renal function. A renal ultrasound, however, demonstrated enlarged, echogenic kidneys which later developed punctate foci indicative of renal microcysts.(Figure 4.1B) She exhibited mildly delayed growth and development but an MRI of her brain was normal, importantly excluding the molar tooth sign of the midbrain associated with Joubert syndrome.(Figure 4.1C)

At four years of age she was assessed by a geneticist and was felt to have facial dysmorphic features inconsistent with her parents' appearances. This included a flat facial profile, epicanthic folds, prominent corneas, short nose, long philtre and broad thumbs without polydactyly. A liver ultrasound revealed coarsened and heterogeneous

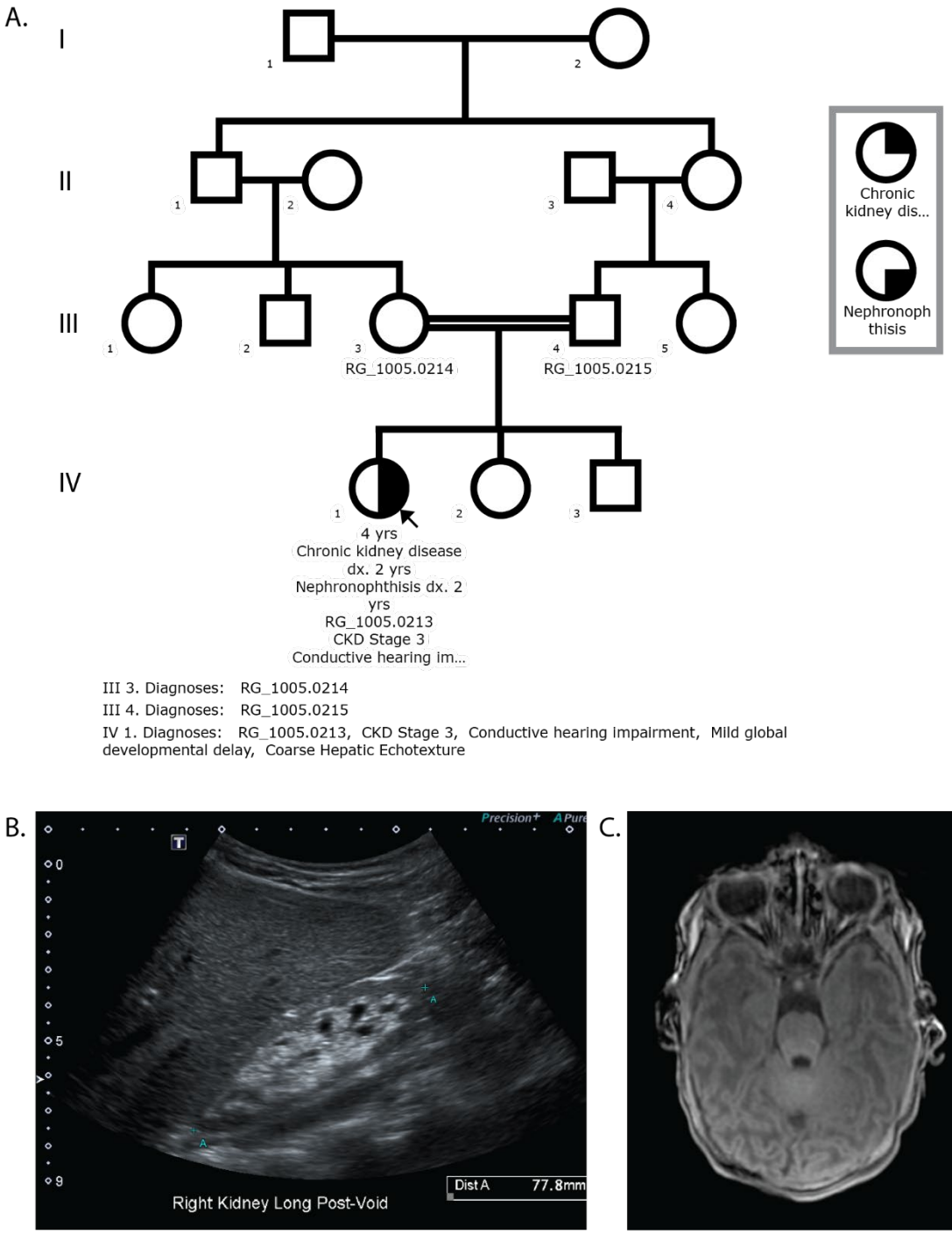

Figure 4.1 Clinical information regarding RG1005.213
(A) Pedigree/genogram for RG1005. (B)Ultrasound of right kidney at 7 years old demonstrating generalised hyper-echogenicity of the kidney (between 'A' callipers) and numerous medullary punctate foci suggestive of micro-cysts. The coarsened echotexture of the liver can be seen above and to the left of the kidney. (C) MRI Brain demonstrating normal midbrain without molar tooth sign of Joubert Syndrome.

echotexture without any focal hepatic lesions. Audiology testing has found mild sensorineural hearing loss and ophthalmology review has identified no significant ocular phenotype.

Importantly, her diagnosis of NPHP had been made on clinical grounds, without tissue biopsy of the kidney or liver. This is broadly the international standard of care for such cases where in the absence of any available treatment beyond the palliation of CKD, the risk of an invasive test cannot be justified.

RG1005.213 is the oldest of three children to consanguineous parents of Lebanese descent with no notable family history of kidney or other inheritable disease.(Figure 4.1A) Her parents are first cousins and her siblings are healthy. She is currently eight years old and has CKD stage 3 with an estimated GFR of 45 ml/min/1.73m^2.

After consultation and genetic counselling with the KidGen Renal Genetics clinic, RG1005.213 underwent whole exome sequencing targeting ciliopathy and cystic kidney disease gene lists which was non-informative.

4.4.2 Novel variant curation prioritises DNAH5 as a gene of interest.

Given the inheritance pattern illustrated by the pedigree and the consanguinity of her parents, homozygous variants were prioritised in the analysis of the trio whole exome sequencing output.(Table 4.1) *DNAH5* c.9751G>C, p.Ala3521Pro was selected for functional modelling in kidney organoids.

DNAH5 c.9751G>C has a low allelic frequency in population databases and high aggregate damage scores.(Table 4.1) The p.Ala3521 displays very high amino acid conservation throughout vertebrates (Figure 4.2) and is positioned in an alpha helix domain in the stalk of the protein. *DNAH5* is expressed in kidney tissue. Olbrich et al. performed Northern blot analysis on mouse tissue and demonstrated the strongest bands in lung and kidney, ahead of brain, heart and testis.(Olbrich et al., 2002) Pathogenic variants in *DNAH5* have an established human phenotype in PCD3 for which no renal phenotype is established. The RG1005.213 proband does not manifest any clinical evidence of a motile ciliary deficit (ie. dextrocardia, chronic suppurative lung disease).

Genomic Position	Gene Name	Change	Predicted Consequence	Max AF	Damage Score
Chr16:27231905	KDM8/JMJD5	G>T (Asp407Tyr)	Missense variant; non-coding transcript exon variant	0.003	7
Chr5:13769215	DNAH5	C>G (Ala3251Pro)	Missense variant; non-coding transcript exon variant	0.0001	7
Chr2:192711230	CAVIN2	C>T (Arg141Gln)	Missense variant; upstream gene variant	0.0000	6
Chr7:56144566	SUMF2	G>A (Arg211His)	Missense variant; synonymous variant; 3 prime UTR variant; non-coding transcript exon variant	0.015	6
Chr12:48374717	COL2A1	G>A (Ala833Val)	Missense variant; non-coding transcript exon variant	0.0000	4
Chr2:217315774	SMARCAL1	C>T (Thr686Ile)	Missense variant; non-coding transcript exon variant	0.0000	4
Chr12:29521198	ERGIC2	T>C (Ile80Val)	Missense variant	0.0014	3
Chr2:210699664	UNC80	G>A (Gly991Ser)	Missense variant; non-coding transcript exon variant	0.0000	2

Table 4.1 Prioritised homozygous variants for RG1005.213 following trio whole exome sequencing
Max AF indicates the maximum allelic frequency documented in any subpopulation of the ExAC or 1000G databases.
Damage Score is a rudimentary aggregate damage score essentially provides the number of damage prediction algorithms that predict the variant to be damaging, pathogenic or likely pathogenic. Algorithms include: SIFT, Polyphen, LRT, MutationTaster, MutationAssessor, FATHMM, PROVEAN & CADD.

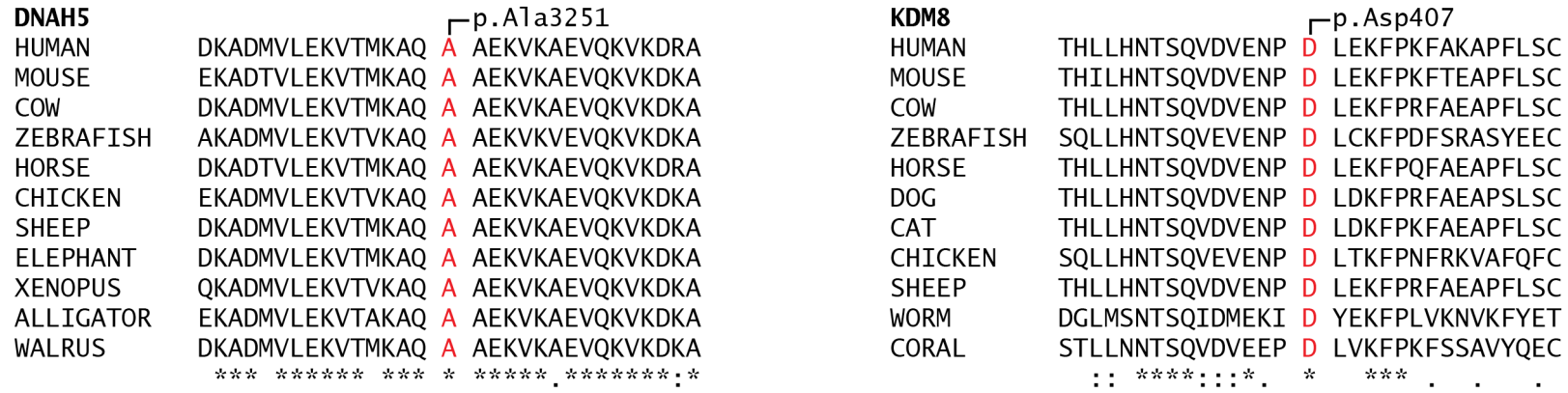

Figure 4.2 Interspecies amino acid conservation for *DNAH5* and *KDM8* variants
WORM: Trichinella spiralis, CORAL: Stylophora pistillata. Generated by Uniprot, https://www.uniprot.org/

However, the vast majority of clinically reported *DNAH5* variants affect premature termination or frameshift of the protein (Olbrich et al., 2002) and it is possible that more subtle variants could produce alternative phenotypes. The ENU derived *Dnah5*^{b2b1003Clo} homozygous mouse phenotyped by the Jackson Laboratory illustrates kidney cysts and duplication in addition to *situs inversus* and immotile respiratory cilia.(https://www.jax.org/strain/013684, accessed 8th October 2018) Of relevance, *DNAH5* was significantly differentially downregulated in the DGE analysis performed for the *IFT140* modelling project.(Forbes et al., 2018) It was hypothesised that *DNAH5* c.9751G>C variant kidney organoids would demonstrate similar abnormalities in ciliary morphology, cyst culture and gene expression, to that seen in the IFT140 project.

Considering this information, a decision was made to validate this variant in both kidney organoids and mice. As no foreseeable clinical opportunity to collect a skin biopsy from the patient existed, iPSC were reprogrammed from patient PBMC by the MCRI iPSC Core Facility. These iPSC cells underwent gene correction for the NM_001369.2:c.9751G>C variant by the MCRI Gene Editing Core Facility. Genotypes were validated by Sanger sequencing and, pluripotency was confirmed by flow cytometry and SNP microarray confirmed no major structural genomic imbalances.(Figure 5.11)

4.4.3 DNAH5 c.9751G>C kidney organoids do not demonstrate abnormal ciliary morphology or polarisation defects compared to gene edited control.

The differentiation protocols were optimised for patient-derived and gene-corrected iPSC clones in E6 media. In order to determine the ideal CHIR duration for the iPSC, both clones were treated with each of three, four and five days of CHIR99021 during the cell monolayer phase of differentiation.(Figure 4.3a and 4.3b) Kidney organoid end point was validated by the presence of all four segments of the nephron by immunofluorescence.(Figure 4.4) Consistent with the original published protocol, longer relative CHIR exposure was associated with more proximally patterned nephrons, demonstrating the ability to alter the nephron patterning of the organoid by manipulating the relative time cultured in CHIR99021 versus FGF9 prior to dissociation.(Takasato et al., 2015) Paradoxically, for the patient iPSC clone, the greatest representation of ECAD+/GATA3+ epithelium was in the 5 day CHIR condition, forming a central, reticulated network linking the surrounding nephrons.(Figure 4.4) Whilst this is a

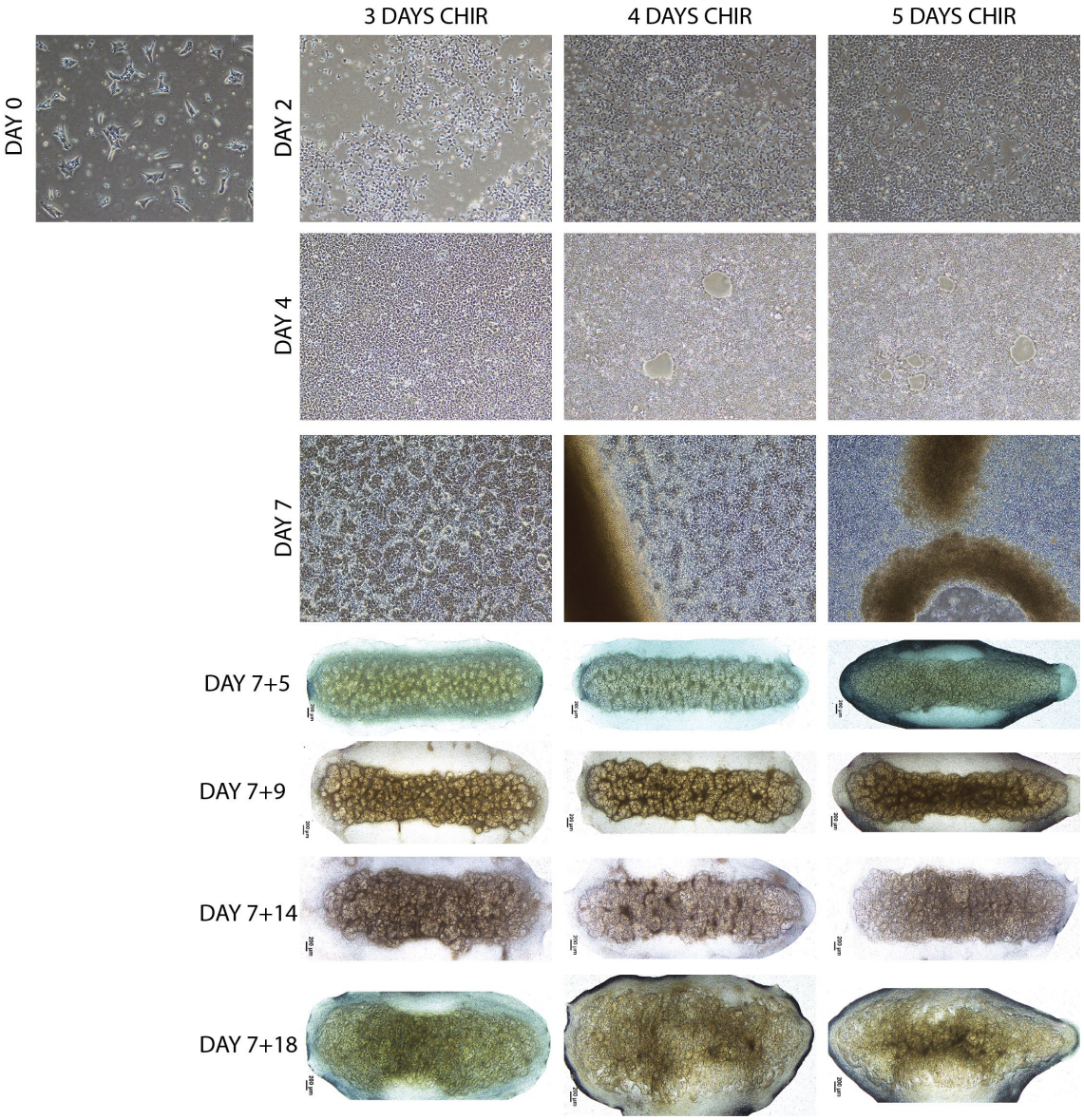

Figure 4.3a Optimisation differentiation experiment for *DNAH5* PT and GC iPSC clones
The differentiation of the patient clone is pictured above. To establish the ideal differentiation conditions for each iPSC clone, duration of CHIR99021 treatment of the monolayer was varies between 3 and 5 days. The 3 day CHIR condition was subsequently treated with 4 days of FGF9 before dissociation and bioprinting, the 4 day CHIR condition with 3 days of FGF9, and so on. The remainder of the protocol continued as indicated. Whilst bright field images are able to illustrate the development of structures, in the absence of any inbuilt fluorescent reporter expression, bright field morphology is poorly predictive of nephron patterning. Scale bars 200 um.
.

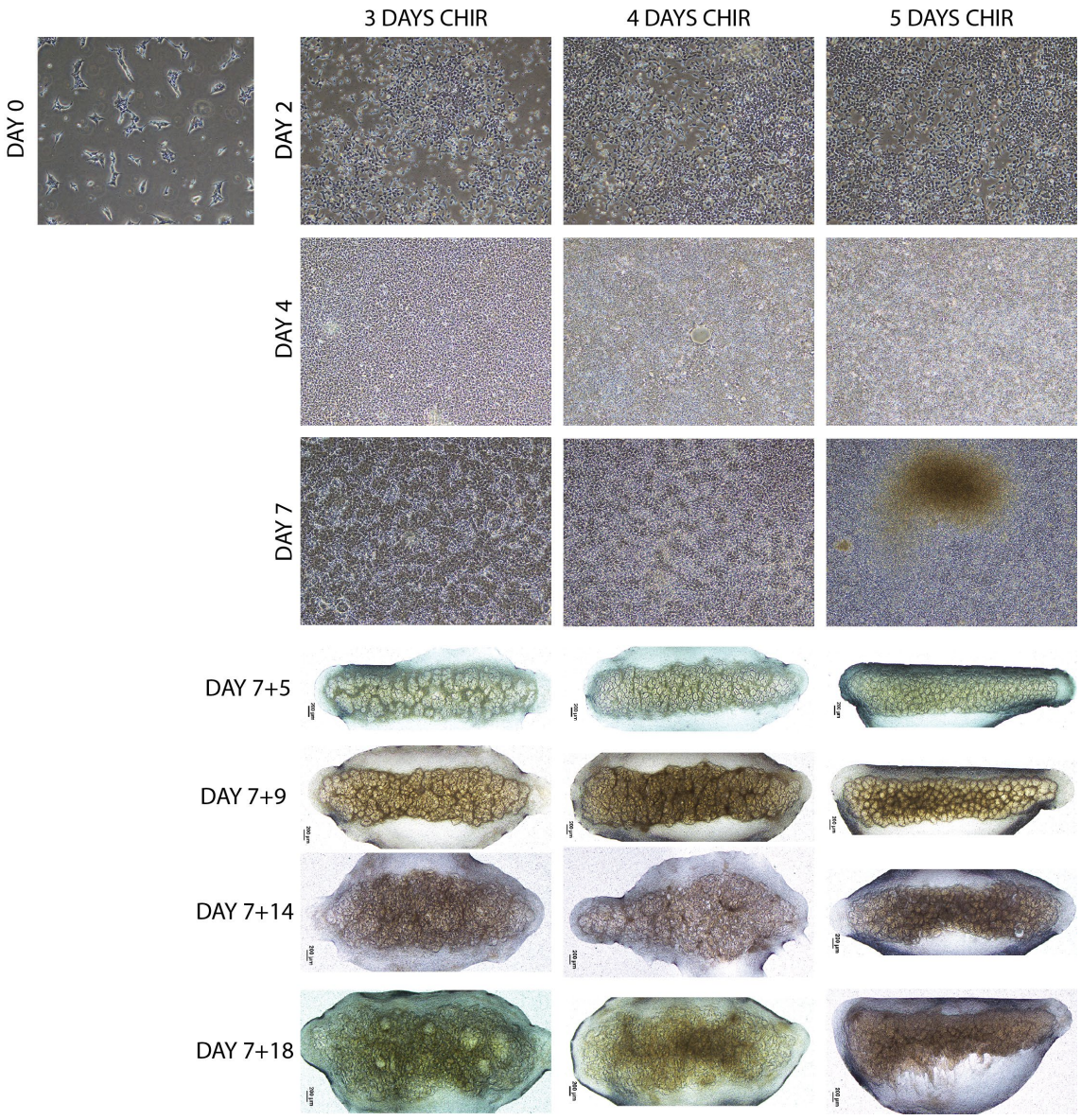

Figure 4.3b Optimisation differentiation experiment for *DNAH5* PT and GC iPSC clones
The differentiation of the DNAH5-GC clone is pictured above. Scale bars 200 um.

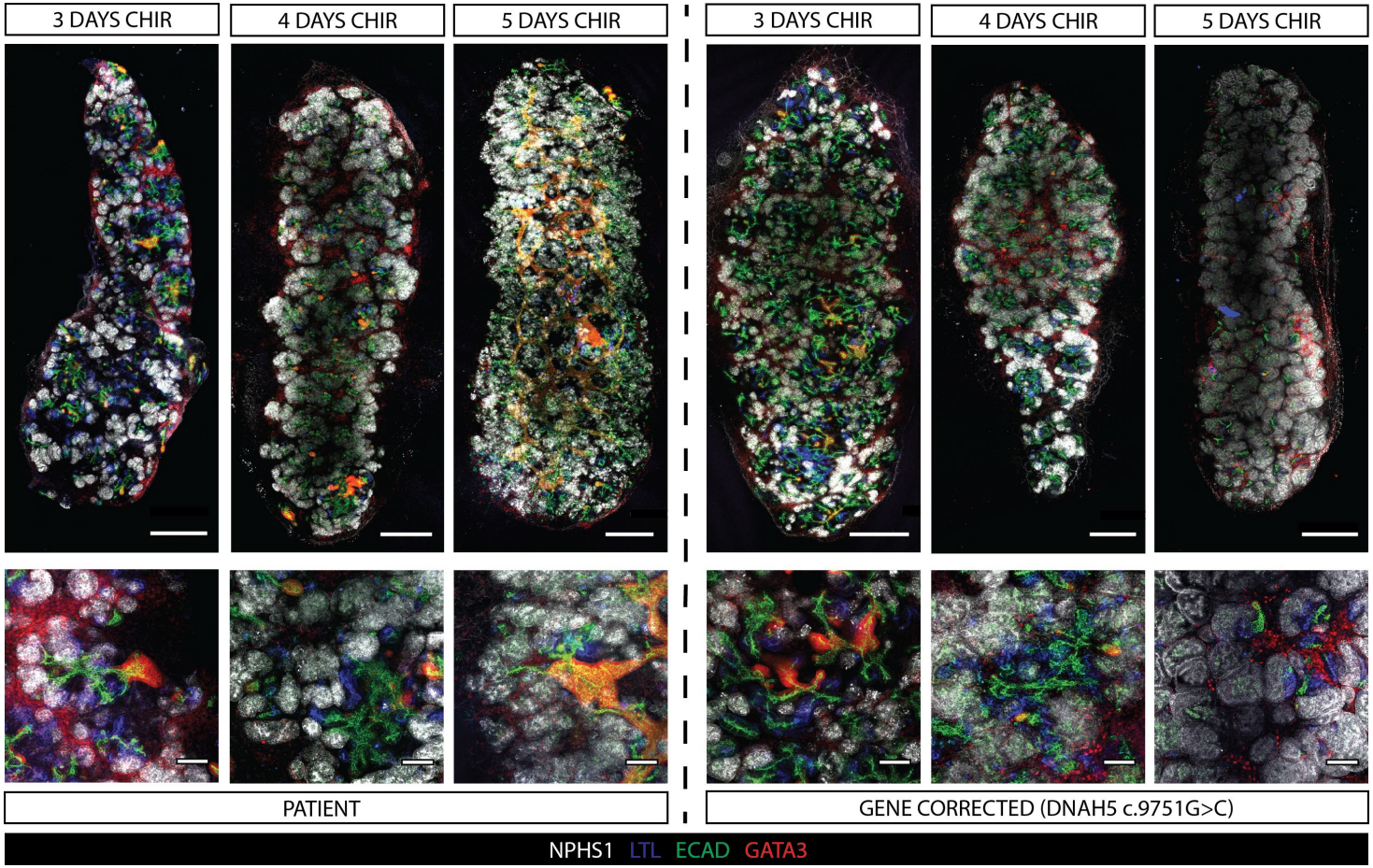

Figure 4.4 Immunofluorescent validation of optimisation differentiation experiments at day 7+18
Glomeruli are stained with NPHS1 (white), proximal tubule is stained with LTL (blue), distal tubule is stained with ECAD (CDH1, green) and collecting duct is coimmunofluorescent for ECAD and GATA3 (green and red respectively). For both lines with increasing CHIR99021 duration, there is an increased representation of glomerular structures. Paradoxically the patient line 5 day CHIR organoids developed a network of ECAD+/GATA3+ epithelial tubules linking nephron structures. This has been observed previously and is not well understood.

morphology our laboratory has witnessed on previous occasion in other iPSC clones at higher CHIR concentrations, it is not understood how it arises. Whilst this would have been an ideal organoid for epithelial characterisation, the same condition from the gene-corrected iPSC clone provided the opposite extreme of nephron patterning. These organoids demonstrated dense NPHS1+ glomeruli and only few ECAD+/GATA3+ structures precluding a comparative analysis of tubular epithelium. (Figure 4.4) The 3 day conditions were selected for further analysis as they were the most similarly patterned paired differentiation, with acceptable and feasibly reproducible tubular representation.

Correction of the *DNAH5* c.9751G>C variant did not affect ciliary length or morphology in wholemount ECAD+ organoid tubules.(Figure 4.5A,B) The mean primary ciliary length within patient tubules (1.61 um, SEM 0.02 um, n = 726) was not different to that measured in gene-corrected tubules (1.62 um, SEM 0.02 um, n = 800; p = 0.53). An similar proportion of distal tubular cilia demonstrated a straight, wild type morphology in both PT (49.7%) and DNAH5-GC (48.8%) organoids.(Figure 4.5C) Indeed, an increased proportion of DNAH5-GC cilia revealed a clubbed morphology (26.0% vs 15.0%).(Figure 4.5C)

Matrigel cyst culture of EPCAM+ MACS sorted epithelial cells from both organoids did not reveal differences in polarisation or open lumen formation.(Figure 4.5D,E) The percentage of cysts demonstrating apical expression of ZO-1 and F-ACTIN was the same in patient and gene-corrected conditions (PT 80.00% vs GC 83.24%, p = 0.46).(Figure 4.5E) No difference in cyst size by cross-sectional area was evident between the genotypes (μ: PT 3877 μm^2 vs GC 3134 μm^2; Δμ 742, 95%CI -1.6 to 0.09; n = 160). (Figure 4.5F) There was a trend towards increased mean cyst perimeter (μ: PT 282 μm vs GC 247 μm; Δμ -34, 95%CI -62 to -7) and maximum diameter (μ: PT 96 μm vs GC 85 μm; Δμ -11, 95%CI -21 to -2) in the patient cysts compared to gene corrected. However the magnitude of difference was not felt to be significant, was in the opposite direction to that hypothesised and failed to reach statistical significance following adjustment of false discovery rate for multiple comparisons of co-dependent variables.(Figure 4.5G,H)

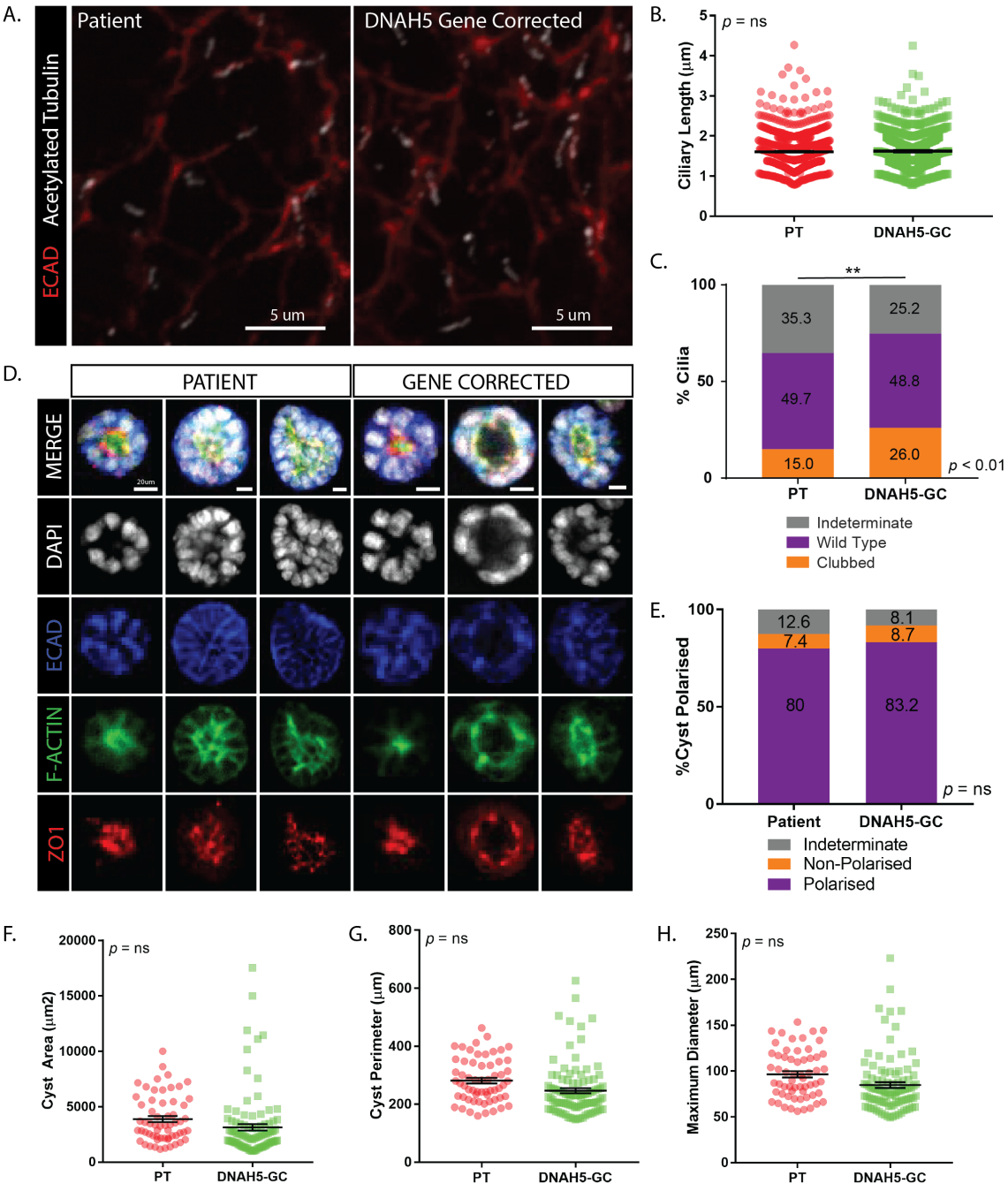

Figure 4.5 Ciliary analysis and epithelial cyst culture from PT and DNAH5-GC organoids
(A) Ciliary morphology was examined by immunofluorescence for acetylated tubulin in ECAD+ regions of whole mount kidney organoids. (B) No difference was found in ciliary length between PT and DNAH5-GC organoids. (C) There was no difference in the proportion of cilia with wild type morphology. DNAH5-GC cilia had slightly higher proportion of clubbed cilia but fewer cilia of indeterminate morphology. (D) Matrigel cyst culture of MACS sorted epithelium demonstrated no difference in ECAD+ polarised cyst formation (E), cyst area (F), perimeter (G) or diameter (H). Error bars: standard error of mean. Scale bars as marked. Categorical variable assessed with chi squared test, continuous variables with unpaired t test.

4.4.4 DNAH5 *c.9751G>C kidney organoid epithelium does not demonstrate transcriptional abnormalities in axonemal dynein assembly.*

The original selection to model the *DNAH5* c.9751G>C variant was partly founded on the observation of downregulation of *DNAH5* in *IFT140* organoid epithelium compared to DNAH5-GC control. Using qPCR the transcriptional activity of other components of the axonemal dynein assembly pathway was compared in RNA lysates obtained from EPCAM+ MACS sorted epithelium from the PT and DNAH5-GC organoids. (Figure 4.6A) There was no evidence of differential downregulation of *DNAH5* or other dynein axonemal assembly genes (*DNAAF1, DNAH1, DNAI1 or CCDC114*) between the two epithelial cell isolates. For completeness, qPCR was also examined for the other differentially expressed genes from the IFT140 project. No significant difference in expression of polarity, EGF signalling or cell-junction component pathways was found. (Figure 4.6A)

Given the lack of evidence of differential gene expression between patient and gene corrected organoids, it was possible that *DNAH5* c.9751G>C was not the causative variant. As such, both patient and gene corrected lines would show an equivalent phenotype. To investigate this possibility, a non-isogenic, wild type control iPSC clone (CRL1502.3) was simultaneously differentiated alongside a paired differentiation of the patient and DNAH5-GC lines. Regrettably, technical difficulties precluded replication of qPCR for any gene within this three-way comparison besides *DNAH5* which was significantly downregulated in both PT and DNAH5-GC compared to non-isogenic control. With only one replicate from the non-isogenic control, it was not possible to perform statistics for other qPCR comparisons.

4.4.5 KDM8 *c.1219G>T is an alternative candidate genetic variant for RG1005.213*

The results thus far have been unable to establish a differential phenotype between *DNAH5* c.9751G>C variant organoids and a gene edited control. Simultaneously, a local collaborator had engineered a mouse model carrying the homozygous *DNAH5* c.9751G>C variant and has been unable to demonstrate a renal phenotype in post-natal mice up to 1 year of age. (Ian Smyth, personal communication)

A.

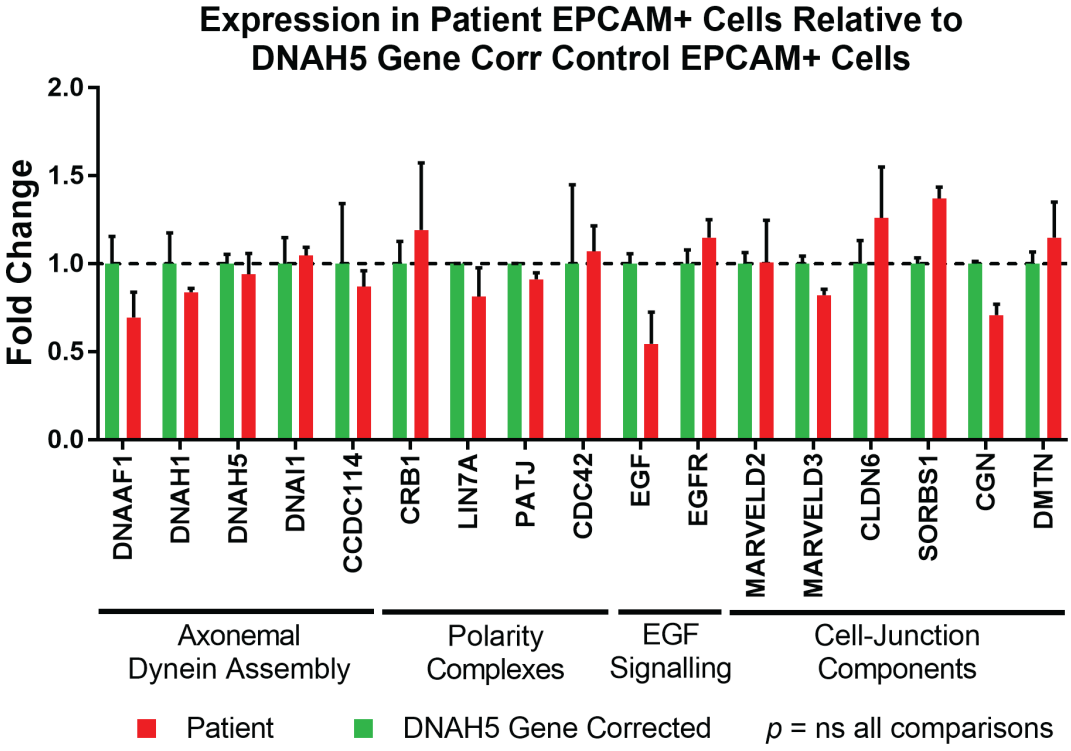

B.

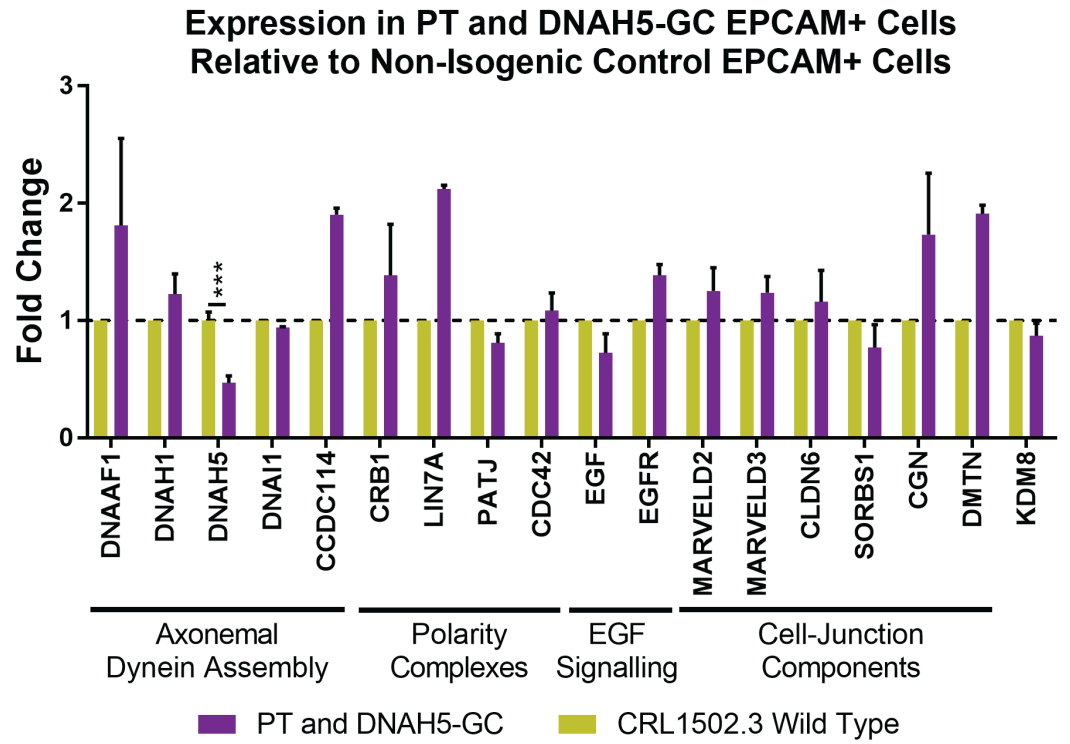

Figure 4.6 qPCR analysis of PT and DNAH5 EpCAM+ cells
(A) One of the reasons for selecting *DNAH5* for modelling was the fact it was downregulated in the IFT140 RNASeq dataset under the GO term Axonemal Dynein Assembly. No transcriptional difference in this set of genes or any other identified in the IFT140 project was observed between PT and DNAH5-GC cells. (B) An attempt to transcriptionally compare the combined PT and DNAH5-GC EpCAM together to a non-isogenic control demonstrated upregulation of these some of these genes by interpretation was limited by technical difficulties.

Considering the likelihood that the *DNAH5* c.9751G>C variant is not associated with RG1005.213's phenotype, the exome sequencing variant list was re-examined in an attempt to prioritise another potential variant. RG1005.213 carries a homozygous c.1219G>T variant in *Lysine demethylase 8* (*KDM8*; also known as '*Jumonji-C domain containing protein 5*' or *JMJD5*; OMIM: 611917). This variant is predicted as moderately damaging by all *in silico* programs used by the database (includes SIFT, M-CAP, Polyphen, LRT, MutationTaster, PROVEAN and CADD) and shows a low (but not rare) allelic frequency in the ExAC and 1000 genome databases of 0.003. The GnomAD database reports a single homozygous individual with no documented phenotype. Unlike *DNAH5*, no existing human phenotype is associated for pathogenic variants in *KDM8*. *KDM8* is expressed in the epithelial bulk RNA sequencing datasets from the IFT140 project (without differential expression between patient and control) and in our laboratory's wild type organoid single cell RNA sequencing database (data not shown). The affected amino acid is conserved throughout vertebrates to nematode and coral.(Figure 4.2)

KDM8 is a putative tumour suppressor gene. The protein acts in a complex with RCCD1 as a histone H3 lysine demethylase epigenetically regulating genes controlling cell cycle progression.(Ishimura et al., 2012, Marcon et al., 2014) During mitosis KDM8 colocalises at the mitotic spindle, increasing microtubular stability by α-tubulin acetylation and interkinetochore tension, satisfying the spindle assembly checkpoint, necessary to complete mitosis.(He et al., 2016) KDM8 interacts with the DNA binding domain of p53, negatively regulating its activity explaining why p53 transcriptional target gene *Ckdn1a* expression is upregulated in both *KDM8* knockout mouse and cellular models.(Ishimura et al., 2012, Huang et al., 2015) Mouse embryonic fibroblasts collected from embryos carrying a hypomorphic *KDM8* allele demonstrated severely reduced proliferation rate, which was rescued by siRNA knockdown of *Cdkn1a*.(Ishimura et al., 2012) Knockdown of either *KDM8* or *RCCD1* in HEK293 cells resulted in abnormal mitotic figures characterised by supernumerary centrosomes, disorganised multipolar spindle assembly and multidirectional chromosome segregation.(Marcon et al., 2014) Wu et al additionally localised KDM8 to the cell cytoplasm and established a role for microtubule stabilisation by regulation of MAP1B protein levels.(Wu et al., 2016) In this study, siRNA knockdown in HeLa cells decreased acetylation and detryosination of cytoplasmic α-tubulin, and

H2AX increased cell sensitivity to microtubule destabilisation agents.(Wu et al., 2016) Finally, *KDM8* siRNA knockdown in differentiated *in vitro* osteoclasts produced accelerated osteoclastogenesis by a reduced protein hydroxylation of NFATC1, a key osteoclastogenic transcription factor.(Youn et al., 2012)

There exists a number of similarities between *KDM8* function and other established NPHP-associated genes. Firstly, its association with mitotic spindle poles during mitosis is shared by MAPKBP1, a non-ciliary protein recruiting to the mitotic spindles poles during mitosis and associated with increased DNA damage response by ɣH2AX immunofluorescence in patient fibroblasts and renal biopsies samples.(Macia et al., 2017) A recent report from Bizet et al highlighted a role for IFT52 in the regulation of cytoplasmic microtubule stabilisation through interaction with MAP4 (Bizet et al., 2015), and this represents another proposed *KDM8* function.(Wu et al., 2016)

Whilst the literature suggests embryonic lethality in the setting of *KDM8* variants, most of the current literature on *KDM8* has been performed with siRNA knockdown or knockout models, raising feasibility that a hypomorphic missense variant could be associated with a more mild human disease phenotype.

D7+18 patient organoids were examined by whole mount immunofluorescence for phosphohistone H3. Repeated examination was unable to find any pHH3+ figures in either patient or DNAH5-GC tubules despite the regular appearance of normal appearing mitotic figures in the stromal regions of the organoids.(data not shown) When compared to non-isogenic control, *KDM8* transcription was similar between non-isogenic control, patient and DNAH5-GC epithelium.(Figure 4.6)

4.4.6 An attempt to utilise primary patient urine derived cells to validate KDM8 *as a candidate variant, ahead of commitment to organoid modelling.*

The gene correction of a second candidate variant in a patient iPSC cell line and the subsequent differentiation experiments represented a significant investment of time and money. Human urine derived renal epithelial cells (HURECs) are painless to collect and represent a straightforward approach for obtaining primary renal cellular material from

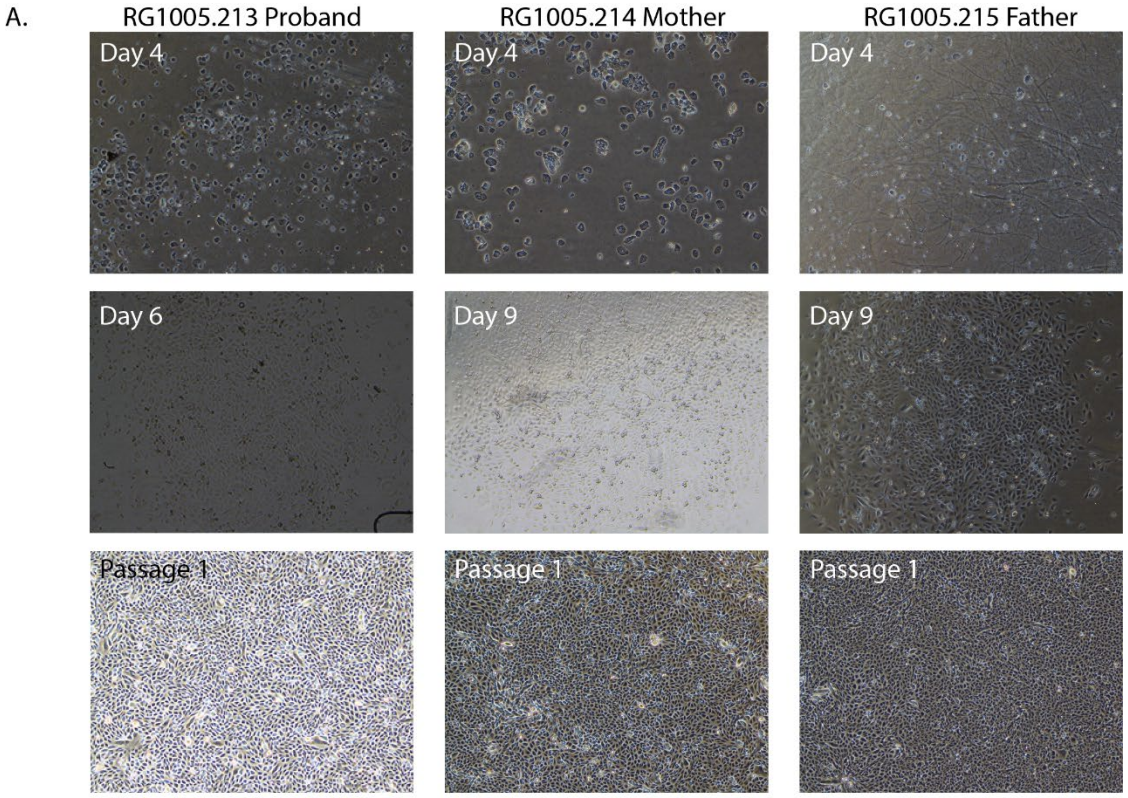
A.
RG1005.213 Proband
RG1005.214 Mother
RG1005.215 Father
Day 4
Day 4
Day 4
Day 6
Day 9
Day 9
Passage 1
Passage 1
Passage 1

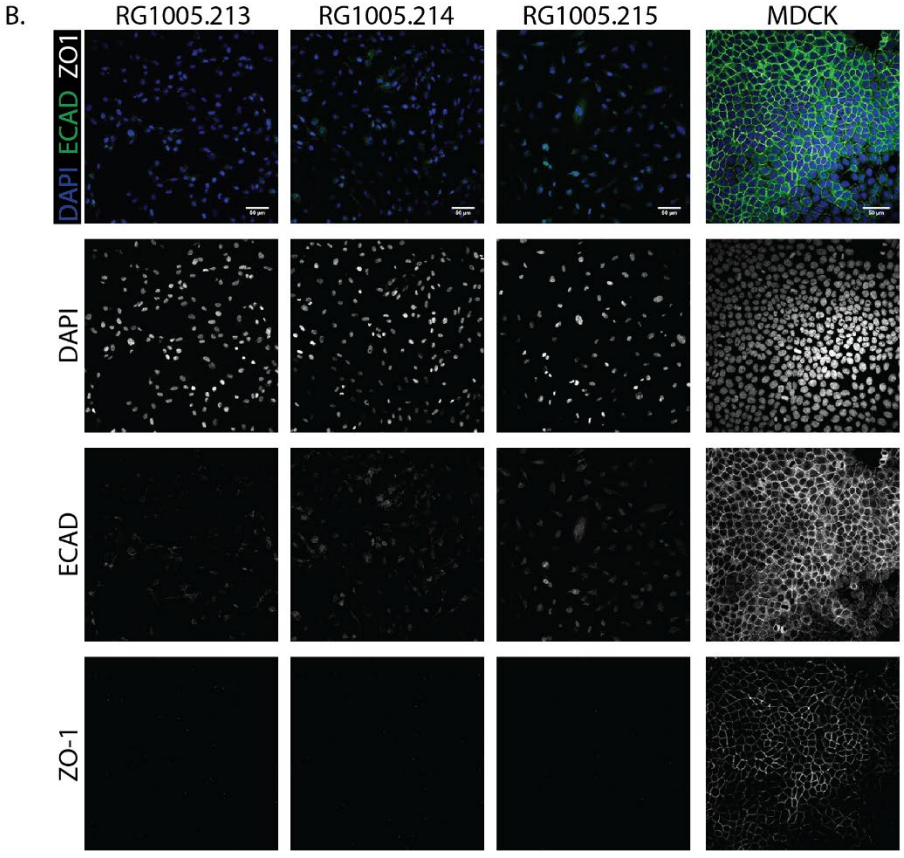
B.
RG1005.213
RG1005.214
RG1005.215
MDCK
DAPI ECAD ZO1
DAPI
ECAD
ZO-1

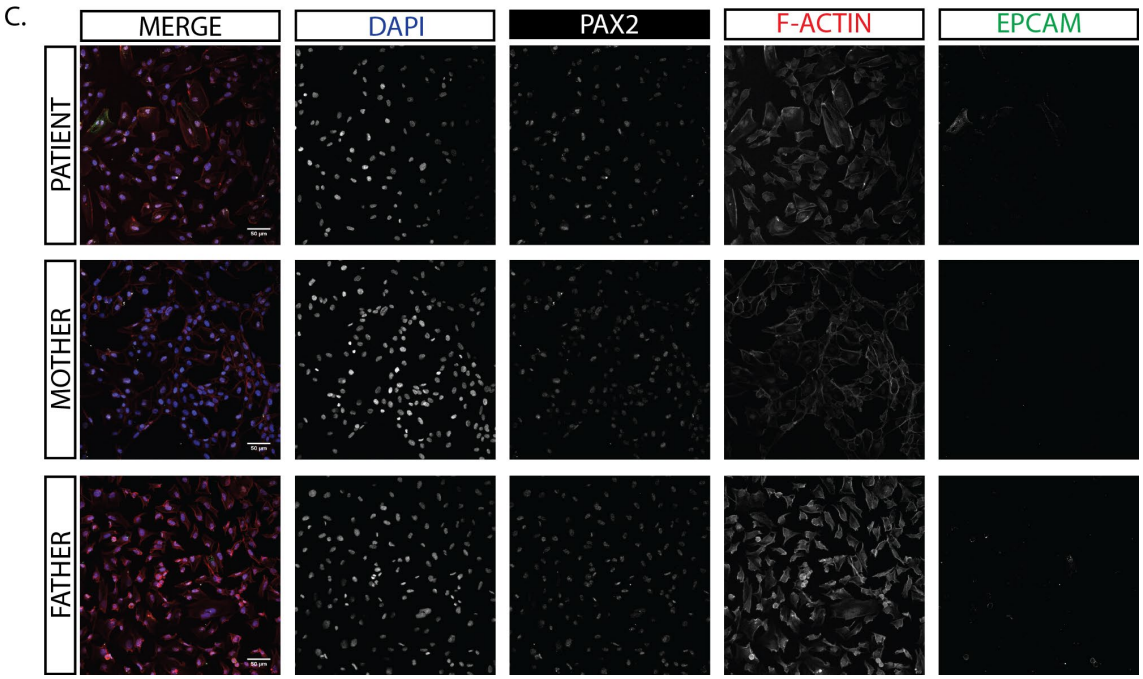

Figure 4.7 Culture of primary HURECs
(A) Bright field images taken during culture of HURECs from urine samples from patient, mother and father. (B) HURECs from all subjects were negative for ECAD and ZO1. (C) HUREC cultures were negative for EPCAM but positive for PAX2. Cell cultures were low in confluence and may improve epithelial marker expression at higher confluence. Scale bars 50 um.

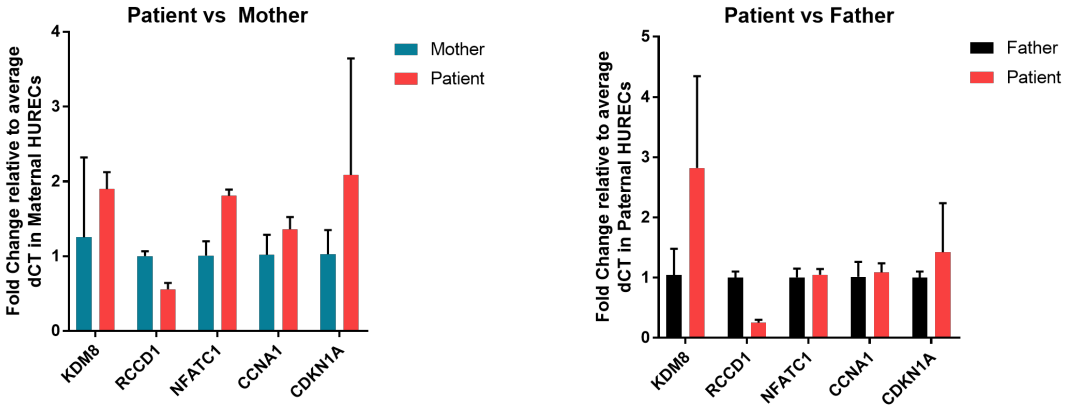

Figure 4.8 qPCR of HUREC cultures
Lysates were generated from two separate HUREC cultures. *KDM8* expression appears higher in patient HURECs than for either parent. *RCCD1* expression appears lower. *CDKN1A* expression was variable. None of the changes were statistically significant. (n = 2, students t test).

patients for preliminary functional genomic modelling or iPSC reprogramming.(Zhou et al., 2012) In an attempt to develop supporting evidence for the pathogenicity of the *KDM8* variant prior to further iPSC gene editing we cultured HURECs from patient and both parental urine samples.

All urine samples gave rise to cell colonies which proliferated at similar rates and appeared morphologically consistent to images presented in the Zhou et al. (2012) protocol.(Figure 4.7A) Bulk RNA sequencing of the patient HURECs (not the parental HURECs) was performed by a collaborating laboratory as part of a mutually exclusive project. This did not reveal any obvious qualitative canonical splicing abnormalities in any of the genes of interest, including *DNAH5* and *KDM8*.(Cas Simons, personal communication) Immunofluorescence of all lines was disappointingly negative for epithelial antigens including EPCAM, ECAD and ZO1 (Figure 4.7B,C), however this may reflect the low confluence of the cultures used for immunostaining. All lines demonstrated nuclear expression of PAX2 which would suggest a renal epithelial origin.(Figure 4.7C) qPCR of HUREC RNA lysates provided variable results that failed to reach statistical significance.(Figure 4.8)

Differential KDM8 protein expression between patient and parental HUREC lysates by SimpleWes capillary Western blot was unable to be reproducibly optimised prior to thesis submission but will be pursued as a potential means of prioritising this alternative genetic variant.

4.5 Discussion

This chapter describes an unsuccessful attempt to validate *DNAH5* c.9751G>C as a novel genotype for presumed NPHP. There are a number of factors that may have contributed to this negative finding. One probability is that *DNAH5* c.9751G>C is not the variant responsible for the renal disease in RG1005.213, which would suggest a need to optimise variant selection methods and thresholds. It is also possible that the variant was correct but the organoid assays performed were not of sufficient fidelity to demonstrate it. In spite of the lack of success in validating a variant for this pedigree, there are a number of learning points from this project which stand to improve our approach to prospective disease modelling projects.

Once believed to be a distinct disorder, NPHP is now understood to be a heterogeneous group of disorders with a broad genetic underpinning.(Braun and Hildebrandt, 2016) In clinical practice, renal biopsy is rarely performed in NPHP because the procedural risk of the biopsy procedure is greater than any benefit derived from a histological diagnosis, given there is no targeted treatment available. Accordingly it is well outside the scope of ethical genomic research to pursue such a procedure if it will be purely for academic benefit. This creates a challenge for research focused on novel gene discovery based entirely on an individual patient. RG1005.213 is presumed to have a diagnosis of NPHP on the basis of likely autosomal recessive inheritance, echogenic kidneys with evidence of microcystic change on ultrasound, a coarsened liver echotexture and soft facial dysmorphic features. However, there is no histological phenotype for this case and it is plausible that a biopsy could demonstrate segment specific features that may have directed alternative lines of inquiry within the organoid model. This project was approached assuming a distal tubular or pantubular pathology, an assumption that may have been incorrect. It is even plausible that RG1005.213 suffers from a non-ciliary renal dysplasia on the spectrum of congenital abnormalities of the kidney and urinary tract (CAKUT). Whilst one clear prospective benefit of diagnostic sequencing for renal disease is the ability to make a diagnosis without renal biopsy, it is possible that with an increasing understanding of the heterogeneity of diseases like NPHP, deep histological phenotyping could play an active role in characterising disease and directing functional genomic analyses in patients referred for research genomics.

Assuming that the definitive phenotype for RG1005.213 *is* NPHP, one could reasonably argue it was ambitious to attempt to redefine a novel phenotype for a gene with an already strongly associated phenotype, as PCD3 is for *DNAH5*. Whilst rare, the association between motile and non-motile ciliopathy is described. Mutant mouse models of *INVS/NPHS2* demonstrate reduced ciliary beating frequency and angle in respiratory cilia.(Tsuji et al., 2016) Similarly, a patient with tracheal motile ciliary dyskinesia and NPHP associated with a truncating variant in *IVNS/NPHP2* has been described.(Moalem et al., 2013) Variants in *CCDC114* previously associated with isolated PCD (Knowles et al., 2013) have recently been described in patients with comorbid renal dysplasia and sensorineural hearing loss.(Li et al., 2019) A recent, unpublished, local study of motile cilia function in patients with genetically proven NPHP has identified subtle slowing of

ciliary beat frequency and increased mean ciliary deviation. (Phil Robinson & Catherine Quinlan, personal communication). Taken together this evidence suggests a less mutually exclusive clinical phenotype between primary and motile ciliopathies than previously thought, which is not surprising given the profound ultrastructural similarities between the two types of cilia. Given the rarity that a mutually exclusive phenotype is presented for a gene with an established link to a monogenic disease, pursuing such a scenario in the future is likely to be of similarly low yield.

Published research describing novel Mendelian gene discovery for NPHP has frequently involved positional cloning, linkage analysis and/or homozygosity mapping across multiple unrelated individuals with a similar genotype and phenotype.(Hildebrandt et al., 1997, Haider et al., 1998, Mollet et al., 2002, Sayer et al., 2006, Otto et al., 2010) By comparison to most established international renal genomic databases, the KidGen research genomics database is young. Having collected prospective data from genetically unresolved patients for only 5 years, this database is unlikely to contain multiple unrelated patients with collective variants in ultra-rare disease genes. Therefore, collaboration with more established databases as well as international genotype matching programs such as Matchmaker Exchange (https://www.matchmakerexchange.org/ accessed 24/09/19), will be paramount to our group's ability to identify multiple affected families affected by our candidate genotypes prior to investing in organoid modelling projects. We have inquired with an international collaborator who was unable to find any homozygous variants in *KDM8* in a database of around 400 unsolved NPHP probands.

A major aspect of the decision to model the *DNAH5* c.9751G>C variant was the observation of transcriptional downregulation of *DNAH5* in the IFT140 project DGE analysis. This would not be the first cytoplasmic dynein motor protein described to interact with an IFT protein. DNAAF1 [OMIM 613190] is dynein motor assembly protein typically associated with Primary Ciliary Dyskinesia Type 13 that displays variable cardiac phenotype and interacts with IFT88 for its proper function.(Hartill et al., 2018) Because of the link to the IFT140 transcriptional profiling, we hypothesised that the same set of assays would demonstrate differential results. However, no difference was observed in ciliary length or morphology between iPSC-derived PT and DNAH5-GC organoid epithelium. This would suggest that the transcriptional downregulation of *DNAH5* in the

IFT140 dataset is a consequence of disordered retrograde IFT, rather than disordered retrograde IFT ensuing from dynein motor assembly defects. There was also no difference between PT and DNAH5-GC epithelium capability to form polarised cysts from single cells. The percentage of polarised ECAD+ cysts was higher in both patient and gene-corrected conditions (~80%) than seen in the IFT140 dataset (40-60%). Potential explanations for this include: (i) not aspect of the disease phenotype; (ii) improved technical skill in handling the MACS sorted cells with lower cell trauma or (iii) reduced contamination of the analysis by non-epithelial or dedifferentiated cells by ECAD+ cyst isolation. The sampling speed from the spinning disk microscope allowed us to improve the cyst culture analysis by imaging the entire Chamberslide well for each genotype and then filtering out ECAD positive cysts and shuffling them for blinded assessment. On one hand this filtering approach standardises the comparison by isolating cysts that have arisen from a cells of a defined nephron segment, reducing the potential for differential nephron patterning to bias results. Alternatively, there is a risk that the defined segment may not express the cyst phenotype which could then be missed.

Unable to demonstrate a validating phenotype using the above methods, the variant prioritisation list was revisited to consider other potential candidates. This included differentiating a third non-isogenic iPSC clone as an external control to the *DNAH5* comparison. Disappointingly, the cyst culture from this three way experiment failed due to technical issues following mounting the slides, but given the cyst polarisation rate in the diseased lines was so high, it is unlikely the non-isogenic control would have been superior. The higher expression of genes involved in dynein motor assembly, crumbs polarity complex and cell-cell junction components demonstrated by qPCR in the diseased lines highlights the importance of isogenic controls in the field of iPSC derived organoid disease modelling. Whilst replicates of this experiment would have strengthened the data, it was exceptionally difficult to coordinate three simultaneous differentiations side by side, and unfortunately it was beyond the scope and funding of this project to repeat this.

Since the decision to model *DNAH5* c.9751G>C was made, a number of single cell RNA sequencing databases have been published illustrating low transcriptional activity of *DNAH5* in both human kidney and kidney organoids.(Wu et al., 2018a, Wu et al., 2018b,

Phipson et al., 2019) *DNAH5* is expressed at low levels in the renal epithelium single cell RNA sequencing datasets from healthy adult kidney biopsies, most prominently in the loop of Henle (~6% of cells) but also the proximal tubule and principle cells of the collecting duct (both ~4% of cells)[**].(Wu et al., 2018a, Wu et al., 2018b) Our own organoid single cell RNA sequencing dataset demonstrates some *DNAH5* expression in the organoid epithelial cluster (~6% cells)(Phipson et al., 2019), though it was more poorly expressed when the Takasato organoid protocol was replicated by Wu and colleagues (~1.2%).(Wu et al., 2018b) *KDM8* is expressed at even lower levels again in human kidney (~2% of cells)(Wu et al., 2018a) and organoid (~4% of cells)(Phipson et al., 2019) epithelium. It is possible that the lower sequencing depth in single cell RNA sequencing (as compared to bulk RNA sequencing) may underrepresent the expression of these relatively lowly expressed genes. For example, *NEK8* is a well-established genotype for NPHP(Choi et al., 2013a, Grampa et al., 2016, Habbig et al., 2012, Otto et al., 2011, Otto et al., 2008) but is only expressed in <1% and 6% of the human kidney epithelial single cell RNA sequencing datasets respectively.(Wu et al., 2018a, Wu et al., 2018b) Gene expression also varies significantly in these datasets due to technical reasons with *NEK8* expression seen in up to 3% of various epithelial segments in the Wu et al replicate of the Takasato protocol(Wu et al., 2018b) but 25% of cells in the Phipson et al report of our protocol.(Phipson et al., 2019) Whilst these datasets may not be able to unequivocally advocate for gene expression in human kidney and organoid models, they represent an additional resource to contribute to the curation of future candidate variants.

Given that the *DNAH5* c.9751G>C variant was proposed on the basis of a single case, in a gene with relatively low expression in human kidney, and that ciliary length, morphology, cyst culture and focussed transcriptional signature have not revealed any significant differences, our provisional conclusion is that this variant is not disease-associated in RG1005.213.

One alternative approach to variant prioritisation is to utilise cheaper and faster preliminary *in vitro* methods to develop evidence in support of genes and variants prioritised by research genomic pipelines, before committing to organoid modelling.

[**] Accessed 29/9/2019 via online KIT Platform: http://humphreyslab.com/SingleCell/#. Published in this thesis with permission from Prof Ben Humphries.

Human urine derived renal epithelial cells (HURECs) are a source of primary cellular material from patients which represent a number of distinct advantages for our disease modelling program. In children, the collection of primary cells for disease modelling involves some distress, be it by skin biopsy or blood taking. Our ethical framework dictates that we cannot perform a skin biopsy or blood sample from a patient unless that procedure coincides with a clinically necessary venepuncture or anaesthetic. At present the gene editing core facility at MCRI is unable to utilise PBMC for combined reprogramming and gene correction, which is cheaper and gives rise to more clonal iPSC cell populations than a two-step process.(Howden et al., 2015, Howden et al., 2018) HURECs, however, are painless to collect, cheap to passage, tolerate freeze and thaw and maintain a high proliferation rate which is desirable for CRISPR-Cas9 gene editing. The generation of iPSC from HURECs is well documented.(Zhou et al., 2012, Zhang et al., 2015, Shi et al., 2016)

Previous reports have demonstrated the functional genomic utility of HURECs. Molinari et al characterised the tissue specific splicing of a synonymous putative splicing *NPHP3* variants in two NPHP patients with where blood and fibroblast mRNA transcript analysis was uninformative.(Molinari et al., 2018) The same group described profoundly elongated primary cilia in HURECs obtained from two siblings with compound heterozygote variants in *CEP290* and demonstrated a reduction in ciliary length when treated with Shh pathway stimulator purmorphamine and cyclin D kinase inhibitor roscovitine.(Srivastava et al., 2017b) For RG1005.213, no splicing abnormalities were identified in any of the candidate genes following whole exome sequencing of the patient HURECs. Ultimately, we had insufficient time during this candidature to optimise HUREC culture techniques, qPCR and Western blot protocols for this project. These protocols require further optimisation in our laboratory.

In summary we have been unable to validate a candidate variant for this pedigree at this time, which ultimately remains unresolved. The project has illustrated a number of learning opportunities for our program with respect to novel variant curation. A defined set of more stringent criteria, against which future candidate variants can be judged ahead of functional validation, will be necessary to optimise yield and efficiency for future projects, including but not limited to:

i. histological phenotyping or high confidence clinical phenotyping by syndromic associations,
ii. avoidance of genes with already established histological phenotypes,
iii. demonstration of genotype-phenotype correlation across multiple unrelated pedigrees,
iv. in the case of NPHP, evidence of gene product association with the primary cilia, centrosome or mitotic spindle in wild type immortalised or patient-derived cells, and/or
v. demonstration of direct a clear truncating effect of gene or protein expression using primary cells derived from patient and related control.

Chapter 5 Kidney organoids validate *NOS1AP* as a novel, patient-derived genotype for steroid resistant nephrotic syndrome.

5.1 Introduction

The previous chapters have described iPSC derived kidney organoid modelling of NPHP, a fibrocystic kidney disease arising from the dysfunction of the renal tubular epithelium. In this chapter kidney organoids are employed to model a novel genotype associated with SRNS, an inherited glomerular disease and the second most common cause of CKD in childhood.(Fletcher et al., 2013, 2014)

5.1.1 Steroid resistant nephrotic syndrome

NS describes severe proteinuria, sufficient to lower serum protein levels to the point of decreased plasma oncotic pressure resulting in tissue oedema. In the healthy state, protein filtration across the glomerular filtration barrier is prevented by the size and charge selectivity of the slit diaphragm, a specialised protein structure bridging the foot processes of glomerular podocytes. In nephrotic syndrome, these foot processes efface and the slit

diaphragm is lost allowing large amounts of protein to cross the glomerular filtration barrier.

A proportion of patients with SRNS suffer from a genetic form of the disease. Unlike idiopathic or SSNS, genetic SRNS represent intrinsic diseases of the podocyte as evidenced by the fact that an overwhelming majority of genotypes encode proteins that are highly expressed in podocytes and essential for their structure and function.(Löwik et al., 2009, Ashraf et al., 2018, Lovric et al., 2016, Warejko et al., 2018, Machuca et al., 2009) Between 11% and 45% of SRNS patients with onset under 25 years of age show evidence for a monogenic aetiology on whole exome sequencing.(Sadowski et al., 2015, Warejko et al., 2018, Tan et al., 2018) Indeed, there are now a sufficient number of SRNS genotypes identified to cohort gene products into functional podocyte pathways including slit diaphragm associated proteins, actin binding proteins, Rho/Rac/Cdc42 regulation of actin dynamics, coenzyme Q10 biosynthesis, integrin/laminin receptor interaction and nuclear transcription factors.(Lovric et al., 2016, Preston et al., 2019)(Figure 2.5)

Clinically, genetic nephrotic syndrome is often associated with progressive, fibrotic glomerulosclerosis and an expectant decline in kidney function leading to dialysis or transplantation.(D'Agati et al., 2011) To date there are no clinically available targeted therapies for most genetic forms of NS, however potential novel therapeutic targets are emerging as the understanding of NS pathogenesis increases.(Starr et al., 2018, Zhou et al., 2017, Greenbaum et al., 2012)

5.1.2 Kidney organoids as a model of glomerular disease.

By transcriptional profiling, human iPSC derived kidney organoids have been demonstrated as equivalent to trimester 1-2 human fetal kidney.(Takasato et al., 2015) As such, the organoid platform is best placed to model inherited diseases with onset in infancy. Three-dimensional glomeruli isolated from iPSC-derived kidney organoids have been comprehensively transcriptionally characterised, showing that they represent superior models of human glomeruli to the previously established gold standard, conditionally immortalised 2D human podocytes.(Hale et al., 2018) In human iPSC derived from patients with congenital nephrotic syndrome due to variants in *NPHS1*, expression of the gene product nephrin and slit diaphragm development was significantly

reduced.(Hale et al., 2018, Tanigawa et al., 2018) These reports demonstrate the feasibility of iPSC derived kidney organoid glomeruli as human disease models for the validation of novel gene discoveries.

5.1.3 Nitric oxide synthase 1 adaptor protein as a novel genotype for SRNS

Next generation sequencing has dramatically increased the rate of gene discovery in SRNS and our understanding of the molecular basis for genetic forms of SRNS.(Vivante and Hildebrandt, 2016, Lovric et al., 2016, Sadowski et al., 2015, Tan et al., 2018, Warejko et al., 2018) A subset of SRNS associated genes have been described in mice and humans which regulate the podocyte actin cytoskeleton include Rho GTPase cell division control protein 42 (*CDC42*), RhoGTPase cofactor Rho GDP Dissociation Inhibitor Alpha (*ARHGDIA)* guanine exchange factors intersectin 1 and 2 (*ITSN1* and *ITSN2*) and neutral Wiskott-Aldrich syndrome protein (*N-WASP*).(Gee et al., 2013, Scott et al., 2012, Ashraf et al., 2018, Schell et al., 2013)

CDC42 belongs to the Rho family small GTPases, alongside *RHOA* and *RAC1*. These GTPase proteins are involved in the regulation of actin cytoskeleton dynamics, maintenance of cell adhesion, cell polarity and motility.(Etienne-Manneville and Hall, 2002, Jaffe and Hall, 2005) The maintenance of cell polarity is via the interaction of CDC42 with the PAR polarity complex. When active CDC42 binds to the CRIB domain of PAR6, it induces a conformational change in the PDZ domain which releases aPKC from its binding domain.(Yamanaka et al., 2001) Both aPkc and Par3 have been localised to the anchor point of the slit diaphragm in immunogold EM of mouse pododcyte foot processes.(Hartleben et al., 2013, Hartleben et al., 2008) Also in mice, inhibition and podocyte specific knockout of *aPkc* and *Cdc42* lead to foot process effacement and the development of nephrotic range proteinuria.(Scott et al., 2012, Choi et al., 2013b, Huang et al., 2016)

Within their database of more than 2000 genetically unresolved patients with steroid resistant nephrotic syndrome, the laboratory of Prof Hildebrandt (Boston Children's Hospital) has identified two unrelated families presenting with onset of SRNS in infancy. Probands from both families carry homozygous variants in *Nitric Oxide Synthase 1 Adaptor Protein* (*NOS1AP*), a novel candidate genotype for SRNS.(Majmundar et al.

unpublished) The Hildebrandt group have demonstrated the podocyte specific expression of *NOS1AP* in both rat and human kidney in single cell RNA sequencing datasets. The have characterised HEK293 and conditionally immortalised 2D podocyte cell lines overexpressing wild type and patient-derived *NOS1AP* mutant vectors. Cells expressing *NOS1AP* mutant vectors demonstrated the reduced expression of active CDC42 levels, reduced podocyte migration and reduced podocyte expression of actin rich filopodia and podosomes.(Majmundar et al. unpublished)

In an invited collaboration with the Hildebrandt group, we set out to characterise organoids carrying homozygous, patient-derived variants in *NOS1AP*.

5.2 Methods

5.2.1 Generation of iPSC lines

A sgRNA plasmid specific to exon 5 of the *NOS1AP* locus (pSMART-sgRNA-*NOS1AP*) was generated by annealing ODNs CACCGTTACACCTGAAGATATTGC and AAACGCAATATCTTCAGGTGTAAC followed by ligation into the *BbsI* sites of the pSMART-sgRNA vector(Howden et al., 2018). To generate the *NOS1AP* template for HDR, a gblock (Integrated DNA Technologies) comprising 434 bp and 555 bp flanking the c.428G>A mutation was ligated into the pSMART-HCKan plasmid vector (Lucigen) (Figure 5.11A). A 3 bp CAG>TTC synonymous change was also included just upstream of the c.428G>A mutation to block Cas9 re-cutting and facilitate screening by allele-specific PCR. Plasmid DNA was propagated in DH5-alpha E.Coli (BIOLINE) and prepared for transfection using a Plasmid Maxi kit (QIAGEN). Transfections were performed using the Neon Transfection System (Thermo Fisher Scientific). iPSCs (derived from ATTC CRL-1502 and ATTC PCS-201010 fibroblasts) were harvested with TrypLE (Thermo Fisher) 2 days after passaging and resuspended in Buffer R at a final concentration of 1 X 10^7 cells/ml and added to a tube containing pSMART-sgRNA-NOS1AP, mRNA encoding Cas9-Gem (Howden et al., 2018, Howden et al., 2016) and the NOS1AP template plasmid. Electroporation was performed in a 100 µl tip using 1100 V, 30 ms, 1 pulse. Electroporated iPSCs were plated on 6-well Matrigel-coated plates containing Essential 8 medium with 5 µM Y-27632 (Tocris). Colonies containing the desired knock-in were screened by PCR followed by Sanger sequencing to confirm homozygosity of the c.428G>A mutation. Colonies containing successfully edited iPSCs

were subjected to a subsequent round of subcloning and screening to ensure a clonal population of gene-edited iPSCs. iPSCs were maintained and expanded at 37˚C, 5% CO_2 and 5% O_2 in Essential 8 medium (Thermo Fisher Scientific) on Matrigel-coated plates with daily media changes and passaged every 3–4 days with EDTA in 1X PBS as previously described(Chen et al., 2011).

5.2.2 Differentiation if iPSC derived kidney organoids

Kidney organoids were differentiated adapting a previously reported protocol (Takasato et al., 2015) depicted in Figure 5.1C. In brief 75,000 iPSC were seeded in 6 well plates on Growth Factor Reduced Matrigel in E8 media supplemented with Revitacell (Thermo Fisher). Cells were treated with 3 days CHIR99021 (7 µM, R&D Systems, refreshed day 2) followed by 4 days FGF9 (200ng/mL) and heparin (1µg/mL) in TeSR-E6 (STEMCELL Technologies) refreshed daily. Monolayers were dissociated to a single cell suspension using TrypLE on day 7 and resuspended in 5 µL TeSR-E6 media per million cells. Cells were bioprinted as previously described.(Higgins et al., 2018) The cell suspension was aspirated into a 100uL Gastight syringe with a 21-guage Removable Needle (Hamilton) and loaded onto a NovoGen MMX bioprinter (Organovo). Eight x 4mm lines of cells were printed onto 0.4 um membrane 6 well Transwell inserts (Corning). Transwells were treated with 5 µM CHIR99021 for one hour then 5 days of FGF9/Heparin, followed by 2 days all trans retinoic acid (2µM) before withdrawal of all growth factors. TeSR-E6 was then refreshed to transwells three times weekly.

5.2.3 Cyclohexamide Treatment

Kidney organoids were treated from day 7+17 with cyclohexamide 100 µg/mL (Merck) from for 18 hours prior to RNA lysis (Bioline Isolate II). qPCR was performed according to methods outline in previous chapters.

5.2.4 Simple Western Blot

Two whole organoids were lysed in RIPA buffer with protease inhibitor (1:500) for 15 minutes on ice. Lysates were vortexed for 45 seconds and centrifuged at 13.3g for 10 minutes at 4°C. The supernatant was collected and diluted 1:5 with 1x Sample Buffer (ProteinSimple). Protein quantification was performed using a 66-440kDa plate in a

ProteinSimple Wes Capillary Western Blot analyser according to the manufacturer's instructions, modified by denaturation for 8 minutes instead of 5 minutes at 95°C.

5.2.5 Periodic acid Schiff stain and glomerular tuft analysis.

Organoids were fixed in 4% PFA for 6 hours. They were set in 2% agar prior to tissue processing for standard paraffin wax histology. Organoid sections were cut at 3 µm and stained with periodic acid and Schiff's reagents (PAS). Organoid glomerular tufts were defined as linear organised monolayers of podocytes lining an established extracellular matrix.

5.2.6 Immunofluorescence

Organoids were fixed in 2% paraformaldehyde for 20 mins on ice and washed with PBS. Whole organoids were cut from the Transwell filter and blocked/permeabilised for 3 hours in 10% Donkey serum/0.3% Triton X/PBS. Both primary and secondary antibodies were incubated overnight at 4 degrees and washed with 0.3% Triton X/PBS. DAPI and phalloidin-568 were incubated for 3 hours at room temperature. Whole mounts were cleared with 90% glycerol. Images were obtained with an Andor Dragonfly Spinning Disk confocal microscope.

5.2.7 Quantitative immunofluorescence analysis

Following immunofluorescent staining, three cross sectional images were obtained from each organoid using an Andor Dragonfly Spinning Disk confocal microscope using identical microscope settings. Images were blinded and shuffled. Tiff images isolating the synaptopodin channel and aPKC/PAR3 were generated and manually thresholded. These thresholds were incorporated into an automated ImageJ workflow which converted the synaptopodin threshold into a binary mask to isolate the glomerular aPKC/PAR3 signal from the non-glomerular signal. The mean fluorescence intensity ratio was calculated by dividing the glomerular MFI by the tubular MFI for each individual image.

5.2.8 Electron microscopy

Organoids were fixed in 2% paraformaldehyde, 2.5% glutaraldehyde in 0.1M sodium cacodylate buffer and post-fixed in 1% osmium tetroxide, 1.5% potassium ferrocyanide

in 0.1M sodium cacodylate buffer. Organoids were subsequently rinsed in distilled water then dehydrated through a graded series of alcohols before embedding in Spurrs Resin(Spurr, 1969) according to standard electron microscopy protocol. Ultrathin sections were cut with a diamond knife (Diatome, Austria) using a Leica UC7 ultra-microtome (Austria), contrasted with aqueous uranyl acetate and lead citrate before viewing in a JEOL JEM 1400Flash (Japan) transmission electron microscope at 80kV.

5.2.9 Glomerular sieving from kidney organoids

Glomeruli were isolated from kidney organoids using a previously published protocol.(Hale et al., 2018) Twelve to sixteen whole organoids were washed with PBS and dissociated in TrypLE Select (1mL per 4 organoids per well of a 6 well plate). The dissociation was incubated at 37°C and titurated with a P1000 every three minutes until a homogenous solution was formed (roughly 15-18 minutes total). The cell-TrypLE solution was passed through 2 x 70 µm cell strainers (Falcon) and cells gently pushed through the strainer with the plunger of a 1 mL syringe before washing with 50 mL with washing buffer (5% fetal bovine serum in PBS) per strainer. The 70 µm strainers were discarded and the flow through passed sequentially through a 40 µm cell strainer (Falcon) and a 30 µm cell strainer (Miltenyi biotech), each washed with 50 mL of washing buffer. 40 µm and 30 µm were held upside down over a 92 mm petri dish and washed retrograde with washing buffer to isolate glomeruli. Isolated glomeruli were centrifuged at 2000g for 5 mins and lysed in RNA lysis buffer (Bioline).

5.2.10 Bulk RNA sequencing

Bulk RNA sequencing was performed using a similar protocol to that used in Chapter 3.5.6. RNA was used to generate libraries for paired-end sequencing using an Illumina Novoseq 6000 sequencer. Reads were trimmed using Trimmomatic 0.35 (Bolger et al., 2014) and mapped to the human genome (GRCh38) with STAR aligner 2.5.3a (Dobin et al., 2013) using the quantMode feature to generate gene count matrices. Limma 3.40.6 (Ritchie et al., 2015) and EdgeR 3.26.7 (Robinson et al., 2009) were used for library normalization and differential gene expression testing. The Goana function in EdgeR was used for gene ontology enrichment testing of differentially expressed gene lists.

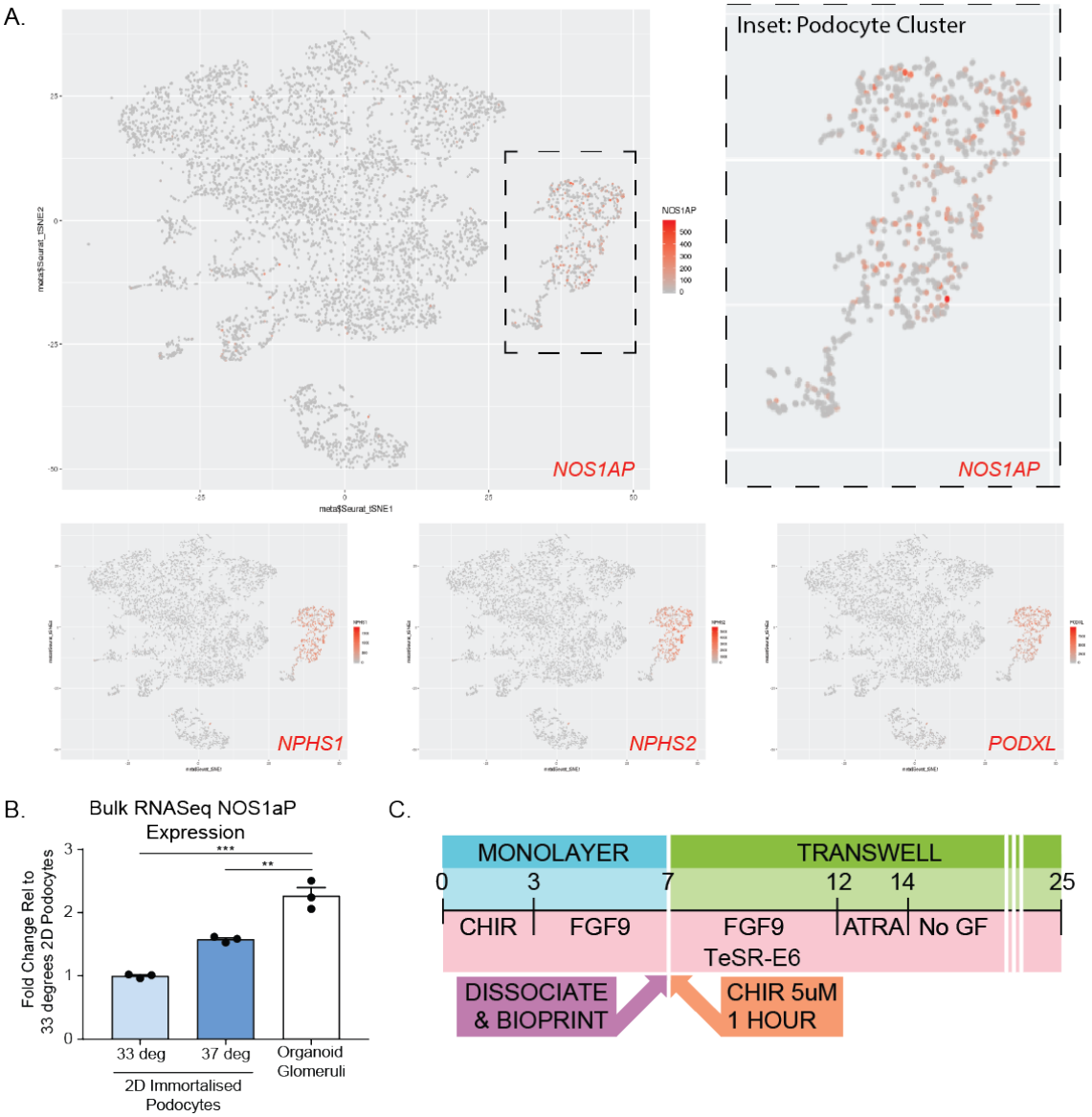

Figure 5.1 Transcriptional evidence of NOS1AP in kidney organoids
(A)Single cell RNA sequencing tSNE plot illustrating *NOS1AP* expression greatest in the podocyte cell cluster identified by strong co-expression of NPHS1, NPHS2 and podocalyxin. (B) Bulk RNA Expression of glomeruli isolated from WT kidney organoids demonstrates stronger expression of NOS1AP than 2D podocyte cultures. (C) Modified differentiation protocol.

5.2.11 Statistics

Statistical analyses of continuous variables were performed in GraphPad Prism (version 7.04) using unpaired t test with Welch's correction for unequal variance. A type I error rate of 0.05 was considered significant.

5.3 Results

5.3.1 Kidney organoid glomeruli express more NOS1AP *than 2D podocyte cultures*

As has been presented in earlier chapters, prior to functionally modelling a genotype with a kidney organoid, it is important to establish the expression pattern of that gene in the organoid. Therefore, single cell RNA sequencing datasets generated from Takasato protocol kidney organoids (Takasato et al., 2015, Phipson et al., 2017) were interrogated for *NOS1AP* expression. Consistent with the findings of the Hildebrandt laboratory in human and rat glomeruli, *NOS1AP* expression was strongest in the podocyte cluster of human kidney organoids.(Figure 5.1A) Additionally, the expression of *NOS1AP* in human organoid glomeruli was superior to 2D conditionally immortalised podocyte cultures.(Figure 5.1B)

5.3.2 Selection of NOS1AP *c.428G>A for iPSC kidney organoid modelling*

Dr Sara Howden performed combined reprogramming and *NOS1AP* c.428G>A variant insertion into CRL1502.3 (female) and ATTC PCS201010 (male) wild type cell lines. For all derived clones genotype was confirmed by Sanger sequencing. Mycoplasma screening was negative.

5.3.3 The NOS1AP *c.428G>A allele produces a misfolded protein.*

Having established NOS1AP was expressed in organoid glomeruli, we examined the protein localisation in the organoids by immunofluorescence. In WT organoids, whole mount immunofluorescence localised NOS1AP to the slit diaphragm, co-localising with synaptopodin (SYNPO) on the apical surface of podocytes and encircling a basement membrane represented by laminin-α5 (LAMA5) immunostaining.(Figure 5.2A) Consistent with single cell RNA sequencing transcriptional data, no NOS1AP protein expression was detectable in proximal or distal tubular segments.(Figure 5.2B) Using the

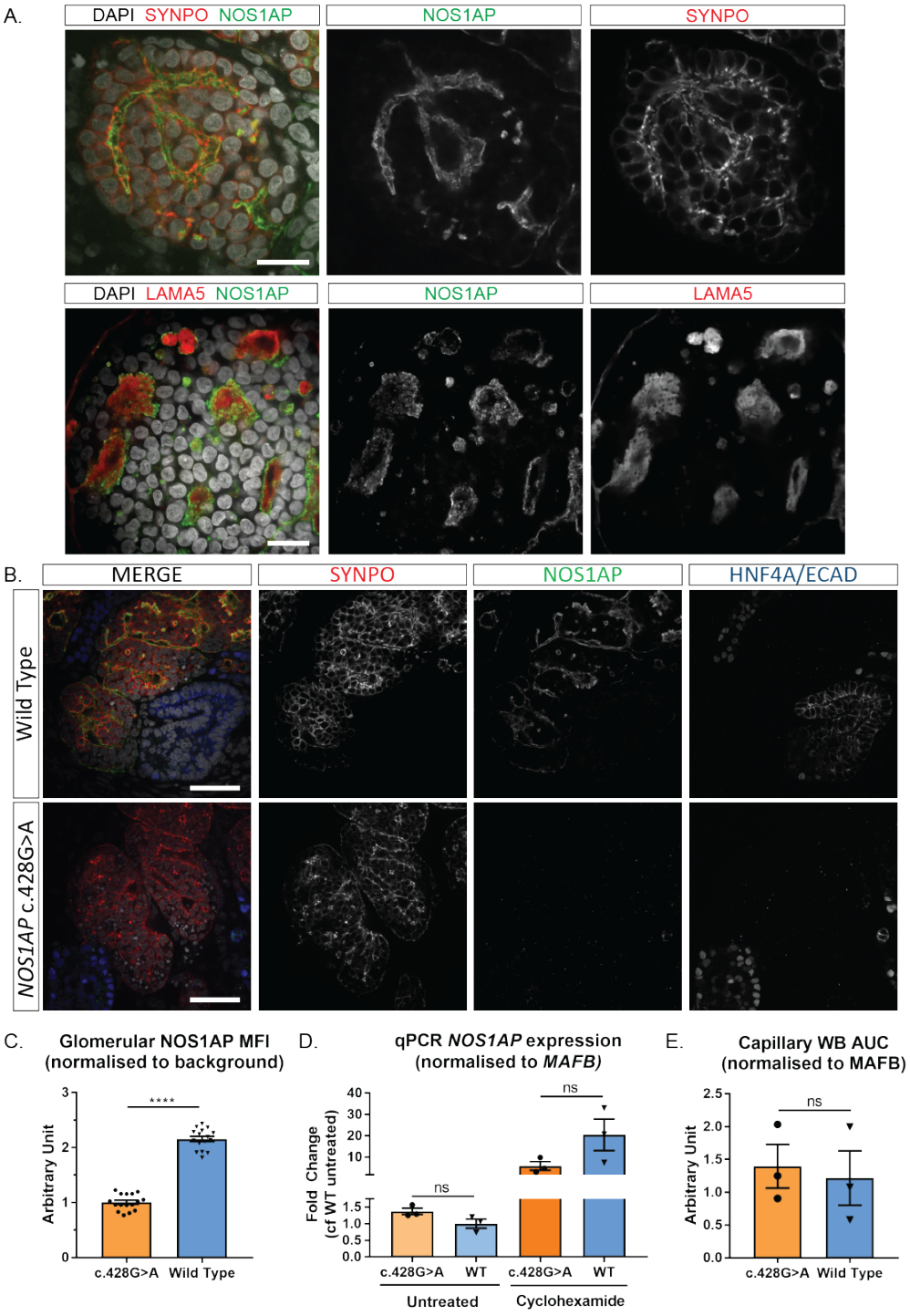

Figure 5.2 NOS1AP expression in organoids
(A) WT organoid immunofluorescence demonstrating NOS1AP protein expression at slit diaphragm between synaptopodin (SYNPO) and lamanin-A5 (LAMA5). Scale 20um. (B) Wild type organoids demonstrate isolation of NOS1AP expression to glomeruli (SYNPO) with no signal evident in proximal (HNF4A, nuclear) or distal (ECAD, cell wall) tubules. NOS1AP c.428G>A organoids demonstrated no detectable NOS1AP expression. Scale bar 50um. (C) Quantification of mean fluorescence intensity of NOS1AP in SYNPO+ glomeruli. Mean +/- SEM. Colours represent individual experiments, shapes represent genotypes (students t test, p <0.0001) (D) qPCR of untreated and cyclohexamide (nonsense mediated decay inhibitor) treated whole organoids demonstrated no significant difference in *NOS1AP* expression. *MAFB* was used as a housekeeping gene to control for organoid glomerular content. (E) Simple Wes capillary western blot demonstrates no difference in NOS1AP protein levels in denatured lysate, once again corrected for MAFB expression.

same antibody in *NOS1AP*-variant organoids, no detectable NOS1AP immunofluorescent signal was demonstrated across both male and female iPSC background genomes and multiple differentiation experiments. (Figure 5.2B,C) In whole organoid lysates, levels of *NOS1AP* mRNA were not different when normalised to *MAFB* expression to correct for glomerular content (Figure 5.2D). Organoids treated with cyclohexamide, an inhibitor of nonsense mediated decay, showed an increase in *NOS1AP* mRNA for both lines (Figure 5.2D), suggesting the loss of immunofluorescent signal in the *NOS1AP*-variant organoid was not due to nonsense mediated mRNA decay. Similarly, NOS1AP protein expression measured by capillary Western blot was comparable between *NOS1AP*-variant and WT organoids (Figure 5.2E). When mapped on the protein amino acid sequence, the p.Cys143Tyr substitution created by the c.428G>A variant lies only six amino acids from the NOS1AP antibody immunogen (NBP2-38758).(Figure 5.3) Considered together this data suggests the absence of the NOS1AP immunofluorescent signal from the *NOS1AP*-variant organoid glomeruli is due to misfolding of the protein, which makes the epitope inaccessible to the NOS1AP antibody (Novus Biologicals - NBP2-38758).

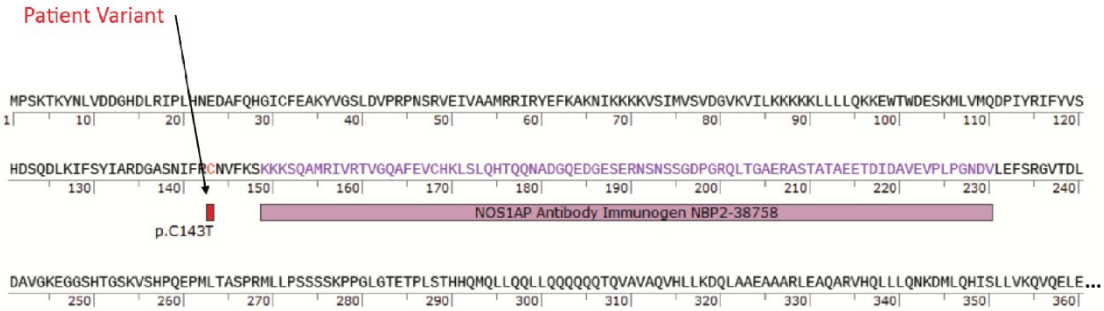

Figure 5.3 Proximity of NOS1AP p.Cys143Tyr substitution to antibody epitope.
Amino acid sequence of NOS1AP protein demonstrates the amino acid substitution is only 6 base pairs from the NOS1AP (NBP2-38758) antibody immunogen.

5.3.4 NOS1AP c.428G>A glomeruli demonstrate disordered glomerular tuft development and increased podocyte apoptosis.

Immunofluorescence analysis for slit diaphragm markers nephrin and podocin suggested a disorganisation of the *NOS1AP*-variant glomerular tissue structure. *NOS1AP*-variant glomeruli showed scattered, and in some cases punctate, nephrin/podocin co-immunofluorescence, whilst WT glomeruli demonstrated linear, organised expression of nephrin/podocin.(Figure 5.4A) This was further investigated in paraffin embedded, sectioned and periodic acid Schiff (PAS) stained organoids. *NOS1AP*-variant organoid glomeruli demonstrated abnormal glomerulogenesis, including impaired glomerular tuft

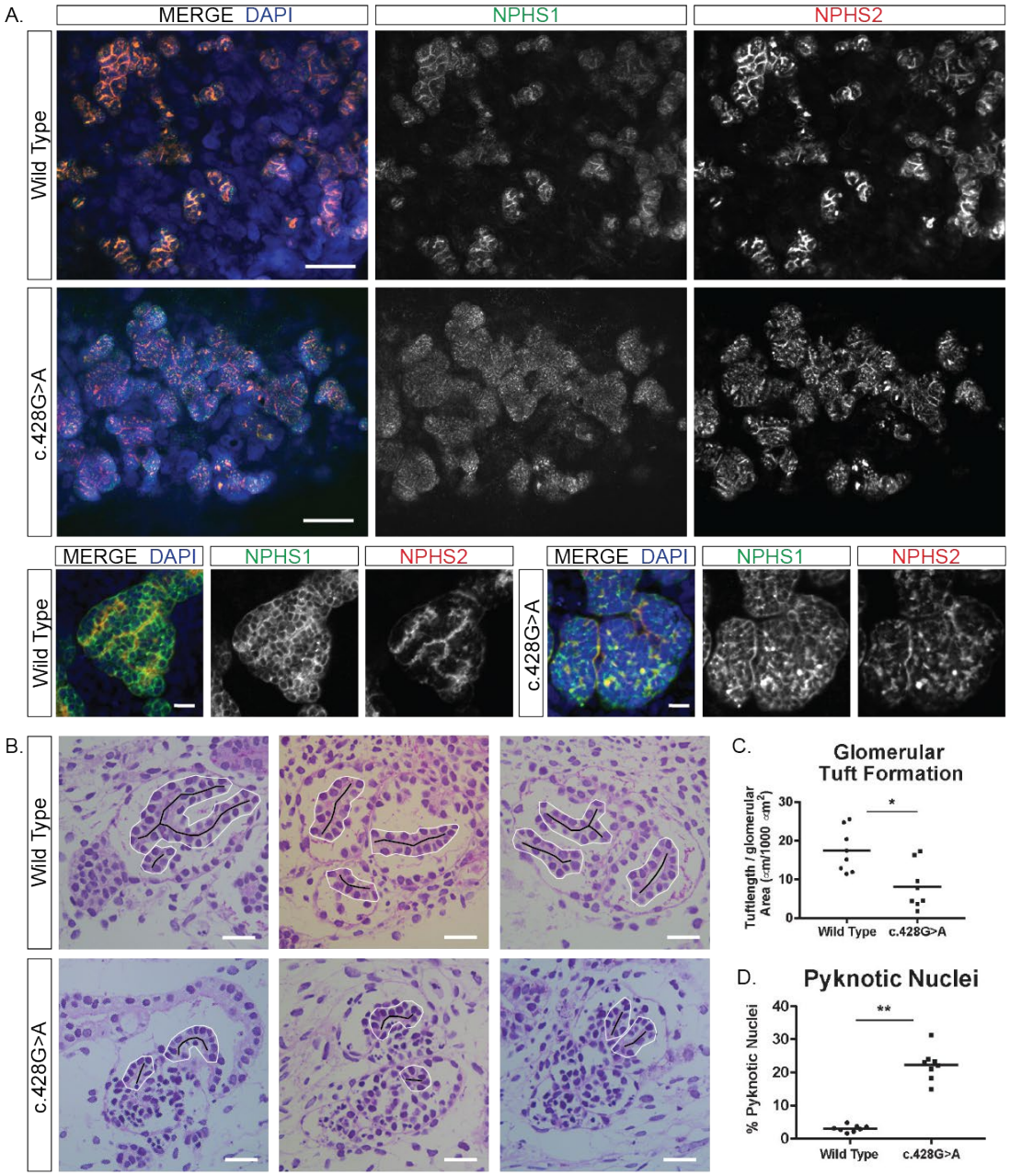

Figure 5.4 *NOS1AP*-variant organoids demonstrate abnormal glomerular development and increased podocyte apoptosis

(A)Immunofluorescent nephrin (green) and podocin (red) staining of kidney organoids demonstrating strong, linear slit diaphragm formation in WT glomeruli and disorganised pattern in *NOS1AP*-variant organoids with small focal intensities. (scale bar 200um larger images, 20 um smaller images) (B) PAS Staining of WT glomeruli reveals organised tufts of podocyte monolayers lining basement membrane (BM). *NOS1AP*-variant glomeruli are disorganised and hypercellular with poorly formed BM and apoptotic figures. (scale bar 20 um) (C-D) *NOS1AP*-variant organoids demonstrate reduced glomerular tuft length and increased pyknotic cell nuclei compared to isogenic, WT control. (students t test. mean)

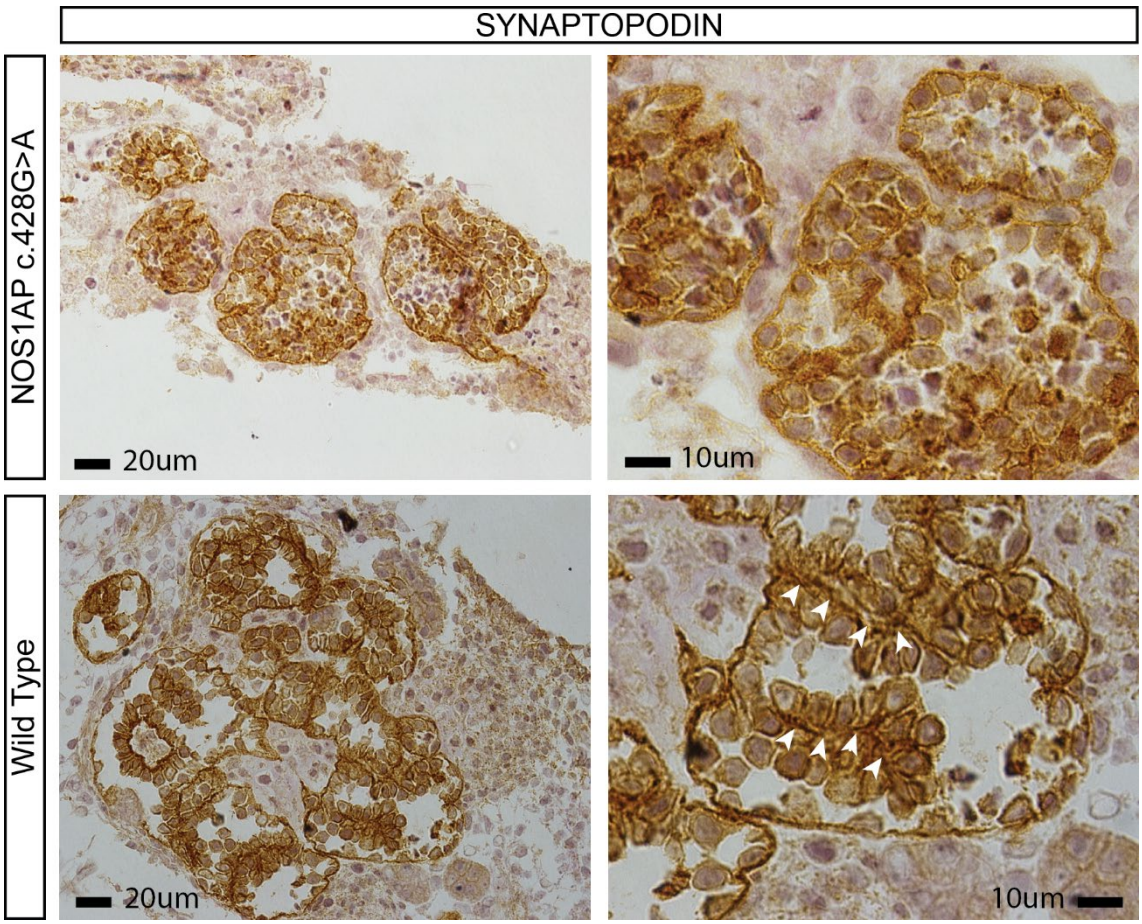

Figure 5.5 Synaptopodin IHC of paraffin embedded organoid sections
Immunohistochemistry demonstrates apical concentration of synaptopodin expression in WT organoids compared to more poorly organised expression in *NOS1AP*-variant glomeruli.

formation (defined as organised monolayers of podocytes lining an area of extracellular matrix) compared to WT controls.(Figure 5.4B,C) IHC staining demonstrated apical concentration of SYNPO in WT organoids along glomerular tufts, but was more diffuse in *NOS1AP*-variant glomeruli.(Figure 5.5) *NOS1AP*-variant organoids also demonstrated an increase in pyknotic nuclei compared to control.(Figure 5.4B,D) This observation was restricted to glomeruli and did not affect tubules. This latter finding was validated by immunofluorescence for apoptosis marker caspase-3 (CASP3). *NOS1AP*-variant glomeruli demonstrated a greater mean percentage area (*NOS1AP* 18.2% vs WT 2.3%, Δμ 15.9%, 95%CI 12.0-19.9%, $p<0.0001$) and glomerular MFI normalised to tubular signal gated on HNF4A expression (*NOS1AP* 1.66 vs WT 0.98, Δμ 0.68, 95%CI 0.51-0.84, $p<0.0001$) of CASP3 expression.(Figure 5.6) This observation was once again confined to the glomerular segment.

5.3.5 Electron microscopy of organoid glomeruli demonstrates reduction of foot process generation in NOS1AP-variant organoids.

The fundamental podocyte morphological defect in all forms of nephrotic syndrome is the effacement of the foot processes sitting on a GBM. Given the immaturity of the GBM within a kidney organoid, previous reports have vascularised organoids by renal subcapsular transplantation in mice.(van den Berg et al., 2018, Sharmin et al., 2016, Tanigawa et al., 2018) We attempted to transplant organoids under the renal capsule of immunocompromised mice in an effort vascularise the glomeruli and demonstrate foot process effacement on a more physiological capillary basement membrane, however at explant organoids appeared to have undergone extensive stromal expansion without any residual nephron structures.(data not shown)

We therefore attempted EM of untransplanted organoids. Transmission EM of non-transplanted organoids was challenging due to the absence of any capillaries within the glomerulus. We were able to qualitatively illustrate a reduction in villous-like cellular projections between podocytes of *NOS1AP*-variant organoids compared to WT. (Figure 5.7) This was admittedly variable and may have been related to the position of the grid section within the 3D glomerulus.

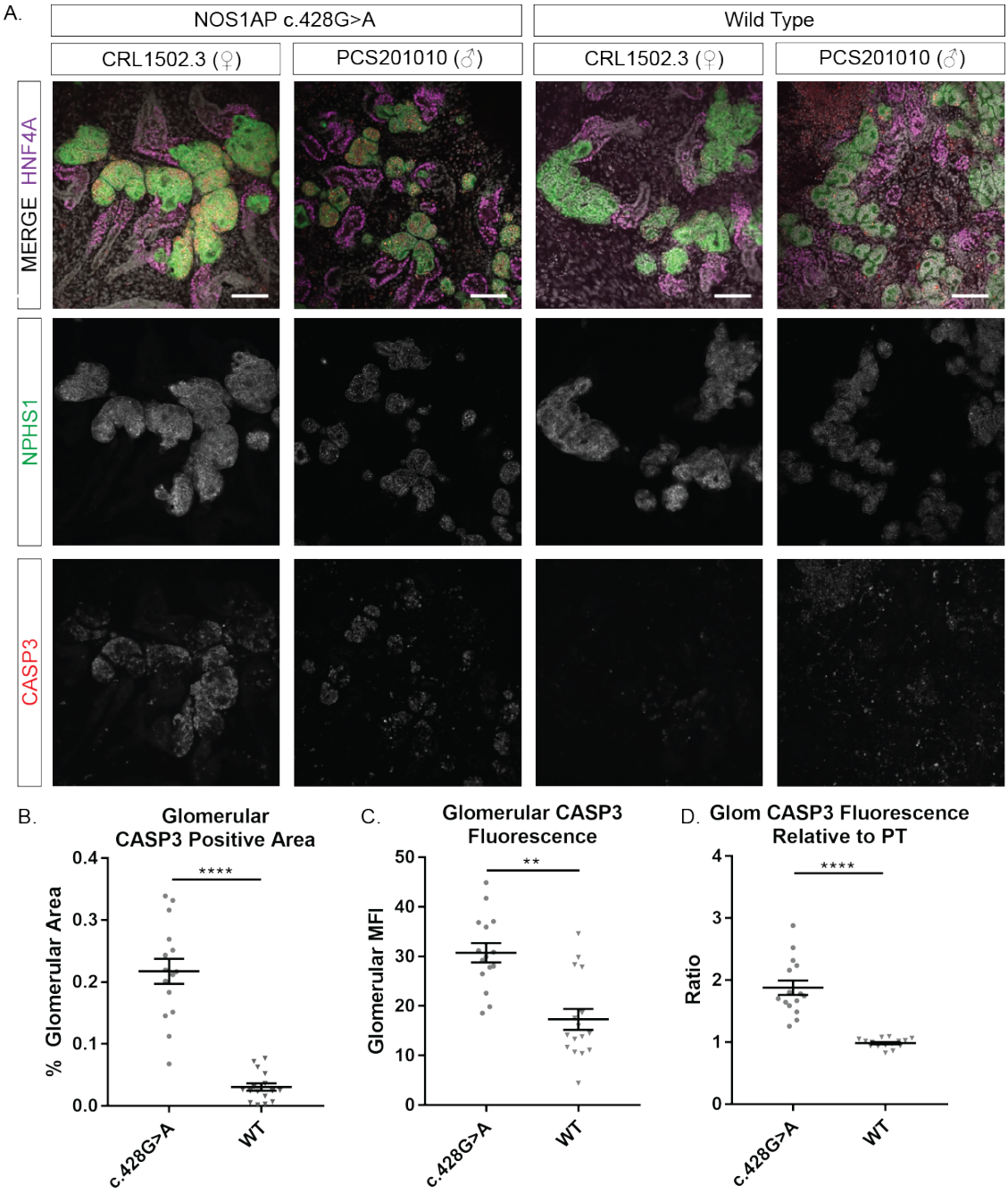

Figure 5.6 Increased caspase 3 expression of NOS1AP c.428G>A homozygous kidney organoids
(A) Immunofluorescence of whole mount organoids demonstrates increased ASP3+(red) apoptosis signal restricted to glomeruli (NPHS1, green) and absent from proximal tubule (HNF4A, magenta). Scale bar 100um. (B-D) Quantification of CASP3 signal across three paired differentiation experiments. *NOS1AP* c.428G>A homozygous organoids demonstrated increased area (B) and mean CASP3 fluorescence intensity in NPHS1+ regions with (D) and without (C) normalisation to proximal tubular (PT) signal. Error bars represent mean +/- standard error of mean.

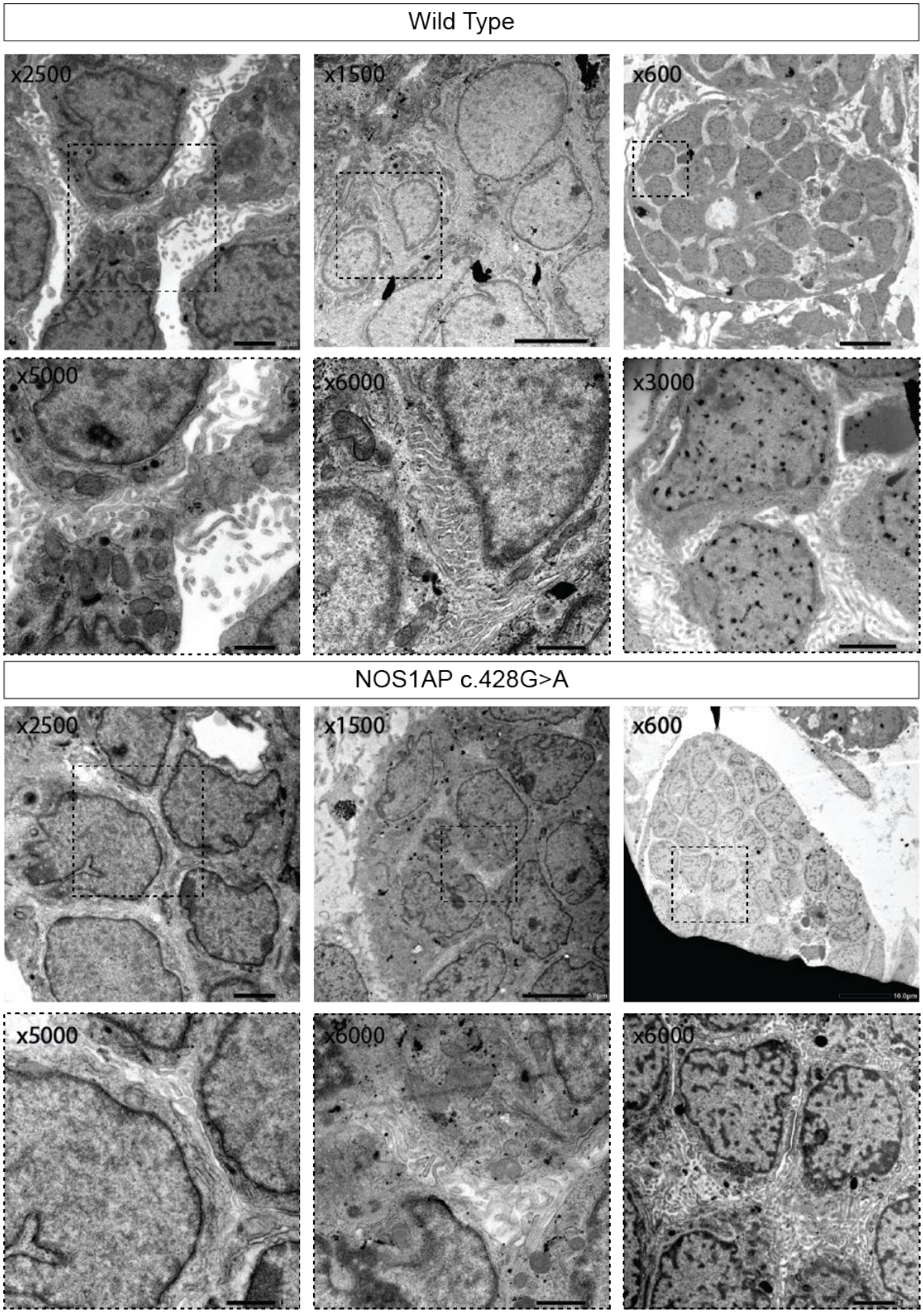

Figure 5.7 Electron microscopy
EM of non-transplanted organoids demonstrated variably reduced presence of villous, foot process like cellular projections in *NOS1AP*-variant organoids compared to WT control (only female background iPSC clones examined).

5.3.6 NOS1AP c.428G>A variant impairs podocyte polarity via dysfunction of the PAR polarity complex.

The Hildebrandt laboratory had illustrated a role for NOS1AP in the promotion of active (or GTP-bound) CDC42 levels.(Majmundar et al, unpublished) Active CDC42-GTP is recognised to regulate activity of the PAR polarity complex.(Yamanaka et al., 2001). We hypothesised that the expression of PAR polarity complex proteins within *NOS1AP*-variant organoid glomeruli would be disturbed. Using blinded manual thresholding within an automated ImageJ processing macro, we illustrated reduced MFI of both aPKC (*NOS1AP* 0.46 vs WT 0.65, Δμ 0.19, 95%CI 0.10-0.27, $p<0.0001$) and PAR3 (*NOS1AP* 0.53 vs WT 0.70, Δμ 0.17, 95%CI 0.08-0.26, $p<0.0001$) in SYNPO gated glomerular regions of *NOS1AP*-variant organoids compared to WT, normalised to tubular signal.(Figure 5.8) This was consistent across multiple differentiations and both genomic backgrounds.

Because the aPKC and PAR3 analyses relied on SYNPO expression to gate for the glomerular segment, differential SYNPO expression observed on IHC (Figure 5.5) may have influenced the aPKC and PAR3 immunofluorescent readout between the two organoids. However, the SYNPO immunofluorescent signal appeared clean and thresholds were converted to a binary mask of the glomerular segment, thus we feel subtle qualitative difference in SYNPO expression on IHC is unlikely to impact on this assay. Examples of thresholding are provided in Figure 5.9.

5.3.7 Bulk RNA sequencing of isolated organoid glomeruli is unable to illustrate NOS1AP disease specific transcriptional pathways

Our group has previously demonstrated an ability to isolate glomeruli from kidney organoids by dissociation and sieving.(Hale et al., 2018) We hypothesised that transcriptional profiling of isolated glomeruli from the *NOS1AP*-variant and WT organoids would demonstrate dysfunctional cellular pathways specific to *NOS1AP* mediated SRNS. Glomerular isolation was performed in technical triplicate from a single paired differentiation of the two iPSC lines. Replicates clustered by genotype on principal component analysis.(Figure 5.10A) Glomerular gene expression was lower in *NOS1AP*-variant glomeruli compared to WT glomeruli and some variability was observed between

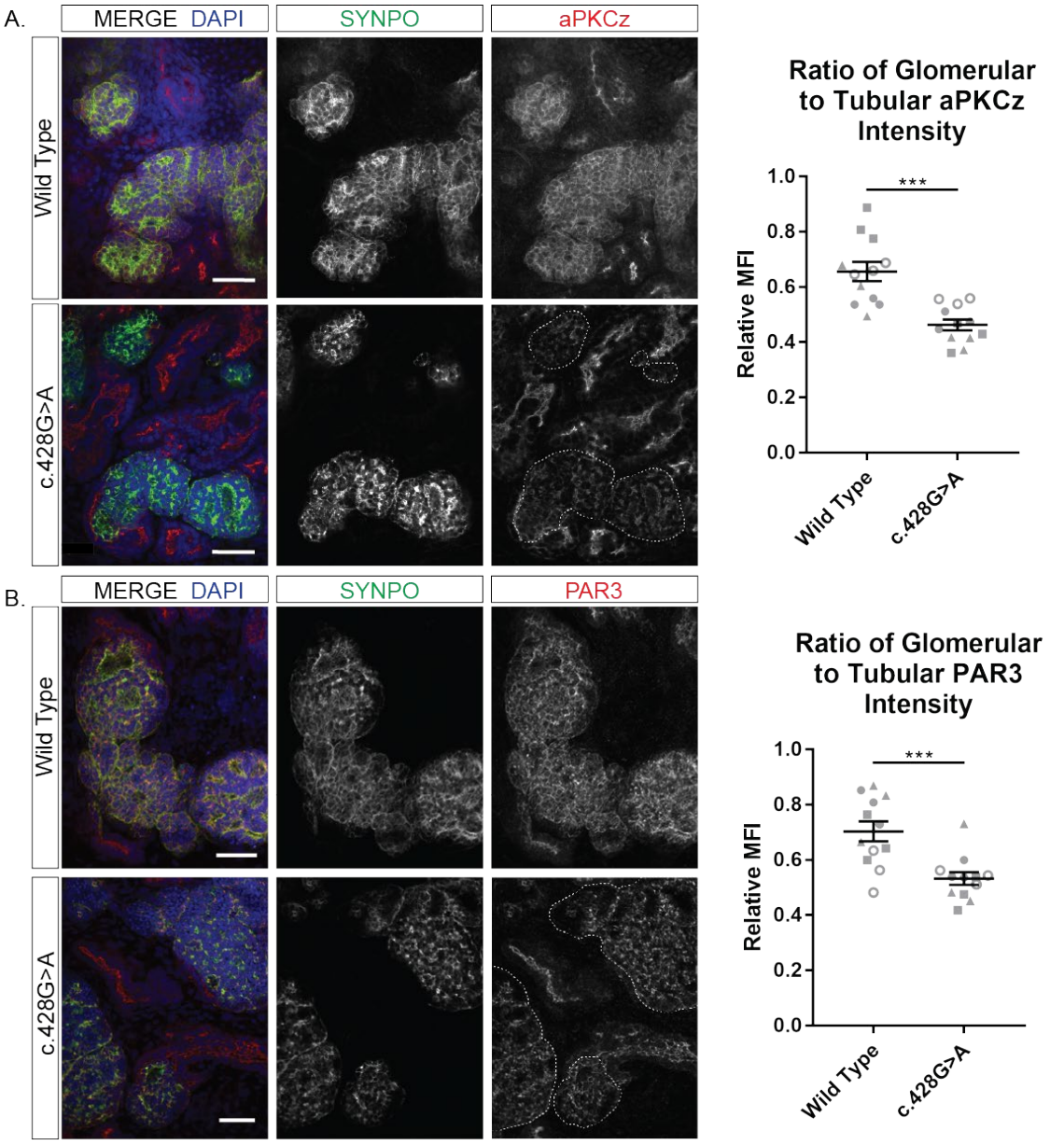

Figure 5.8 Analysis of polarity protein expression
(A) Reduced aPKC (red) immunofluorescence in glomeruli (synaptopodin, green) of *NOS1AP*-variant organoids compared to WT. When normalised to adjacent tubular aPKC intensity, NOS1AP-variant glomeruli demonstrate reduced glomerular aPKC mean fluorescence intensity (3 images from each of 4 paired distinct differentiations). (B) Same for PAR3. Symbols represent paired differentiations.

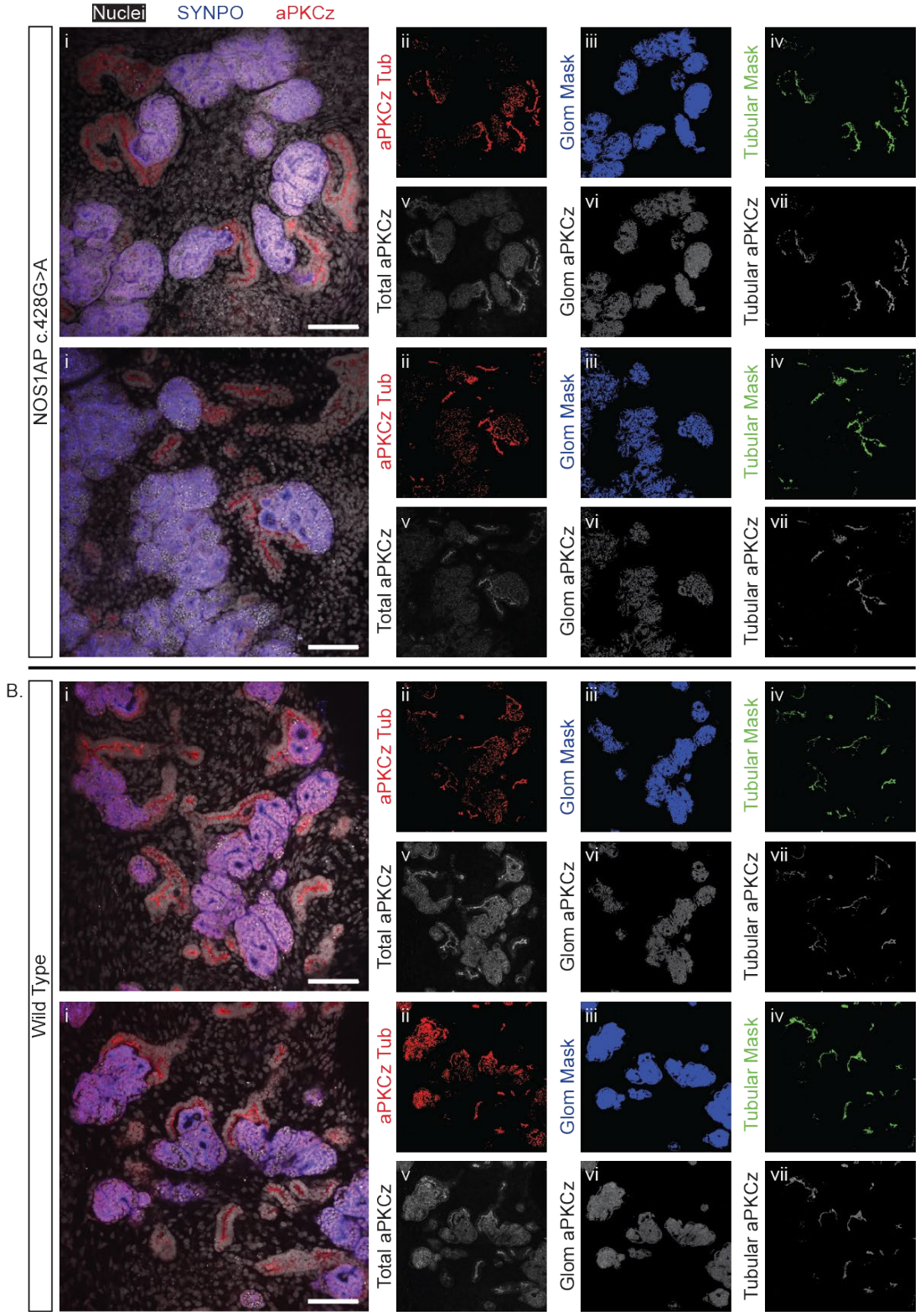

Figure 5.9 Measurement of glomerular to tubular aPKC fluorescence intensity ratio
Organoids were stained with synaptopodin (SYNPO, Blue) and aPKC (Red, Scale 100 um) and 3 images obtained by confocal microscopy(i). A blinded operator set intensity thresholds to highlight tubular aPKC (ii, red) and glomeruli (iii, SYNPO, blue) and converted these to binary masks. Subtraction of glomerular from tubular aPKC masks provided a mask that highlighted only tubular regions (iv, green). Mean intensity readouts from raw aPKC data (v) were restricted to SYNPO and Tubular masks (vi and vii). Two examples of each condition are displayed: A. NOS1AP c.428G>A and B. Results of glomerular:tubular aPKC and PAR3 ratio analysis are presented in Figure 5.6.

WT replicates, indicating some technical variability in the within the sieving protocol.(Figure 5.10B). Differential gene expression analysis highlighted GO terms associated with cell-cell adhesion and extracellular matrix expression.(Figure 5.10C)

Differential expression within these GO terms was largely dominated by protocadherins and ECM proteins (collagens, contactins, integrins and laminin) that we were not able to link to the proposed *NOS1AP*-variant or SRNS disease mechanisms. Furthermore, there was no evidence of an apoptotic signal consistent with the CASP3 immunofluorescence. Additionally, ion transporters were upregulated in the *NOS1AP* samples (Figure 5.10C), suggestive of the potential contamination of the glomerular lysates with tubular cells. We hypothesise that the apoptosis within *NOS1AP*-variant glomeruli rendered them more liable dissociation which may have adversely affected the efficacy of the sieving protocol, trapping tubular segments in the sieves. Consequently it is difficult to make meaningful conclusions from this bulk RNA sequencing experiment with regards to *NOS1AP* or SRNS disease pathobiology.

5.4 Discussion

The data presented in this chapter contributes to the functional genomic validation of *NOS1AP* as a novel gene associated with SRNS and extends the molecular understanding of the effect of *NOS1AP* variants on glomerular development beyond maintenance of active CDC42 levels to demonstrate disturbances in podocyte polarity.

Consistent with findings in mouse and human kidney single cell RNA sequencing datasets (Majmundar et al. unpublished), we confirm *NOS1AP* expression is isolated to the podocyte in wild-type human kidney organoids. Furthermore, we demonstrate that 3D modelling of wild-type podocytes permits increased *NOS1AP* expression compared to 2D modelling. The superior expression of podocyte genes in 3D organoid culture over 2D podocyte culture is previously established.(Hale et al., 2018) However, in this project we demonstrate that the benefits of 3D podocyte culture are not limited to improved gene expression. The organoid platform validated the spatial expression of NOS1AP protein within the human glomerulus to be slit diaphragm associated. Furthermore, organoids portrayed a segment specific tissue consequence of the *NOS1AP* patient variant in the form of aberrant glomerular development, reduced polarity expression and increased

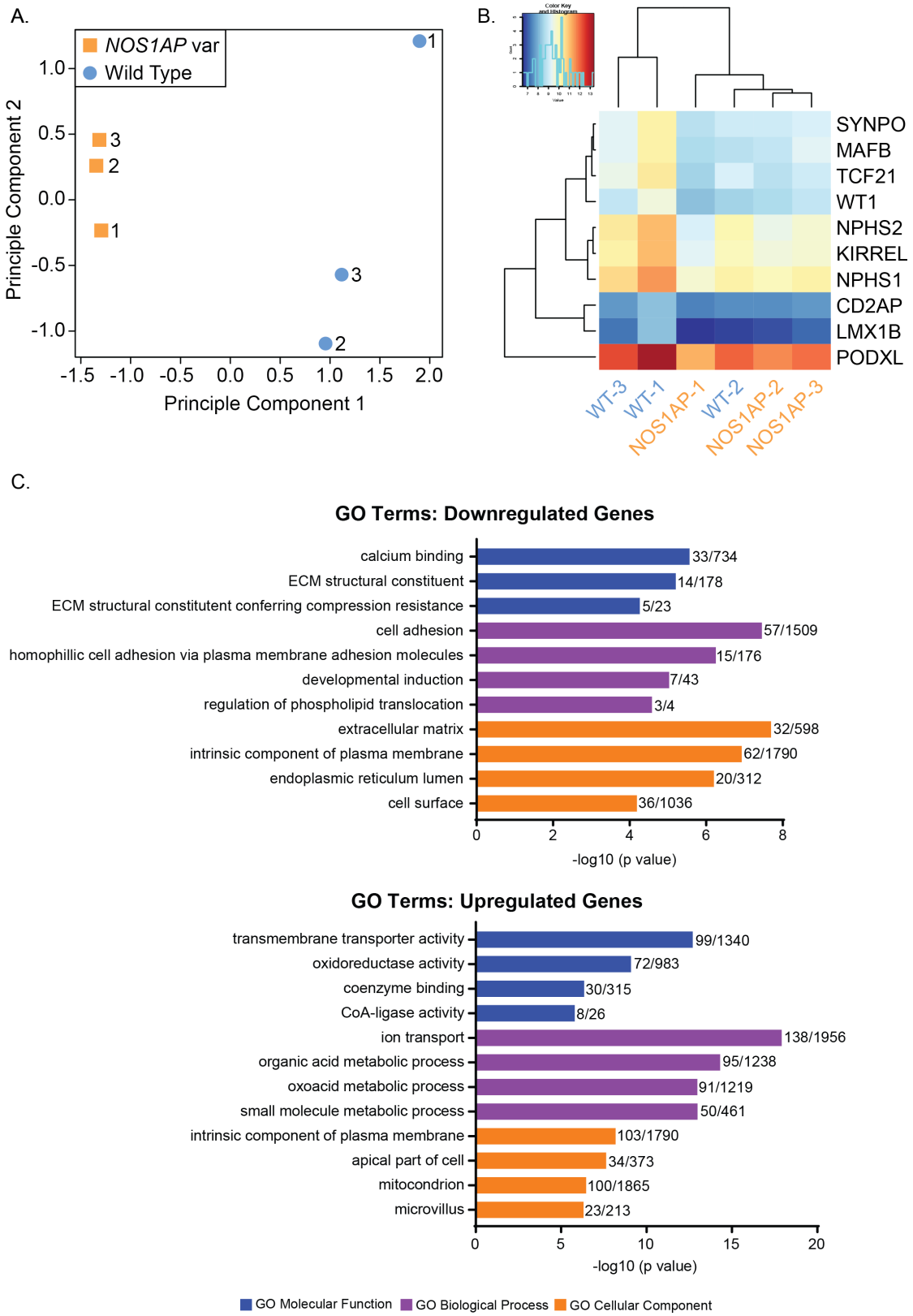

Figure 5.10 Bulk RNA Sequencing and differential gene expression analysis of glomeruli isolated from *NOS1AP-var* and WT kidney organoids.
(A) Principle component analysis demonstrates clustering of technical replicates by genotype. (B) Expression of key glomerular genes was increased in WT compared to control but also more variable, potentially due to technical variability introduced by the sieving protocol. (C) Differential expression analysis produces ambiguous GO terms unable to be linked to *NOS1AP* gene or podocyte dysfunction.

podocyte apoptosis, representing a key advantage to organoid based disease modelling over 2D podocyte culture. The observation of no detectable signal in the NOS1AP c.428G>A variant organoids is most likely due to misfolding of the protein. This is consistent with *in silico* modelling of *NOS1AP*-variant protein crystal structure performed by the Hildebrandt group predicting instability of the protein and steric clashes with adjacent amino acids (Majmundar et al, unpublished) Additionally, the Hildebrandt group have been able to detect *myc*-tagged mutant vectors transfected into 2D podocytes by immunofluorescence for the myc epitope, indicating viability of the mutant NOS1AP protein within the cell. The ultimate evidence for protein misfolding will be the ability to successfully stain whole mount organoids for the mutant protein using alternative NOS1AP antibodies, which are in the process of being shipped from our collaborator.

The findings of aberrant glomerular development, reduced tuft length and increased podocyte apoptosis are consistent with existing literature on *aPkc* and *Cdc42* knockout models. During normal capillary loop development, podocytes extend radially inwards to encircle glomerular capillaries. In a dual knockout *aPkcλ/aPkcζ* mouse model, Hartleben et al (2013) demonstrate failure of the glomerular development at the capillary loop stage with reduced radial extension of the podocyte processes, incomplete capillary loop formation, simplified glomerular structures and proteinuria. PAS stained sections of mouse glomeruli pictured in other *aPkc* and *Cdc42* knockout mouse models illustrate similar changes and dark, condensed nuclei albeit without frank pyknosis.(Scott et al., 2012, Hirose et al., 2009) An increase in podocyte apoptosis has been demonstrated in *Cdc42* siRNA knockdown podocytes and mice treated with Cdc42 inhibitors.(Huang et al., 2016)

Increased apoptosis is possibly more prominent in kidney organoid glomeruli due to the less physiological *in vitro* environment as well as the lack of vasculature and mesangial support for the podocytes. This may also be because the knockout of the *Cdc42/aPkc* genes in these mouse models are driven by *Nphs2* expression and therefore affect only later glomerular development. In contrast, the homozygous *NOS1AP* variant in our organoids is somatic and expressed throughout the development of the organoid. The peripheral nature of the CASP3 signal noted on immunofluorescent analysis of the *NOS1AP*-variant organoid glomeruli is reminiscent of the collapsing glomerulosclerosis

seen in *Cdc42* and *aPKC* knockout mouse models as well as the proband biopsy. *NOS1AP* is heavily expressed in the brain where it is involved in axonal projection.(Carrel et al., 2009, Carrel et al., 2015) Clinically, *NOS1AP* variants have been associated with neurodegenerative disease, stroke, mental illness, and cardiac rhythm disturbances. (Treuer and Gonzalez, 2014, Delorme et al., 2010, Freudenberg et al., 2015) NOS1AP is known to carry dynamic O-linked N-acetylglucosamine (O-GlcNAc) post-translational modifications on serine residues, which protect neurons from apoptosis when placed under stress by decreasing association with nNOS, modifying NF-κβ and MAPK pathways.(Zhu et al., 2015, Zou et al., 2009, Fulop et al., 2007)When the *NOS1AP* gene was mutated in rat phaeochromocytoma (PC12) cells to remove serine residues known to carry O-GlcNAc residues, cell apoptosis increased.(Zhu et al., 2015) Whilst the amino acid substitution caused by the c.428G>A variant doesn't involve a serine residue, it is possible that misfolding of the mutant NOS1AP protein reduces O-GlcNAc modification of the protein and leaves the cell vulnerable to an uncontrolled apoptotic response to stress. Whilst further work is required to demonstrate that this phenomenon is active in podocytes, it provides a possible link between *NOS1AP* variants and the apoptosis seen in our organoid glomeruli.

We demonstrate the reduced expression of nephrin and podocin in our *NOS1AP*-variant organoid glomeruli, as well as the reduced glomerular expression of aPKC and PAR3. Immunofluorescent study of the *Cdc42* knockout mouse glomeruli demonstrated punctate immunofluorescent expression of nephrin and podocin and reduced expression of aPKC, PAR3 and ZO-1, (Scott et al., 2012) also consistent with our findings. This mouse, as well as those discussed previously, develop foot process effacement and nephrotic range proteinuria by birth, consistent with the patient phenotype.(Hirose et al., 2009, Hartleben et al., 2008, Scott et al., 2012, Huang et al., 2016, Hartleben et al., 2013) Both PAR3 and aPKC have been demonstrated to localise to the anchor point of the mouse slit diaphragm on immunogold EM.(Hartleben et al., 2008, Scott et al., 2012) The reduced linear expression of nephrin/podocin in *NOS1AP* variant organoids is also consistent with images of SYNPO and ZO-1 expression in a *PODXL*$^{-/-}$ iPSC organoid glomerulus, another established genotype for infant onset SRNS.(Freedman et al., 2015, Kang et al., 2017, Barua et al., 2014a)

The glomerular characterisation of our *NOS1AP c.428G>A* homozygous organoids differs from previous organoids modelling of congenital nephrotic syndrome due to variants in *NPHS1*.(Hale et al., 2018, Tanigawa et al., 2018) Both reports utilise different protocols to model nephrin expression within patient-derived, compound heterozygous *NPHS1* variant kidney organoids.(Tanigawa et al., 2018, Hale et al., 2018) Immunofluorescent images provided in both manuscripts do not demonstrate aberrant glomerular development or podocyte apoptosis, suggesting this organoid glomerular phenotype is specific to *NOS1AP* genotype and not SRNS genes more broadly.

The success of this project validates the lessons learned from the less successful *DNAH5* variant curation and disease modelling experience. The likelihood of pathogenicity was increased by the demonstration of segregation between two unrelated families and the preliminary work performed by our collaborators. The transcriptional immaturity of the organoid model prompted the selection of the variant carried by proband (*NOS1AP* c.428G>A) for modelling in iPSC derived kidney organoids as this proband presented at a younger age (4 days). Additionally, in spite of a seemly less pathogenic missense variant, this patient demonstrated more severe proteinuria and renal dysfunction thus was thought to represent a greater likelihood of establishing an *in vitro* phenotype from the immature organoid model. Finally, this proband and had undergone renal biopsy, providing us with a histological confirmation of the primary phenotype and therefore an increased level of certainty in the variant.

In this project we elected to CRISPR edit the patient variant into a wild type iPSC cell line ("knock in") rather than derive and gene edit patient iPSC. This decision was made largely on practical grounds. The derivation of patient iPSC would have required: (i) amendment to our existing HREC for recruitment of an international patient; (ii) coordination of the patient fibroblast collection (iii) expansion and transport of patient fibroblasts from a third, international collaborating centre and (iv) execution of combined reprogramming and gene correction. Collectively this process represented at best a 6-9 month delay before modelling could commence. The disadvantage of the knock-in approach includes the inability to account for any contribution of the patient's background genome to disease phenotype. However, in this circumstance, we recapitulate our findings across two wild type iPSC backgrounds and therefore confidently confirm that this single

gene mutation is responsible for the phenotype seen in the organoids. One future advantage of the knock in approach would be to extend our research of SRNS by knocking in multiple SRNS genotypes into one reference iPSC control line, allowing all mutant clones one control, thereby minimising (i) technical variability that may otherwise arise between non-isogenic controls as well as (ii) differentiation protocol optimisation which is required for each individual line.

Our laboratory has established that organoid glomeruli are relatively more resistant to dissociation than the tubules and stroma and published protocols for their isolation.(Hale et al., 2018) The ability to generate reproducible glomerular isolation from *diseased* organoids has not been demonstrated. We propose that a lack of integrity within *NOS1AP*-variant glomeruli sufficiently confounded the ability to generate a representative glomerular lysate using this protocol. One must also consider the potential low fidelity of transcriptional profiling when studying a gene with little to no role in transcriptional regulation, such as *NOS1AP.* In other words, even if the glomerular isolates were pure, the molecular disturbance in this particular context may lack the transcriptional magnitude to be detected by bulk RNA sequencing. This argument, along with our results, also highlight the benefits of examining the whole mount organoid in preference to dissociating or disturbing the live micro-tissues.

EM of organoid glomeruli was challenging due to the lack of a capillary and glomerular basement membrane to provide a surface on which podocytes can align. Previous reports have vascularised organoids using murine subcapsular transplantation and demonstrated EM images of the glomerular filtration barrier very similar to that expected *in vivo*.(Tanigawa et al., 2018, van den Berg et al., 2018) Our attempts to replicate these protocols were unsuccessful and require optimisation. Accordingly, we analysed non-transplanted organoids and were able to appreciate a decrease in villous like cellular projections extending between NOS1AP variant podocytes compared to wild type, however this was variable and difficult to quantitate. Similar wild-type podocyte projections have been illustrated in previous reports and labelled as putative foot processes.(Hale et al., 2018, van den Berg et al., 2018) There are no previous reports of glomerular disease in kidney organoids examined in non-transplanted kidney organoids however 2D podocyte cultures regularly describe actin rich cell projections labelled

filopodia and podosomes as a surrogate marker of actin dynamics and podocyte function.(Welsch et al., 2001, Scott et al., 2012, Schell et al., 2013, Mattila and Lappalainen, 2008) Ultimately optimisation of murine transplantation protocols will be essential to this approach.

In conclusion, kidney organoids provided a human, *in vitro* model in which we were able to localise the spatial, 3D NOS1AP protein expression with a human glomerular slit diaphragm. Additionally, we were able to demonstrate a podocyte specific consequence of a patient specific *NOS1AP* variant including increased podocyte apoptosis and reduced glomerular tuft length, providing a link from the 2D podocyte work performed by Professor Hildebrandt's laboratory and an established murine glomerular disease phenotype in *Cdc42* conditional knockout models. At the time of writing, this is the first report of the use of kidney organoids for the validation of a novel gene for inherited kidney disease.

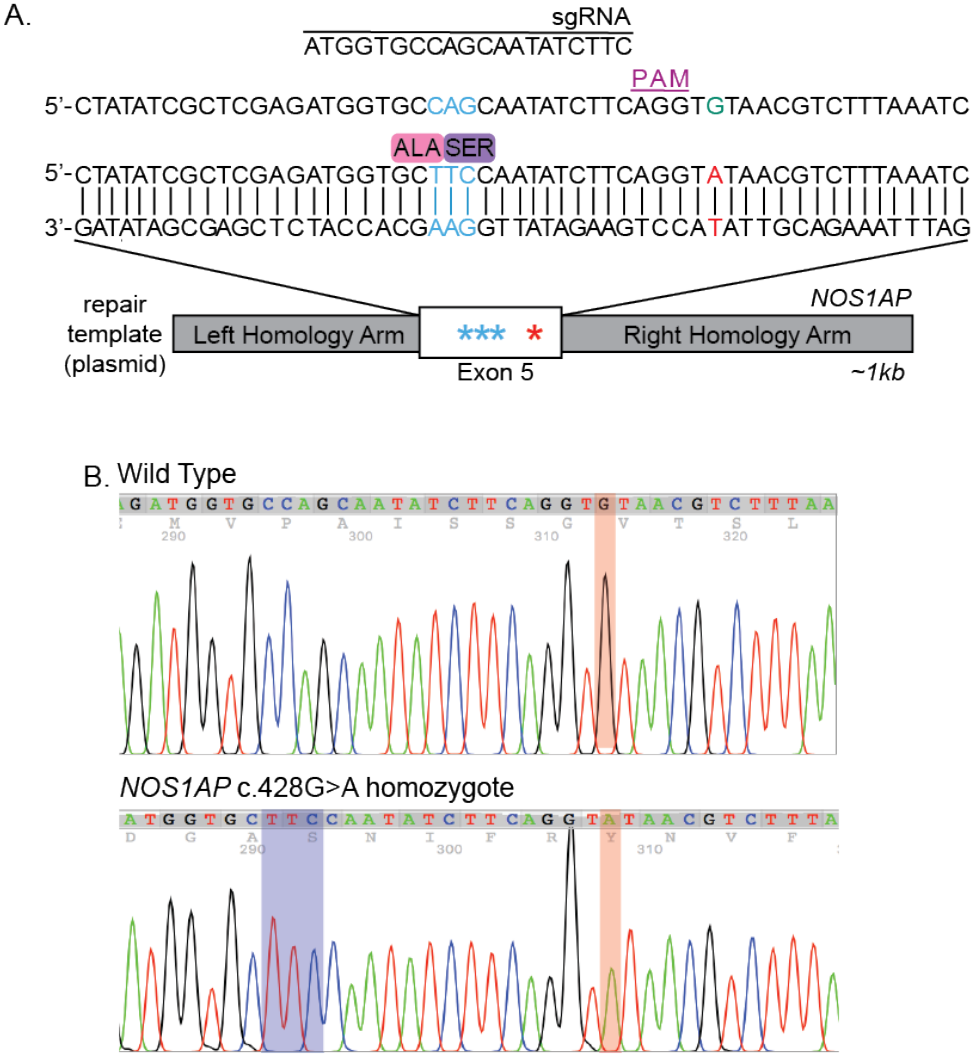

Figure 5.11 NOS1AP gene editing approach by Dr Sara Howden
(A) CRISPR Guide RNA and DNA repair template inducing missense variant A (red) for G (green) as well as synonymous 3bp change (blue) upstream for ease of identification of edited clones. (B) Sanger sequences of gDNA of WT and PT clones show knock-in of c.428G>A missense variant (red) and synonymous 3bp change (blue).

Chapter 6 Conclusions and Future Directions

This PhD commenced shortly after the first publication of iPSC-derived kidney organoid protocols.(Takasato et al., 2015, Morizane et al., 2015, Takasato et al., 2014, Freedman et al., 2015, Taguchi et al., 2014) At this time, it was unknown whether organoids differentiated from the reprogrammed iPSC of patients with inherited kidney disease would be capable of faithfully modelling disease phenotypes. This thesis sought to demonstrate the capabilities of the organoid model for the functional genomic research of glomerular and tubular disorders, first in a previously validated genotype and subsequently for novel genes associated with kidney disease.

The projects presented in this thesis, alongside those published in the field during the period of candidature (Chapter 2.6.2), demonstrate the breadth of utility of kidney organoids in the modelling of both glomerular and tubular disease. Given the developmental immaturity of the organoids, (Takasato et al., 2015) we approached diseases with onset in infancy and childhood. This rationale was based on maximising the likelihood of observing a morphological disease phenotype directly from the organoid. A

gene specific phenotype was observed in both the *IFT140* and *NOS1AP* mutant organoids. Other groups have successfully approached adult onset disease such as ADTKD-*UMOD* (Dvela-Levitt et al., 2019) and ADPKD (Cruz et al., 2017). Thus one might conclude that the sole prerequisite to studying a genetic disease in an organoid is the expression of that gene by the organoid, regardless of the age of disease onset. This may well be the case, however the absence of mature channel and transporter expression from current organoid protocols may alter the observed phenotypes seen in adult onset disease models.

One aspect of kidney organoid disease modelling that has changed little over the period of this candidature is the spectrum of diseases unable to be modelled. There exist multiple reports at vascularising organoids either using *in vitro* flow (Homan et al., 2019) or through transplantation into mice (Sharmin et al., 2016, van den Berg et al., 2018, Tanigawa et al., 2018, Subramanian et al., 2019) but despite improvements in glomerular filtration barrier formation, a model of Alport syndrome is yet to be achieved. Furthermore, very recent evidence suggests that murine subcapsular transplantation can only achieve maturation to a finite extent.(Nam et al., 2019) Protocols for the iPSC derived modelling of glomerular disease are progressing at rapid speed including 'organ on a chip' models.(Musah et al., 2018, Musah et al., 2017, Petrosyan et al., 2019) and protocol amendments aimed at eliminating off-target differentiated cell types.(Wu et al., 2018b)

In Chapter 3 and 4 patient-derived iPSC are used to generate organoids. However in Chapter 5, knocking the patient *NOS1AP* variant into a WT reference iPSC line was more practical. Both are reasonable approaches. The former approach requires re-optimisation of differentiation conditions for each derived iPSC clone which we have found to be cumbersome and therefore expensive. It is also more expensive if the patient iPSC reprogramming and gene correction are performed separately. The 'knock in' approach may reduce optimisation and cost however, in order to progress to clinically relevant personalised therapeutic screening assays, patient iPSC will eventually need to be derived and optimised. Whatever the approach, CRISPR remains an indispensable tool in generating isogenic control iPSC lines to isolate the genetic variant of interest within the experimental comparison. This is now gold standard within the field.

The multicellular nature of kidney organoids provides an *in vitro* micro-environment that more accurately reflects *in vivo* cell-cell communication and tissue function.(Pampaloni et al., 2007) The drawback of this model is the need to isolate the cell types of interest for molecular interrogation, a process not required in 2D cell cultures. This thesis illustrates methods for isolation of epithelial cells (by MACS) and glomeruli (by sieving) for bulk RNA sequencing and DGE analysis. Unsurprisingly these isolation methods are not perfect and these approaches require optimisation. For example, the differential gene expression analysis in the *IFT140* project required correction for variable nephron patterning. In future, at the expense of sequencing depth, this may be overcome by single cell RNA sequencing permitting inclusion of transcriptionally comparable cell clusters into the DGE analysis. In the *NOS1AP* project DGE did not reflect the apoptotic signals seen in whole mount staining, presumably because the apoptotic cells were washed away during the dissociation prior to glomerular isolation. Whilst these DGE analyses were able to imply dysfunctional transcriptional pathways they were not able to provide highly granular insights into molecular pathogenesis. Furthermore, dissociation is recognised to produce cellular stress responses which may pollute transcriptional analyses.(Wu et al., 2019b) Additionally, transcriptional profiling may not be an adequately sensitive modality to characterise the molecular effect of gene variants that are not transcription factors. Quantitative proteomics may be more effective in this circumstance.

Consequently, both within the projects described in this thesis and within the wider organoid disease modelling literature,(Dvela-Levitt et al., 2019, Czerniecki et al., 2018, Przepiorski et al., 2018, Hollywood et al., 2019) the greatest analytical yield has been derived from undissociated, whole mount organoid preparations. In the *IFT140* and *DNAH5* projects we performed quantitative and qualitative analysis of primary cilia morphology within a three dimensional whole mount organoid using state of the art high-resolution confocal microscopy and partially automated analysis programs. In the *NOS1AP* project we performed a fully automated, quantitative analysis of apoptosis using caspase 3 immunofluorescence. This caspase 3 assay is a candidate for a high content analysis screen of compounds which modulate CDC42 GTPase activity. However, existing attempts to culture organoids in high throughput platforms has demonstrated a high degree of variability.(Czerniecki et al., 2018) Accounting for this variability, the expense of organoid culture and sheer number of compounds in libraries available for

screening (measured in thousands), it is likely that more straightforward, 2D cell cultures will be used for primary high throughput compound screening with validation of identified candidates then tested in organoids. This elegantly illustrated by Associate Professor Anna Greka's laboratory in the characterisation of a proposed novel compound for ADTKD-*UMOD*.(Dvela-Levitt et al., 2019) Far from fantasy, the use of organoids to identify subjects that may respond to specific pharmacological treatments is already in preclinical practice. The use of primary rectal organoid assays from patients with cystic fibrosis has been shown to correlate with respiratory function test results and model respiratory response to CFTR modulation therapies.(Dekkers et al., 2016, Dekkers et al., 2013)

In Chapter 4, the unsuccessful attempt to ratify *DNAH5* as a novel genotype for NPHP highlights the importance of high quality genomic variant curation prior to the commitment to organoid modelling and the pitfall of approaching a gene for validation based on only a single affected case. Additionally, the fact that we were unable to identify any phenotypic difference between the *DNAH5* patient and gene corrected organoids within this project also speaks to the fidelity of the results in the previous *IFT140* chapter. In future, the established workflow from undiagnosed patient to organoid disease model is likely to involve greater collaboration between international clinical renal genomic databases and an element of preliminary 2D cell culture assays as an acid test, before the expense of organoid modelling can be justified.

In summary, kidney organoids represent exciting, novel, functional genomic models, clearly capable of expanding our knowledge of inherited glomerular and tubular kidney disease. Current protocols do not allow the modelling of all kidney diseases and thus organoids stand to complement existing functional genomic models, rather than replace them. The diseases best suited to modelling with kidney organoids are those where an immunofluorescent morphological readout of protein localisation, structural tissue development or function can be obtained. Isolation of specific cell types from organoids is possible but prone to technical variation which can be overcome by a sound understanding of the inherent variation in the differentiation protocol in use.

The initial hype of regenerative medicine revolved around the future prospects of culturing autologous nephron masses for use as transplantable renal replacement therapy. Kidney organoid disease modelling, however provides a far more immediately realisable clinical translation in the form of novel gene discovery, improved pathomolecular understanding, and ultimately tailored patient therapy using personalised, *in vitro* therapeutic screening. As new technologies are superimposed on existing kidney regeneration approaches, the breadth of diseases able to be modelled and thus the clinical translation of discoveries will only increase.

Chapter 7 Bibliography

AALTO-SETÄLÄ, K., CONKLIN, B. R. & LO, B. 2009. Obtaining Consent for Future Research with Induced Pluripotent Cells: Opportunities and Challenges. *PLOS Biology,* 7**,** e1000042.

ABDELHAMED, Z. A., WHEWAY, G., SZYMANSKA, K., NATARAJAN, S., TOOMES, C., INGLEHEARN, C. & JOHNSON, C. A. 2013. Variable expressivity of ciliopathy neurological phenotypes that encompass Meckel-Gruber syndrome and Joubert syndrome is caused by complex de-regulated ciliogenesis, Shh and Wnt signalling defects. *Hum Mol Genet,* 22**,** 1358-72.

ABRAHAMSON, D. R. 2012. Role of the podocyte (and glomerular endothelium) in building the GBM. *Semin Nephrol,* 32**,** 342-9.

AFZELIUS, B. A. 1976. A human syndrome caused by immotile cilia. *Science,* 193**,** 317-9.

AGARWAL, A. K., ZHOU, X. J., HALL, R. K., NICHOLLS, K., BANKIER, A., VAN ESCH, H., FRYNS, J. P. & GARG, A. 2006. Focal segmental glomerulosclerosis in patients with mandibuloacral dysplasia owing to ZMPSTE24 deficiency. *J Investig Med,* 54**,** 208-13.

AGUILAR, A. 2016. Efficacy of eculizumab in paediatric aHUS. *Nature Reviews Nephrology,* 12**,** 198-198.

AIHW 2012. Dialysis and kidney transplantation in Australia: 1991–2010. Cat. no. PHE 162. Canberra: AIHW.

AIHW 2014. Projections of the prevalence of treated end-stage kidney diseasein Australia 2012–2020. Cat. no. PHE 176. Canberra: AIHW.

AKCHURIN, O. & REIDY, K. J. 2015. Genetic causes of proteinuria and nephrotic syndrome: impact on podocyte pathobiology. *Pediatr Nephrol,* 30**,** 221-33.

AKILESH, S., SULEIMAN, H., YU, H., STANDER, M. C., LAVIN, P., GBADEGESIN, R., ANTIGNAC, C., POLLAK, M., KOPP, J. B., WINN, M. P. & SHAW, A. S. 2011. Arhgap24 inactivates Rac1 in mouse podocytes, and a mutant form is associated with familial focal segmental glomerulosclerosis. *J Clin Invest,* 121**,** 4127-37.

ANDERSON, M., KIM, E. Y., HAGMANN, H., BENZING, T. & DRYER, S. E. 2013. Opposing effects of podocin on the gating of podocyte TRPC6 channels evoked by membrane stretch or diacylglycerol. *Am J Physiol Cell Physiol,* 305**,** C276-89.

ARAOKA, T., MAE, S., KUROSE, Y., UESUGI, M., OHTA, A., YAMANAKA, S. & OSAFUNE, K. 2014. Efficient and rapid induction of human iPSCs/ESCs into nephrogenic intermediate mesoderm using small molecule-based differentiation methods. *PLoS One,* 9**,** e84881.

ARIF, E. & NIHALANI, D. 2013. Glomerular Filtration Barrier Assembly: An insight. *Postdoc J,* 1**,** 33-45.

ARTS, H. H., BONGERS, E. M., MANS, D. A., VAN BEERSUM, S. E., OUD, M. M., BOLAT, E., SPRUIJT, L., CORNELISSEN, E. A., SCHUURS-HOEIJMAKERS, J. H., DE LEEUW, N., CORMIER-DAIRE, V., BRUNNER, H. G., KNOERS, N. V. & ROEPMAN, R. 2011. C14ORF179 encoding IFT43 is mutated in Sensenbrenner syndrome. *J Med Genet,* 48**,** 390-5.

ASHRAF, S., GEE, H. Y., WOERNER, S., XIE, L. X., VEGA-WARNER, V., LOVRIC, S., FANG, H., SONG, X., CATTRAN, D. C., AVILA-CASADO, C., PATERSON, A. D., NITSCHKE, P., BOLE-FEYSOT, C., COCHAT, P., ESTEVE-RUDD, J., HABERBERGER, B., ALLEN, S. J., ZHOU, W., AIRIK, R., OTTO, E. A., BARUA, M., AL-HAMED, M. H., KARI, J. A., EVANS, J., BIERZYNSKA, A., SALEEM, M. A., BOCKENHAUER, D., KLETA, R., EL DESOKY, S., HACIHAMDIOGLU, D. O., GOK, F., WASHBURN, J., WIGGINS, R. C., CHOI, M., LIFTON, R. P., LEVY, S., HAN, Z., SALVIATI, L., PROKISCH, H., WILLIAMS, D. S., POLLAK, M., CLARKE, C. F., PEI, Y., ANTIGNAC, C. & HILDEBRANDT, F. 2013. ADCK4 mutations promote steroid-resistant nephrotic syndrome through CoQ10 biosynthesis disruption. *J Clin Invest,* 123**,** 5179-89.

ASHRAF, S., KUDO, H., RAO, J., KIKUCHI, A., WIDMEIER, E., LAWSON, J. A., TAN, W., HERMLE, T., WAREJKO, J. K., SHRIL, S., AIRIK, M., JOBST-SCHWAN, T., LOVRIC, S., BRAUN, D. A., GEE, H. Y., SCHAPIRO, D., MAJMUNDAR, A. J., SADOWSKI, C. E., PABST, W. L., DAGA, A., VAN DER VEN, A. T., SCHMIDT, J. M., LOW, B. C., GUPTA, A. B., TRIPATHI, B. K., WONG, J., CAMPBELL, K., METCALFE, K., SCHANZE, D., NIIHORI, T., KAITO, H., NOZU, K., TSUKAGUCHI, H., TANAKA, R., HAMAHIRA, K., KOBAYASHI, Y., TAKIZAWA, T., FUNAYAMA, R., NAKAYAMA, K., AOKI, Y., KUMAGAI, N., IIJIMA, K., FEHRENBACH, H., KARI, J. A., EL DESOKY, S., JALALAH, S., BOGDANOVIC, R., STAJIC, N., ZAPPEL, H., RAKHMETOVA, A., WASSMER, S. R., JUNGRAITHMAYR, T., STREHLAU, J., KUMAR, A. S., BAGGA, A., SOLIMAN, N. A., MANE, S. M., KAUFMAN, L., LOWY, D. R., JAIRAJPURI, M. A., LIFTON, R. P., PEI, Y., ZENKER, M., KURE, S. & HILDEBRANDT, F. 2018. Mutations in six nephrosis genes delineate a pathogenic pathway amenable to treatment. *Nat Commun,* 9**,** 1960.

ATTANASIO, M., UHLENHAUT, N. H., SOUSA, V. H., O'TOOLE, J. F., OTTO, E., ANLAG, K., KLUGMANN, C., TREIER, A. C., HELOU, J., SAYER, J. A., SEELOW, D., NÜRNBERG, G., BECKER, C., CHUDLEY, A. E., NÜRNBERG, P., HILDEBRANDT, F. & TREIER, M. 2007. Loss of GLIS2 causes nephronophthisis in humans and mice by increased apoptosis and fibrosis. *Nature Genetics,* 39**,** 1018-1024.

ATTISANO, L. & WRANA, J. L. 2002. Signal transduction by the TGF-beta superfamily. *Science,* 296**,** 1646-7.

ATTREE, O., OLIVOS, I. M., OKABE, I., BAILEY, L. C., NELSON, D. L., LEWIS, R. A., MCINNES, R. R. & NUSSBAUM, R. L. 1992. The Lowe's oculocerebrorenal syndrome gene encodes a protein highly homologous to inositol polyphosphate-5-phosphatase. *Nature,* 358**,** 239-42.

BAERT, L. 1978. Hereditary polycystic kidney disease (adult form): a microdissection study of two cases at an early stage of the disease. *Kidney Int,* 13**,** 519-25.

BAGHERIE-LACHIDAN, M., REGINENSI, A., PAN, Q., ZAVERI, H. P., SCOTT, D. A., BLENCOWE, B. J., HELMBACHER, F. & MCNEILL, H. 2015. Stromal Fat4 acts non-autonomously with Dchs1/2 to restrict the nephron progenitor pool. *Development,* 142**,** 2564-73.

BAKEBERG, J. L., TAMMACHOTE, R., WOOLLARD, J. R., HOGAN, M. C., TUAN, H. F., LI, M., VAN DEURSEN, J. M., WU, Y., HUANG, B. Q., TORRES, V. E., HARRIS, P. C. & WARD, C. J. 2011. Epitope-tagged Pkhd1 tracks the processing, secretion, and localization of fibrocystin. *J Am Soc Nephrol,* 22**,** 2266-77.

BARAK, H., HUH, S. H., CHEN, S., JEANPIERRE, C., MARTINOVIC, J., PARISOT, M., BOLE-FEYSOT, C., NITSCHKE, P., SALOMON, R., ANTIGNAC, C., ORNITZ, D. M. & KOPAN, R. 2012. FGF9 and FGF20 maintain the stemness of nephron progenitors in mice and man. *Dev Cell,* 22**,** 1191-207.

BARD, J. B., GORDON, A., SHARP, L. & SELLERS, W. I. 2001. Early nephron formation in the developing mouse kidney. *J Anat,* 199**,** 385-92.

BARKER, D. F., HOSTIKKA, S. L., ZHOU, J., CHOW, L. T., OLIPHANT, A. R., GERKEN, S. C., GREGORY, M. C., SKOLNICK, M. H., ATKIN, C. L. & TRYGGVASON, K. 1990. Identification of mutations in the COL4A5 collagen gene in Alport syndrome. *Science,* 248**,** 1224-7.

BARKER, N., ROOKMAAKER, M. B., KUJALA, P., NG, A., LEUSHACKE, M., SNIPPERT, H., VAN DE WETERING, M., TAN, S., VAN ES, J. H., HUCH, M., POULSOM, R., VERHAAR, M. C.,

PETERS, P. J. & CLEVERS, H. 2012. Lgr5(+ve) stem/progenitor cells contribute to nephron formation during kidney development. *Cell Rep,* 2**,** 540-52.

BARROW, J. R., HOWELL, W. D., RULE, M., HAYASHI, S., THOMAS, K. R., CAPECCHI, M. R. & MCMAHON, A. P. 2007. Wnt3 signaling in the epiblast is required for proper orientation of the anteroposterior axis. *Dev Biol,* 312**,** 312-20.

BARUA, M., SHIEH, E., SCHLONDORFF, J., GENOVESE, G., KAPLAN, B. S. & POLLAK, M. R. 2014a. Exome sequencing and in vitro studies identified podocalyxin as a candidate gene for focal and segmental glomerulosclerosis. *Kidney Int,* 85**,** 124-33.

BARUA, M., STELLACCI, E., STELLA, L., WEINS, A., GENOVESE, G., MUTO, V., CAPUTO, V., TOKA, H. R., CHAROONRATANA, V. T., TARTAGLIA, M. & POLLAK, M. R. 2014b. Mutations in PAX2 associate with adult-onset FSGS. *J Am Soc Nephrol,* 25**,** 1942-53.

BASTEN, S. G. & GILES, R. H. 2013. Functional aspects of primary cilia in signaling, cell cycle and tumorigenesis. *Cilia,* 2.

BEALS, R. K. & WELEBER, R. G. 2007. Conorenal dysplasia: a syndrome of cone-shaped epiphysis, renal disease in childhood, retinitis pigmentosa and abnormality of the proximal femur. *Am J Med Genet A,* 143A**,** 2444-7.

BEHAL, R. H., MILLER, M. S., QIN, H., LUCKER, B. F., JONES, A. & COLE, D. G. 2012. Subunit interactions and organization of the Chlamydomonas reinhardtii intraflagellar transport complex A proteins. *J Biol Chem,* 287**,** 11689-703.

BEN-HAIM, N., LU, C., GUZMAN-AYALA, M., PESCATORE, L., MESNARD, D., BISCHOFBERGER, M., NAEF, F., ROBERTSON, E. J. & CONSTAM, D. B. 2006. The nodal precursor acting via activin receptors induces mesoderm by maintaining a source of its convertases and BMP4. *Dev Cell,* 11**,** 313-23.

BENZING, T., GERKE, P., HOPKER, K., HILDEBRANDT, F., KIM, E. & WALZ, G. 2001. Nephrocystin interacts with Pyk2, p130(Cas), and tensin and triggers phosphorylation of Pyk2. *Proc Natl Acad Sci U S A,* 98**,** 9784-9.

BEPPU, H., KAWABATA, M., HAMAMOTO, T., CHYTIL, A., MINOWA, O., NODA, T. & MIYAZONO, K. 2000. BMP type II receptor is required for gastrulation and early development of mouse embryos. *Dev Biol,* 221**,** 249-58.

BERG, S., KUTRA, D., KROEGER, T., STRAEHLE, C. N., KAUSLER, B. X., HAUBOLD, C., SCHIEGG, M., ALES, J., BEIER, T., RUDY, M., EREN, K., CERVANTES, J. I., XU, B., BEUTTENMUELLER, F., WOLNY, A., ZHANG, C., KOETHE, U., HAMPRECHT, F. A. & KRESHUK, A. 2019. ilastik: interactive machine learning for (bio)image analysis. *Nature Methods,* 16**,** 1226-1232.

BERGMANN, C., FLIEGAUF, M., BRUCHLE, N. O., FRANK, V., OLBRICH, H., KIRSCHNER, J., SCHERMER, B., SCHMEDDING, I., KISPERT, A., KRANZLIN, B., NURNBERG, G., BECKER, C., GRIMM, T., GIRSCHICK, G., LYNCH, S. A., KELEHAN, P., SENDEREK, J., NEUHAUS, T. J., STALLMACH, T., ZENTGRAF, H., NURNBERG, P., GRETZ, N., LO, C., LIENKAMP, S., SCHAFER, T., WALZ, G., BENZING, T., ZERRES, K. & OMRAN, H. 2008. Loss of nephrocystin-3 function can cause embryonic lethality, Meckel-Gruber-like syndrome, situs inversus, and renal-hepatic-pancreatic dysplasia. *Am J Hum Genet,* 82**,** 959-70.

BERKOVIC, S. F., DIBBENS, L. M., OSHLACK, A., SILVER, J. D., KATERELOS, M., VEARS, D. F., LÜLLMANN-RAUCH, R., BLANZ, J., ZHANG, K. W., STANKOVICH, J., KALNINS, R. M., DOWLING, J. P., ANDERMANN, E., ANDERMANN, F., FALDINI, E., D'HOOGE, R., VADLAMUDI, L., MACDONELL, R. A., HODGSON, B. L., BAYLY, M. A., SAVIGE, J., MULLEY, J. C., SMYTH, G. K., POWER, D. A., SAFTIG, P. & BAHLO, M. 2008. Array-Based Gene Discovery with Three Unrelated Subjects Shows SCARB2/LIMP-2 Deficiency Causes Myoclonus Epilepsy and Glomerulosclerosis. *The American Journal of Human Genetics,* 82**,** 673-684.

BERNSTEIN, H. S., BISHOP, D. F., ASTRIN, K. H., KORNREICH, R., ENG, C. M., SAKURABA, H. & DESNICK, R. J. 1989. Fabry disease: six gene rearrangements and an exonic point mutation in the alpha-galactosidase gene. *J Clin Invest,* 83**,** 1390-9.

BERRIDGE, M. J. 2016. The Inositol Trisphosphate/Calcium Signaling Pathway in Health and Disease. *Physiol Rev,* 96**,** 1261-96.

BI, J., CHASE, S. E., PELLENZ, C. D., KURIHARA, H., FANNING, A. S. & KRENDEL, M. 2013. Myosin 1e is a component of the glomerular slit diaphragm complex that regulates actin reorganization during cell-cell contact formation in podocytes. *Am J Physiol Renal Physiol,* 305**,** F532-44.

BIERZYNSKA, A., MCCARTHY, H. J., SODERQUEST, K., SEN, E. S., COLBY, E., DING, W. Y., NABHAN, M. M., KERECUK, L., HEGDE, S., HUGHES, D., MARKS, S., FEATHER, S., JONES, C., WEBB, N. J., OGNJANOVIC, M., CHRISTIAN, M., GILBERT, R. D., SINHA, M. D., LORD, G. M., SIMPSON, M., KOZIELL, A. B., WELSH, G. I. & SALEEM, M. A. 2017. Genomic and clinical profiling of a national nephrotic syndrome cohort advocates a precision medicine approach to disease management. *Kidney Int,* 91**,** 937-947.

BIZET, A. A., BECKER-HECK, A., RYAN, R., WEBER, K., FILHOL, E., KRUG, P., HALBRITTER, J., DELOUS, M., LASBENNES, M. C., LINGHU, B., OAKELEY, E. J., ZARHRATE, M., NITSCHKE, P., GARFA-TRAORE, M., SERLUCA, F., YANG, F., BOUWMEESTER, T., PINSON, L., CASSUTO, E., DUBOT, P., ELSHAKHS, N. A., SAHEL, J. A., SALOMON, R., DRUMMOND, I. A., GUBLER, M. C., ANTIGNAC, C., CHIBOUT, S., SZUSTAKOWSKI, J. D., HILDEBRANDT, F., LORENTZEN, E., SAILER, A. W., BENMERAH, A., SAINT-MEZARD, P. & SAUNIER, S. 2015. Mutations in TRAF3IP1/IFT54 reveal a new role for IFT proteins in microtubule stabilization. *Nat Commun,* 6**,** 8666.

BLACQUE, O. E., LI, C., INGLIS, P. N., ESMAIL, M. A., OU, G., MAH, A. K., BAILLIE, D. L., SCHOLEY, J. M. & LEROUX, M. R. 2006. The WD repeat-containing protein IFTA-1 is required for retrograde intraflagellar transport. *Mol Biol Cell,* 17**,** 5053-62.

BLISNICK, T., BUISSON, J., ABSALON, S., MARIE, A., CAYET, N. & BASTIN, P. 2014. The intraflagellar transport dynein complex of trypanosomes is made of a heterodimer of dynein heavy chains and of light and intermediate chains of distinct functions. *Mol Biol Cell,* 25**,** 2620-33.

BLOODGOOD, R. A. 2000. Protein targeting to flagella of trypanosomatid protozoa. *Cell Biol Int,* 24**,** 857-62.

BODDU, R., YANG, C., O'CONNOR, A. K., HENDRICKSON, R. C., BOONE, B., CUI, X., GARCIA-GONZALEZ, M., IGARASHI, P., ONUCHIC, L. F., GERMINO, G. G. & GUAY-WOODFORD, L. M. 2014. Intragenic motifs regulate the transcriptional complexity of Pkhd1/PKHD1. *J Mol Med (Berl),* 92**,** 1045-56.

BOERKOEL, C. F., TAKASHIMA, H., JOHN, J., YAN, J., STANKIEWICZ, P., ROSENBARKER, L., ANDRE, J. L., BOGDANOVIC, R., BURGUET, A., COCKFIELD, S., CORDEIRO, I., FRUND, S., ILLIES, F., JOSEPH, M., KAITILA, I., LAMA, G., LOIRAT, C., MCLEOD, D. R., MILFORD, D. V., PETTY, E. M., RODRIGO, F., SARAIVA, J. M., SCHMIDT, B., SMITH, G. C., SPRANGER, J., STEIN, A., THIELE, H., TIZARD, J., WEKSBERG, R., LUPSKI, J. R. & STOCKTON, D. W. 2002. Mutant chromatin remodeling protein SMARCAL1 causes Schimke immuno-osseous dysplasia. *Nat Genet,* 30**,** 215-20.

BOLGER, A. M., LOHSE, M. & USADEL, B. 2014. Trimmomatic: a flexible trimmer for Illumina sequence data. *Bioinformatics,* 30**,** 2114-20.

BOOIJ, T. H., BANGE, H., LEONHARD, W. N., YAN, K., FOKKELMAN, M., KUNNEN, S. J., DAUWERSE, J. G., QIN, Y., VAN DE WATER, B., VAN WESTEN, G. J. P., PETERS, D. J. M. & PRICE, L. S. 2017. High-Throughput Phenotypic Screening of Kinase Inhibitors to Identify Drug Targets for Polycystic Kidney Disease. *SLAS Discov,* 22**,** 974-984.

BOUCHARD, M., SOUABNI, A., MANDLER, M., NEUBUSER, A. & BUSSLINGER, M. 2002. Nephric lineage specification by Pax2 and Pax8. *Genes Dev,* 16**,** 2958-70.

BOUTE, N., GRIBOUVAL, O., ROSELLI, S., BENESSY, F., LEE, H., FUCHSHUBER, A., DAHAN, K., GUBLER, M. C., NIAUDET, P. & ANTIGNAC, C. 2000. NPHS2, encoding the glomerular protein podocin, is mutated in autosomal recessive steroid-resistant nephrotic syndrome. *Nat Genet,* 24**,** 349-54.

BOYER, O., WOERNER, S., YANG, F., OAKELEY, E. J., LINGHU, B., GRIBOUVAL, O., TETE, M. J., DUCA, J. S., KLICKSTEIN, L., DAMASK, A. J., SZUSTAKOWSKI, J. D., HEIBEL, F., MATIGNON, M., BAUDOUIN, V., CHANTREL, F., CHAMPIGNEULLE, J., MARTIN, L., NITSCHKE, P., GUBLER, M. C., JOHNSON, K. J., CHIBOUT, S. D. & ANTIGNAC, C. 2013. LMX1B mutations cause hereditary FSGS without extrarenal involvement. *J Am Soc Nephrol,* 24**,** 1216-22.

BOYLE, S., MISFELDT, A., CHANDLER, K. J., DEAL, K. K., SOUTHARD-SMITH, E. M., MORTLOCK, D. P., BALDWIN, H. S. & DE CAESTECKER, M. 2008. Fate mapping using Cited1-CreERT2 mice demonstrates that the cap mesenchyme contains self-renewing progenitor cells and gives rise exclusively to nephronic epithelia. *Dev Biol,* 313**,** 234-45.

BOYLE, S. C., KIM, M., VALERIUS, M. T., MCMAHON, A. P. & KOPAN, R. 2011. Notch pathway activation can replace the requirement for Wnt4 and Wnt9b in mesenchymal-to-epithelial transition of nephron stem cells. *Development,* 138**,** 4245-54.

BRAUN, D. A. & HILDEBRANDT, F. 2016. Ciliopathies. *Cold Spring Harbor Perspectives in Biology*.

BRAUN, D. A., SADOWSKI, C. E., KOHL, S., LOVRIC, S., ASTRINIDIS, S. A., PABST, W. L., GEE, H. Y., ASHRAF, S., LAWSON, J. A., SHRIL, S., AIRIK, M., TAN, W., SCHAPIRO, D., RAO, J., CHOI, W. I., HERMLE, T., KEMPER, M. J., POHL, M., OZALTIN, F., KONRAD, M., BOGDANOVIC, R., BUSCHER, R., HELMCHEN, U., SERDAROGLU, E., LIFTON, R. P., ANTONIN, W. & HILDEBRANDT, F. 2016. Mutations in nuclear pore genes NUP93, NUP205 and XPO5 cause steroid-resistant nephrotic syndrome. *Nat Genet,* 48**,** 457-65.

BRAUN, D. A., WAREJKO, J. K., ASHRAF, S., TAN, W., DAGA, A., SCHNEIDER, R., HERMLE, T., JOBST-SCHWAN, T., WIDMEIER, E., MAJMUNDAR, A. J., NAKAYAMA, M., SCHAPIRO, D., RAO, J., SCHMIDT, J. M., HOOGSTRATEN, C. A., HUGO, H., BAKKALOGLU, S. A., KARI, J. A., EL DESOKY, S., DAOUK, G., MANE, S., LIFTON, R. P., SHRIL, S. & HILDEBRANDT, F. 2019. Genetic variants in the LAMA5 gene in pediatric nephrotic syndrome. *Nephrol Dial Transplant,* 34**,** 485-493.

BREDRUP, C., SAUNIER, S., OUD, M. M., FISKERSTRAND, T., HOISCHEN, A., BRACKMAN, D., LEH, S. M., MIDTBO, M., FILHOL, E., BOLE-FEYSOT, C., NITSCHKE, P., GILISSEN, C., HAUGEN, O. H., SANDERS, J. S., STOLTE-DIJKSTRA, I., MANS, D. A., STEENBERGEN, E. J., HAMEL, B. C., MATIGNON, M., PFUNDT, R., JEANPIERRE, C., BOMAN, H., RODAHL, E., VELTMAN, J. A., KNAPPSKOG, P. M., KNOERS, N. V., ROEPMAN, R. & ARTS, H. H. 2011. Ciliopathies with skeletal anomalies and renal insufficiency due to mutations in the IFT-A gene WDR19. *Am J Hum Genet,* 89**,** 634-43.

BRIGGS, M. W. & SACKS, D. B. 2003. IQGAP proteins are integral components of cytoskeletal regulation. *EMBO Rep,* 4**,** 571-4.

BRISCOE, J. & THEROND, P. P. 2013. The mechanisms of Hedgehog signalling and its roles in development and disease. *Nat Rev Mol Cell Biol,* 14**,** 416-29.

BROWN, E. J., SCHLONDORFF, J. S., BECKER, D. J., TSUKAGUCHI, H., TONNA, S. J., USCINSKI, A. L., HIGGS, H. N., HENDERSON, J. M. & POLLAK, M. R. 2010. Mutations in the formin gene INF2 cause focal segmental glomerulosclerosis. *Nat Genet,* 42**,** 72-6.

BROWN, J. M., COCHRAN, D. A., CRAIGE, B., KUBO, T. & WITMAN, G. B. 2015. Assembly of IFT trains at the ciliary base depends on IFT74. *Curr Biol,* 25**,** 1583-93.

BROWN, J. M. & WITMAN, G. B. 2014. Cilia and Diseases. *Bioscience,* 64**,** 1126-1137.

BRUNSKILL, E. W., ARONOW, B. J., GEORGAS, K., RUMBALLE, B., VALERIUS, M. T., ARONOW, J., KAIMAL, V., JEGGA, A. G., YU, J., GRIMMOND, S., MCMAHON, A. P., PATTERSON, L. T., LITTLE, M. H. & POTTER, S. S. 2008. Atlas of gene expression in the developing kidney at microanatomic resolution. *Dev Cell,* 15**,** 781-91.

BUKANOV, N. O., MORENO, S. E., NATOLI, T. A., ROGERS, K. A., SMITH, L. A., LEDBETTER, S. R., OUMATA, N., GALONS, H., MEIJER, L. & IBRAGHIMOV-BESKROVNAYA, O. 2012. CDK inhibitors R-roscovitine and S-CR8 effectively block renal and hepatic cystogenesis in an orthologous model of ADPKD. *Cell Cycle,* 11**,** 4040-4046.

BUKANOV, N. O., SMITH, L. A., KLINGER, K. W., LEDBETTER, S. R. & IBRAGHIMOV-BESKROVNAYA, O. 2006. Long-lasting arrest of murine polycystic kidney disease with CDK inhibitor roscovitine. *Nature,* 444**,** 949-952.

BURN, S. F., WEBB, A., BERRY, R. L., DAVIES, J. A., FERRER-VAQUER, A., HADJANTONAKIS, A. K., HASTIE, N. D. & HOHENSTEIN, P. 2011. Calcium/NFAT signalling promotes early nephrogenesis. *Dev Biol,* 352**,** 288-98.

BYRON, A., RANDLES, M. J., HUMPHRIES, J. D., MIRONOV, A., HAMIDI, H., HARRIS, S., MATHIESON, P. W., SALEEM, M. A., SATCHELL, S. C., ZENT, R., HUMPHRIES, M. J. & LENNON, R. 2014. Glomerular cell cross-talk influences composition and assembly of extracellular matrix. *J Am Soc Nephrol,* 25**,** 953-66.

CARREL, D., DU, Y., KOMLOS, D., HADZIMICHALIS, N. M., KWON, M., WANG, B., BRZUSTOWICZ, L. M. & FIRESTEIN, B. L. 2009. NOS1AP regulates dendrite patterning of hippocampal neurons through a carboxypeptidase E-mediated pathway. *The Journal of neuroscience : the official journal of the Society for Neuroscience,* 29**,** 8248-8258.

CARREL, D., HERNANDEZ, K., KWON, M., MAU, C., TRIVEDI, M. P., BRZUSTOWICZ, L. M. & FIRESTEIN, B. L. 2015. Nitric oxide synthase 1 adaptor protein, a protein implicated in schizophrenia, controls radial migration of cortical neurons. *Biological psychiatry,* 77**,** 969-978.

CARROLL, T. J., PARK, J. S., HAYASHI, S., MAJUMDAR, A. & MCMAHON, A. P. 2005. Wnt9b plays a central role in the regulation of mesenchymal to epithelial transitions underlying organogenesis of the mammalian urogenital system. *Dev Cell,* 9**,** 283-92.

CASS A, C. S., GALLAGHER M, HOWARD K, JONES A, MCDONALD S, SNELLING P, WHITE S 2010. The Economic Impact of End-Stage Kidney Disease in Australia. Melbourne: Kidney Health Australia.

CASTELLETTI, F., DONADELLI, R., BANTERLA, F., HILDEBRANDT, F., ZIPFEL, P. F., BRESIN, E., OTTO, E., SKERKA, C., RENIERI, A., TODESCHINI, M., CAPRIOLI, J., CARUSO, R. M., ARTUSO, R., REMUZZI, G. & NORIS, M. 2008. Mutations in FN1 cause glomerulopathy with fibronectin deposits. *Proc Natl Acad Sci U S A,* 105**,** 2538-43.

CHAKI, M., AIRIK, R., GHOSH, A. K., GILES, R. H., CHEN, R., SLAATS, G. G., WANG, H., HURD, T. W., ZHOU, W., CLUCKEY, A., GEE, H. Y., RAMASWAMI, G., HONG, C. J., HAMILTON, B. A., CERVENKA, I., GANJI, R. S., BRYJA, V., ARTS, H. H., VAN REEUWIJK, J., OUD, M. M., LETTEBOER, S. J., ROEPMAN, R., HUSSON, H., IBRAGHIMOV-BESKROVNAYA, O., YASUNAGA, T., WALZ, G., ELEY, L., SAYER, J. A., SCHERMER, B., LIEBAU, M. C., BENZING, T., LE CORRE, S., DRUMMOND, I., JANSSEN, S., ALLEN, S. J., NATARAJAN, S., O'TOOLE, J. F., ATTANASIO, M., SAUNIER, S., ANTIGNAC, C., KOENEKOOP, R. K., REN, H., LOPEZ, I., NAYIR, A., STOETZEL, C., DOLLFUS, H., MASSOUDI, R., GLEESON, J. G., ANDREOLI, S. P., DOHERTY, D. G., LINDSTRAD, A., GOLZIO, C., KATSANIS, N., PAPE, L., ABBOUD, E. B., AL-RAJHI, A. A., LEWIS, R. A., OMRAN, H., LEE, E. Y., WANG, S., SEKIGUCHI, J. M., SAUNDERS, R., JOHNSON, C. A., GARNER, E., VANSELOW, K., ANDERSEN, J. S., SHLOMAI, J., NURNBERG, G., NURNBERG, P., LEVY, S., SMOGORZEWSKA, A., OTTO, E. A. & HILDEBRANDT, F. 2012. Exome capture reveals ZNF423 and CEP164 mutations, linking renal ciliopathies to DNA damage response signaling. *Cell,* 150**,** 533-48.

CHANG, S. S., GRUNDER, S., HANUKOGLU, A., ROSLER, A., MATHEW, P. M., HANUKOGLU, I., SCHILD, L., LU, Y., SHIMKETS, R. A., NELSON-WILLIAMS, C., ROSSIER, B. C. & LIFTON, R. P. 1996. Mutations in subunits of the epithelial sodium channel cause salt wasting with hyperkalaemic acidosis, pseudohypoaldosteronism type 1. *Nat Genet,* 12**,** 248-53.

CHATTERJEE, R., HOFFMAN, M., CLIFTEN, P., SESHAN, S., LIAPIS, H. & JAIN, S. 2013. Targeted exome sequencing integrated with clinicopathological information reveals novel and rare mutations in atypical, suspected and unknown cases of Alport syndrome or proteinuria. *PLoS One,* 8**,** e76360.

CHATTERJEE, R., RAMOS, E., HOFFMAN, M., VANWINKLE, J., MARTIN, D. R., DAVIS, T. K., HOSHI, M., HMIEL, S. P., BECK, A., HRUSKA, K., COPLEN, D., LIAPIS, H., MITRA, R., DRULEY, T., AUSTIN, P. & JAIN, S. 2012. Traditional and targeted exome sequencing reveals common, rare and novel functional deleterious variants in RET-signaling complex in a cohort of living US patients with urinary tract malformations. *Hum Genet,* 131**,** 1725-38.

CHEN, G., GULBRANSON, D. R., HOU, Z., BOLIN, J. M., RUOTTI, V., PROBASCO, M. D., SMUGA-OTTO, K., HOWDEN, S. E., DIOL, N. R., PROPSON, N. E., WAGNER, R., LEE, G. O., ANTOSIEWICZ-BOURGET, J., TENG, J. M. C. & THOMSON, J. A. 2011. Chemically defined conditions for human iPSC derivation and culture. *Nat Meth,* 8**,** 424-429.

CHEN, J., BARDES, E. E., ARONOW, B. J. & JEGGA, A. G. 2009. ToppGene Suite for gene list enrichment analysis and candidate gene prioritization. *Nucleic Acids Res,* 37**,** W305-11.

CHEN, L., LEE, J. W., CHOU, C.-L., NAIR, A. V., BATTISTONE, M. A., PĂUNESCU, T. G., MERKULOVA, M., BRETON, S., VERLANDER, J. W., WALL, S. M., BROWN, D., BURG, M. B. & KNEPPER, M. A. 2017. Transcriptomes of major renal collecting duct cell types in mouse identified by single-cell RNA-seq. *Proceedings of the National Academy of Sciences,* 114**,** E9989-E9998.

CHEN, Y. M., ZHOU, Y., GO, G., MARMERSTEIN, J. T., KIKKAWA, Y. & MINER, J. H. 2013. Laminin beta2 gene missense mutation produces endoplasmic reticulum stress in podocytes. *J Am Soc Nephrol,* 24**,** 1223-33.

CHENG, H. T., KIM, M., VALERIUS, M. T., SURENDRAN, K., SCHUSTER-GOSSLER, K., GOSSLER, A., MCMAHON, A. P. & KOPAN, R. 2007. Notch2, but not Notch1, is required for proximal fate acquisition in the mammalian nephron. *Development,* 134**,** 801-11.

CHENNATHUKUZHI, V., MORALES, C. R., EL-ALFY, M. & HECHT, N. B. 2003. The kinesin KIF17b and RNA-binding protein TB-RBP transport specific cAMP-responsive element modulator-regulated mRNAs in male germ cells. *Proc Natl Acad Sci U S A,* 100**,** 15566-71.

CHERRY, A. B. & DALEY, G. Q. 2013. Reprogrammed cells for disease modeling and regenerative medicine. *Annu Rev Med,* 64**,** 277-90.

CHEW, C. & LENNON, R. 2018. Basement Membrane Defects in Genetic Kidney Diseases. *Frontiers in pediatrics,* 6**,** 11-11.

CHI, X., MICHOS, O., SHAKYA, R., RICCIO, P., ENOMOTO, H., LICHT, J. D., ASAI, N., TAKAHASHI, M., OHGAMI, N., KATO, M., MENDELSOHN, C. & COSTANTINI, F. 2009. Ret-dependent cell rearrangements in the Wolffian duct epithelium initiate ureteric bud morphogenesis. *Dev Cell,* 17**,** 199-209.

CHOI, H. J., LIN, J. R., VANNIER, J. B., SLAATS, G. G., KILE, A. C., PAULSEN, R. D., MANNING, D. K., BEIER, D. R., GILES, R. H., BOULTON, S. J. & CIMPRICH, K. A. 2013a. NEK8 links the ATR-regulated replication stress response and S phase CDK activity to renal ciliopathies. *Mol Cell,* 51**,** 423-39.

CHOI, S. Y., CHACON-HESZELE, M. F., HUANG, L., MCKENNA, S., WILSON, F. P., ZUO, X. & LIPSCHUTZ, J. H. 2013b. Cdc42 deficiency causes ciliary abnormalities and cystic kidneys. *J Am Soc Nephrol,* 24**,** 1435-50.

CINGOLANI, P., PLATTS, A., WANG LE, L., COON, M., NGUYEN, T., WANG, L., LAND, S. J., LU, X. & RUDEN, D. M. 2012. A program for annotating and predicting the effects of single nucleotide polymorphisms, SnpEff: SNPs in the genome of Drosophila melanogaster strain w1118; iso-2; iso-3. *Fly (Austin),* 6**,** 80-92.

CLEARY, J. G., BRAITHWAITE, R., GAASTRA, K., HILBUSH, B. S., INGLIS, S., IRVINE, S. A., JACKSON, A., LITTIN, R., NOHZADEH-MALAKSHAH, S., RATHOD, M., WARE, D., TRIGG, L. & DE LA VEGA, F. M. 2014. Joint variant and de novo mutation identification on pedigrees from high-throughput sequencing data. *J Comput Biol,* 21**,** 405-19.

CLISSOLD, R. L., HAMILTON, A. J., HATTERSLEY, A. T., ELLARD, S. & BINGHAM, C. 2015. HNF1B-associated renal and extra-renal disease-an expanding clinical spectrum. *Nat Rev Nephrol,* 11**,** 102-12.

COLIN, E., HUYNH CONG, E., MOLLET, G., GUICHET, A., GRIBOUVAL, O., ARRONDEL, C., BOYER, O., DANIEL, L., GUBLER, M. C., EKINCI, Z., TSIMARATOS, M., CHABROL, B., BODDAERT, N., VERLOES, A., CHEVROLLIER, A., GUEGUEN, N., DESQUIRET-DUMAS, V., FERRE, M., PROCACCIO, V., RICHARD, L., FUNALOT, B., MONCLA, A., BONNEAU, D. & ANTIGNAC, C. 2014. Loss-of-function mutations in WDR73 are responsible for microcephaly and steroid-resistant nephrotic syndrome: Galloway-Mowat syndrome. *Am J Hum Genet,* 95**,** 637-48.

COLLET, J., SPIKE, C. A., LUNDQUIST, E. A., SHAW, J. E. & HERMAN, R. K. 1998. Analysis of osm-6, a gene that affects sensory cilium structure and sensory neuron function in Caenorhabditis elegans. *Genetics,* 148**,** 187-200.

COLVIN, J. S., FELDMAN, B., NADEAU, J. H., GOLDFARB, M. & ORNITZ, D. M. 1999. Genomic organization and embryonic expression of the mouse fibroblast growth factor 9 gene. *Dev Dyn,* 216**,** 72-88.

COMBES, A. N., PHIPSON, B., LAWLOR, K. T., DORISON, A., PATRICK, R., ZAPPIA, L., HARVEY, R. P., OSHLACK, A. & LITTLE, M. H. 2019a. Single cell analysis of the developing mouse kidney provides deeper insight into marker gene expression and ligand-receptor crosstalk. *Development,* 146.

COMBES, A. N., SHORT, K. M., LEFEVRE, J., HAMILTON, N. A., LITTLE, M. H. & SMYTH, I. M. 2014. An integrated pipeline for the multidimensional analysis of branching morphogenesis. *Nat Protoc,* 9**,** 2859-79.

COMBES, A. N., WILSON, S., PHIPSON, B., BINNIE, B. B., JU, A., LAWLOR, K. T., CEBRIAN, C., WALTON, S. L., SMYTH, I. M., MORITZ, K. M., KOPAN, R., OSHLACK, A. & LITTLE, M. H. 2018. Haploinsufficiency for the Six2 gene increases nephron progenitor proliferation promoting branching and nephron number. *Kidney International,* 93**,** 589-598.

COMBES, A. N., ZAPPIA, L., ER, P. X., OSHLACK, A. & LITTLE, M. H. 2019b. Single-cell analysis reveals congruence between kidney organoids and human fetal kidney. *Genome Med,* 11**,** 3.

CONLON, F. L., LYONS, K. M., TAKAESU, N., BARTH, K. S., KISPERT, A., HERRMANN, B. & ROBERTSON, E. J. 1994. A primary requirement for nodal in the formation and maintenance of the primitive streak in the mouse. *Development,* 120**,** 1919-28.

COOPER, C. J., DUTTA, N. T., MARTIN, C. E., PISCIONE, T. D., THORNER, P. S. & JONES, N. 2018. Characterization of a novel disease-associated mutation within NPHS1 and its effects on nephrin phosphorylation and signaling. *PLoS One,* 13**,** e0203905.

CORTELLINO, S., WANG, C., WANG, B., BASSI, M. R., CARETTI, E., CHAMPEVAL, D., CALMONT, A., JARNIK, M., BURCH, J., ZARET, K. S., LARUE, L. & BELLACOSA, A. 2009. Defective ciliogenesis, embryonic lethality and severe impairment of the Sonic Hedgehog pathway caused by inactivation of the mouse complex A intraflagellar transport gene Ift122/Wdr10, partially overlapping with the DNA repair gene Med1/Mbd4. *Dev Biol,* 325**,** 225-37.

COSTANTINI, F. & KOPAN, R. 2010. Patterning a complex organ: branching morphogenesis and nephron segmentation in kidney development. *Dev Cell,* 18**,** 698-712.

CRUZ, N. M., SONG, X., CZERNIECKI, S. M., GULIEVA, R. E., CHURCHILL, A. J., KIM, Y. K., WINSTON, K., TRAN, L. M., DIAZ, M. A., FU, H., FINN, L. S., PEI, Y., HIMMELFARB, J. & FREEDMAN, B. S. 2017. Organoid cystogenesis reveals a critical role of microenvironment in human polycystic kidney disease. *Nat Mater,* 16**,** 1112-1119.

CURTHOYS, N. P. & MOE, O. W. 2014. Proximal Tubule Function and Response to Acidosis. *Clinical Journal of the American Society of Nephrology,* 9**,** 1627-1638.

CYBULSKY, A. V., TAKANO, T., PAPILLON, J., BIJIAN, K., GUILLEMETTE, J. & KENNEDY, C. R. J. 2009. Glomerular epithelial cell injury associated with mutant alpha-actinin-4. *American Journal of Physiology-Renal Physiology,* 297**,** F987-F995.

CZERNIECKI, S. M., CRUZ, N. M., HARDER, J. L., MENON, R., ANNIS, J., OTTO, E. A., GULIEVA, R. E., ISLAS, L. V., KIM, Y. K., TRAN, L. M., MARTINS, T. J., PIPPIN, J. W., FU, H., KRETZLER, M., SHANKLAND, S. J., HIMMELFARB, J., MOON, R. T., PARAGAS, N. & FREEDMAN, B. S. 2018. High-Throughput Screening Enhances Kidney Organoid Differentiation from Human Pluripotent Stem Cells and Enables Automated Multidimensional Phenotyping. *Cell Stem Cell*.

D'AGATI, V. D., KASKEL, F. J. & FALK, R. J. 2011. Focal segmental glomerulosclerosis. *N Engl J Med,* 365**,** 2398-411.

DAGA, A., MAJMUNDAR, A. J., BRAUN, D. A., GEE, H. Y., LAWSON, J. A., SHRIL, S., JOBST-SCHWAN, T., VIVANTE, A., SCHAPIRO, D., TAN, W., WAREJKO, J. K., WIDMEIER, E., NELSON, C. P., FATHY, H. M., GUCEV, Z., SOLIMAN, N. A., HASHMI, S., HALBRITTER, J., HALTY, M., KARI, J. A., EL-DESOKY, S., FERGUSON, M. A., SOMERS, M. J. G., TRAUM, A. Z., STEIN, D. R., DAOUK, G. H., RODIG, N. M., KATZ, A., HANNA, C., SCHWADERER, A. L., SAYER, J. A., WASSNER, A. J., MANE, S., LIFTON, R. P., MILOSEVIC, D., TASIC, V., BAUM, M. A. & HILDEBRANDT, F. 2018. Whole exome sequencing frequently detects a monogenic cause in early onset nephrolithiasis and nephrocalcinosis. *Kidney Int,* 93**,** 204-213.

DAMERLA, R. R., CUI, C., GABRIEL, G. C., LIU, X., CRAIGE, B., GIBBS, B. C., FRANCIS, R., LI, Y., CHATTERJEE, B., SAN AGUSTIN, J. T., EGUETHER, T., SUBRAMANIAN, R., WITMAN, G. B., MICHAUD, J. L., PAZOUR, G. J. & LO, C. W. 2015. Novel Jbts17 mutant mouse model of Joubert syndrome with cilia transition zone defects and cerebellar and other ciliopathy related anomalies. *Hum Mol Genet,* 24**,** 3994-4005.

DANDAPANI, S. V., SUGIMOTO, H., MATTHEWS, B. D., KOLB, R. J., SINHA, S., GERSZTEN, R. E., ZHOU, J., INGBER, D. E., KALLURI, R. & POLLAK, M. R. 2007. Alpha-actinin-4 is required for normal podocyte adhesion. *J Biol Chem,* 282**,** 467-77.

DAS, A., TANIGAWA, S., KARNER, C. M., XIN, M., LUM, L., CHEN, C., OLSON, E. N., PERANTONI, A. O. & CARROLL, T. J. 2013. Stromal-epithelial crosstalk regulates kidney progenitor cell differentiation. *Nat Cell Biol,* 15**,** 1035-44.

DASGUPTA, A. & AMACK, J. D. 2016. Cilia in vertebrate left-right patterning. *Philosophical transactions of the Royal Society of London. Series B, Biological sciences,* 371**,** 20150410.

DAVIS, E. E., ZHANG, Q., LIU, Q., DIPLAS, B. H., DAVEY, L. M., HARTLEY, J., STOETZEL, C., SZYMANSKA, K., RAMASWAMI, G., LOGAN, C. V., MUZNY, D. M., YOUNG, A. C., WHEELER, D. A., CRUZ, P., MORGAN, M., LEWIS, L. R., CHERUKURI, P., MASKERI, B., HANSEN, N. F., MULLIKIN, J. C., BLAKESLEY, R. W., BOUFFARD, G. G., PROGRAM, N. C. S., GYAPAY, G., RIEGER, S., TONSHOFF, B., KERN, I., SOLIMAN, N. A., NEUHAUS, T. J., SWOBODA, K. J., KAYSERILI, H., GALLAGHER, T. E., LEWIS, R. A., BERGMANN, C., OTTO, E. A., SAUNIER, S., SCAMBLER, P. J., BEALES, P. L., GLEESON, J. G., MAHER, E. R., ATTIE-BITACH, T., DOLLFUS, H., JOHNSON, C. A., GREEN, E. D., GIBBS, R. A., HILDEBRANDT, F., PIERCE, E. A. & KATSANIS, N. 2011. TTC21B contributes both causal and modifying alleles across the ciliopathy spectrum. *Nat Genet,* 43**,** 189-96.

DAVIS, T. K., HOSHI, M. & JAIN, S. 2014. To bud or not to bud: the RET perspective in CAKUT. *Pediatr Nephrol,* 29**,** 597-608.

DE JONG, J. C., VAN DER VLIET, W. A., VAN DEN HEUVEL, L. P., WILLEMS, P. H., KNOERS, N. V. & BINDELS, R. J. 2002. Functional expression of mutations in the human NaCl cotransporter: evidence for impaired routing mechanisms in Gitelman's syndrome. *J Am Soc Nephrol,* 13**,** 1442-8.

DE ROUFFIGNAC, C. 1972. Physiological role of the loop of Henle in urinary concentration. *Kidney International,* 2**,** 297-303.

DECRAMER, S., PARANT, O., BEAUFILS, S., CLAUIN, S., GUILLOU, C., KESSLER, S., AZIZA, J., BANDIN, F., SCHANSTRA, J. P. & BELLANNE-CHANTELOT, C. 2007. Anomalies of the TCF2 gene are the main cause of fetal bilateral hyperechogenic kidneys. *J Am Soc Nephrol,* 18**,** 923-33.

DEKKERS, J. F., BERKERS, G., KRUISSELBRINK, E., VONK, A., DE JONGE, H. R., JANSSENS, H. M., BRONSVELD, I., VAN DE GRAAF, E. A., NIEUWENHUIS, E. E., HOUWEN, R. H., VLEGGAAR, F. P., ESCHER, J. C., DE RIJKE, Y. B., MAJOOR, C. J., HEIJERMAN, H. G., DE WINTER-DE GROOT, K. M., CLEVERS, H., VAN DER ENT, C. K. & BEEKMAN, J. M. 2016. Characterizing responses to CFTR-modulating drugs using rectal organoids derived from subjects with cystic fibrosis. *Sci Transl Med,* 8**,** 344ra84.

DEKKERS, J. F., WIEGERINCK, C. L., DE JONGE, H. R., BRONSVELD, I., JANSSENS, H. M., DE WINTER-DE GROOT, K. M., BRANDSMA, A. M., DE JONG, N. W., BIJVELDS, M. J., SCHOLTE, B. J., NIEUWENHUIS, E. E., VAN DEN BRINK, S., CLEVERS, H., VAN DER ENT, C. K., MIDDENDORP, S. & BEEKMAN, J. M. 2013. A functional CFTR assay using primary cystic fibrosis intestinal organoids. *Nat Med,* 19**,** 939-45.

DELORME, R., BETANCUR, C., SCHEID, I., ANCKARSATER, H., CHASTE, P., JAMAIN, S., SCHUROFF, F., NYGREN, G., HERBRECHT, E., DUMAINE, A., MOUREN, M. C., RASTAM, M., LEBOYER, M., GILLBERG, C. & BOURGERON, T. 2010. Mutation screening of NOS1AP gene in a large sample of psychiatric patients and controls. *BMC Med Genet,* 11**,** 108.

DELOUS, M., HELLMAN, N. E., GAUDE, H. M., SILBERMANN, F., LE BIVIC, A., SALOMON, R., ANTIGNAC, C. & SAUNIER, S. 2009. Nephrocystin-1 and nephrocystin-4 are required for epithelial morphogenesis and associate with PALS1/PATJ and Par6. *Hum Mol Genet,* 18**,** 4711-23.

DELTAS, C., SAVVA, I., VOSKARIDES, K., PAPAZACHARIOU, L. & PIERIDES, A. 2015. Carriers of Autosomal Recessive Alport Syndrome with Thin Basement Membrane Nephropathy Presenting as Focal Segmental Glomerulosclerosis in Later Life. *Nephron,* 130**,** 271-80.

DEN HOLLANDER, A. I., HECKENLIVELY, J. R., VAN DEN BORN, L. I., DE KOK, Y. J., VAN DER VELDE-VISSER, S. D., KELLNER, U., JURKLIES, B., VAN SCHOONEVELD, M. J., BLANKENAGEL, A., ROHRSCHNEIDER, K., WISSINGER, B., CRUYSBERG, J. R., DEUTMAN, A. F., BRUNNER, H. G., APFELSTEDT-SYLLA, E., HOYNG, C. B. & CREMERS, F. P. 2001. Leber congenital amaurosis and retinitis pigmentosa with Coats-like exudative vasculopathy are associated with mutations in the crumbs homologue 1 (CRB1) gene. *Am J Hum Genet,* 69**,** 198-203.

DESGRANGE, A., HELIOT, C., SKOVORODKIN, I., AKRAM, S. U., HEIKKILA, J., RONKAINEN, V. P., MIINALAINEN, I., VAINIO, S. J. & CEREGHINI, S. 2017. HNF1B controls epithelial organization and cell polarity during ureteric bud branching and collecting duct morphogenesis. *Development,* 144**,** 4704-4719.

DESMET, F. O., HAMROUN, D., LALANDE, M., COLLOD-BEROUD, G., CLAUSTRES, M. & BEROUD, C. 2009. Human Splicing Finder: an online bioinformatics tool to predict splicing signals. *Nucleic Acids Res,* 37**,** e67.

DEVLIN, L. A. & SAYER, J. A. 2019. Renal ciliopathies. *Current Opinion in Genetics & Development,* 56**,** 49-60.

DEVUYST, O., KNOERS, N. V., REMUZZI, G., SCHAEFER, F., BOARD OF THE WORKING GROUP FOR INHERITED KIDNEY DISEASES OF THE EUROPEAN RENAL, A., EUROPEAN, D. & TRANSPLANT, A. 2014. Rare inherited kidney diseases: challenges, opportunities, and perspectives. *Lancet,* 383**,** 1844-59.

DIOMEDI-CAMASSEI, F., DI GIANDOMENICO, S., SANTORELLI, F. M., CARIDI, G., PIEMONTE, F., MONTINI, G., GHIGGERI, G. M., MURER, L., BARISONI, L., PASTORE, A., MUDA, A. O., VALENTE, M. L., BERTINI, E. & EMMA, F. 2007. COQ2 nephropathy: a newly described inherited mitochondriopathy with primary renal involvement. *J Am Soc Nephrol,* 18**,** 2773-80.

DISHINGER, J. F., KEE, H. L., JENKINS, P. M., FAN, S., HURD, T. W., HAMMOND, J. W., TRUONG, Y. N., MARGOLIS, B., MARTENS, J. R. & VERHEY, K. J. 2010. Ciliary entry of the kinesin-2 motor KIF17 is regulated by importin-beta2 and RanGTP. *Nat Cell Biol,* 12**,** 703-10.

DOBIN, A., DAVIS, C. A., SCHLESINGER, F., DRENKOW, J., ZALESKI, C., JHA, S., BATUT, P., CHAISSON, M. & GINGERAS, T. R. 2013. STAR: ultrafast universal RNA-seq aligner. *Bioinformatics,* 29**,** 15-21.

DONALDSON, J. C., DEMPSEY, P. J., REDDY, S., BOUTON, A. H., COFFEY, R. J. & HANKS, S. K. 2000. Crk-associated substrate p130(Cas) interacts with nephrocystin and both proteins localize to cell-cell contacts of polarized epithelial cells. *Exp Cell Res,* 256**,** 168-78.

DONALDSON, J. C., DISE, R. S., RITCHIE, M. D. & HANKS, S. K. 2002. Nephrocystin-conserved domains involved in targeting to epithelial cell-cell junctions, interaction with filamins, and establishing cell polarity. *J Biol Chem,* 277**,** 29028-35.

DRAGON-DUREY, M.-A., FRÉMEAUX-BACCHI, V., LOIRAT, C., BLOUIN, J., NIAUDET, P., DESCHENES, G., COPPO, P., HERMAN FRIDMAN, W. & WEISS, L. 2004. Heterozygous and Homozygous Factor H Deficiencies Associated with Hemolytic Uremic Syndrome or Membranoproliferative Glomerulonephritis: Report and Genetic Analysis of 16 Cases. *Journal of the American Society of Nephrology,* 15**,** 787-795.

DVELA-LEVITT, M., KOST-ALIMOVA, M., EMANI, M., KOHNERT, E., THOMPSON, R., SIDHOM, E. H., RIVADENEIRA, A., SAHAKIAN, N., ROIGNOT, J., PAPAGREGORIOU, G., MONTESINOS, M. S., CLARK, A. R., MCKINNEY, D., GUTIERREZ, J., ROTH, M., RONCO, L., ELONGA, E., CARTER, T. A., GNIRKE, A., MELANSON, M., HARTLAND, K., WIEDER, N., HSU, J. C., DELTAS, C., HUGHEY, R., BLEYER, A. J., KMOCH, S., ZIVNA, M., BARESOVA, V., KOTA, S., SCHLONDORFF, J., HEIMAN, M., ALPER, S. L., WAGNER, F., WEINS, A., GOLUB, T. R., LANDER, E. S. & GREKA, A. 2019. Small Molecule Targets TMED9 and Promotes Lysosomal Degradation to Reverse Proteinopathy. *Cell,* 178**,** 521-535 e23.

EBARASI, L., ASHRAF, S., BIERZYNSKA, A., GEE, H. Y., MCCARTHY, H. J., LOVRIC, S., SADOWSKI, C. E., PABST, W., VEGA-WARNER, V., FANG, H., KOZIELL, A., SIMPSON, M. A., DURSUN, I., SERDAROGLU, E., LEVY, S., SALEEM, M. A., HILDEBRANDT, F. & MAJUMDAR, A. 2015. Defects of CRB2 cause steroid-resistant nephrotic syndrome. *Am J Hum Genet,* 96**,** 153-61.

EIRAKU, M., TAKATA, N., ISHIBASHI, H., KAWADA, M., SAKAKURA, E., OKUDA, S., SEKIGUCHI, K., ADACHI, T. & SASAI, Y. 2011. Self-organizing optic-cup morphogenesis in three-dimensional culture. *Nature,* 472**,** 51-56.

ELEY, L., GABRIELIDES, C., ADAMS, M., JOHNSON, C. A., HILDEBRANDT, F. & SAYER, J. A. 2008. Jouberin localizes to collecting ducts and interacts with nephrocystin-1. *Kidney Int,* 74**,** 1139-49.

ESPOSITO, T., LEA, R. A., MAHER, B. H., MOSES, D., COX, H. C., MAGLIOCCA, S., ANGIUS, A., NYHOLT, D. R., TITUS, T., KAY, T., GRAY, N. A., RASTALDI, M. P., PARNHAM, A., GIANFRANCESCO, F. & GRIFFITHS, L. R. 2013. Unique X-linked familial FSGS with co-segregating heart block disorder is associated with a mutation in the NXF5 gene. *Hum Mol Genet,* 22**,** 3654-66.

ESTEVEZ, R., BOETTGER, T., STEIN, V., BIRKENHAGER, R., OTTO, E., HILDEBRANDT, F. & JENTSCH, T. J. 2001. Barttin is a Cl- channel beta-subunit crucial for renal Cl- reabsorption and inner ear K+ secretion. *Nature,* 414**,** 558-61.

ETIENNE-MANNEVILLE, S. & HALL, A. 2002. Rho GTPases in cell biology. *Nature,* 420**,** 629-35.

FAGUER, S., CHASSAING, N., BANDIN, F., PROUHEZE, C., CHAUVEAU, D. & DECRAMER, S. 2012. Should SIX2 be routinely tested in patients with isolated congenital abnormalities of kidneys and/or urinary tract (CAKUT)? *Eur J Med Genet,* 55**,** 688-9.

FAILLY, M., BARTOLONI, L., LETOURNEAU, A., MUNOZ, A., FALCONNET, E., ROSSIER, C., DE SANTI, M. M., SANTAMARIA, F., SACCO, O., DELOZIER-BLANCHET, C. D., LAZOR, R. & BLOUIN, J. L. 2009. Mutations in DNAH5 account for only 15% of a non-preselected cohort of patients with primary ciliary dyskinesia. *J Med Genet,* 46**,** 281-6.

FALLERINI, C., BALDASSARRI, M., TREVISSON, E., MORBIDONI, V., LA MANNA, A., LAZZARIN, R., PASINI, A., BARBANO, G., PINCIAROLI, A. R., GAROSI, G., FRULLANTI, E., PINTO, A. M., MENCARELLI, M. A., MARI, F., RENIERI, A. & ARIANI, F. 2017. Alport syndrome: impact of digenic inheritance in patients management. *Clinical Genetics,* 92**,** 34-44.

FALLERINI, C., DOSA, L., TITA, R., DEL PRETE, D., FERIOZZI, S., GAI, G., CLEMENTI, M., LA MANNA, A., MIGLIETTI, N., MANCINI, R., MANDRILE, G., GHIGGERI, G. M., PIAGGIO, G., BRANCATI, F., DIANO, L., FRATE, E., PINCIAROLI, A. R., GIANI, M., CASTORINA, P., BRESIN, E., GIACHINO, D., DE MARCHI, M., MARI, F., BRUTTINI, M., RENIERI, A. & ARIANI, F. 2014. Unbiased next generation sequencing analysis confirms the existence of autosomal dominant Alport syndrome in a relevant fraction of cases. *Clin Genet,* 86**,** 252-7.

FAUL, C., DONNELLY, M., MERSCHER-GOMEZ, S., CHANG, Y. H., FRANZ, S., DELFGAAUW, J., CHANG, J. M., CHOI, H. Y., CAMPBELL, K. N., KIM, K., REISER, J. & MUNDEL, P. 2008. The actin cytoskeleton of kidney podocytes is a direct target of the antiproteinuric effect of cyclosporine A. *Nat Med,* 14**,** 931-8.

FISCH, C. & DUPUIS-WILLIAMS, P. 2011. Ultrastructure of cilia and flagella - back to the future! *Biol Cell,* 103**,** 249-70.

FISCHER, E., LEGUE, E., DOYEN, A., NATO, F., NICOLAS, J. F., TORRES, V., YANIV, M. & PONTOGLIO, M. 2006. Defective planar cell polarity in polycystic kidney disease. *Nature Genetics,* 38**,** 21-23.

FISSELL, W. H. & MINER, J. H. 2018. What Is the Glomerular Ultrafiltration Barrier? *J Am Soc Nephrol,* 29**,** 2262-2264.

FLEMING, B. M., YELIN, R., JAMES, R. G. & SCHULTHEISS, T. M. 2013. A role for Vg1/Nodal signaling in specification of the intermediate mesoderm. *Development,* 140**,** 1819-29.

FLETCHER, J., MCDONALD, S., ALEXANDER, S. I., AUSTRALIAN & NEW ZEALAND PEDIATRIC NEPHROLOGY, A. 2013. Prevalence of genetic renal disease in children. *Pediatr Nephrol,* 28**,** 251-6.

FLIEGAUF, M., HORVATH, J., VON SCHNAKENBURG, C., OLBRICH, H., MULLER, D., THUMFART, J., SCHERMER, B., PAZOUR, G. J., NEUMANN, H. P., ZENTGRAF, H., BENZING, T. & OMRAN, H. 2006. Nephrocystin specifically localizes to the transition zone of renal and respiratory cilia and photoreceptor connecting cilia. *J Am Soc Nephrol,* 17**,** 2424-33.

FORBES, T. A., HOWDEN, S. E., LAWLOR, K., PHIPSON, B., MAKSIMOVIC, J., HALE, L., WILSON, S., QUINLAN, C., HO, G., HOLMAN, K., BENNETTS, B., CRAWFORD, J., TRNKA, P., OSHLACK, A., PATEL, C., MALLETT, A., SIMONS, C. & LITTLE, M. H. 2018. Patient-iPSC-Derived Kidney Organoids Show Functional Validation of a Ciliopathic Renal Phenotype and Reveal Underlying Pathogenetic Mechanisms. *The American Journal of Human Genetics,* 102**,** 816-831.

FRANKE, I., AYDIN, M., KURYLOWICZ, L., LOPEZ, C. E. L., GANSCHOW, R., LENTZE, M. J. & BORN, M. 2019. Clinical course & management of childhood nephrotic syndrome in Germany: a large epidemiological ESPED study. *BMC Nephrology,* 20**,** 45.

FREEDMAN, B. S., BROOKS, C. R., LAM, A. Q., FU, H., MORIZANE, R., AGRAWAL, V., SAAD, A. F., LI, M. K., HUGHES, M. R., WERFF, R. V., PETERS, D. T., LU, J., BACCEI, A., SIEDLECKI, A. M., VALERIUS, M. T., MUSUNURU, K., MCNAGNY, K. M., STEINMAN, T. I., ZHOU, J., LEROU, P. H. & BONVENTRE, J. V. 2015. Modelling kidney disease with CRISPR-mutant kidney organoids derived from human pluripotent epiblast spheroids. *Nat Commun,* 6**,** 8715.

FREEDMAN, B. S., LAM, A. Q., SUNDSBAK, J. L., IATRINO, R., SU, X., KOON, S. J., WU, M., DAHERON, L., HARRIS, P. C., ZHOU, J. & BONVENTRE, J. V. 2013. Reduced ciliary polycystin-2 in induced pluripotent stem cells from polycystic kidney disease patients with PKD1 mutations. *J Am Soc Nephrol,* 24**,** 1571-86.

FREUDENBERG, F., ALTTOA, A. & REIF, A. 2015. Neuronal nitric oxide synthase (NOS1) and its adaptor, NOS1AP, as a genetic risk factors for psychiatric disorders. *Genes Brain Behav,* 14**,** 46-63.

FRIIS, U. G., MADSEN, K., STUBBE, J., HANSEN, P. B., SVENNINGSEN, P., BIE, P., SKOTT, O. & JENSEN, B. L. 2013. Regulation of renin secretion by renal juxtaglomerular cells. *Pflugers Arch,* 465**,** 25-37.

FULOP, N., ZHANG, Z., MARCHASE, R. B. & CHATHAM, J. C. 2007. Glucosamine cardioprotection in perfused rat hearts associated with increased O-linked N-acetylglucosamine protein modification and altered p38 activation. *Am J Physiol Heart Circ Physiol,* 292**,** H2227-36.

FUNA, N. S., SCHACHTER, K. A., LERDRUP, M., EKBERG, J., HESS, K., DIETRICH, N., HONORE, C., HANSEN, K. & SEMB, H. 2015. beta-Catenin Regulates Primitive Streak Induction through Collaborative Interactions with SMAD2/SMAD3 and OCT4. *Cell Stem Cell,* 16**,** 639-52.

GAGNADOUX, M. F., BACRI, J. L., BROYER, M. & HABIB, R. 1989. Infantile chronic tubulo-interstitial nephritis with cortical microcysts: variant of nephronophthisis or new disease entity? *Pediatr Nephrol,* 3**,** 50-5.

GARCIA-GONZALO, F. R., CORBIT, K. C., SIREROL-PIQUER, M. S., RAMASWAMI, G., OTTO, E. A., NORIEGA, T. R., SEOL, A. D., ROBINSON, J. F., BENNETT, C. L., JOSIFOVA, D. J., GARCIA-VERDUGO, J. M., KATSANIS, N., HILDEBRANDT, F. & REITER, J. F. 2011. A transition zone complex regulates mammalian ciliogenesis and ciliary membrane composition. *Nat Genet,* 43**,** 776-84.

GARCIA-GONZALO, F. R. & REITER, J. F. 2012. Scoring a backstage pass: mechanisms of ciliogenesis and ciliary access. *J Cell Biol,* 197**,** 697-709.

GARCIA-GONZALO, F. R. & REITER, J. F. 2016. Open Sesame: How Transition Fibers and the Transition Zone Control Ciliary Composition. *Cold Spring Harb Perspect Biol*.

GARG, P., VERMA, R., COOK, L., SOOFI, A., VENKATAREDDY, M., GEORGE, B., MIZUNO, K., GURNIAK, C., WITKE, W. & HOLZMAN, L. B. 2010. Actin-depolymerizing factor cofilin-1 is necessary in maintaining mature podocyte architecture. *J Biol Chem,* 285**,** 22676-88.

GAST, C., PENGELLY, R. J., LYON, M., BUNYAN, D. J., SEABY, E. G., GRAHAM, N., VENKAT-RAMAN, G. & ENNIS, S. 2016. Collagen (COL4A) mutations are the most frequent mutations underlying adult focal segmental glomerulosclerosis. *Nephrol Dial Transplant,* 31**,** 961-70.

GBADEGESIN, R. A., HALL, G., ADEYEMO, A., HANKE, N., TOSSIDOU, I., BURCHETTE, J., WU, G., HOMSTAD, A., SPARKS, M. A., GOMEZ, J., JIANG, R., ALONSO, A., LAVIN, P., CONLON, P., KORSTANJE, R., STANDER, M. C., SHAMSAN, G., BARUA, M., SPURNEY, R., SINGHAL, P. C., KOPP, J. B., HALLER, H., HOWELL, D., POLLAK, M. R., SHAW, A. S., SCHIFFER, M. & WINN, M. P. 2014. Mutations in the gene that encodes the F-actin binding protein anillin cause FSGS. *J Am Soc Nephrol,* 25**,** 1991-2002.

GEE, HEON Y., ASHRAF, S., WAN, X., VEGA-WARNER, V., ESTEVE-RUDD, J., LOVRIC, S., FANG, H., HURD, TOBY W., SADOWSKI, CAROLIN E., ALLEN, SUSAN J., OTTO, EDGAR A., KORKMAZ, E., WASHBURN, J., LEVY, S., WILLIAMS, DAVID S., BAKKALOGLU, SEVCAN A., ZOLOTNITSKAYA, A., OZALTIN, F., ZHOU, W. & HILDEBRANDT, F. 2014a. Mutations in EMP2 Cause Childhood-Onset Nephrotic Syndrome. *The American Journal of Human Genetics,* 94**,** 884-890.

GEE, H. Y., OTTO, E. A., HURD, T. W., ASHRAF, S., CHAKI, M., CLUCKEY, A., VEGA-WARNER, V., SAISAWAT, P., DIAZ, K. A., FANG, H., KOHL, S., ALLEN, S. J., AIRIK, R., ZHOU, W., RAMASWAMI, G., JANSSEN, S., FU, C., INNIS, J. L., WEBER, S., VESTER, U., DAVIS, E. E., KATSANIS, N., FATHY, H. M., JECK, N., KLAUS, G., NAYIR, A., RAHIM, K. A., AL ATTRACH, I., AL HASSOUN, I., OZTURK, S., DROZDZ, D., HELMCHEN, U., O'TOOLE, J. F., ATTANASIO, M., LEWIS, R. A., NURNBERG, G., NURNBERG, P., WASHBURN, J., MACDONALD, J., INNIS, J. W., LEVY, S. & HILDEBRANDT, F. 2014b. Whole-exome resequencing distinguishes cystic kidney diseases from phenocopies in renal ciliopathies. *Kidney Int,* 85**,** 880-7.

GEE, H. Y., SADOWSKI, C. E., AGGARWAL, P. K., PORATH, J. D., YAKULOV, T. A., SCHUELER, M., LOVRIC, S., ASHRAF, S., BRAUN, D. A., HALBRITTER, J., FANG, H., AIRIK, R., VEGA-WARNER, V., CHO, K. J., CHAN, T. A., MORRIS, L. G., FFRENCH-CONSTANT, C., ALLEN, N., MCNEILL, H., BUSCHER, R., KYRIELEIS, H., WALLOT, M., GASPERT, A., KISTLER, T., MILFORD, D. V., SALEEM, M. A., KENG, W. T., ALEXANDER, S. I., VALENTINI, R. P., LICHT, C., TEH, J. C., BOGDANOVIC, R., KOZIELL, A., BIERZYNSKA, A., SOLIMAN, N. A., OTTO, E. A., LIFTON, R. P., HOLZMAN, L. B., SIBINGA, N. E., WALZ, G., TUFRO, A. & HILDEBRANDT, F. 2016. FAT1 mutations cause a glomerulotubular nephropathy. *Nat Commun,* 7**,** 10822.

GEE, H. Y., SAISAWAT, P., ASHRAF, S., HURD, T. W., VEGA-WARNER, V., FANG, H., BECK, B. B., GRIBOUVAL, O., ZHOU, W., DIAZ, K. A., NATARAJAN, S., WIGGINS, R. C., LOVRIC, S., CHERNIN, G., SCHOEB, D. S., OVUNC, B., FRISHBERG, Y., SOLIMAN, N. A., FATHY, H. M., GOEBEL, H., HOEFELE, J., WEBER, L. T., INNIS, J. W., FAUL, C., HAN, Z., WASHBURN, J., ANTIGNAC, C., LEVY, S., OTTO, E. A. & HILDEBRANDT, F. 2013. ARHGDIA mutations cause nephrotic syndrome via defective RHO GTPase signaling. *J Clin Invest,* 123**,** 3243-53.

GEE, H. Y., ZHANG, F., ASHRAF, S., KOHL, S., SADOWSKI, C. E., VEGA-WARNER, V., ZHOU, W., LOVRIC, S., FANG, H., NETTLETON, M., ZHU, J. Y., HOEFELE, J., WEBER, L. T., PODRACKA, L., BOOR, A., FEHRENBACH, H., INNIS, J. W., WASHBURN, J., LEVY, S., LIFTON, R. P., OTTO, E. A., HAN, Z. & HILDEBRANDT, F. 2015. KANK deficiency leads to podocyte dysfunction and nephrotic syndrome. *J Clin Invest,* 125**,** 2375-84.

GELLERMANN, J., STEFANIDIS, C. J., MITSIONI, A. & QUERFELD, U. 2010. Successful treatment of steroid-resistant nephrotic syndrome associated with WT1 mutations. *Pediatr Nephrol,* 25**,** 1285-9.

GENOVESE, G., FRIEDMAN, D. J., ROSS, M. D., LECORDIER, L., UZUREAU, P., FREEDMAN, B. I., BOWDEN, D. W., LANGEFELD, C. D., OLEKSYK, T. K., USCINSKI KNOB, A. L., BERNHARDY, A. J., HICKS, P. J., NELSON, G. W., VANHOLLEBEKE, B., WINKLER, C. A., KOPP, J. B., PAYS, E. & POLLAK, M. R. 2010. Association of trypanolytic ApoL1 variants with kidney disease in African Americans. *Science,* 329**,** 841-5.

GEORGAS, K., RUMBALLE, B., VALERIUS, M. T., CHIU, H. S., THIAGARAJAN, R. D., LESIEUR, E., ARONOW, B. J., BRUNSKILL, E. W., COMBES, A. N., TANG, D., TAYLOR, D., GRIMMOND, S. M., POTTER, S. S., MCMAHON, A. P. & LITTLE, M. H. 2009. Analysis of

early nephron patterning reveals a role for distal RV proliferation in fusion to the ureteric tip via a cap mesenchyme-derived connecting segment. *Dev Biol,* 332**,** 273-86.

GHOSH, S., SPAGNOLI, G. C., MARTIN, I., PLOEGERT, S., DEMOUGIN, P., HEBERER, M. & RESCHNER, A. 2005. Three-dimensional culture of melanoma cells profoundly affects gene expression profile: a high density oligonucleotide array study. *J Cell Physiol,* 204**,** 522-31.

GIACOMELLI, E., BELLIN, M., SALA, L., VAN MEER, B. J., TERTOOLEN, L. G. J., ORLOVA, V. V. & MUMMERY, C. L. 2017. Three-dimensional cardiac microtissues composed of cardiomyocytes and endothelial cells co-differentiated from human pluripotent stem cells. *Development (Cambridge, England),* 144**,** 1008-1017.

GIGANTE, M., PIEMONTESE, M., GESUALDO, L., IOLASCON, A. & AUCELLA, F. 2011. Molecular and Genetic Basis of Inherited Nephrotic Syndrome. *International Journal of Nephrology,* 2011.

GIGLIO, S., PROVENZANO, A., MAZZINGHI, B., BECHERUCCI, F., GIUNTI, L., SANSAVINI, G., RAVAGLIA, F., ROPERTO, R. M., FARSETTI, S., BENETTI, E., ROTONDI, M., MURER, L., LAZZERI, E., LASAGNI, L., MATERASSI, M. & ROMAGNANI, P. 2015. Heterogeneous Genetic Alterations in Sporadic Nephrotic Syndrome Associate with Resistance to Immunosuppression. *Journal of the American Society of Nephrology,* 26**,** 230-236.

GILES, R. H., AJZENBERG, H. & JACKSON, P. K. 2014. 3D spheroid model of mIMCD3 cells for studying ciliopathies and renal epithelial disorders. *Nat Protoc,* 9**,** 2725-31.

GONG, K. Q., YALLOWITZ, A. R., SUN, H., DRESSLER, G. R. & WELLIK, D. M. 2007. A Hox-Eya-Pax complex regulates early kidney developmental gene expression. *Mol Cell Biol,* 27**,** 7661-8.

GORDON, R. D. 1986. Syndrome of hypertension and hyperkalemia with normal glomerular filtration rate. *Hypertension,* 8**,** 93-102.

GRAHAMMER, F., SCHELL, C. & HUBER, T. B. 2013. The podocyte slit diaphragm—from a thin grey line to a complex signalling hub. *Nature Reviews Nephrology,* 9**,** 587-598.

GRAMPA, V., DELOUS, M., ZAIDAN, M., ODYE, G., THOMAS, S., ELKHARTOUFI, N., FILHOL, E., NIEL, O., SILBERMANN, F., LEBRETON, C., COLLARDEAU-FRACHON, S., ROUVET, I., ALESSANDRI, J. L., DEVISME, L., DIEUX-COESLIER, A., CORDIER, M. P., CAPRI, Y., KHUNG-SAVATOVSKY, S., SIGAUDY, S., SALOMON, R., ANTIGNAC, C., GUBLER, M. C., BENMERAH, A., TERZI, F., ATTIE-BITACH, T., JEANPIERRE, C. & SAUNIER, S. 2016. Novel NEK8 Mutations Cause Severe Syndromic Renal Cystic Dysplasia through YAP Dysregulation. *PLoS Genet,* 12**,** e1005894.

GREBENYUK, S. & RANGA, A. 2019. Engineering Organoid Vascularization. *Frontiers in Bioengineering and Biotechnology,* 7.

GREENBAUM, L. A., BENNDORF, R. & SMOYER, W. E. 2012. Childhood nephrotic syndrome—current and future therapies. *Nature Reviews Nephrology,* 8**,** 445-458.

GREGER, R. 1985. Ion transport mechanisms in thick ascending limb of Henle's loop of mammalian nephron. *Physiological Reviews,* 65**,** 760-797.

GREKA, A. & MUNDEL, P. 2012. Calcium regulates podocyte actin dynamics. *Seminars in nephrology,* 32**,** 319-326.

GROTE, D., SOUABNI, A., BUSSLINGER, M. & BOUCHARD, M. 2006. Pax 2/8-regulated Gata 3 expression is necessary for morphogenesis and guidance of the nephric duct in the developing kidney. *Development,* 133**,** 53-61.

GUYTON, A. C., LANGSTON, J. B. & NAVAR, G. 1964. THEORY FOR RENAL AUTOREGULATION BY FEEDBACK AT THE JUXTAGLOMERULAR APPARATUS. *Circ Res,* 15**,** Suppl:187-97.

HABBIG, S., BARTRAM, M. P., MULLER, R. U., SCHWARZ, R., ANDRIOPOULOS, N., CHEN, S., SAGMULLER, J. G., HOEHNE, M., BURST, V., LIEBAU, M. C., REINHARDT, H. C., BENZING, T. & SCHERMER, B. 2011. NPHP4, a cilia-associated protein, negatively regulates the Hippo pathway. *J Cell Biol,* 193**,** 633-42.

HABBIG, S., BARTRAM, M. P., SAGMULLER, J. G., GRIESSMANN, A., FRANKE, M., MULLER, R. U., SCHWARZ, R., HOEHNE, M., BERGMANN, C., TESSMER, C., REINHARDT, H. C., BURST, V., BENZING, T. & SCHERMER, B. 2012. The ciliopathy disease protein NPHP9 promotes nuclear delivery and activation of the oncogenic transcriptional regulator TAZ. *Hum Mol Genet,* 21**,** 5528-38.

HACKL, M. J., BURFORD, J. L., VILLANUEVA, K., LAM, L., SUSZTAK, K., SCHERMER, B., BENZING, T. & PETI-PETERDI, J. 2013. Tracking the fate of glomerular epithelial cells in vivo using serial multiphoton imaging in new mouse models with fluorescent lineage tags. *Nat Med,* 19**,** 1661-6.

HAIDER, N. B., CARMI, R., SHALEV, H., SHEFFIELD, V. C. & LANDAU, D. 1998. A Bedouin kindred with infantile nephronophthisis demonstrates linkage to chromosome 9 by homozygosity mapping. *American Journal of Human Genetics,* 63**,** 1404-1410.

HALBRITTER, J., PORATH, J. D., DIAZ, K. A., BRAUN, D. A., KOHL, S., CHAKI, M., ALLEN, S. J., SOLIMAN, N. A., HILDEBRANDT, F., OTTO, E. A. & GROUP, G. P. N. S. 2013. Identification of 99 novel mutations in a worldwide cohort of 1,056 patients with a nephronophthisis-related ciliopathy. *Hum Genet,* 132**,** 865-84.

HALE, L. J., HOWDEN, S. E., PHIPSON, B., LONSDALE, A., ER, P. X., GHOBRIAL, I., HOSAWI, S., WILSON, S., LAWLOR, K. T., KHAN, S., OSHLACK, A., QUINLAN, C., LENNON, R. & LITTLE, M. H. 2018. 3D organoid-derived human glomeruli for personalised podocyte disease modelling and drug screening. *Nat Commun,* 9**,** 5167.

HALL, J. E. 2016. Urine Concentration and Dilution; Regulation of Extracellular Fluid Osmolarity and Sodium Concentration. *In:* HALL, J. E. (ed.) *Guyton and Hall Textbook of Medical Physiology.* 13 ed.: Saunders.

HAMM, L. L., NAKHOUL, N. & HERING-SMITH, K. S. 2015. Acid-Base Homeostasis. *Clinical Journal of the American Society of Nephrology,* 10**,** 2232-2242.

HANNAN, N. R. F., SEGERITZ, C.-P., TOUBOUL, T. & VALLIER, L. 2013. Production of hepatocyte-like cells from human pluripotent stem cells. *Nature protocols,* 8**,** 430-437.

HARIHARAN, K., KURTZ, A. & SCHMIDT-OTT, K. M. 2015. Assembling Kidney Tissues from Cells: The Long Road from Organoids to Organs. *Front Cell Dev Biol,* 3**,** 70.

HARSKAMP, L. R., GANSEVOORT, R. T., VAN GOOR, H. & MEIJER, E. 2016. The epidermal growth factor receptor pathway in chronic kidney diseases. *Nat Rev Nephrol,* 12**,** 496-506.

HART, A. H., WILLSON, T. A., WONG, M., PARKER, K. & ROBB, L. 2005. Transcriptional regulation of the homeobox gene Mixl1 by TGF-beta and FoxH1. *Biochem Biophys Res Commun,* 333**,** 1361-9.

HARTILL, V. L., VAN DE HOEK, G., PATEL, M. P., LITTLE, R., WATSON, C. M., BERRY, I. R., SHOEMARK, A., ABDELMOTTALEB, D., PARKES, E., BACCHELLI, C., SZYMANSKA, K., KNOERS, N. V., SCAMBLER, P. J., UEFFING, M., BOLDT, K., YATES, R., WINYARD, P. J., ADLER, B., MOYA, E., HATTINGH, L., SHENOY, A., HOGG, C., SHERIDAN, E., ROEPMAN, R., NORRIS, D., MITCHISON, H. M., GILES, R. H. & JOHNSON, C. A. 2018. DNAAF1 links heart laterality with the AAA+ ATPase RUVBL1 and ciliary intraflagellar transport. *Hum Mol Genet,* 27**,** 529-545.

HARTLEBEN, B., SCHWEIZER, H., LÜBBEN, P., BARTRAM, M. P., MÖLLER, C. C., HERR, R., WEI, C., NEUMANN-HAEFELIN, E., SCHERMER, B., ZENTGRAF, H., KERJASCHKI, D., REISER, J., WALZ, G., BENZING, T. & HUBER, T. B. 2008. Neph-Nephrin Proteins Bind the Par3-Par6-Atypical Protein Kinase C (aPKC) Complex to Regulate Podocyte Cell Polarity. *Journal of Biological Chemistry,* 283**,** 23033-23038.

HARTLEBEN, B., WIDMEIER, E., SUHM, M., WORTHMANN, K., SCHELL, C., HELMSTÄDTER, M., WIECH, T., WALZ, G., LEITGES, M., SCHIFFER, M. & HUBER, T. B. 2013. aPKCλ/ι and aPKCζ Contribute to Podocyte Differentiation and Glomerular Maturation. *Journal of the American Society of Nephrology,* 24**,** 253-267.

HARTMAN, H. A., LAI, H. L. & PATTERSON, L. T. 2007. Cessation of renal morphogenesis in mice. *Dev Biol,* 310**,** 379-87.

HAS, C., SPARTA, G., KIRITSI, D., WEIBEL, L., MOELLER, A., VEGA-WARNER, V., WATERS, A., HE, Y., ANIKSTER, Y., ESSER, P., STRAUB, B. K., HAUSSER, I., BOCKENHAUER, D., DEKEL, B., HILDEBRANDT, F., BRUCKNER-TUDERMAN, L. & LAUBE, G. F. 2012. Integrin alpha3 mutations with kidney, lung, and skin disease. *N Engl J Med,* 366**,** 1508-14.

HASSELBACHER, K., WIGGINS, R. C., MATEJAS, V., HINKES, B. G., MUCHA, B., HOSKINS, B. E., OZALTIN, F., NURNBERG, G., BECKER, C., HANGAN, D., POHL, M., KUWERTZ-BROKING, E., GRIEBEL, M., SCHUMACHER, V., ROYER-POKORA, B., BAKKALOGLU, A., NURNBERG, P., ZENKER, M. & HILDEBRANDT, F. 2006. Recessive missense mutations in LAMB2 expand the clinical spectrum of LAMB2-associated disorders. *Kidney Int,* 70**,** 1008-12.

HE, F., CHEN, S., WANG, H., SHAO, N., TIAN, X., JIANG, H., LIU, J., ZHU, Z., MENG, X. & ZHANG, C. 2011. Regulation of CD2-associated protein influences podocyte endoplasmic reticulum stress-mediated apoptosis induced by albumin overload. *Gene,* 484**,** 18-25.

HE, Z., WU, J., SU, X., ZHANG, Y., PAN, L., WEI, H., FANG, Q., LI, H., WANG, D.-L. & SUN, F.-L. 2016. JMJD5 (Jumonji Domain-containing 5) Associates with Spindle Microtubules and Is Required for Proper Mitosis. *The Journal of Biological Chemistry,* 291**,** 4684-4697.

HEASMAN, S. J. & RIDLEY, A. J. 2008. Mammalian Rho GTPases: new insights into their functions from in vivo studies. *Nat Rev Mol Cell Biol,* 9**,** 690-701.

HECHT, D., ZIMMERMAN, N., BEDFORD, M., AVIVI, A. & YAYON, A. 1995. Identification of fibroblast growth factor 9 (FGF9) as a high affinity, heparin dependent ligand for FGF receptors 3 and 2 but not for FGF receptors 1 and 4. *Growth Factors,* 12**,** 223-33.

HEERINGA, S. F., CHERNIN, G., CHAKI, M., ZHOU, W., SLOAN, A. J., JI, Z., XIE, L. X., SALVIATI, L., HURD, T. W., VEGA-WARNER, V., KILLEN, P. D., RAPHAEL, Y., ASHRAF, S., OVUNC, B., SCHOEB, D. S., MCLAUGHLIN, H. M., AIRIK, R., VLANGOS, C. N., GBADEGESIN, R., HINKES, B., SAISAWAT, P., TREVISSON, E., DOIMO, M., CASARIN, A., PERTEGATO, V., GIORGI, G., PROKISCH, H., ROTIG, A., NURNBERG, G., BECKER, C., WANG, S., OZALTIN, F., TOPALOGLU, R., BAKKALOGLU, A., BAKKALOGLU, S. A., MULLER, D., BEISSERT, A., MIR, S., BERDELI, A., VARPIZEN, S., ZENKER, M., MATEJAS, V., SANTOS-OCANA, C., NAVAS, P., KUSAKABE, T., KISPERT, A., AKMAN, S., SOLIMAN, N. A., KRICK, S., MUNDEL, P., REISER, J., NURNBERG, P., CLARKE, C. F., WIGGINS, R. C., FAUL, C. & HILDEBRANDT, F. 2011. COQ6 mutations in human patients produce nephrotic syndrome with sensorineural deafness. *J Clin Invest,* 121**,** 2013-24.

HEIDET, L., DECRAMER, S., PAWTOWSKI, A., MORINIERE, V., BANDIN, F., KNEBELMANN, B., LEBRE, A. S., FAGUER, S., GUIGONIS, V., ANTIGNAC, C. & SALOMON, R. 2010. Spectrum of HNF1B mutations in a large cohort of patients who harbor renal diseases. *Clin J Am Soc Nephrol,* 5**,** 1079-90.

HELMS, L., GOMEZ, I., CRUZ, N. M. & FREEDMAN, B. S. 2019. Myosin Activation as a Novel Therapeutic Strategy to Treat PKD in Human Kidney Organoids and Mice. *American Society of Nephrology.* Washington D.C.

HENNIGAR, R. A., SCHULTE, B. A. & SPICER, S. S. 1985. Heterogeneous distribution of glycoconjugates in human kidney tubules. *Anat Rec,* 211**,** 376-90.

HENTZE, H., SOONG, P. L., WANG, S. T., PHILLIPS, B. W., PUTTI, T. C. & DUNN, N. R. 2009. Teratoma formation by human embryonic stem cells: evaluation of essential parameters for future safety studies. *Stem Cell Res,* 2**,** 198-210.

HIGGINS, J. W., CHAMBON, A., BISHARD, K., HARTUNG, A., ARNDT, D., BRUGNANO, J., ER, P. X., LAWLOR, K. T., VANSLAMBROUCK, J. M., WILSON, S., COMBES, A. N., HOWDEN, S. E., TAN, K. S., KUMAR, S. V., HALE, L. J., SHEPHERD, B., PENTONEY, S., PRESNELL, S. C., CHEN, A. E. & LITTLE, M. H. 2018. Bioprinted pluripotent stem cell-derived kidney organoids provide opportunities for high content screening. *bioRxiv***,** 505396.

HILDEBRANDT, F. 1999. Nephronophthisis. *Pediatric Nephrology***,** 453-458.

HILDEBRANDT, F. 2016. Nephronophthisis and Medullary Cystic Kidney Disease in Children. *In:* AVNER, E. D., HARMON, W. E., NIAUDET, P., YOSHIKAWA, N., EMMA, F. & GOLDSTEIN, S. L. (eds.) *Pediatric Nephrology.* Berlin, Heidelberg: Springer Berlin Heidelberg.

HILDEBRANDT, F., BENZING, T. & KATSANIS, N. 2011. Ciliopathies. *New England Journal of Medicine,* 364**,** 1533-1543.

HILDEBRANDT, F. & HEERINGA, S. F. 2009. Specific podocin mutations determine age of onset of nephrotic syndrome all the way into adult life. *Kidney Int,* 75**,** 669-71.

HILDEBRANDT, F. & OTTO, E. 2005. Cilia and centrosomes: A unifying pathogenic concept for cystic kidney disease? *Nature Reviews Genetics,* 6**,** 928-940.

HILDEBRANDT, F., STRAHM, B., NOTHWANG, H. G., GRETZ, N., SCHNIEDERS, B., SINGH-SAWHNEY, I., KUTT, R., VOLLMER, M. & BRANDIS, M. 1997. Molecular genetic identification of families with juvenile nephronophthisis type 1: rate of progression to renal failure. APN Study Group. Arbeitsgemeinschaft fur Padiatrische Nephrologie. *Kidney Int,* 51**,** 261-9.

HILDEBRANDT, F., WALDHERR, R., KUTT, R. & BRANDIS, M. 1992. The nephronophthisis complex: clinical and genetic aspects. *Clin Investig,* 70**,** 802-8.

HILDEBRANDT, F. & ZHOU, W. 2007. Nephronophthisis-associated ciliopathies. *J Am Soc Nephrol,* 18**,** 1855-71.

HINCHLIFFE, S. A., SARGENT, P. H., HOWARD, C. V., CHAN, Y. F. & VAN VELZEN, D. 1991. Human intrauterine renal growth expressed in absolute number of glomeruli assessed by the disector method and Cavalieri principle. *Lab Invest,* 64**,** 777-84.

HINKES, B., WIGGINS, R. C., GBADEGESIN, R., VLANGOS, C. N., SEELOW, D., NURNBERG, G., GARG, P., VERMA, R., CHAIB, H., HOSKINS, B. E., ASHRAF, S., BECKER, C., HENNIES, H. C., GOYAL, M., WHARRAM, B. L., SCHACHTER, A. D., MUDUMANA, S., DRUMMOND, I., KERJASCHKI, D., WALDHERR, R., DIETRICH, A., OZALTIN, F., BAKKALOGLU, A., CLEPER, R., BASEL-VANAGAITE, L., POHL, M., GRIEBEL, M.,

TSYGIN, A. N., SOYLU, A., MULLER, D., SORLI, C. S., BUNNEY, T. D., KATAN, M., LIU, J., ATTANASIO, M., O'TOOLE J, F., HASSELBACHER, K., MUCHA, B., OTTO, E. A., AIRIK, R., KISPERT, A., KELLEY, G. G., SMRCKA, A. V., GUDERMANN, T., HOLZMAN, L. B., NURNBERG, P. & HILDEBRANDT, F. 2006. Positional cloning uncovers mutations in PLCE1 responsible for a nephrotic syndrome variant that may be reversible. *Nat Genet,* 38**,** 1397-405.

HINKES, B. G., MUCHA, B., VLANGOS, C. N., GBADEGESIN, R., LIU, J., HASSELBACHER, K., HANGAN, D., OZALTIN, F., ZENKER, M., HILDEBRANDT, F. & ARBEITSGEMEINSCHAFT FUR PAEDIATRISCHE NEPHROLOGIE STUDY, G. 2007. Nephrotic syndrome in the first year of life: two thirds of cases are caused by mutations in 4 genes (NPHS1, NPHS2, WT1, and LAMB2). *Pediatrics,* 119**,** e907-19.

HIRANO, T., KATOH, Y. & NAKAYAMA, K. 2016. Intraflagellar transport-A complex mediates ciliary entry as well as retrograde trafficking of ciliary G protein-coupled receptors. *Mol Biol Cell*.

HIROSE, T., SATOH, D., KURIHARA, H., KUSAKA, C., HIROSE, H., AKIMOTO, K., MATSUSAKA, T., ICHIKAWA, I., NODA, T. & OHNO, S. 2009. An essential role of the universal polarity protein, aPKClambda, on the maintenance of podocyte slit diaphragms. *PLoS One,* 4**,** e4194.

HISATSUNE, C., KURODA, Y., NAKAMURA, K., INOUE, T., NAKAMURA, T., MICHIKAWA, T., MIZUTANI, A. & MIKOSHIBA, K. 2004. Regulation of TRPC6 channel activity by tyrosine phosphorylation. *J Biol Chem,* 279**,** 18887-94.

HOEFELE, J., WOLF, M. T., O'TOOLE, J. F., OTTO, E. A., SCHULTHEISS, U., DESCHENES, G., ATTANASIO, M., UTSCH, B., ANTIGNAC, C. & HILDEBRANDT, F. 2007. Evidence of oligogenic inheritance in nephronophthisis. *J Am Soc Nephrol,* 18**,** 2789-95.

HOFMEISTER, A. F., KOMHOFF, M., WEBER, S. & GRGIC, I. 2017. Disease modeling in genetic kidney diseases: mice. *Cell Tissue Res,* 369**,** 159-170.

HOLLYWOOD, J. A., PRZEPIORSKI, A., HARRISON, P. T., WOLVETANG, E. J., DAVIDSON, A. J. & HOLM, T. M. 2019. Use of human iPSCs and kidney organoids to develop a cysteamine/mTOR inhibition combination therapy to treat cystinosis. *bioRxiv***,** 595264.

HOMAN, K. A., GUPTA, N., KROLL, K. T., KOLESKY, D. B., SKYLAR-SCOTT, M., MIYOSHI, T., MAU, D., VALERIUS, M. T., FERRANTE, T., BONVENTRE, J. V., LEWIS, J. A. & MORIZANE, R. 2019. Flow-enhanced vascularization and maturation of kidney organoids in vitro. *Nature Methods*.

HOMAN, K. A., KOLESKY, D. B., SKYLAR-SCOTT, M. A., HERRMANN, J., OBUOBI, H., MOISAN, A. & LEWIS, J. A. 2016. Bioprinting of 3D Convoluted Renal Proximal Tubules on Perfusable Chips. *Sci Rep,* 6**,** 34845.

HORANI, A. & FERKOL, T. W. 2018. Advances in the Genetics of Primary Ciliary Dyskinesia: Clinical Implications. *Chest,* 154**,** 645-652.

HOU, Y., QIN, H., FOLLIT, J. A., PAZOUR, G. J., ROSENBAUM, J. L. & WITMAN, G. B. 2007. Functional analysis of an individual IFT protein: IFT46 is required for transport of outer dynein arms into flagella. *J Cell Biol,* 176**,** 653-65.

HOWDEN, S. E., MAUFORT, J. P., DUFFIN, B. M., ELEFANTY, A. G., STANLEY, E. G. & THOMSON, J. A. 2015. Simultaneous Reprogramming and Gene Correction of Patient Fibroblasts. *Stem Cell Reports,* 5**,** 1109-18.

HOWDEN, S. E., MCCOLL, B., GLASER, A., VADOLAS, J., PETROU, S., LITTLE, M. H., ELEFANTY, A. G. & STANLEY, E. G. 2016. A Cas9 Variant for Efficient Generation of Indel-Free Knockin or Gene-Corrected Human Pluripotent Stem Cells. *Stem Cell Reports,* 7**,** 508-517.

HOWDEN, S. E., THOMSON, J. A. & LITTLE, M. H. 2018. Simultaneous reprogramming and gene editing of human fibroblasts. *Nat Protoc,* 13**,** 875-898.

HOWDEN, S. E., VANSLAMBROUCK, J. M., WILSON, S. B., TAN, K. S. & LITTLE, M. H. 2019. Reporter-based fate mapping in human kidney organoids confirms nephron lineage relationships and reveals synchronous nephron formation. *EMBO reports,* 20**,** e47483.

HOY, W. E., DOUGLAS-DENTON, R. N., HUGHSON, M. D., CASS, A., JOHNSON, K. & BERTRAM, J. F. 2003. A stereological study of glomerular number and volume: preliminary findings in a multiracial study of kidneys at autopsy. *Kidney Int Suppl***,** S31-7.

HSIEH, W.-C., RAMADESIKAN, S., FEKETE, D. & AGUILAR, R. C. 2018. Kidney-differentiated cells derived from Lowe Syndrome patient's iPSCs show ciliogenesis defects and Six2 retention at the Golgi complex. *PloS one,* 13**,** e0192635-e0192635.

HUANG, X., ZHANG, S., QI, H., WANG, Z., CHEN, H.-W., SHAO, J. & SHEN, J. 2015. JMJD5 interacts with p53 and negatively regulates p53 function in control of cell cycle and proliferation. *Biochimica et Biophysica Acta (BBA) - Molecular Cell Research,* 1853**,** 2286-2295.

HUANG, Z., ZHANG, L., CHEN, Y., ZHANG, H., ZHANG, Q., LI, R., MA, J., LI, Z., YU, C., LAI, Y., LIN, T., ZHAO, X., ZHANG, B., YE, Z., LIU, S., WANG, W., LIANG, X., LIAO, R. & SHI, W. 2016. Cdc42 deficiency induces podocyte apoptosis by inhibiting the Nwasp/stress fibers/YAP pathway. *Cell Death & Disease,* 7**,** e2142-e2142.

HUANGFU, D., LIU, A., RAKEMAN, A. S., MURCIA, N. S., NISWANDER, L. & ANDERSON, K. V. 2003. Hedgehog signalling in the mouse requires intraflagellar transport proteins. *Nature,* 426**,** 83-7.

HUBER, T. B., HARTLEBEN, B., KIM, J., SCHMIDTS, M., SCHERMER, B., KEIL, A., EGGER, L., LECHA, R. L., BORNER, C., PAVENSTADT, H., SHAW, A. S., WALZ, G. & BENZING, T. 2003a. Nephrin and CD2AP associate with phosphoinositide 3-OH kinase and stimulate AKT-dependent signaling. *Mol Cell Biol,* 23**,** 4917-28.

HUBER, T. B., SIMONS, M., HARTLEBEN, B., SERNETZ, L., SCHMIDTS, M., GUNDLACH, E., SALEEM, M. A., WALZ, G. & BENZING, T. 2003b. Molecular basis of the functional podocin–nephrin complex: mutations in the NPHS2 gene disrupt nephrin targeting to lipid raft microdomains. *Human Molecular Genetics,* 12**,** 3397-3405.

HUGHSON, M., FARRIS, A. B., 3RD, DOUGLAS-DENTON, R., HOY, W. E. & BERTRAM, J. F. 2003. Glomerular number and size in autopsy kidneys: the relationship to birth weight. *Kidney Int,* 63**,** 2113-22.

HURD, T. W. & HILDEBRANDT, F. 2011. Mechanisms of nephronophthisis and related ciliopathies. *Nephron Exp Nephrol,* 118**,** e9-14.

HUSSON, H., MORENO, S., SMITH, L. A., SMITH, M. M., RUSSO, R. J., PITSTICK, R., SERGEEV, M., LEDBETTER, S. R., BUKANOV, N. O., LANE, M., ZHANG, K., BILLOT, K., CARLSON, G., SHAH, J., MEIJER, L., BEIER, D. R. & IBRAGHIMOV-BESKROVNAYA, O. 2016. Reduction of ciliary length through pharmacologic or genetic inhibition of CDK5 attenuates polycystic kidney disease in a model of nephronophthisis. *Hum Mol Genet*.

HUYNH CONG, E., BIZET, A. A., BOYER, O., WOERNER, S., GRIBOUVAL, O., FILHOL, E., ARRONDEL, C., THOMAS, S., SILBERMANN, F., CANAUD, G., HACHICHA, J., BEN DHIA, N., PERALDI, M. N., HARZALLAH, K., IFTENE, D., DANIEL, L., WILLEMS, M., NOEL, L. H., BOLE-FEYSOT, C., NITSCHKE, P., GUBLER, M. C., MOLLET, G., SAUNIER, S. & ANTIGNAC, C. 2014. A homozygous missense mutation in the ciliary gene TTC21B causes familial FSGS. *J Am Soc Nephrol,* 25**,** 2435-43.

HWANG, D. Y., DWORSCHAK, G. C., KOHL, S., SAISAWAT, P., VIVANTE, A., HILGER, A. C., REUTTER, H. M., SOLIMAN, N. A., BOGDANOVIC, R., KEHINDE, E. O., TASIC, V. & HILDEBRANDT, F. 2014. Mutations in 12 known dominant disease-causing genes clarify many congenital anomalies of the kidney and urinary tract. *Kidney Int,* 85**,** 1429-33.

HYNES, A. M., GILES, R. H., SRIVASTAVA, S., ELEY, L., WHITEHEAD, J., DANILENKO, M., RAMAN, S., SLAATS, G. G., COLVILLE, J. G., AJZENBERG, H., KROES, H. Y., THELWALL, P. E., SIMMONS, N. L., MILES, C. G. & SAYER, J. A. 2014. Murine Joubert syndrome reveals Hedgehog signaling defects as a potential therapeutic target for nephronophthisis. *Proc Natl Acad Sci U S A,* 111**,** 9893-8.

IGLESIAS, C. G., TORRES, V. E., OFFORD, K. P., HOLLEY, K. E., BEARD, C. M. & KURLAND, L. T. 1983. Epidemiology of adult polycystic kidney disease, Olmsted County, Minnesota: 1935-1980. *Am J Kidney Dis,* 2**,** 630-9.

IMBERTI, B., TOMASONI, S., CIAMPI, O., PEZZOTTA, A., DEROSAS, M., XINARIS, C., RIZZO, P., PAPADIMOU, E., NOVELLI, R., BENIGNI, A., REMUZZI, G. & MORIGI, M. 2015. Renal progenitors derived from human iPSCs engraft and restore function in a mouse model of acute kidney injury. *Sci Rep,* 5**,** 8826.

IOMINI, C., BABAEV-KHAIMOV, V., SASSAROLI, M. & PIPERNO, G. 2001. Protein particles in Chlamydomonas flagella undergo a transport cycle consisting of four phases. *J Cell Biol,* 153**,** 13-24.

ISHIKAWA, H., THOMPSON, J., YATES, J. R., 3RD & MARSHALL, W. F. 2012. Proteomic analysis of mammalian primary cilia. *Curr Biol,* 22**,** 414-9.

ISHIMURA, A., MINEHATA, K.-I., TERASHIMA, M., KONDOH, G., HARA, T. & SUZUKI, T. 2012. Jmjd5, an H3K36me2 histone demethylase, modulates embryonic cell proliferation through the regulation of Cdkn1a expression. *Development,* 139**,** 749-759.

IZU, A., YANAGIDA, H., SUGIMOTO, K., FUJITA, S., SAKATA, N., WADA, N., OKADA, M. & TAKEMURA, T. 2011. Pathogenesis of focal segmental glomerular sclerosis in a girl with the partial deletion of chromosome 6p. *Tohoku J Exp Med,* 223**,** 187-92.

JAFFE, A. B. & HALL, A. 2005. Rho GTPases: biochemistry and biology. *Annu Rev Cell Dev Biol,* 21**,** 247-69.

JAIN, S. 2009. The many faces of RET dysfunction in kidney. *Organogenesis,* 5**,** 177-90.

JAISWAL, M., FANSA, E. K., DVORSKY, R. & AHMADIAN, M. R. 2013. New insight into the molecular switch mechanism of human Rho family proteins: shifting a paradigm. *Biol Chem,* 394**,** 89-95.

JAMES, R. G., KAMEI, C. N., WANG, Q., JIANG, R. & SCHULTHEISS, T. M. 2006. Odd-skipped related 1 is required for development of the metanephric kidney and regulates formation and differentiation of kidney precursor cells. *Development,* 133**,** 2995-3004.

JAMES, R. G. & SCHULTHEISS, T. M. 2003. Patterning of the avian intermediate mesoderm by lateral plate and axial tissues. *Dev Biol,* 253**,** 109-24.

JANSEN, J., DE NAPOLI, I. E., FEDECOSTANTE, M., SCHOPHUIZEN, C. M., CHEVTCHIK, N. V., WILMER, M. J., VAN ASBECK, A. H., CROES, H. J., PERTIJS, J. C., WETZELS, J. F., HILBRANDS, L. B., VAN DEN HEUVEL, L. P., HOENDEROP, J. G., STAMATIALIS, D. & MASEREEUW, R. 2015. Human proximal tubule epithelial cells cultured on hollow fibers: living membranes that actively transport organic cations. *Sci Rep,* 5**,** 16702.

JARAD, G., CUNNINGHAM, J., SHAW, A. S. & MINER, J. H. 2006. Proteinuria precedes podocyte abnormalities inLamb2-/- mice, implicating the glomerular basement membrane as an albumin barrier. *J Clin Invest,* 116**,** 2272-9.

JAYASINGHE, K., QUINLAN, C., STARK, Z., PATEL, C., MALLAWAARACHCHI, A., WARDROP, L., KERR, P. G., TRNKA, P., MALLETT, A. J. & COLLABORATIVE, O. B. O. T. K. 2019. Renal genetics in Australia: Kidney medicine in the genomic age. *Nephrology,* 24**,** 279-286.

JIANG, L., DING, J., TSAI, H., LI, L., FENG, Q., MIAO, J. & FAN, Q. 2011. Over-expressing transient receptor potential cation channel 6 in podocytes induces cytoskeleton rearrangement through increases of intracellular Ca2+ and RhoA activation. *Exp Biol Med (Maywood),* 236**,** 184-93.

JONASSEN, J. A., SANAGUSTIN, J., BAKER, S. P. & PAZOUR, G. J. 2012. Disruption of IFT complex A causes cystic kidneys without mitotic spindle misorientation. *J Am Soc Nephrol,* 23**,** 641-51.

JOO, K., KIM, C. G., LEE, M. S., MOON, H. Y., LEE, S. H., KIM, M. J., KWEON, H. S., PARK, W. Y., KIM, C. H., GLEESON, J. G. & KIM, J. 2013. CCDC41 is required for ciliary vesicle docking to the mother centriole. *Proc Natl Acad Sci U S A,* 110**,** 5987-92.

JOSHI, S., ANDERSEN, R., JESPERSEN, B. & RITTIG, S. 2013. Genetics of steroid-resistant nephrotic syndrome: a review of mutation spectrum and suggested approach for genetic testing. *Acta Paediatr,* 102**,** 844-56.

KAMBHAM, N., TANJI, N., SEIGLE, R. L., MARKOWITZ, G. S., PULKKINEN, L., UITTO, J. & D'AGATI, V. D. 2000. Congenital focal segmental glomerulosclerosis associated with beta4 integrin mutation and epidermolysis bullosa. *Am J Kidney Dis,* 36**,** 190-6.

KANG, H. G., LEE, M., LEE, K. B., HUGHES, M., KWON, B. S., LEE, S., MCNAGNY, K. M., AHN, Y. H., KO, J. M., HA, I. S., CHOI, M. & CHEONG, H. I. 2017. Loss of podocalyxin causes a novel syndromic type of congenital nephrotic syndrome. *Exp Mol Med,* 49**,** e414.

KANTARCI, S., AL-GAZALI, L., HILL, R. S., DONNAI, D., BLACK, G. C., BIETH, E., CHASSAING, N., LACOMBE, D., DEVRIENDT, K., TEEBI, A., LOSCERTALES, M., ROBSON, C., LIU, T., MACLAUGHLIN, D. T., NOONAN, K. M., RUSSELL, M. K., WALSH, C. A., DONAHOE, P. K. & POBER, B. R. 2007. Mutations in LRP2, which encodes the multiligand receptor megalin, cause Donnai-Barrow and facio-oculo-acoustico-renal syndromes. *Nat Genet,* 39**,** 957-9.

KAPLAN, J. M., KIM, S. H., NORTH, K. N., RENNKE, H., CORREIA, L. A., TONG, H. Q., MATHIS, B. J., RODRIGUEZ-PEREZ, J. C., ALLEN, P. G., BEGGS, A. H. & POLLAK, M. R. 2000. Mutations in ACTN4, encoding alpha-actinin-4, cause familial focal segmental glomerulosclerosis. *Nat Genet,* 24**,** 251-6.

KARLSTROM, R. O., TYURINA, O. V., KAWAKAMI, A., NISHIOKA, N., TALBOT, W. S., SASAKI, H. & SCHIER, A. F. 2003. Genetic analysis of zebrafish gli1 and gli2 reveals divergent requirements for gli genes in vertebrate development. *Development,* 130**,** 1549-64.

KARNER, C. M., DAS, A., MA, Z., SELF, M., CHEN, C., LUM, L., OLIVER, G. & CARROLL, T. J. 2011. Canonical Wnt9b signaling balances progenitor cell expansion and differentiation during kidney development. *Development,* 138**,** 1247-57.

KEE, H. L., DISHINGER, J. F., BLASIUS, T. L., LIU, C. J., MARGOLIS, B. & VERHEY, K. J. 2012. A size-exclusion permeability barrier and nucleoporins characterize a ciliary pore complex that regulates transport into cilia. *Nat Cell Biol,* 14**,** 431-7.

KELLER, G., ZIMMER, G., MALL, G., RITZ, E. & AMANN, K. 2003. Nephron number in patients with primary hypertension. *N Engl J Med,* 348**,** 101-8.

KERLIN, B. A., HAWORTH, K. & SMOYER, W. E. 2014. Venous thromboembolism in pediatric nephrotic syndrome. *Pediatr Nephrol,* 29**,** 989-97.

KESTILA, M., LENKKERI, U., MANNIKKO, M., LAMERDIN, J., MCCREADY, P., PUTAALA, H., RUOTSALAINEN, V., MORITA, T., NISSINEN, M., HERVA, R., KASHTAN, C. E., PELTONEN, L., HOLMBERG, C., OLSEN, A. & TRYGGVASON, K. 1998. Positionally cloned gene for a novel glomerular protein--nephrin--is mutated in congenital nephrotic syndrome. *Mol Cell,* 1**,** 575-82.

KIDGEN. 2017. *Kidgen. Researching the causes of kidney disease across generations.* [Online]. Available: http://www.kidgen.org.au/ [Accessed 29th August 2019].

KIM, E., ARNOULD, T., SELLIN, L. K., BENZING, T., FAN, M. J., GRUNING, W., SOKOL, S. Y., DRUMMOND, I. & WALZ, G. 1999. The polycystic kidney disease 1 gene product modulates Wnt signaling. *J Biol Chem,* 274**,** 4947-53.

KIM, Y. S., KANG, H. S. & JETTEN, A. M. 2007. The Kruppel-like zinc finger protein Glis2 functions as a negative modulator of the Wnt/beta-catenin signaling pathway. *FEBS Lett,* 581**,** 858-64.

KIRBY, A., GNIRKE, A., JAFFE, D. B., BARESOVA, V., POCHET, N., BLUMENSTIEL, B., YE, C., AIRD, D., STEVENS, C., ROBINSON, J. T., CABILI, M. N., GAT-VIKS, I., KELLIHER, E., DAZA, R., DEFELICE, M., HULKOVA, H., SOVOVA, J., VYLET'AL, P., ANTIGNAC, C., GUTTMAN, M., HANDSAKER, R. E., PERRIN, D., STEELMAN, S., SIGURDSSON, S., SCHEINMAN, S. J., SOUGNEZ, C., CIBULSKIS, K., PARKIN, M., GREEN, T., ROSSIN, E., ZODY, M. C., XAVIER, R. J., POLLAK, M. R., ALPER, S. L., LINDBLAD-TOH, K., GABRIEL, S., HART, P. S., REGEV, A., NUSBAUM, C., KMOCH, S., BLEYER, A. J., LANDER, E. S. & DALY, M. J. 2013. Mutations causing medullary cystic kidney disease type 1 lie in a large VNTR in MUC1 missed by massively parallel sequencing. *Nat Genet,* 45**,** 299-303.

KNOWLES, M. R., LEIGH, M. W., OSTROWSKI, L. E., HUANG, L., CARSON, J. L., HAZUCHA, M. J., YIN, W., BERG, J. S., DAVIS, S. D., DELL, S. D., FERKOL, T. W., ROSENFELD, M., SAGEL, S. D., MILLA, C. E., OLIVIER, K. N., TURNER, E. H., LEWIS, A. P., BAMSHAD, M. J., NICKERSON, D. A., SHENDURE, J., ZARIWALA, M. A. & GENETIC DISORDERS OF MUCOCILIARY CLEARANCE, C. 2013. Exome sequencing identifies mutations in CCDC114 as a cause of primary ciliary dyskinesia. *Am J Hum Genet,* 92**,** 99-106.

KOBAYASHI, A., VALERIUS, M. T., MUGFORD, J. W., CARROLL, T. J., SELF, M., OLIVER, G. & MCMAHON, A. P. 2008. Six2 defines and regulates a multipotent self-renewing nephron progenitor population throughout mammalian kidney development. *Cell Stem Cell,* 3**,** 169-81.

KOKKO, J. P. 1970. Sodium chloride and water transport in the descending limb of Henle. *The Journal of Clinical Investigation,* 49**,** 1838-1846.

KOPAN, R., CHENG, H. T. & SURENDRAN, K. 2007. Molecular insights into segmentation along the proximal-distal axis of the nephron. *J Am Soc Nephrol,* 18**,** 2014-20.

KOPP, J. B., SMITH, M. W., NELSON, G. W., JOHNSON, R. C., FREEDMAN, B. I., BOWDEN, D. W., OLEKSYK, T., MCKENZIE, L. M., KAJIYAMA, H., AHUJA, T. S., BERNS, J. S., BRIGGS, W., CHO, M. E., DART, R. A., KIMMEL, P. L., KORBET, S. M., MICHEL, D. M., MOKRZYCKI, M. H., SCHELLING, J. R., SIMON, E., TRACHTMAN, H., VLAHOV, D. & WINKLER, C. A. 2008. MYH9 is a major-effect risk gene for focal segmental glomerulosclerosis. *Nat Genet,* 40**,** 1175-84.

KOZMINSKI, K. G., BEECH, P. L. & ROSENBAUM, J. L. 1995. The Chlamydomonas kinesin-like protein FLA10 is involved in motility associated with the flagellar membrane. *J Cell Biol,* 131**,** 1517-27.

KOZMINSKI, K. G., JOHNSON, K. A., FORSCHER, P. & ROSENBAUM, J. L. 1993. A motility in the eukaryotic flagellum unrelated to flagellar beating. *Proc Natl Acad Sci U S A,* 90**,** 5519-23.

KRANZ, C., DENECKE, J., LEHLE, L., SOHLBACH, K., JESKE, S., MEINHARDT, F., ROSSI, R., GUDOWIUS, S. & MARQUARDT, T. 2004. Congenital disorder of glycosylation type Ik (CDG-Ik): a defect of mannosyltransferase I. *American journal of human genetics,* 74**,** 545-551.

KRENDEL, M., KIM, S. V., WILLINGER, T., WANG, T., KASHGARIAN, M., FLAVELL, R. A. & MOOSEKER, M. S. 2009. Disruption of Myosin 1e Promotes Podocyte Injury. *Journal of the American Society of Nephrology,* 20**,** 86-94.

KUMAR, S. V., ER, P. X., LAWLOR, K. T., MOTAZEDIAN, A., SCURR, M., GHOBRIAL, I., COMBES, A. N., ZAPPIA, L., OSHLACK, A., STANLEY, E. G. & LITTLE, M. H. 2019. Kidney micro-organoids in suspension culture as a scalable source of human pluripotent stem cell-derived kidney cells. *Development,* 146**,** dev172361.

KUURE, S., POPSUEVA, A., JAKOBSON, M., SAINIO, K. & SARIOLA, H. 2007. Glycogen synthase kinase-3 inactivation and stabilization of beta-catenin induce nephron differentiation in isolated mouse and rat kidney mesenchymes. *J Am Soc Nephrol,* 18**,** 1130-9.

LACOMBE, C., DA SILVA, J. L., BRUNEVAL, P., CASADEVALL, N., CAMILLERI, J. P., BARIETY, J., TAMBOURIN, P. & VARET, B. 1991. Erythropoietin: sites of synthesis and regulation of secretion. *Am J Kidney Dis,* 18**,** 14-9.

LAM, A. Q., FREEDMAN, B. S. & BONVENTRE, J. V. 2014a. Directed differentiation of pluripotent stem cells to kidney cells. *Semin Nephrol,* 34**,** 445-61.

LAM, A. Q., FREEDMAN, B. S., MORIZANE, R., LEROU, P. H., VALERIUS, M. T. & BONVENTRE, J. V. 2014b. Rapid and efficient differentiation of human pluripotent stem cells into intermediate mesoderm that forms tubules expressing kidney proximal tubular markers. *J Am Soc Nephrol,* 25**,** 1211-25.

LANCASTER, M. A. & GLEESON, J. G. 2010. Cystic kidney disease: the role of Wnt signaling. *Trends Mol Med,* 16**,** 349-60.

LANCASTER, M. A. & KNOBLICH, J. A. 2014. Organogenesis in a dish: Modeling development and disease using organoid technologies. *Science,* 345**,** 1247125.

LANCASTER, M. A., LOUIE, C. M., SILHAVY, J. L., SINTASATH, L., DECAMBRE, M., NIGAM, S. K., WILLERT, K. & GLEESON, J. G. 2009. Impaired Wnt-beta-catenin signaling disrupts adult renal homeostasis and leads to cystic kidney ciliopathy. *Nat Med,* 15**,** 1046-54.

LANCASTER, M. A., RENNER, M., MARTIN, C. A., WENZEL, D., BICKNELL, L. S., HURLES, M. E., HOMFRAY, T., PENNINGER, J. M., JACKSON, A. P. & KNOBLICH, J. A. 2013. Cerebral organoids model human brain development and microcephaly. *Nature,* 501**,** 373-9.

LANTINGA-VAN LEEUWEN, I. S., DAUWERSE, J. G., BAELDE, H. J., LEONHARD, W. N., VAN DE WAL, A., WARD, C. J., VERBEEK, S., DERUITER, M. C., BREUNING, M. H., DE HEER, E. & PETERS, D. J. 2004. Lowering of Pkd1 expression is sufficient to cause polycystic kidney disease. *Hum Mol Genet,* 13**,** 3069-77.

LAW, C. W., CHEN, Y., SHI, W. & SMYTH, G. K. 2014. voom: Precision weights unlock linear model analysis tools for RNA-seq read counts. *Genome Biol,* 15**,** R29.

LAWLOR, K. T., ZAPPIA, L., LEFEVRE, J., PARK, J.-S., HAMILTON, N. A., OSHLACK, A., LITTLE, M. H. & COMBES, A. N. 2019. Nephron progenitor commitment is a stochastic process influenced by cell migration. *eLife,* 8**,** e41156.

LECHTRECK, K. F. 2015. IFT-Cargo Interactions and Protein Transport in Cilia. *Trends Biochem Sci,* 40**,** 765-78.

LEE, E., SIVAN-LOUKIANOVA, E., EBERL, D. F. & KERNAN, M. J. 2008. An IFT-A protein is required to delimit functionally distinct zones in mechanosensory cilia. *Curr Biol,* 18**,** 1899-906.

LEE, J. W., CHOU, C. L. & KNEPPER, M. A. 2015. Deep Sequencing in Microdissected Renal Tubules Identifies Nephron Segment-Specific Transcriptomes. *J Am Soc Nephrol,* 26**,** 2669-77.

LEGLAND, D., ARGANDA-CARRERAS, I. & ANDREY, P. 2016. MorphoLibJ: integrated library and plugins for mathematical morphology with ImageJ. *Bioinformatics,* 32**,** 3532-3534.

LEHTONEN, S., RYAN, J. J., KUDLICKA, K., IINO, N., ZHOU, H. & FARQUHAR, M. G. 2005. Cell junction-associated proteins IQGAP1, MAGI-2, CASK, spectrins, and α-actinin are components of the nephrin multiprotein complex. *Proceedings of the National Academy of Sciences of the United States of America,* 102**,** 9814-9819.

LEK, M., KARCZEWSKI, K. J., MINIKEL, E. V., SAMOCHA, K. E., BANKS, E., FENNELL, T., O'DONNELL-LURIA, A. H., WARE, J. S., HILL, A. J., CUMMINGS, B. B., TUKIAINEN, T., BIRNBAUM, D. P., KOSMICKI, J. A., DUNCAN, L. E., ESTRADA, K., ZHAO, F., ZOU, J., PIERCE-HOFFMAN, E., BERGHOUT, J., COOPER, D. N., DEFLAUX, N., DEPRISTO, M., DO, R., FLANNICK, J., FROMER, M., GAUTHIER, L., GOLDSTEIN, J., GUPTA, N., HOWRIGAN, D., KIEZUN, A., KURKI, M. I., MOONSHINE, A. L., NATARAJAN, P., OROZCO, L., PELOSO, G. M., POPLIN, R., RIVAS, M. A., RUANO-RUBIO, V., ROSE, S. A., RUDERFER, D. M., SHAKIR, K., STENSON, P. D., STEVENS, C., THOMAS, B. P., TIAO, G., TUSIE-LUNA, M. T., WEISBURD, B., WON, H. H., YU, D., ALTSHULER, D. M., ARDISSINO, D., BOEHNKE, M., DANESH, J., DONNELLY, S., ELOSUA, R., FLOREZ, J. C., GABRIEL, S. B., GETZ, G., GLATT, S. J., HULTMAN, C. M., KATHIRESAN, S., LAAKSO, M., MCCARROLL, S., MCCARTHY, M. I., MCGOVERN, D., MCPHERSON, R., NEALE, B. M., PALOTIE, A., PURCELL, S. M., SALEHEEN, D., SCHARF, J. M., SKLAR, P., SULLIVAN, P. F., TUOMILEHTO, J., TSUANG, M. T., WATKINS, H. C., WILSON, J. G., DALY, M. J., MACARTHUR, D. G. & EXOME AGGREGATION, C. 2016. Analysis of protein-coding genetic variation in 60,706 humans. *Nature,* 536**,** 285-91.

LEMMINK, H. H., MOCHIZUKI, T., VAN DEN HEUVEL, L. P., SCHRODER, C. H., BARRIENTOS, A., MONNENS, L. A., VAN OOST, B. A., BRUNNER, H. G., REEDERS, S. T. & SMEETS, H. J. 1994. Mutations in the type IV collagen alpha 3 (COL4A3) gene in autosomal recessive Alport syndrome. *Hum Mol Genet,* 3**,** 1269-73.

LENNON, R., RANDLES, M. J. & HUMPHRIES, M. J. 2014. The importance of podocyte adhesion for a healthy glomerulus. *Front Endocrinol (Lausanne),* 5**,** 160.

LEVY, M. & FEINGOLD, J. 2000. Estimating prevalence in single-gene kidney diseases progressing to renal failure. *Kidney Int,* 58**,** 925-43.

LI, P., HE, Y., CAI, G., XIAO, F., YANG, J., LI, Q. & CHEN, X. 2019. CCDC114 is mutated in patient with a complex phenotype combining primary ciliary dyskinesia, sensorineural deafness, and renal disease. *J Hum Genet,* 64**,** 39-48.

LIAO, Y., SMYTH, G. K. & SHI, W. 2014. featureCounts: an efficient general purpose program for assigning sequence reads to genomic features. *Bioinformatics,* 30**,** 923-30.

LIEM, K. F., JR., ASHE, A., HE, M., SATIR, P., MORAN, J., BEIER, D., WICKING, C. & ANDERSON, K. V. 2012. The IFT-A complex regulates Shh signaling through cilia structure and membrane protein trafficking. *J Cell Biol,* 197**,** 789-800.

LINDEMANN, C. B. & LESICH, K. A. 2010. Flagellar and ciliary beating: the proven and the possible. *J Cell Sci,* 123**,** 519-28.

LINDSTROM, N. O., GUO, J., KIM, A. D., TRAN, T., GUO, Q., DE SENA BRANDINE, G., RANSICK, A., PARVEZ, R. K., THORNTON, M. E., BASKING, L., GRUBBS, B., MCMAHON, J. A., SMITH, A. D. & MCMAHON, A. P. 2018a. Conserved and Divergent Features of Mesenchymal Progenitor Cell Types within the Cortical Nephrogenic Niche of the Human and Mouse Kidney. *J Am Soc Nephrol,* 29**,** 806-824.

LINDSTROM, N. O., LAWRENCE, M. L., BURN, S. F., JOHANSSON, J. A., BAKKER, E. R., RIDGWAY, R. A., CHANG, C. H., KAROLAK, M. J., OXBURGH, L., HEADON, D. J., SANSOM, O. J., SMITS, R., DAVIES, J. A. & HOHENSTEIN, P. 2014. Integrated beta-catenin, BMP, PTEN, and Notch signalling patterns the nephron. *Elife,* 3**,** e04000.

LINDSTROM, N. O., LAWRENCE, M. L., BURN, S. F., JOHANSSON, J. A., BAKKER, E. R., RIDGWAY, R. A., CHANG, C. H., KAROLAK, M. J., OXBURGH, L., HEADON, D. J., SANSOM, O. J., SMITS, R., DAVIES, J. A. & HOHENSTEIN, P. 2015. Integrated beta-catenin, BMP, PTEN, and Notch signalling patterns the nephron. *Elife,* 3**,** e04000.

LINDSTROM, N. O., MCMAHON, J. A., GUO, J., TRAN, T., GUO, Q., RUTLEDGE, E., PARVEZ, R. K., SARIBEKYAN, G., SCHULER, R. E., LIAO, C., KIM, A. D., ABDELHALIM, A., RUFFINS, S. W., THORNTON, M. E., BASKING, L., GRUBBS, B., KESSELMAN, C. & MCMAHON, A. P. 2018b. Conserved and Divergent Features of Human and Mouse Kidney Organogenesis. *J Am Soc Nephrol,* 29**,** 785-805.

LINDSTROM, N. O., TRAN, T., GUO, J., RUTLEDGE, E., PARVEZ, R. K., THORNTON, M. E., GRUBBS, B., MCMAHON, J. A. & MCMAHON, A. P. 2018c. Conserved and Divergent Molecular and Anatomic Features of Human and Mouse Nephron Patterning. *J Am Soc Nephrol,* 29**,** 825-840.

LITINGTUNG, Y. & CHIANG, C. 2000. Specification of ventral neuron types is mediated by an antagonistic interaction between Shh and Gli3. *Nat Neurosci,* 3**,** 979-85.

LITTLE, M. H. 2015. Improving our resolution of kidney morphogenesis across time and space. *Current Opinion in Genetics & Development,* 32**,** 135-143.

LITTLE, M. H. & COMBES, A. N. 2019. Kidney organoids: accurate models or fortunate accidents. *Genes Dev,* 33**,** 1319-1345.

LITTLE, M. H., COMBES, A. N. & TAKASATO, M. 2016. Understanding kidney morphogenesis to guide renal tissue regeneration. *Nature Reviews Nephrology,* 12**,** 624.

LITTLE, M. H. & MCMAHON, A. P. 2012. Mammalian kidney development: principles, progress, and projections. *Cold Spring Harb Perspect Biol,* 4.

LIU, A., WANG, B. & NISWANDER, L. A. 2005. Mouse intraflagellar transport proteins regulate both the activator and repressor functions of Gli transcription factors. *Development,* 132**,** 3103-11.

LIU, L., DONE, S. C., KHOSHNOODI, J., BERTORELLO, A., WARTIOVAARA, J., BERGGREN, P. O. & TRYGGVASON, K. 2001. Defective nephrin trafficking caused by missense mutations in the NPHS1 gene: insight into the mechanisms of congenital nephrotic syndrome. *Hum Mol Genet,* 10**,** 2637-44.

LLOYD, S. E., PEARCE, S. H. S., FISHER, S. E., STEINMEYER, K., SCHWAPPACH, B., SCHEINMAN, S. J., HARDING, B., BOLINO, A., DEVOTO, M., GOODYER, P., RIGDEN, S.

P. A., WRONG, O., JENTSCH, T. J., CRAIG, I. W. & THAKKER, R. V. 1996. A common molecular basis for three inherited kidney stone diseases. *Nature,* 379**,** 445-449.

LOPEZ, L. C., SCHUELKE, M., QUINZII, C. M., KANKI, T., RODENBURG, R. J., NAINI, A., DIMAURO, S. & HIRANO, M. 2006. Leigh syndrome with nephropathy and CoQ10 deficiency due to decaprenyl diphosphate synthase subunit 2 (PDSS2) mutations. *Am J Hum Genet,* 79**,** 1125-9.

LOVRIC, S., ASHRAF, S., TAN, W. & HILDEBRANDT, F. 2016. Genetic testing in steroid-resistant nephrotic syndrome: when and how? *Nephrol Dial Transplant,* 31**,** 1802-1813.

LOVRIC, S., GONCALVES, S., GEE, H. Y., OSKOUIAN, B., SRINIVAS, H., CHOI, W. I., SHRIL, S., ASHRAF, S., TAN, W., RAO, J., AIRIK, M., SCHAPIRO, D., BRAUN, D. A., SADOWSKI, C. E., WIDMEIER, E., JOBST-SCHWAN, T., SCHMIDT, J. M., GIRIK, V., CAPITANI, G., SUH, J. H., LACHAUSSEE, N., ARRONDEL, C., PATAT, J., GRIBOUVAL, O., FURLANO, M., BOYER, O., SCHMITT, A., VUIBLET, V., HASHMI, S., WILCKEN, R., BERNIER, F. P., INNES, A. M., PARBOOSINGH, J. S., LAMONT, R. E., MIDGLEY, J. P., WRIGHT, N., MAJEWSKI, J., ZENKER, M., SCHAEFER, F., KUSS, N., GREIL, J., GIESE, T., SCHWARZ, K., CATHELINE, V., SCHANZE, D., FRANKE, I., SZNAJER, Y., TRUANT, A. S., ADAMS, B., DESIR, J., BIEMANN, R., PEI, Y., ARS, E., LLOBERAS, N., MADRID, A., DHARNIDHARKA, V. R., CONNOLLY, A. M., WILLING, M. C., COOPER, M. A., LIFTON, R. P., SIMONS, M., RIEZMAN, H., ANTIGNAC, C., SABA, J. D. & HILDEBRANDT, F. 2017. Mutations in sphingosine-1-phosphate lyase cause nephrosis with ichthyosis and adrenal insufficiency. *J Clin Invest,* 127**,** 912-928.

LOWENTHAL, J., LIPNICK, S., RAO, M. & HULL, S. C. 2012. Specimen collection for induced pluripotent stem cell research: harmonizing the approach to informed consent. *Stem cells translational medicine,* 1**,** 409-421.

LÖWIK, M. M., GROENEN, P. J., LEVTCHENKO, E. N., MONNENS, L. A. & VAN DEN HEUVEL, L. P. 2009. Molecular genetic analysis of podocyte genes in focal segmental glomerulosclerosis—a review. *European Journal of Pediatrics,* 168**,** 1291.

LOWIK, M. M., GROENEN, P. J., PRONK, I., LILIEN, M. R., GOLDSCHMEDING, R., DIJKMAN, H. B., LEVTCHENKO, E. N., MONNENS, L. A. & VAN DEN HEUVEL, L. P. 2007. Focal segmental glomerulosclerosis in a patient homozygous for a CD2AP mutation. *Kidney Int,* 72**,** 1198-203.

LU, W., FAN, X., BASORA, N., BABAKHANLOU, H., LAW, T., RIFAI, N., HARRIS, P. C., PEREZ-ATAYDE, A. R., RENNKE, H. G. & ZHOU, J. 1999. Late onset of renal and hepatic cysts in Pkd1-targeted heterozygotes. *Nat Genet,* 21**,** 160-1.

LUDINGTON, W. B., WEMMER, K. A., LECHTRECK, K. F., WITMAN, G. B. & MARSHALL, W. F. 2013. Avalanche-like behavior in ciliary import. *Proc Natl Acad Sci U S A,* 110**,** 3925-30.

MACDONALD, B. T., TAMAI, K. & HE, X. 2009. Wnt/beta-catenin signaling: components, mechanisms, and diseases. *Dev Cell,* 17**,** 9-26.

MACHUCA, E., BENOIT, G. & ANTIGNAC, C. 2009. Genetics of nephrotic syndrome: connecting molecular genetics to podocyte physiology. *Hum Mol Genet,* 18**,** R185-94.

MACIA, M. S., HALBRITTER, J., DELOUS, M., BREDRUP, C., GUTTER, A., FILHOL, E., MELLGREN, A. E., LEH, S., BIZET, A., BRAUN, D. A., GEE, H. Y., SILBERMANN, F., HENRY, C., KRUG, P., BOLE-FEYSOT, C., NITSCHKE, P., JOLY, D., NICOUD, P., PAGET, A., HAUGLAND, H., BRACKMANN, D., AHMET, N., SANDFORD, R., CENGIZ, N., KNAPPSKOG, P. M., BOMAN, H., LINGHU, B., YANG, F., OAKELEY, E. J., SAINT MEZARD, P., SAILER, A. W., JOHANSSON, S., RODAHL, E., SAUNIER, S., HILDEBRANDT, F. & BENMERAH, A. 2017. Mutations in MAPKBP1 Cause Juvenile or Late-Onset Cilia-Independent Nephronophthisis. *Am J Hum Genet*.

MAE, S., SHONO, A., SHIOTA, F., YASUNO, T., KAJIWARA, M., GOTODA-NISHIMURA, N., ARAI, S., SATO-OTUBO, A., TOYODA, T., TAKAHASHI, K., NAKAYAMA, N., COWAN, C. A., AOI, T., OGAWA, S., MCMAHON, A. P., YAMANAKA, S. & OSAFUNE, K. 2013. Monitoring and robust induction of nephrogenic intermediate mesoderm from human pluripotent stem cells. *Nat Commun,* 4**,** 1367.

MAE, S. I., RYOSAKA, M., TOYODA, T., MATSUSE, K., OSHIMA, Y., TSUJIMOTO, H., OKUMURA, S., SHIBASAKI, A. & OSAFUNE, K. 2018. Generation of branching ureteric bud tissues from human pluripotent stem cells. *Biochem Biophys Res Commun,* 495**,** 954-961.

MAGELLA, B., ADAM, M., POTTER, A. S., VENKATASUBRAMANIAN, M., CHETAL, K., HAY, S. B., SALOMONIS, N. & POTTER, S. S. 2018. Cross-platform single cell analysis of kidney development shows stromal cells express Gdnf. *Dev Biol,* 434**,** 36-47.

MAJUMDAR, A., VAINIO, S., KISPERT, A., MCMAHON, J. & MCMAHON, A. P. 2003. Wnt11 and Ret/Gdnf pathways cooperate in regulating ureteric branching during metanephric kidney development. *Development,* 130**,** 3175-85.

MALLETT, A., FOWLES, L. F., MCGAUGHRAN, J., HEALY, H. & PATEL, C. 2016. A multidisciplinary renal genetics clinic improves patient diagnosis. *Med J Aust,* 204**,** 58-9.

MALLETT, A., MCCARTHY, H. J., HO, G., HOLMAN, K., FARNSWORTH, E., PATEL, C., FLETCHER, J., QUINLAN, C., BENNETT, B. J. & ALEXANDER, S. I. 2017. A National Testing Approach Using Massively Parallel Sequencing and Targeted Exomes in Familial Kidney Disease. *Kidney International*.

MALLETT, A., PATEL, C., MAIER, B., MCGAUGHRAN, J., GABBETT, M., TAKASATO, M., CAMERON, A., TRNKA, P., ALEXANDER, S. I., RANGAN, G., TCHAN, M. C., CARUANA, G., JOHN, G., QUINLAN, C., MCCARTHY, H. J., HYLAND, V., HOY, W. E., WOLVETANG, E., TAFT, R., SIMONS, C., HEALY, H. & LITTLE, M. 2015. A protocol for the identification and validation of novel genetic causes of kidney disease. *BMC Nephrol,* 16**,** 152.

MALLETT, A., PATEL, C., SALISBURY, A., WANG, Z., HEALY, H. & HOY, W. 2014. The prevalence and epidemiology of genetic renal disease amongst adults with chronic kidney disease in Australia. *Orphanet J Rare Dis,* 9**,** 98.

MAO, Y., FRANCIS-WEST, P. & IRVINE, K. D. 2015. Fat4/Dchs1 signaling between stromal and cap mesenchyme cells influences nephrogenesis and ureteric bud branching. *Development,* 142**,** 2574-85.

MARCON, E., NI, Z., PU, S., TURINSKY, A. L., TRIMBLE, S. S., OLSEN, J. B., SILVERMAN-GAVRILA, R., SILVERMAN-GAVRILA, L., PHANSE, S., GUO, H., ZHONG, G., GUO, X., YOUNG, P., BAILEY, S., ROUDEVA, D., ZHAO, D., HEWEL, J., LI, J., GRASLUND, S., PADUCH, M., KOSSIAKOFF, A. A., LUPIEN, M., EMILI, A., WODAK, S. J. & GREENBLATT, J. 2014. Human-chromatin-related protein interactions identify a demethylase complex required for chromosome segregation. *Cell Rep,* 8**,** 297-310.

MAROSE, T. D., MERKEL, C. E., MCMAHON, A. P. & CARROLL, T. J. 2008. Beta-catenin is necessary to keep cells of ureteric bud/Wolffian duct epithelium in a precursor state. *Dev Biol,* 314**,** 112-26.

MARSZALEK, J. R., RUIZ-LOZANO, P., ROBERTS, E., CHIEN, K. R. & GOLDSTEIN, L. S. 1999. Situs inversus and embryonic ciliary morphogenesis defects in mouse mutants lacking the KIF3A subunit of kinesin-II. *Proc Natl Acad Sci U S A,* 96**,** 5043-8.

MASSA, F., GARBAY, S., BOUVIER, R., SUGITANI, Y., NODA, T., GUBLER, M. C., HEIDET, L., PONTOGLIO, M. & FISCHER, E. 2013. Hepatocyte nuclear factor 1beta controls nephron tubular development. *Development,* 140**,** 886-96.

MASSAGUE, J., SEOANE, J. & WOTTON, D. 2005. Smad transcription factors. *Genes Dev,* 19**,** 2783-810.

MATEER, S. C., WANG, N. & BLOOM, G. S. 2003. IQGAPs: integrators of the cytoskeleton, cell adhesion machinery, and signaling networks. *Cell Motil Cytoskeleton,* 55**,** 147-55.

MATISE, M. P., EPSTEIN, D. J., PARK, H. L., PLATT, K. A. & JOYNER, A. L. 1998. Gli2 is required for induction of floor plate and adjacent cells, but not most ventral neurons in the mouse central nervous system. *Development,* 125**,** 2759-70.

MATTILA, P. K. & LAPPALAINEN, P. 2008. Filopodia: molecular architecture and cellular functions. *Nat Rev Mol Cell Biol,* 9**,** 446-54.

MAY, S. R., ASHIQUE, A. M., KARLEN, M., WANG, B., SHEN, Y., ZARBALIS, K., REITER, J., ERICSON, J. & PETERSON, A. S. 2005. Loss of the retrograde motor for IFT disrupts localization of Smo to cilia and prevents the expression of both activator and repressor functions of Gli. *Dev Biol,* 287**,** 378-89.

MCCARTHY, H. J., BIERZYNSKA, A., WHERLOCK, M., OGNJANOVIC, M., KERECUK, L., HEGDE, S., FEATHER, S., GILBERT, R. D., KRISCHOCK, L., JONES, C., SINHA, M. D., WEBB, N. J., CHRISTIAN, M., WILLIAMS, M. M., MARKS, S., KOZIELL, A., WELSH, G. I., SALEEM, M. A. & GROUP, R. T. U. S. S. 2013. Simultaneous sequencing of 24 genes associated with steroid-resistant nephrotic syndrome. *Clin J Am Soc Nephrol,* 8**,** 637-48.

MCCRACKEN, K. W., CATÁ, E. M., CRAWFORD, C. M., SINAGOGA, K. L., SCHUMACHER, M., ROCKICH, B. E., TSAI, Y.-H., MAYHEW, C. N., SPENCE, J. R., ZAVROS, Y. & WELLS, J. M. 2014. Modelling human development and disease in pluripotent stem-cell-derived gastric organoids. *Nature,* 516**,** 400-404.

MCGAVIN, M. K., BADOUR, K., HARDY, L. A., KUBISESKI, T. J., ZHANG, J. & SIMINOVITCH, K. A. 2001. The intersectin 2 adaptor links Wiskott Aldrich Syndrome protein (WASp)-mediated actin polymerization to T cell antigen receptor endocytosis. *J Exp Med,* 194**,** 1777-87.

MCINTYRE, P. & CRAIG, J. 1998. Prevention of serious bacterial infection in children with nephrotic syndrome. *Journal of Paediatrics and Child Health,* 34**,** 314-317.

MCLAREN, A. 2001. Ethical and social considerations of stem cell research. *Nature,* 414**,** 129-131.

MCNAMARA, B. J., DIOUF, B., HUGHSON, M. D., DOUGLAS-DENTON, R. N., HOY, W. E. & BERTRAM, J. F. 2008. Renal pathology, glomerular number and volume in a West African urban community. *Nephrol Dial Transplant,* 23**,** 2576-85.

MELE, C., IATROPOULOS, P., DONADELLI, R., CALABRIA, A., MARANTA, R., CASSIS, P., BUELLI, S., TOMASONI, S., PIRAS, R., KRENDEL, M., BETTONI, S., MORIGI, M., DELLEDONNE, M., PECORARO, C., ABBATE, I., CAPOBIANCHI, M. R., HILDEBRANDT, F., OTTO, E., SCHAEFER, F., MACCIARDI, F., OZALTIN, F., EMRE, S., IBSIRLIOGLU, T., BENIGNI, A., REMUZZI, G., NORIS, M. & PODONET, C. 2011. MYO1E mutations and childhood familial focal segmental glomerulosclerosis. *N Engl J Med,* 365**,** 295-306.

MENDELSOHN, H. B., KRAUSS, M., BERANT, M. & LICHTIG, C. 1982. Familial early-onset nephrotic syndrome: diffuse mesangial sclerosis. Clinico-pathological study of a kindred. *Acta Paediatr Scand,* 71**,** 753-8.

MENEZES, L. F., CAI, Y., NAGASAWA, Y., SILVA, A. M., WATKINS, M. L., DA SILVA, A. M., SOMLO, S., GUAY-WOODFORD, L. M., GERMINO, G. G. & ONUCHIC, L. F. 2004. Polyductin, the PKHD1 gene product, comprises isoforms expressed in plasma membrane, primary cilium, and cytoplasm. *Kidney Int,* 66**,** 1345-55.

MICALLEF, S. J., LI, X., ELEFANTY, A. G. & STANLEY, E. G. 2007. Pancreas differentiation of mouse ES cells. *Curr Protoc Stem Cell Biol,* Chapter 1**,** Unit 1G 2.

MICHAUD, J. L., CHAISSON, K. M., PARKS, R. J. & KENNEDY, C. R. 2006. FSGS-associated alpha-actinin-4 (K256E) impairs cytoskeletal dynamics in podocytes. *Kidney Int,* 70**,** 1054-61.

MILL, P., LOCKHART, P. J., FITZPATRICK, E., MOUNTFORD, H. S., HALL, E. A., REIJNS, M. A., KEIGHREN, M., BAHLO, M., BROMHEAD, C. J., BUDD, P., AFTIMOS, S., DELATYCKI, M. B., SAVARIRAYAN, R., JACKSON, I. J. & AMOR, D. J. 2011. Human and mouse mutations in WDR35 cause short-rib polydactyly syndromes due to abnormal ciliogenesis. *Am J Hum Genet,* 88**,** 508-15.

MILLER, K. A., AH-CANN, C. J., WELFARE, M. F., TAN, T. Y., POPE, K., CARUANA, G., FRECKMANN, M. L., SAVARIRAYAN, R., BERTRAM, J. F., DOBBIE, M. S., BATEMAN, J. F. & FARLIE, P. G. 2013. Cauli: a mouse strain with an Ift140 mutation that results in a skeletal ciliopathy modelling Jeune syndrome. *PLoS Genet,* 9**,** e1003746.

MINER, J. H. & LI, C. 2000. Defective glomerulogenesis in the absence of laminin alpha5 demonstrates a developmental role for the kidney glomerular basement membrane. *Dev Biol,* 217**,** 278-89.

MIYAKE, N., TSUKAGUCHI, H., KOSHIMIZU, E., SHONO, A., MATSUNAGA, S., SHIINA, M., MIMURA, Y., IMAMURA, S., HIROSE, T., OKUDELA, K., NOZU, K., AKIOKA, Y., HATTORI, M., YOSHIKAWA, N., KITAMURA, A., CHEONG, H. I., KAGAMI, S., YAMASHITA, M., FUJITA, A., MIYATAKE, S., TSURUSAKI, Y., NAKASHIMA, M., SAITSU, H., OHASHI, K., IMAMOTO, N., RYO, A., OGATA, K., IIJIMA, K. & MATSUMOTO, N. 2015. Biallelic Mutations in Nuclear Pore Complex Subunit NUP107 Cause Early-Childhood-Onset Steroid-Resistant Nephrotic Syndrome. *Am J Hum Genet,* 97**,** 555-66.

MOALEM, S., KEATING, S., SHANNON, P., THOMPSON, M., MILLAR, K., NYKAMP, K., FORSTER, A., NOOR, A. & CHITAYAT, D. 2013. Broadening the ciliopathy spectrum: motile cilia dyskinesia, and nephronophthisis associated with a previously unreported homozygous mutation in the INVS/NPHP2 gene. *Am J Med Genet A,* 161A**,** 1792-6.

MOCHIZUKI, T., LEMMINK, H. H., MARIYAMA, M., ANTIGNAC, C., GUBLER, M. C., PIRSON, Y., VERELLEN-DUMOULIN, C., CHAN, B., SCHRODER, C. H., SMEETS, H. J. & ET AL. 1994. Identification of mutations in the alpha 3(IV) and alpha 4(IV) collagen genes in autosomal recessive Alport syndrome. *Nat Genet,* 8**,** 77-81.

MOE, O. W., UJIIE, K., STAR, R. A., MILLER, R. T., WIDELL, J., ALPERN, R. J. & HENRICH, W. L. 1993. Renin expression in renal proximal tubule. *J Clin Invest,* 91**,** 774-9.

MOLINARI, E., DECKER, E., MABILLARD, H., TELLEZ, J., SRIVASTAVA, S., RAMAN, S., WOOD, K., KEMPF, C., ALKANDERI, S., RAMSBOTTOM, S. A., MILES, C. G., JOHNSON, C. A., HILDEBRANDT, F., BERGMANN, C. & SAYER, J. A. 2018. Human urine-derived renal epithelial cells provide insights into kidney-specific alternate splicing variants. *European Journal of Human Genetics,* 26**,** 1791-1796.

MOLLET, G., SALOMON, R., GRIBOUVAL, O., SILBERMANN, F., BACQ, D., LANDTHALER, G., MILFORD, D., NAYIR, A., RIZZONI, G., ANTIGNAC, C. & SAUNIER, S. 2002. The gene

mutated in juvenile nephronophthisis type 4 encodes a novel protein that interacts with nephrocystin. *Nature Genetics,* 32**,** 300-305.

MORENO, S., IBRAGHIMOV-BESKROVNAYA, O. & BUKANOV, N. O. 2008. Serum and urinary biomarker signatures for rapid preclinical in vivo assessment of CDK inhibition as a therapeutic approach for PKD. *Cell Cycle,* 7**,** 1856-64.

MORIZANE, R., LAM, A. Q., FREEDMAN, B. S., KISHI, S., VALERIUS, M. T. & BONVENTRE, J. V. 2015. Nephron organoids derived from human pluripotent stem cells model kidney development and injury. *Nat Biotechnol,* 33**,** 1193-200.

MORRIS, R. L., ENGLISH, C. N., LOU, J. E., DUFORT, F. J., NORDBERG, J., TERASAKI, M. & HINKLE, B. 2004. Redistribution of the kinesin-II subunit KAP from cilia to nuclei during the mitotic and ciliogenic cycles in sea urchin embryos. *Dev Biol,* 274**,** 56-69.

MOSER, M., MATTHIESEN, S., KIRFEL, J., SCHORLE, H., BERGMANN, C., SENDEREK, J., RUDNIK-SCHONEBORN, S., ZERRES, K. & BUETTNER, R. 2005. A mouse model for cystic biliary dysgenesis in autosomal recessive polycystic kidney disease (ARPKD). *Hepatology,* 41**,** 1113-21.

MUGFORD, J. W., SIPILA, P., KOBAYASHI, A., BEHRINGER, R. R. & MCMAHON, A. P. 2008. Hoxd11 specifies a program of metanephric kidney development within the intermediate mesoderm of the mouse embryo. *Dev Biol,* 319**,** 396-405.

MUGFORD, J. W., YU, J., KOBAYASHI, A. & MCMAHON, A. P. 2009. High-resolution gene expression analysis of the developing mouse kidney defines novel cellular compartments within the nephron progenitor population. *Dev Biol,* 333**,** 312-23.

MUKHOPADHYAY, S., WEN, X., CHIH, B., NELSON, C. D., LANE, W. S., SCALES, S. J. & JACKSON, P. K. 2010. TULP3 bridges the IFT-A complex and membrane phosphoinositides to promote trafficking of G protein-coupled receptors into primary cilia. *Genes Dev,* 24**,** 2180-93.

MUKHOPADHYAY, S., WEN, X., RATTI, N., LOKTEV, A., RANGELL, L., SCALES, S. J. & JACKSON, P. K. 2013. The ciliary G-protein-coupled receptor Gpr161 negatively regulates the Sonic hedgehog pathway via cAMP signaling. *Cell,* 152**,** 210-23.

MURALI, A. & RAJALINGAM, K. 2014. Small Rho GTPases in the control of cell shape and mobility. *Cell Mol Life Sci,* 71**,** 1703-21.

MUSAH, S., DIMITRAKAKIS, N., CAMACHO, D. M., CHURCH, G. M. & INGBER, D. E. 2018. Directed differentiation of human induced pluripotent stem cells into mature kidney podocytes and establishment of a Glomerulus Chip. *Nat Protoc,* 13**,** 1662-1685.

MUSAH, S., MAMMOTO, A., FERRANTE, T. C., JEANTY, S. S. F., HIRANO-KOBAYASHI, M., MAMMOTO, T., ROBERTS, K., CHUNG, S., NOVAK, R., INGRAM, M., FATANAT-DIDAR, T., KOSHY, S., WEAVER, J. C., CHURCH, G. M. & INGBER, D. E. 2017. Mature induced-pluripotent-stem-cell-derived human podocytes reconstitute kidney glomerular-capillary-wall function on a chip. *Nat Biomed Eng,* 1.

MUTHUKRISHNAN, S. D., YANG, X., FRIESEL, R. & OXBURGH, L. 2015. Concurrent BMP7 and FGF9 signalling governs AP-1 function to promote self-renewal of nephron progenitor cells. *Nat Commun,* 6**,** 10027.

NACHURY, M. V., SEELEY, E. S. & JIN, H. 2010. Trafficking to the ciliary membrane: how to get across the periciliary diffusion barrier? *Annu Rev Cell Dev Biol,* 26**,** 59-87.

NAGASAWA, Y., MATTHIESEN, S., ONUCHIC, L. F., HOU, X., BERGMANN, C., ESQUIVEL, E., SENDEREK, J., REN, Z., ZELTNER, R., FURU, L., AVNER, E., MOSER, M., SOMLO, S., GUAY-WOODFORD, L., BUTTNER, R., ZERRES, K. & GERMINO, G. G. 2002. Identification and characterization of Pkhd1, the mouse orthologue of the human ARPKD gene. *J Am Soc Nephrol,* 13**,** 2246-58.

NAM, S. A., SEO, E., KIM, J. W., KIM, H. W., KIM, H. L., KIM, K., KIM, T.-M., JU, J. H., GOMEZ, I. G., UCHIMURA, K., HUMPHREYS, B. D., YANG, C. W., LEE, J. Y., KIM, J., CHO, D. W., FREEDMAN, B. S. & KIM, Y. K. 2019. Graft immaturity and safety concerns in transplanted human kidney organoids. *Experimental & Molecular Medicine,* 51**,** 145.

NAPRTCS. 2014. *NAPRTCS 2014 Annual Report* [Online]. Available: https://web.emmes.com/study/ped/annlrept/annualrept2014.pdf [Accessed 24th August 2019].

NAULI, S. M., ROSSETTI, S., KOLB, R. J., ALENGHAT, F. J., CONSUGAR, M. B., HARRIS, P. C., INGBER, D. E., LOGHMAN-ADHAM, M. & ZHOU, J. 2006. Loss of polycystin-1 in human cyst-lining epithelia leads to ciliary dysfunction. *J Am Soc Nephrol,* 17**,** 1015-25.

NEMET, I., ROPELEWSKI, P. & IMANISHI, Y. 2015. Rhodopsin Trafficking and Mistrafficking: Signals, Molecular Components, and Mechanisms. *Prog Mol Biol Transl Sci,* 132**,** 39-71.

NG, E. S., AZZOLA, L., SOURRIS, K., ROBB, L., STANLEY, E. G. & ELEFANTY, A. G. 2005. The primitive streak gene Mixl1 is required for efficient haematopoiesis and BMP4-induced ventral mesoderm patterning in differentiating ES cells. *Development,* 132**,** 873-84.

NIEDERREITHER, K., SUBBARAYAN, V., DOLLE, P. & CHAMBON, P. 1999. Embryonic retinoic acid synthesis is essential for early mouse post-implantation development. *Nat Genet,* 21**,** 444-8.

NIELSEN, R., CHRISTENSEN, E. I. & BIRN, H. 2016. Megalin and cubilin in proximal tubule protein reabsorption: from experimental models to human disease. *Kidney Int,* 89**,** 58-67.

NIGG, E. A. & RAFF, J. W. 2009. Centrioles, centrosomes, and cilia in health and disease. *Cell,* 139**,** 663-78.

NONAKA, S., SHIRATORI, H., SAIJOH, Y. & HAMADA, H. 2002. Determination of left-right patterning of the mouse embryo by artificial nodal flow. *Nature,* 418**,** 96-9.

NOONE, D. G., IIJIMA, K. & PAREKH, R. 2018. Idiopathic nephrotic syndrome in children. *The Lancet,* 392**,** 61-74.

NOSTRO, M. C., CHENG, X., KELLER, G. M. & GADUE, P. 2008. Wnt, activin, and BMP signaling regulate distinct stages in the developmental pathway from embryonic stem cells to blood. *Cell Stem Cell,* 2**,** 60-71.

NYKJAER, A., DRAGUN, D., WALTHER, D., VORUM, H., JACOBSEN, C., HERZ, J., MELSEN, F., CHRISTENSEN, E. I. & WILLNOW, T. E. 1999. An endocytic pathway essential for renal uptake and activation of the steroid 25-(OH) vitamin D3. *Cell,* 96**,** 507-15.

O'BRIEN, L. L., GUO, Q., LEE, Y., TRAN, T., BENAZET, J.-D., WHITNEY, P. H., VALOUEV, A. & MCMAHON, A. P. 2016. Differential regulation of mouse and human nephron progenitors by the Six family of transcriptional regulators. *Development (Cambridge, England),* 143**,** 595-608.

O'SHAUGHNESSY, K. M. 2015. Gordon Syndrome: a continuing story. *Pediatric Nephrology,* 30**,** 1903-1908.

OBARA-ISHIHARA, T., KUHLMAN, J., NISWANDER, L. & HERZLINGER, D. 1999. The surface ectoderm is essential for nephric duct formation in intermediate mesoderm. *Development,* 126**,** 1103-8.

OCBINA, P. J., EGGENSCHWILER, J. T., MOSKOWITZ, I. & ANDERSON, K. V. 2011. Complex interactions between genes controlling trafficking in primary cilia. *Nat Genet,* 43**,** 547-53.

OHASHI, T., UCHIDA, K., UCHIDA, S., SASAKI, S. & NIHEI, H. 2003. Intracellular mislocalization of mutant podocin and correction by chemical chaperones. *Histochemistry and Cell Biology,* 119**,** 257-264.

OKADA, Y., NONAKA, S., TANAKA, Y., SAIJOH, Y., HAMADA, H. & HIROKAWA, N. 1999. Abnormal nodal flow precedes situs inversus in iv and inv mice. *Molecular Cell,* 4**,** 459-468.

OLBRICH, H., FLIEGAUF, M., HOEFELE, J., KISPERT, A., OTTO, E., VOLZ, A., WOLF, M. T., SASMAZ, G., TRAUER, U., REINHARDT, R., SUDBRAK, R., ANTIGNAC, C., GRETZ, N., WALZ, G., SCHERMER, B., BENZING, T., HILDEBRANDT, F. & OMRAN, H. 2003. Mutations in a novel gene, NPHP3, cause adolescent nephronophthisis, tapeto-retinal degeneration and hepatic fibrosis. *Nat Genet,* 34**,** 455-9.

OLBRICH, H., HAFFNER, K., KISPERT, A., VOLKEL, A., VOLZ, A., SASMAZ, G., REINHARDT, R., HENNIG, S., LEHRACH, H., KONIETZKO, N., ZARIWALA, M., NOONE, P. G., KNOWLES, M., MITCHISON, H. M., MEEKS, M., CHUNG, E. M., HILDEBRANDT, F., SUDBRAK, R. & OMRAN, H. 2002. Mutations in DNAH5 cause primary ciliary dyskinesia and randomization of left-right asymmetry. *Nat Genet,* 30**,** 143-4.

OMRAN, H., FERNANDEZ, C., JUNG, M., HAFFNER, K., FARGIER, B., VILLAQUIRAN, A., WALDHERR, R., GRETZ, N., BRANDIS, M., RUSCHENDORF, F., REIS, A. & HILDEBRANDT, F. 2000a. Identification of a new gene locus for adolescent nephronophthisis, on chromosome 3q22 in a large Venezuelan pedigree. *Am J Hum Genet,* 66**,** 118-27.

OMRAN, H., HAFFNER, K., VOLKEL, A., KUEHR, J., KETELSEN, U. P., ROSS, U. H., KONIETZKO, N., WIENKER, T., BRANDIS, M. & HILDEBRANDT, F. 2000b. Homozygosity mapping of a gene locus for primary ciliary dyskinesia on chromosome 5p and identification of the heavy dynein chain DNAH5 as a candidate gene. *Am J Respir Cell Mol Biol,* 23**,** 696-702.

OTTO, E., KISPERT, A., SCHATZLE, LESCHER, B., RENSING, C. & HILDEBRANDT, F. 2000. Nephrocystin: gene expression and sequence conservation between human, mouse, and Caenorhabditis elegans. *J Am Soc Nephrol,* 11**,** 270-82.

OTTO, E. A., HURD, T. W., AIRIK, R., CHAKI, M., ZHOU, W., STOETZEL, C., PATIL, S. B., LEVY, S., GHOSH, A. K., MURGA-ZAMALLOA, C. A., VAN REEUWIJK, J., LETTEBOER, S. J., SANG, L., GILES, R. H., LIU, Q., COENE, K. L., ESTRADA-CUZCANO, A., COLLIN, R. W., MCLAUGHLIN, H. M., HELD, S., KASANUKI, J. M., RAMASWAMI, G., CONTE, J., LOPEZ,

I., WASHBURN, J., MACDONALD, J., HU, J., YAMASHITA, Y., MAHER, E. R., GUAY-WOODFORD, L. M., NEUMANN, H. P., OBERMULLER, N., KOENEKOOP, R. K., BERGMANN, C., BEI, X., LEWIS, R. A., KATSANIS, N., LOPES, V., WILLIAMS, D. S., LYONS, R. H., DANG, C. V., BRITO, D. A., DIAS, M. B., ZHANG, X., CAVALCOLI, J. D., NURNBERG, G., NURNBERG, P., PIERCE, E. A., JACKSON, P. K., ANTIGNAC, C., SAUNIER, S., ROEPMAN, R., DOLLFUS, H., KHANNA, H. & HILDEBRANDT, F. 2010. Candidate exome capture identifies mutation of SDCCAG8 as the cause of a retinal-renal ciliopathy. *Nat Genet,* 42**,** 840-50.

OTTO, E. A., RAMASWAMI, G., JANSSEN, S., CHAKI, M., ALLEN, S. J., ZHOU, W., AIRIK, R., HURD, T. W., GHOSH, A. K., WOLF, M. T., HOPPE, B., NEUHAUS, T. J., BOCKENHAUER, D., MILFORD, D. V., SOLIMAN, N. A., ANTIGNAC, C., SAUNIER, S., JOHNSON, C. A., HILDEBRANDT, F. & GROUP, G. P. N. S. 2011. Mutation analysis of 18 nephronophthisis associated ciliopathy disease genes using a DNA pooling and next generation sequencing strategy. *J Med Genet,* 48**,** 105-16.

OTTO, E. A., SCHERMER, B., OBARA, T., O'TOOLE, J. F., HILLER, K. S., MUELLER, A. M., RUF, R. G., HOEFELE, J., BEEKMANN, F., LANDAU, D., FOREMAN, J. W., GOODSHIP, J. A., STRACHAN, T., KISPERT, A., WOLF, M. T., GAGNADOUX, M. F., NIVET, H., ANTIGNAC, C., WALZ, G., DRUMMOND, I. A., BENZING, T. & HILDEBRANDT, F. 2003. Mutations in INVS encoding inversin cause nephronophthisis type 2, linking renal cystic disease to the function of primary cilia and left-right axis determination. *Nat Genet,* 34**,** 413-20.

OTTO, E. A., TRAPP, M. L., SCHULTHEISS, U. T., HELOU, J., QUARMBY, L. M. & HILDEBRANDT, F. 2008. NEK8 mutations affect ciliary and centrosomal localization and may cause nephronophthisis. *Journal of the American Society of Nephrology,* 19**,** 587-592.

OVUNC, B., OTTO, E. A., VEGA-WARNER, V., SAISAWAT, P., ASHRAF, S., RAMASWAMI, G., FATHY, H. M., SCHOEB, D., CHERNIN, G., LYONS, R. H., YILMAZ, E. & HILDEBRANDT, F. 2011. Exome sequencing reveals cubilin mutation as a single-gene cause of proteinuria. *J Am Soc Nephrol,* 22**,** 1815-20.

OZALTIN, F., IBSIRLIOGLU, T., TASKIRAN, EKIM Z., BAYDAR, DILEK E., KAYMAZ, F., BUYUKCELIK, M., KILIC, BELTINGE D., BALAT, A., IATROPOULOS, P., ASAN, E., AKARSU, NURTEN A., SCHAEFER, F., YILMAZ, E. & BAKKALOGLU, A. 2011. Disruption of PTPRO Causes Childhood-Onset Nephrotic Syndrome. *The American Journal of Human Genetics,* 89**,** 139-147.

PAMPALONI, F., REYNAUD, E. G. & STELZER, E. H. 2007. The third dimension bridges the gap between cell culture and live tissue. *Nat Rev Mol Cell Biol,* 8**,** 839-45.

PAN, J., SEEGER-NUKPEZAH, T. & GOLEMIS, E. A. 2013. The role of the cilium in normal and abnormal cell cycles: emphasis on renal cystic pathologies. *Cell Mol Life Sci,* 70**,** 1849-74.

PAPAZACHARIOU, L., PAPAGREGORIOU, G., HADJIPANAGI, D., DEMOSTHENOUS, P., VOSKARIDES, K., KOUTSOFTI, C., STYLIANOU, K., IOANNOU, P., XYDAKIS, D., TZANAKIS, I., PAPADAKI, A., KALLIVRETAKIS, N., NIKOLAKAKIS, N., PERYSINAKI, G., GALE, D. P., DIAMANTOPOULOS, A., GOUDAS, P., GOUMENOS, D., SOLOUKIDES, A., BOLETIS, I., MELEXOPOULOU, C., GEORGAKI, E., FRYSIRA, E., KOMIANOU, F., GREKAS, D., PALIOURAS, C., ALIVANIS, P., VERGOULAS, G., PIERIDES, A., DAPHNIS, E. & DELTAS, C. 2017. Frequent COL4 mutations in familial microhematuria accompanied by later-onset Alport nephropathy due to focal segmental glomerulosclerosis. *Clin Genet,* 92**,** 517-527.

PARFITT, D. A., LANE, A., RAMSDEN, C. M., CARR, A. J., MUNRO, P. M., JOVANOVIC, K., SCHWARZ, N., KANUGA, N., MUTHIAH, M. N., HULL, S., GALLO, J. M., DA CRUZ, L., MOORE, A. T., HARDCASTLE, A. J., COFFEY, P. J. & CHEETHAM, M. E. 2016. Identification and Correction of Mechanisms Underlying Inherited Blindness in Human iPSC-Derived Optic Cups. *Cell Stem Cell,* 18**,** 769-81.

PARK, H. L., BAI, C., PLATT, K. A., MATISE, M. P., BEEGHLY, A., HUI, C. C., NAKASHIMA, M. & JOYNER, A. L. 2000. Mouse Gli1 mutants are viable but have defects in SHH signaling in combination with a Gli2 mutation. *Development,* 127**,** 1593-605.

PARK, J. S., VALERIUS, M. T. & MCMAHON, A. P. 2007. Wnt/beta-catenin signaling regulates nephron induction during mouse kidney development. *Development,* 134**,** 2533-9.

PAZOUR, G. J., DICKERT, B. L., VUCICA, Y., SEELEY, E. S., ROSENBAUM, J. L., WITMAN, G. B. & COLE, D. G. 2000. Chlamydomonas IFT88 and its mouse homologue, polycystic kidney disease gene tg737, are required for assembly of cilia and flagella. *J Cell Biol,* 151**,** 709-18.

PAZOUR, G. J., DICKERT, B. L. & WITMAN, G. B. 1999. The DHC1b (DHC2) isoform of cytoplasmic dynein is required for flagellar assembly. *J Cell Biol,* 144**,** 473-81.

PEARCE, D., SOUNDARARAJAN, R., TRIMPERT, C., KASHLAN, O. B., DEEN, P. M. T. & KOHAN, D. E. 2015. Collecting duct principal cell transport processes and their regulation. *Clinical journal of the American Society of Nephrology : CJASN,* 10**,** 135-146.

PEARCE, D., VIVEK, B. & FUNDER, J. W. 2016. Aldosterone and Mineralocorticoid Receptors: Renal and Extrarenal Roles. *In:* SKORECKI, K., CHERTOW, G. M., MARSDEN, P. A., TAAL, M. W. & YU, A. S. (eds.) *Brenner and Rector's The Kidney.* 10th ed. Philadelphia: Saunders.

PENA-PADILLA, C., MARSHALL, C. R., WALKER, S., SCHERER, S. W., TAVARES-MACIAS, G., RAZO-JIMENEZ, G., BOBADILLA-MORALES, L., ACOSTA-FERNANDEZ, E., CORONA-RIVERA, A., MENDOZA-LONDONO, R. & CORONA-RIVERA, J. R. 2016. Compound heterozygous mutations in the IFT140 gene cause Opitz trigonocephaly C syndrome in a patient with typical features of a ciliopathy. *Clin Genet*.

PEPICELLI, C. V., KISPERT, A., ROWITCH, D. H. & MCMAHON, A. P. 1997. GDNF induces branching and increased cell proliferation in the ureter of the mouse. *Dev Biol,* 192**,** 193-8.

PERLEWITZ, A., PERSSON, A. E. & PATZAK, A. 2012. The juxtaglomerular apparatus. *Acta Physiologica,* 205**,** 6-8.

PERRAULT, I., SAUNIER, S., HANEIN, S., FILHOL, E., BIZET, A. A., COLLINS, F., SALIH, M. A., GERBER, S., DELPHIN, N., BIGOT, K., ORSSAUD, C., SILVA, E., BAUDOUIN, V., OUD, M. M., SHANNON, N., LE MERRER, M., ROCHE, O., PIETREMENT, C., GOUMID, J., BAUMANN, C., BOLE-FEYSOT, C., NITSCHKE, P., ZAHRATE, M., BEALES, P., ARTS, H. H., MUNNICH, A., KAPLAN, J., ANTIGNAC, C., CORMIER-DAIRE, V. & ROZET, J. M. 2012. Mainzer-Saldino syndrome is a ciliopathy caused by IFT140 mutations. *Am J Hum Genet,* 90**,** 864-70.

PETROSYAN, A., CRAVEDI, P., VILLANI, V., ANGELETTI, A., MANRIQUE, J., RENIERI, A., DE FILIPPO, R. E., PERIN, L. & DA SACCO, S. 2019. A glomerulus-on-a-chip to recapitulate the human glomerular filtration barrier. *Nature Communications,* 10**,** 3656.

PHILIPPE, A., NEVO, F., ESQUIVEL, E. L., REKLAITYTE, D., GRIBOUVAL, O., TETE, M. J., LOIRAT, C., DANTAL, J., FISCHBACH, M., POUTEIL-NOBLE, C., DECRAMER, S., HOEHNE, M., BENZING, T., CHARBIT, M., NIAUDET, P. & ANTIGNAC, C. 2008. Nephrin mutations can cause childhood-onset steroid-resistant nephrotic syndrome. *J Am Soc Nephrol,* 19**,** 1871-8.

PHIPSON, B., ER, P. X., COMBES, A. N., FORBES, T. A., HOWDEN, S. E., ZAPPIA, L., YEN, H. J., LAWLOR, K. T., HALE, L. J., SUN, J., WOLVETANG, E., TAKASATO, M., OSHLACK, A. & LITTLE, M. H. 2019. Evaluation of variability in human kidney organoids. *Nat Methods,* 16**,** 79-87.

PHIPSON, B., ER, P. X., HALE, L., YEN, D., LAWLOR, K., TAKASATO, M., SUN, J., WOLVETANG, E., OSHLACK, A. & LITTLE, M. 2017. Transcriptional evaluation of the developmental accuracy, reproducibility and robustness of kidney organoids derived from human pluripotent stem cells. *bioRxiv*.

PIECZYNSKI, J. & MARGOLIS, B. 2011. Protein complexes that control renal epithelial polarity. *American Journal of Physiology - Renal Physiology,* 300**,** F589-F601.

PIPERNO, G., SIUDA, E., HENDERSON, S., SEGIL, M., VAANANEN, H. & SASSAROLI, M. 1998. Distinct mutants of retrograde intraflagellar transport (IFT) share similar morphological and molecular defects. *J Cell Biol,* 143**,** 1591-601.

PRESTON, R., STUART, H. M. & LENNON, R. 2019. Genetic testing in steroid-resistant nephrotic syndrome: why, who, when and how? *Pediatric Nephrology,* 34**,** 195-210.

PRZEPIORSKI, A., SANDER, V., TRAN, T., HOLLYWOOD, J. A., SORRENSON, B., SHIH, J. H., WOLVETANG, E. J., MCMAHON, A. P., HOLM, T. M. & DAVIDSON, A. J. 2018. A Simple Bioreactor-Based Method to Generate Kidney Organoids from Pluripotent Stem Cells. *Stem Cell Reports,* 11**,** 470-484.

PUJO, L., FAGART, J., GARY, F., PAPADIMITRIOU, D. T., CLAES, A., JEUNEMAITRE, X. & ZENNARO, M. C. 2007. Mineralocorticoid receptor mutations are the principal cause of renal type 1 pseudohypoaldosteronism. *Hum Mutat,* 28**,** 33-40.

QIN, J., LIN, Y., NORMAN, R. X., KO, H. W. & EGGENSCHWILER, J. T. 2011. Intraflagellar transport protein 122 antagonizes Sonic Hedgehog signaling and controls ciliary localization of pathway components. *Proc Natl Acad Sci U S A,* 108**,** 1456-61.

RANGHINI, E. & DRESSLER, G. R. 2015. Early Specification and Patterning of the Intermediate Mesoderm: Genetics and Epigenetics. *In:* LITTLE, M. H. (ed.) *Kidney Development, Disease and Regeneration.* Amsterdam: Academic Press.

RAO, R., BHALLA, V. & PASTOR-SOLER, N. M. 2019. Intercalated Cells of the Kidney Collecting Duct in Kidney Physiology. *Semin Nephrol,* 39**,** 353-367.

RECKER, F., ZANIEW, M., BÖCKENHAUER, D., MIGLIETTI, N., BÖKENKAMP, A., MOCZULSKA, A., ROGOWSKA-KALISZ, A., LAUBE, G., SAID-CONTI, V., KASAP-DEMIR, B., NIEMIRSKA, A., LITWIN, M., SITEŃ, G., CHRZANOWSKA, K. H., KRAJEWSKA-WALASEK, M., SETHI, S. K., TASIC, V., ANGLANI, F., ADDIS, M., WASILEWSKA, A., SZCZEPAŃSKA, M., PAWLACZYK, K., SIKORA, P. & LUDWIG, M. 2015. Characterization of 28 novel patients expands the mutational and phenotypic spectrum of Lowe syndrome. *Pediatric Nephrology,* 30**,** 931-943.

REICHMAN, S., SLEMBROUCK, A., GAGLIARDI, G., CHAFFIOL, A., TERRAY, A., NANTEAU, C., POTEY, A., BELLE, M., RABESANDRATANA, O., DUEBEL, J., ORIEUX, G., NANDROT, E. F., SAHEL, J. A. & GOUREAU, O. 2017. Generation of Storable Retinal Organoids and Retinal Pigmented Epithelium from Adherent Human iPS Cells in Xeno-Free and Feeder-Free Conditions. *Stem Cells,* 35**,** 1176-1188.

REISER, J. & ALTINTAS, M. M. 2016. Podocytes. *F1000Research,* 5**,** F1000 Faculty Rev-114.

REISER, J., POLU, K. R., MOLLER, C. C., KENLAN, P., ALTINTAS, M. M., WEI, C., FAUL, C., HERBERT, S., VILLEGAS, I., AVILA-CASADO, C., MCGEE, M., SUGIMOTO, H., BROWN, D., KALLURI, R., MUNDEL, P., SMITH, P. L., CLAPHAM, D. E. & POLLAK, M. R. 2005. TRPC6 is a glomerular slit diaphragm-associated channel required for normal renal function. *Nat Genet,* 37**,** 739-44.

RENKEMA, K. Y., STOKMAN, M. F., GILES, R. H. & KNOERS, N. V. 2014. Next-generation sequencing for research and diagnostics in kidney disease. *Nat Rev Nephrol,* 10**,** 433-44.

RICHARDS, S., AZIZ, N., BALE, S., BICK, D., DAS, S., GASTIER-FOSTER, J., GRODY, W. W., HEGDE, M., LYON, E., SPECTOR, E., VOELKERDING, K., REHM, H. L. & COMMITTEE, A. L. Q. A. 2015. Standards and guidelines for the interpretation of sequence variants: a joint consensus recommendation of the American College of Medical Genetics and Genomics and the Association for Molecular Pathology. *Genet Med,* 17**,** 405-24.

RICHEY, E. A. & QIN, H. 2012. Dissecting the sequential assembly and localization of intraflagellar transport particle complex B in Chlamydomonas. *PLoS One,* 7**,** e43118.

RIGOTHIER, C., AUGUSTE, P., WELSH, G. I., LEPREUX, S., DEMINIERE, C., MATHIESON, P. W., SALEEM, M. A., RIPOCHE, J. & COMBE, C. 2012. IQGAP1 interacts with components of the slit diaphragm complex in podocytes and is involved in podocyte migration and permeability in vitro. *PLoS One,* 7**,** e37695.

RITCHIE, M. E., PHIPSON, B., WU, D., HU, Y., LAW, C. W., SHI, W. & SMYTH, G. K. 2015. limma powers differential expression analyses for RNA-sequencing and microarray studies. *Nucleic Acids Res,* 43**,** e47.

RIVEIRA-MUNOZ, E., CHANG, Q., GODEFROID, N., HOENDEROP, J. G., BINDELS, R. J., DAHAN, K. & DEVUYST, O. 2007. Transcriptional and Functional Analyses of SLC12A3 Mutations: New Clues for the Pathogenesis of Gitelman Syndrome. *Journal of the American Society of Nephrology,* 18**,** 1271-1283.

ROBB, L. & TAM, P. P. 2004. Gastrula organiser and embryonic patterning in the mouse. *Semin Cell Dev Biol,* 15**,** 543-54.

ROBINSON, M. D., MCCARTHY, D. J. & SMYTH, G. K. 2009. edgeR: a Bioconductor package for differential expression analysis of digital gene expression data. *Bioinformatics,* 26**,** 139-140.

ROBINSON, M. D. & OSHLACK, A. 2010. A scaling normalization method for differential expression analysis of RNA-seq data. *Genome Biol,* 11**,** R25.

ROSELLI, S., MOUTKINE, I., GRIBOUVAL, O., BENMERAH, A. & ANTIGNAC, C. 2004. Plasma membrane targeting of podocin through the classical exocytic pathway: effect of NPHS2 mutations. *Traffic,* 5**,** 37-44.

ROSENBAUM, J. L. & WITMAN, G. B. 2002. Intraflagellar transport. *Nat Rev Mol Cell Biol,* 3**,** 813-25.

ROY, A., AL-BATAINEH, M. M. & PASTOR-SOLER, N. M. 2015. Collecting duct intercalated cell function and regulation. *Clin J Am Soc Nephrol,* 10**,** 305-24.

RUF, R. G., LICHTENBERGER, A., KARLE, S. M., HAAS, J. P., ANACLETO, F. E., SCHULTHEISS, M., ZALEWSKI, I., IMM, A., RUF, E. M., MUCHA, B., BAGGA, A., NEUHAUS, T., FUCHSHUBER, A., BAKKALOGLU, A., HILDEBRANDT, F. & ARBEITSGEMEINSCHAFT FUR PADIATRISCHE NEPHROLOGIE STUDY, G. 2004. Patients with mutations in NPHS2

(podocin) do not respond to standard steroid treatment of nephrotic syndrome. *J Am Soc Nephrol,* 15**,** 722-32.

RUMBALLE, B. A., GEORGAS, K. M., COMBES, A. N., JU, A. L., GILBERT, T. & LITTLE, M. H. 2011. Nephron formation adopts a novel spatial topology at cessation of nephrogenesis. *Dev Biol,* 360**,** 110-22.

RUTLEDGE, E. A., BENAZET, J. D. & MCMAHON, A. P. 2017. Cellular heterogeneity in the ureteric progenitor niche and distinct profiles of branching morphogenesis in organ development. *Development,* 144**,** 3177-3188.

RYAN, D., SUTHERLAND, M. R., FLORES, T. J., KENT, A. L., DAHLSTROM, J. E., PUELLES, V. G., BERTRAM, J. F., MCMAHON, A. P., LITTLE, M. H., MOORE, L. & BLACK, M. J. 2018. Development of the Human Fetal Kidney from Mid to Late Gestation in Male and Female Infants. *EBioMedicine,* 27**,** 275-283.

SAADI-KHEDDOUCI, S., BERREBI, D., ROMAGNOLO, B., CLUZEAUD, F., PEUCHMAUR, M., KAHN, A., VANDEWALLE, A. & PERRET, C. 2001. Early development of polycystic kidney disease in transgenic mice expressing an activated mutant of the beta-catenin gene. *Oncogene,* 20**,** 5972-81.

SABATH, E., MEADE, P., BERKMAN, J., DE LOS HEROS, P., MORENO, E., BOBADILLA, N. A., VAZQUEZ, N., ELLISON, D. H. & GAMBA, G. 2004. Pathophysiology of functional mutations of the thiazide-sensitive Na-Cl cotransporter in Gitelman disease. *Am J Physiol Renal Physiol,* 287**,** F195-203.

SADOWSKI, C. E., LOVRIC, S., ASHRAF, S., PABST, W. L., GEE, H. Y., KOHL, S., ENGELMANN, S., VEGA-WARNER, V., FANG, H., HALBRITTER, J., SOMERS, M. J., TAN, W., SHRIL, S., FESSI, I., LIFTON, R. P., BOCKENHAUER, D., EL-DESOKY, S., KARI, J. A., ZENKER, M., KEMPER, M. J., MUELLER, D., FATHY, H. M., SOLIMAN, N. A., GROUP, S. S. & HILDEBRANDT, F. 2015. A single-gene cause in 29.5% of cases of steroid-resistant nephrotic syndrome. *J Am Soc Nephrol,* 26**,** 1279-89.

SALEEM, M. A., NI, L., WITHERDEN, I., TRYGGVASON, K., RUOTSALAINEN, V., MUNDEL, P. & MATHIESON, P. W. 2002. Co-Localization of Nephrin, Podocin, and the Actin Cytoskeleton: Evidence for a Role in Podocyte Foot Process Formation. *The American Journal of Pathology,* 161**,** 1459-1466.

SANDS, J. M. & LAYTON, H. E. 2009. The Physiology of Urinary Concentration: An Update. *Seminars in Nephrology,* 29**,** 178-195.

SANG, L., MILLER, J. J., CORBIT, K. C., GILES, R. H., BRAUER, M. J., OTTO, E. A., BAYE, L. M., WEN, X., SCALES, S. J., KWONG, M., HUNTZICKER, E. G., SFAKIANOS, M. K., SANDOVAL, W., BAZAN, J. F., KULKARNI, P., GARCIA-GONZALO, F. R., SEOL, A. D., O'TOOLE, J. F., HELD, S., REUTTER, H. M., LANE, W. S., RAFIQ, M. A., NOOR, A., ANSAR, M., DEVI, A. R. R., SHEFFIELD, V. C., SLUSARSKI, D. C., VINCENT, J. B., DOHERTY, D. A., HILDEBRANDT, F., REITER, J. F. & JACKSON, P. K. 2011. Mapping the NPHP-JBTS-MKS protein network reveals ciliopathy disease genes and pathways. *Cell,* 145**,** 513-528.

SANTIN, S., BULLICH, G., TAZON-VEGA, B., GARCIA-MASET, R., GIMENEZ, I., SILVA, I., RUIZ, P., BALLARIN, J., TORRA, R. & ARS, E. 2011. Clinical utility of genetic testing in children and adults with steroid-resistant nephrotic syndrome. *Clin J Am Soc Nephrol,* 6**,** 1139-48.

SANTIN, S., GARCIA-MASET, R., RUIZ, P., GIMENEZ, I., ZAMORA, I., PENA, A., MADRID, A., CAMACHO, J. A., FRAGA, G., SANCHEZ-MORENO, A., COBO, M. A., BERNIS, C., ORTIZ, A., DE PABLOS, A. L., PINTOS, G., JUSTA, M. L., HIDALGO-BARQUERO, E., FERNANDEZ-LLAMA, P., BALLARIN, J., ARS, E., TORRA, R. & GROUP, F. S. S. 2009. Nephrin mutations cause childhood- and adult-onset focal segmental glomerulosclerosis. *Kidney Int,* 76**,** 1268-76.

SAUNIER, S., CALADO, J., BENESSY, F., SILBERMANN, F., HEILIG, R., WEISSENBACH, J. & ANTIGNAC, C. 2000. Characterization of the NPHP1 locus: mutational mechanism involved in deletions in familial juvenile nephronophthisis. *Am J Hum Genet,* 66**,** 778-89.

SAVIGE, J., ARIANI, F., MARI, F., BRUTTINI, M., RENIERI, A., GROSS, O., DELTAS, C., FLINTER, F., DING, J., GALE, D. P., NAGEL, M., YAU, M., SHAGAM, L., TORRA, R., ARS, E., HOEFELE, J., GAROSI, G. & STOREY, H. 2019. Expert consensus guidelines for the genetic diagnosis of Alport syndrome. *Pediatric Nephrology,* 34**,** 1175-1189.

SAXEN, L. & LEHTONEN, E. 1987. Embryonic kidney in organ culture. *Differentiation,* 36**,** 2-11.

SAXEN, L. & SARIOLA, H. 1987. Early organogenesis of the kidney. *Pediatr Nephrol,* 1**,** 385-92.

SAYER, J. A., OTTO, E. A., O'TOOLE, J. F., NURNBERG, G., KENNEDY, M. A., BECKER, C., HENNIES, H. C., HELOU, J., ATTANASIO, M., FAUSETT, B. V., UTSCH, B., KHANNA, H., LIU, Y., DRUMMOND, I., KAWAKAMI, I., KUSAKABE, T., TSUDA, M., MA, L., LEE, H., LARSON, R. G., ALLEN, S. J., WILKINSON, C. J., NIGG, E. A., SHOU, C., LILLO, C., WILLIAMS, D. S., HOPPE, B., KEMPER, M. J., NEUHAUS, T., PARISI, M. A., GLASS, I. A., PETRY, M., KISPERT, A., GLOY, J., GANNER, A., WALZ, G., ZHU, X., GOLDMAN, D., NURNBERG, P., SWAROOP, A., LEROUX, M. R. & HILDEBRANDT, F. 2006. The centrosomal protein nephrocystin-6 is mutated in Joubert syndrome and activates transcription factor ATF4. *Nat Genet,* 38**,** 674-81.

SCHELL, C., BAUMHAKL, L., SALOU, S., CONZELMANN, A.-C., MEYER, C., HELMSTÄDTER, M., WREDE, C., GRAHAMMER, F., EIMER, S., KERJASCHKI, D., WALZ, G., SNAPPER, S. & HUBER, T. B. 2013. N-wasp is required for stabilization of podocyte foot processes. *Journal of the American Society of Nephrology : JASN,* 24**,** 713-721.

SCHELL, C. & HUBER, T. B. 2017. The Evolving Complexity of the Podocyte Cytoskeleton. *Journal of the American Society of Nephrology,* 28**,** 3166-3174.

SCHINDELIN, J., ARGANDA-CARRERAS, I., FRISE, E., KAYNIG, V., LONGAIR, M., PIETZSCH, T., PREIBISCH, S., RUEDEN, C., SAALFELD, S., SCHMID, B., TINEVEZ, J. Y., WHITE, D. J., HARTENSTEIN, V., ELICEIRI, K., TOMANCAK, P. & CARDONA, A. 2012. Fiji: an open-source platform for biological-image analysis. *Nat Methods,* 9**,** 676-82.

SCHMIDT, K. N., KUHNS, S., NEUNER, A., HUB, B., ZENTGRAF, H. & PEREIRA, G. 2012. Cep164 mediates vesicular docking to the mother centriole during early steps of ciliogenesis. *J Cell Biol,* 199**,** 1083-101.

SCHMIDTS, M., FRANK, V., EISENBERGER, T., AL TURKI, S., BIZET, A. A., ANTONY, D., RIX, S., DECKER, C., BACHMANN, N., BALD, M., VINKE, T., TOENSHOFF, B., DI DONATO, N., NEUHANN, T., HARTLEY, J. L., MAHER, E. R., BOGDANOVIC, R., PECO-ANTIC, A., MACHE, C., HURLES, M. E., JOKSIC, I., GUC-SCEKIC, M., DOBRICIC, J., BRANKOVIC-MAGIC, M., BOLZ, H. J., PAZOUR, G. J., BEALES, P. L., SCAMBLER, P. J., SAUNIER, S., MITCHISON, H. M. & BERGMANN, C. 2013. Combined NGS approaches identify mutations in the intraflagellar transport gene IFT140 in skeletal ciliopathies with early progressive kidney Disease. *Hum Mutat,* 34**,** 714-24.

SCHNELL, U. & CARROLL, T. J. 2014. Planar cell polarity of the kidney. *Exp Cell Res*.

SCHULTE, B. A. & SPICER, S. S. 1983. Histochemical evaluation of mouse and rat kidneys with lectin-horseradish peroxidase conjugates. *Am J Anat,* 168**,** 345-62.

SCHUTGENS, F., ROOKMAAKER, M. B., MARGARITIS, T., RIOS, A., AMMERLAAN, C., JANSEN, J., GIJZEN, L., VORMANN, M., VONK, A., VIVEEN, M., YENGEJ, F. Y., DERAKHSHAN, S., DE WINTER-DE GROOT, K. M., ARTEGIANI, B., VAN BOXTEL, R., CUPPEN, E., HENDRICKX, A. P. A., VAN DEN HEUVEL-EIBRINK, M. M., HEITZER, E., LANZ, H., BEEKMAN, J., MURK, J.-L., MASEREEUW, R., HOLSTEGE, F., DROST, J., VERHAAR, M. C. & CLEVERS, H. 2019. Tubuloids derived from human adult kidney and urine for personalized disease modeling. *Nature Biotechnology,* 37**,** 303-313.

SCHWARZ, K., SIMONS, M., REISER, J., SALEEM, M. A., FAUL, C., KRIZ, W., SHAW, A. S., HOLZMAN, L. B. & MUNDEL, P. 2001. Podocin, a raft-associated component of the glomerular slit diaphragm, interacts with CD2AP and nephrin. *The Journal of Clinical Investigation,* 108**,** 1621-1629.

SCOTT, R. P., HAWLEY, S. P., RUSTON, J., DU, J., BRAKEBUSCH, C., JONES, N. & PAWSON, T. 2012. Podocyte-specific loss of Cdc42 leads to congenital nephropathy. *J Am Soc Nephrol,* 23**,** 1149-54.

SELLIN, L., HUBER, T. B., GERKE, P., QUACK, I., PAVENSTADT, H. & WALZ, G. 2003. NEPH1 defines a novel family of podocin interacting proteins. *The FASEB Journal,* 17**,** 115-117.

SHANKLAND, S. J., SMEETS, B., PIPPIN, J. W. & MOELLER, M. J. 2014. The emergence of the glomerular parietal epithelial cell. *Nat Rev Nephrol,* 10**,** 158-73.

SHARMIN, S., TAGUCHI, A., KAKU, Y., YOSHIMURA, Y., OHMORI, T., SAKUMA, T., MUKOYAMA, M., YAMAMOTO, T., KURIHARA, H. & NISHINAKAMURA, R. 2016. Human Induced Pluripotent Stem Cell-Derived Podocytes Mature into Vascularized Glomeruli upon Experimental Transplantation. *J Am Soc Nephrol,* 27**,** 1778-91.

SHAWLOT, W. & BEHRINGER, R. R. 1995. Requirement for Lim1 in head-organizer function. *Nature,* 374**,** 425-30.

SHI, H., ENRIQUEZ, A., RAPADAS, M., MARTIN, E. M. M. A., WANG, R., MOREAU, J., LIM, C. K., SZOT, J. O., IP, E., HUGHES, J. N., SUGIMOTO, K., HUMPHREYS, D. T., MCINERNEY-

LEO, A. M., LEO, P. J., MAGHZAL, G. J., HALLIDAY, J., SMITH, J., COLLEY, A., MARK, P. R., COLLINS, F., SILLENCE, D. O., WINLAW, D. S., HO, J. W. K., GUILLEMIN, G. J., BROWN, M. A., KIKUCHI, K., THOMAS, P. Q., STOCKER, R., GIANNOULATOU, E., CHAPMAN, G., DUNCAN, E. L., SPARROW, D. B. & DUNWOODIE, S. L. 2017. NAD Deficiency, Congenital Malformations, and Niacin Supplementation. *New England Journal of Medicine,* 377**,** 544-552.

SHI, L., CUI, Y., LUAN, J., ZHOU, X. & HAN, J. 2016. Urine-derived induced pluripotent stem cells as a modeling tool to study rare human diseases. *Intractable & rare diseases research,* 5**,** 192-201.

SHIMADA, H., LU, Q., INSINNA-KETTENHOFEN, C., NAGASHIMA, K., ENGLISH, M. A., SEMLER, E. M., MAHGEREFTEH, J., CIDECIYAN, A. V., LI, T., BROOKS, B. P., GUNAY-AYGUN, M., JACOBSON, S. G., COGLIATI, T., WESTLAKE, C. J. & SWAROOP, A. 2017. In Vitro Modeling Using Ciliopathy-Patient-Derived Cells Reveals Distinct Cilia Dysfunctions Caused by CEP290 Mutations. *Cell Rep,* 20**,** 384-396.

SHIMELD, S. M., VAN DEN HEUVEL, M., DAWBER, R. & BRISCOE, J. 2007. An amphioxus Gli gene reveals conservation of midline patterning and the evolution of hedgehog signalling diversity in chordates. *PLoS One,* 2**,** e864.

SIGNOR, D., WEDAMAN, K. P., OROZCO, J. T., DWYER, N. D., BARGMANN, C. I., ROSE, L. S. & SCHOLEY, J. M. 1999. Role of a class DHC1b dynein in retrograde transport of IFT motors and IFT raft particles along cilia, but not dendrites, in chemosensory neurons of living Caenorhabditis elegans. *J Cell Biol,* 147**,** 519-30.

SIMONS, M., GLOY, J., GANNER, A., BULLERKOTTE, A., BASHKUROV, M., KRONIG, C., SCHERMER, B., BENZING, T., CABELLO, O. A., JENNY, A., MLODZIK, M., POLOK, B., DRIEVER, W., OBARA, T. & WALZ, G. 2005. Inversin, the gene product mutated in nephronophthisis type II, functions as a molecular switch between Wnt signaling pathways. *Nat Genet,* 37**,** 537-43.

SINGH, V. K., KALSAN, M., KUMAR, N., SAINI, A. & CHANDRA, R. 2015. Induced pluripotent stem cells: applications in regenerative medicine, disease modeling, and drug discovery. *Front Cell Dev Biol,* 3**,** 2.

SINHA, A., SAHA, A., KUMAR, M., SHARMA, S., AFZAL, K., MEHTA, A., KALAIVANI, M., HARI, P. & BAGGA, A. 2015. Extending initial prednisolone treatment in a randomized control trial from 3 to 6 months did not significantly influence the course of illness in children with steroid-sensitive nephrotic syndrome. *Kidney Int,* 87**,** 217-24.

SIVASUBRAMANIAM, S., SUN, X., PAN, Y. R., WANG, S. & LEE, E. Y. 2008. Cep164 is a mediator protein required for the maintenance of genomic stability through modulation of MDC1, RPA, and CHK1. *Genes Dev,* 22**,** 587-600.

SLAATS, G. G., LILIEN, M. R. & GILES, R. H. 2016. Nephronophthisis: should we target cysts or fibrosis? *Pediatr Nephrol,* 31**,** 545-54.

SLAATS, G. G., SALDIVAR, J. C., BACAL, J., ZEMAN, M. K., KILE, A. C., HYNES, A. M., SRIVASTAVA, S., NAZMUTDINOVA, J., DEN OUDEN, K., ZAGERS, M. S., FOLETTO, V., VERHAAR, M. C., MILES, C., SAYER, J. A., CIMPRICH, K. A. & GILES, R. H. 2015. DNA replication stress underlies renal phenotypes in CEP290-associated Joubert syndrome. *J Clin Invest,* 125**,** 3657-66.

SMITH, C., LAMONT, R. E., WADE, A., BERNIER, F. P., PARBOOSINGH, J. S. & INNES, A. M. 2016. A relatively mild skeletal ciliopathy phenotype consistent with cranioectodermal dysplasia is associated with a homozygous nonsynonymous mutation in WDR35. *Am J Med Genet A,* 170**,** 760-5.

SOO, J. Y. C., JANSEN, J., MASEREEUW, R. & LITTLE, M. H. 2018. Advances in predictive in vitro models of drug-induced nephrotoxicity. *Nature Reviews Nephrology,* 14**,** 378-393.

SPASIC, M. & JACOBS, C. R. 2017. Primary cilia: Cell and molecular mechanosensors directing whole tissue function. *Semin Cell Dev Biol,* 71**,** 42-52.

SPENCE, J. R., MAYHEW, C. N., RANKIN, S. A., KUHAR, M. F., VALLANCE, J. E., TOLLE, K., HOSKINS, E. E., KALINICHENKO, V. V., WELLS, S. I., ZORN, A. M., SHROYER, N. F. & WELLS, J. M. 2011. Directed differentiation of human pluripotent stem cells into intestinal tissue in vitro. *Nature,* 470**,** 105-9.

SPURR, A. R. 1969. A low-viscosity epoxy resin embedding medium for electron microscopy. *J Ultrastruct Res,* 26**,** 31-43.

SRIVASTAVA, S., MOLINARI, E., RAMAN, S. & SAYER, J. A. 2017a. Many Genes-One Disease? Genetics of Nephronophthisis (NPHP) and NPHP-Associated Disorders. *Front Pediatr,* 5**,** 287.

SRIVASTAVA, S., RAMSBOTTOM, S. A., MOLINARI, E., ALKANDERI, S., FILBY, A., WHITE, K., HENRY, C., SAUNIER, S., MILES, C. G. & SAYER, J. A. 2017b. A human patient-derived cellular model of Joubert syndrome reveals ciliary defects which can be rescued with targeted therapies. *Hum Mol Genet*.

STARR, M. C., CHANG, I. J., FINN, L. S., SUN, A., LARSON, A. A., GOEBEL, J., HANEVOLD, C., THIES, J., VAN HOVE, J. L. K., HINGORANI, S. R. & LAM, C. 2018. COQ2 nephropathy: a treatable cause of nephrotic syndrome in children. *Pediatr Nephrol,* 33**,** 1257-1261.

STEPANEK, L. & PIGINO, G. 2016. Microtubule doublets are double-track railways for intraflagellar transport trains. *Science,* 352**,** 721-4.

STONE, D. M., HYNES, M., ARMANINI, M., SWANSON, T. A., GU, Q., JOHNSON, R. L., SCOTT, M. P., PENNICA, D., GODDARD, A., PHILLIPS, H., NOLL, M., HOOPER, J. E., DE SAUVAGE, F. & ROSENTHAL, A. 1996. The tumour-suppressor gene patched encodes a candidate receptor for Sonic hedgehog. *Nature,* 384**,** 129-34.

SUBRAMANIAN, A., SIDHOM, E.-H., EMANI, M., SAHAKIAN, N., VERNON, K., ZHOU, Y., KOST-ALIMOVA, M., WEINS, A., SLYPER, M., WALDMAN, J., DIONNE, D., NGUYEN, L., MARSHALL, J. L., ROZENBLATT-ROSEN, O., REGEV, A. & GREKA, A. 2019. Kidney organoid reproducibility across multiple human iPSC lines and diminished off target cells after transplantation revealed by single cell transcriptomics. *bioRxiv***,** 516807.

SUMI, T., TSUNEYOSHI, N., NAKATSUJI, N. & SUEMORI, H. 2008. Defining early lineage specification of human embryonic stem cells by the orchestrated balance of canonical Wnt/beta-catenin, Activin/Nodal and BMP signaling. *Development,* 135**,** 2969-79.

SUN, L., TONG, H., WANG, H., YUE, Z., LIU, T., LIN, H., LI, J. & WANG, C. 2016. High mutation rate of NPHP3 in 18 Chinese infantile nephronophthisis patients. *Nephrology (Carlton),* 21**,** 209-16.

SWEENEY, C. L., TENG, R., WANG, H., MERLING, R. K., LEE, J., CHOI, U., KOONTZ, S., WRIGHT, D. G. & MALECH, H. L. 2016. Molecular Analysis of Neutrophil Differentiation from Human Induced Pluripotent Stem Cells Delineates the Kinetics of Key Regulators of Hematopoiesis. *STEM CELLS,* 34**,** 1513-1526.

SZKLARCZYK, D., FRANCESCHINI, A., WYDER, S., FORSLUND, K., HELLER, D., HUERTA-CEPAS, J., SIMONOVIC, M., ROTH, A., SANTOS, A., TSAFOU, K. P., KUHN, M., BORK, P., JENSEN, L. J. & VON MERING, C. 2015. STRING v10: protein-protein interaction networks, integrated over the tree of life. *Nucleic Acids Res,* 43**,** D447-52.

TAGUCHI, A., KAKU, Y., OHMORI, T., SHARMIN, S., OGAWA, M., SASAKI, H. & NISHINAKAMURA, R. 2014. Redefining the in vivo origin of metanephric nephron progenitors enables generation of complex kidney structures from pluripotent stem cells. *Cell Stem Cell,* 14**,** 53-67.

TAGUCHI, A. & NISHINAKAMURA, R. 2017. Higher-Order Kidney Organogenesis from Pluripotent Stem Cells. *Cell Stem Cell,* 21**,** 730-746 e6.

TAKAHASHI, K., OKITA, K., NAKAGAWA, M. & YAMANAKA, S. 2007. Induction of pluripotent stem cells from fibroblast cultures. *Nat Protoc,* 2**,** 3081-9.

TAKASATO, M., ER, P. X., BECROFT, M., VANSLAMBROUCK, J. M., STANLEY, E. G., ELEFANTY, A. G. & LITTLE, M. H. 2014. Directing human embryonic stem cell differentiation towards a renal lineage generates a self-organizing kidney. *Nat Cell Biol,* 16**,** 118-26.

TAKASATO, M., ER, P. X., CHIU, H. S. & LITTLE, M. H. 2016. Generation of kidney organoids from human pluripotent stem cells. *Nat Protoc,* 11**,** 1681-92.

TAKASATO, M., ER, P. X., CHIU, H. S., MAIER, B., BAILLIE, G. J., FERGUSON, C., PARTON, R. G., WOLVETANG, E. J., ROOST, M. S., CHUVA DE SOUSA LOPES, S. M. & LITTLE, M. H. 2015. Kidney organoids from human iPS cells contain multiple lineages and model human nephrogenesis. *Nature,* 526**,** 564-8.

TAKASATO, M. & LITTLE, M. H. 2015. The origin of the mammalian kidney: implications for recreating the kidney in vitro. *Development,* 142**,** 1937-47.

TAKEDA, S., YONEKAWA, Y., TANAKA, Y., OKADA, Y., NONAKA, S. & HIROKAWA, N. 1999. Left-right asymmetry and kinesin superfamily protein KIF3A: new insights in determination of laterality and mesoderm induction by kif3A-/- mice analysis. *J Cell Biol,* 145**,** 825-36.

TAM, P. P. & LOEBEL, D. A. 2007. Gene function in mouse embryogenesis: get set for gastrulation. *Nat Rev Genet,* 8**,** 368-81.

TAMMACHOTE, R., HOMMERDING, C. J., SINDERS, R. M., MILLER, C. A., CZARNECKI, P. G., LEIGHTNER, A. C., SALISBURY, J. L., WARD, C. J., TORRES, V. E., GATTONE, V. H., 2ND & HARRIS, P. C. 2009. Ciliary and centrosomal defects associated with mutation and depletion of the Meckel syndrome genes MKS1 and MKS3. *Hum Mol Genet,* 18**,** 3311-23.

TAN, W., LOVRIC, S., ASHRAF, S., RAO, J., SCHAPIRO, D., AIRIK, M., SHRIL, S., GEE, H. Y., BAUM, M., DAOUK, G., FERGUSON, M. A., RODIG, N., SOMERS, M. J. G., STEIN, D. R., VIVANTE, A., WAREJKO, J. K., WIDMEIER, E. & HILDEBRANDT, F. 2018. Analysis of 24 genes reveals a monogenic cause in 11.1% of cases with steroid-resistant nephrotic syndrome at a single center. *Pediatr Nephrol,* 33**,** 305-314.

TANIGAWA, S., ISLAM, M., SHARMIN, S., NAGANUMA, H., YOSHIMURA, Y., HAQUE, F., ERA, T., NAKAZATO, H., NAKANISHI, K., SAKUMA, T., YAMAMOTO, T., KURIHARA, H., TAGUCHI, A. & NISHINAKAMURA, R. 2018. Organoids from Nephrotic Disease-Derived iPSCs Identify Impaired NEPHRIN Localization and Slit Diaphragm Formation in Kidney Podocytes. *Stem Cell Reports,* 11**,** 727-740.

TANIGAWA, S., WANG, H., YANG, Y., SHARMA, N., TARASOVA, N., AJIMA, R., YAMAGUCHI, T. P., RODRIGUEZ, L. G. & PERANTONI, A. O. 2011. Wnt4 induces nephronic tubules in metanephric mesenchyme by a non-canonical mechanism. *Dev Biol,* 352**,** 58-69.

TASCHNER, M., BHOGARAJU, S. & LORENTZEN, E. 2012. Architecture and function of IFT complex proteins in ciliogenesis. *Differentiation,* 83**,** S12-22.

TASCHNER, M., KOTSIS, F., BRAEUER, P., KUEHN, E. W. & LORENTZEN, E. 2014. Crystal structures of IFT70/52 and IFT52/46 provide insight into intraflagellar transport B core complex assembly. *J Cell Biol,* 207**,** 269-82.

TASCHNER, M. & LORENTZEN, E. 2016. The Intraflagellar Transport Machinery. *Cold Spring Harbor Perspectives in Biology,* 8.

TASCHNER, M., WEBER, K., MOURAO, A., VETTER, M., AWASTHI, M., STIEGLER, M., BHOGARAJU, S. & LORENTZEN, E. 2016. Intraflagellar transport proteins 172, 80, 57, 54, 38, and 20 form a stable tubulin-binding IFT-B2 complex. *EMBO J,* 35**,** 773-90.

TAUB, D. G. & LIU, Q. 2016. The Role of Intraflagellar Transport in the Photoreceptor Sensory Cilium. *Adv Exp Med Biol,* 854**,** 627-33.

TEENINGA, N., KIST-VAN HOLTHE, J. E., VAN RIJSWIJK, N., DE MOS, N. I., HOP, W. C., WETZELS, J. F., VAN DER HEIJDEN, A. J. & NAUTA, J. 2013. Extending prednisolone treatment does not reduce relapses in childhood nephrotic syndrome. *J Am Soc Nephrol,* 24**,** 149-59.

THATCHER, S. E. 2017. A Brief Introduction into the Renin-Angiotensin-Aldosterone System: New and Old Techniques. *Methods Mol Biol,* 1614**,** 1-19.

THIAGARAJAN, R. D., GEORGAS, K. M., RUMBALLE, B. A., LESIEUR, E., CHIU, H. S., TAYLOR, D., TANG, D. T., GRIMMOND, S. M. & LITTLE, M. H. 2011. Identification of anchor genes during kidney development defines ontological relationships, molecular subcompartments and regulatory pathways. *PLoS One,* 6**,** e17286.

THIVIERGE, C., KURBEGOVIC, A., COUILLARD, M., GUILLAUME, R., COTE, O. & TRUDEL, M. 2006. Overexpression of PKD1 causes polycystic kidney disease. *Mol Cell Biol,* 26**,** 1538-48.

THONG, K. M., XU, Y., COOK, J., TAKOU, A., WAGNER, B., KAWAR, B. & ONG, A. C. 2013. Cosegregation of focal segmental glomerulosclerosis in a family with familial partial lipodystrophy due to a mutation in LMNA. *Nephron Clin Pract,* 124**,** 31-7.

TORY, K., ROUSSET-ROUVIERE, C., GUBLER, M. C., MORINIERE, V., PAWTOWSKI, A., BECKER, C., GUYOT, C., GIE, S., FRISHBERG, Y., NIVET, H., DESCHENES, G., COCHAT, P., GAGNADOUX, M. F., SAUNIER, S., ANTIGNAC, C. & SALOMON, R. 2009. Mutations of NPHP2 and NPHP3 in infantile nephronophthisis. *Kidney Int,* 75**,** 839-47.

TOWN, M., JEAN, G., CHERQUI, S., ATTARD, M., FORESTIER, L., WHITMORE, S. A., CALLEN, D. F., GRIBOUVAL, O., BROYER, M., BATES, G. P., VAN'T HOFF, W. & ANTIGNAC, C. 1998. A novel gene encoding an integral membrane protein is mutated in nephropathic cystinosis. *Nat Genet,* 18**,** 319-24.

TRAN, P. V., HAYCRAFT, C. J., BESSCHETNOVA, T. Y., TURBE-DOAN, A., STOTTMANN, R. W., HERRON, B. J., CHESEBRO, A. L., QIU, H., SCHERZ, P. J., SHAH, J. V., YODER, B. K. & BEIER, D. R. 2008. THM1 negatively modulates mouse sonic hedgehog signal transduction and affects retrograde intraflagellar transport in cilia. *Nat Genet,* 40**,** 403-10.

TREUER, A. V. & GONZALEZ, D. R. 2014. NOS1AP modulates intracellular Ca(2+) in cardiac myocytes and is up-regulated in dystrophic cardiomyopathy. *Int J Physiol Pathophysiol Pharmacol,* 6**,** 37-46.

TSANG, T. E., SHAWLOT, W., KINDER, S. J., KOBAYASHI, A., KWAN, K. M., SCHUGHART, K., KANIA, A., JESSELL, T. M., BEHRINGER, R. R. & TAM, P. P. 2000. Lim1 activity is required for intermediate mesoderm differentiation in the mouse embryo. *Dev Biol,* 223**,** 77-90.

TSAO, C. C. & GOROVSKY, M. A. 2008. Different effects of Tetrahymena IFT172 domains on anterograde and retrograde intraflagellar transport. *Mol Biol Cell,* 19**,** 1450-61.

TSUJI, T., MATSUO, K., NAKAHARI, T., MARUNAKA, Y. & YOKOYAMA, T. 2016. Structural basis of the Inv compartment and ciliary abnormalities in Inv/nphp2 mutant mice. *Cytoskeleton (Hoboken),* 73**,** 45-56.

UNBEKANDT, M. & DAVIES, J. A. 2010. Dissociation of embryonic kidneys followed by reaggregation allows the formation of renal tissues. *Kidney Int,* 77**,** 407-16.

VAN DEN BERG, C. W., RITSMA, L., AVRAMUT, M. C., WIERSMA, L. E., VAN DEN BERG, B. M., LEUNING, D. G., LIEVERS, E., KONING, M., VANSLAMBROUCK, J. M., KOSTER, A. J., HOWDEN, S. E., TAKASATO, M., LITTLE, M. H. & RABELINK, T. J. 2018. Renal Subcapsular Transplantation of PSC-Derived Kidney Organoids Induces Neo-vasculogenesis and Significant Glomerular and Tubular Maturation In Vivo. *Stem Cell Reports,* 10**,** 751-765.

VAN DER KNAAP, M. S., WEVERS, R. A., MONNENS, L., JAKOBS, C., JAEKEN, J. & VAN WIJK, J. A. 1996. Congenital nephrotic syndrome: a novel phenotype of type I carbohydrate-deficient glycoprotein syndrome. *J Inherit Metab Dis,* 19**,** 787-91.

VAN DER VEN, A. T., CONNAUGHTON, D. M., ITYEL, H., MANN, N., NAKAYAMA, M., CHEN, J., VIVANTE, A., HWANG, D. Y., SCHULZ, J., BRAUN, D. A., SCHMIDT, J. M., SCHAPIRO, D., SCHNEIDER, R., WAREJKO, J. K., DAGA, A., MAJMUNDAR, A. J., TAN, W., JOBST-SCHWAN, T., HERMLE, T., WIDMEIER, E., ASHRAF, S., AMAR, A., HOOGSTRAATEN, C. A., HUGO, H., KITZLER, T. M., KAUSE, F., KOLVENBACH, C. M., DAI, R., SPANEAS, L., AMANN, K., STEIN, D. R., BAUM, M. A., SOMERS, M. J. G., RODIG, N. M., FERGUSON, M. A., TRAUM, A. Z., DAOUK, G. H., BOGDANOVIC, R., STAJIC, N., SOLIMAN, N. A., KARI, J. A., EL DESOKY, S., FATHY, H. M., MILOSEVIC, D., AL-SAFFAR, M., AWAD, H. S., EID, L. A., SELVIN, A., SENGUTTUVAN, P., SANNA-CHERCHI, S., REHM, H. L., MACARTHUR, D. G., LEK, M., LARICCHIA, K. M., WILSON, M. W., MANE, S. M., LIFTON, R. P., LEE, R. S., BAUER, S. B., LU, W., REUTTER, H. M., TASIC, V., SHRIL, S. & HILDEBRANDT, F. 2018. Whole-Exome Sequencing Identifies Causative Mutations in Families with Congenital Anomalies of the Kidney and Urinary Tract. *J Am Soc Nephrol,* 29**,** 2348-2361.

VAN DER WALT, S., SCHONBERGER, J. L., NUNEZ-IGLESIAS, J., BOULOGNE, F., WARNER, J. D., YAGER, N., GOUILLART, E. & YU, T. 2014. scikit-image: image processing in Python. *PeerJ,* 2**,** e453.

VANDERVER, A., SIMONS, C., HELMAN, G., CRAWFORD, J., WOLF, N. I., BERNARD, G., PIZZINO, A., SCHMIDT, J. L., TAKANOHASHI, A., MILLER, D., KHOUZAM, A., RAJAN, V., RAMOS, E., CHOWDHURY, S., HAMBUCH, T., RU, K., BAILLIE, G. J., GRIMMOND, S. M., CALDOVIC, L., DEVANEY, J., BLOOM, M., EVANS, S. H., MURPHY, J. L., MCNEILL, N., FOGEL, B. L., LEUKODYSTROPHY STUDY, G., SCHIFFMANN, R., VAN DER KNAAP, M. S. & TAFT, R. J. 2016. Whole exome sequencing in patients with white matter abnormalities. *Ann Neurol,* 79**,** 1031-7.

VERBITSKY, M., WESTLAND, R., PEREZ, A., KIRYLUK, K., LIU, Q., KRITHIVASAN, P., MITROTTI, A., FASEL, D. A., BATOURINA, E., SAMPSON, M. G., BODRIA, M., WERTH, M., KAO, C., MARTINO, J., CAPONE, V. P., VIVANTE, A., SHRIL, S., KIL, B. H., MARASÀ, M., ZHANG, J. Y., NA, Y.-J., LIM, T. Y., AHRAM, D., WENG, P. L., HEINZEN, E. L., CARREA, A., PIAGGIO, G., GESUALDO, L., MANCA, V., MASNATA, G., GIGANTE, M., CUSI, D., IZZI, C., SCOLARI, F., VAN WIJK, J. A. E., SARAGA, M., SANTORO, D., CONTI, G., ZAMBOLI, P., WHITE, H., DROZDZ, D., ZACHWIEJA, K., MIKLASZEWSKA, M., TKACZYK, M., TOMCZYK, D., KRAKOWSKA, A., SIKORA, P., JARMOLIŃSKI, T., BORSZEWSKA-KORNACKA, M. K., PAWLUCH, R., SZCZEPANSKA, M., ADAMCZYK, P., MIZERSKA-WASIAK, M., KRZEMIEN, G., SZMIGIELSKA, A., ZANIEW, M., DOBSON, M. G., DARLOW, J. M., PURI, P., BARTON, D. E., FURTH, S. L., WARADY, B. A., GUCEV, Z., LOZANOVSKI, V. J., TASIC, V., PISANI, I., ALLEGRI, L., RODAS, L. M., CAMPISTOL, J. M., JEANPIERRE, C., ALAM, S., CASALE, P., WONG, C. S., LIN, F., MIRANDA, D. M., OLIVEIRA, E. A., SIMÕES-E-SILVA, A. C., BARASCH, J. M., LEVY, B., WU, N., HILDEBRANDT, F., GHIGGERI, G. M., LATOS-BIELENSKA, A., MATERNA-KIRYLUK, A., ZHANG, F., HAKONARSON, H., PAPAIOANNOU, V. E., MENDELSOHN, C. L., GHARAVI, A. G. & SANNA-CHERCHI, S. 2019. The copy number variation landscape of congenital anomalies of the kidney and urinary tract. *Nature Genetics,* 51**,** 117-127.

VERHEY, K. J., DISHINGER, J. & KEE, H. L. 2011. Kinesin motors and primary cilia. *Biochem Soc Trans,* 39**,** 1120-5.

VERMA, R., KOVARI, I., SOOFI, A., NIHALANI, D., PATRIE, K. & HOLZMAN, L. B. 2006. Nephrin ectodomain engagement results in Src kinase activation, nephrin phosphorylation, Nck recruitment, and actin polymerization. *The Journal of Clinical Investigation,* 116**,** 1346-1359.

VESTER, U., KRANZ, B. & HOYER, P. F. 2010. The diagnostic value of ultrasound in cystic kidney diseases. *Pediatr Nephrol,* 25**,** 231-40.

VIEIRA, O. V., GAUS, K., VERKADE, P., FULLEKRUG, J., VAZ, W. L. & SIMONS, K. 2006. FAPP2, cilium formation, and compartmentalization of the apical membrane in polarized Madin-Darby canine kidney (MDCK) cells. *Proc Natl Acad Sci U S A,* 103**,** 18556-61.

VINCENT, S. D., DUNN, N. R., HAYASHI, S., NORRIS, D. P. & ROBERTSON, E. J. 2003. Cell fate decisions within the mouse organizer are governed by graded Nodal signals. *Genes Dev,* 17**,** 1646-62.

VIVANTE, A. & HILDEBRANDT, F. 2016. Exploring the genetic basis of early-onset chronic kidney disease. *Nat Rev Nephrol,* 12**,** 133-46.

VOKES, S. A., JI, H., MCCUINE, S., TENZEN, T., GILES, S., ZHONG, S., LONGABAUGH, W. J., DAVIDSON, E. H., WONG, W. H. & MCMAHON, A. P. 2007. Genomic characterization of Gli-activator targets in sonic hedgehog-mediated neural patterning. *Development,* 134**,** 1977-89.

VOKES, S. A., JI, H., WONG, W. H. & MCMAHON, A. P. 2008. A genome-scale analysis of the cis-regulatory circuitry underlying sonic hedgehog-mediated patterning of the mammalian limb. *Genes Dev,* 22**,** 2651-63.

WALCZAK-SZTULPA, J., EGGENSCHWILER, J., OSBORN, D., BROWN, D. A., EMMA, F., KLINGENBERG, C., HENNEKAM, R. C., TORRE, G., GARSHASBI, M., TZSCHACH, A., SZCZEPANSKA, M., KRAWCZYNSKI, M., ZACHWIEJA, J., ZWOLINSKA, D., BEALES, P. L., ROPERS, H. H., LATOS-BIELENSKA, A. & KUSS, A. W. 2010. Cranioectodermal Dysplasia, Sensenbrenner syndrome, is a ciliopathy caused by mutations in the IFT122 gene. *Am J Hum Genet,* 86**,** 949-56.

WALDHERR, R., LENNERT, T., WEBER, H. P., FODISCH, H. J. & SCHARER, K. 1982. The nephronophthisis complex. A clinicopathologic study in children. *Virchows Arch A Pathol Anat Histol,* 394**,** 235-54.

WARD, C. J., HOGAN, M. C., ROSSETTI, S., WALKER, D., SNEDDON, T., WANG, X., KUBLY, V., CUNNINGHAM, J. M., BACALLAO, R., ISHIBASHI, M., MILLINER, D. S., TORRES, V. E. & HARRIS, P. C. 2002. The gene mutated in autosomal recessive polycystic kidney disease encodes a large, receptor-like protein. *Nat Genet,* 30**,** 259-69.

WAREJKO, J. K., TAN, W., DAGA, A., SCHAPIRO, D., LAWSON, J. A., SHRIL, S., LOVRIC, S., ASHRAF, S., RAO, J., HERMLE, T., JOBST-SCHWAN, T., WIDMEIER, E., MAJMUNDAR, A. J., SCHNEIDER, R., GEE, H. Y., SCHMIDT, J. M., VIVANTE, A., VAN DER VEN, A. T., ITYEL, H., CHEN, J., SADOWSKI, C. E., KOHL, S., PABST, W. L., NAKAYAMA, M., SOMERS, M. J. G., RODIG, N. M., DAOUK, G., BAUM, M., STEIN, D. R., FERGUSON, M. A., TRAUM, A. Z., SOLIMAN, N. A., KARI, J. A., EL DESOKY, S., FATHY, H., ZENKER, M., BAKKALOGLU, S. A., MULLER, D., NOYAN, A., OZALTIN, F., CADNAPAPHORNCHAI, M. A., HASHMI, S., HOPCIAN, J., KOPP, J. B., BENADOR, N., BOCKENHAUER, D., BOGDANOVIC, R., STAJIC, N., CHERNIN, G., ETTENGER, R., FEHRENBACH, H., KEMPER, M., MUNARRIZ, R. L., PODRACKA, L., BUSCHER, R., SERDAROGLU, E., TASIC, V., MANE, S., LIFTON, R. P., BRAUN, D. A. & HILDEBRANDT, F. 2018. Whole Exome Sequencing of Patients with Steroid-Resistant Nephrotic Syndrome. *Clin J Am Soc Nephrol,* 13**,** 53-62.

WEATHERBEE, S. D., NISWANDER, L. A. & ANDERSON, K. V. 2009. A mouse model for Meckel syndrome reveals Mks1 is required for ciliogenesis and Hedgehog signaling. *Hum Mol Genet,* 18**,** 4565-75.

WEBER, S., TAYLOR, J. C., WINYARD, P., BAKER, K. F., SULLIVAN-BROWN, J., SCHILD, R., KNUPPEL, T., ZUROWSKA, A. M., CALDAS-ALFONSO, A., LITWIN, M., EMRE, S., GHIGGERI, G. M., BAKKALOGLU, A., MEHLS, O., ANTIGNAC, C., NETWORK, E., SCHAEFER, F. & BURDINE, R. D. 2008. SIX2 and BMP4 mutations associate with anomalous kidney development. *J Am Soc Nephrol,* 19**,** 891-903.

WEI, Q., XU, Q., ZHANG, Y., LI, Y., ZHANG, Q., HU, Z., HARRIS, P. C., TORRES, V. E., LING, K. & HU, J. 2013. Transition fibre protein FBF1 is required for the ciliary entry of assembled intraflagellar transport complexes. *Nat Commun,* 4**,** 2750.

WEI, Q., ZHANG, Y., LI, Y., ZHANG, Q., LING, K. & HU, J. 2012. The BBSome controls IFT assembly and turnaround in cilia. *Nat Cell Biol,* 14**,** 950-7.

WEINS, A., KENLAN, P., HERBERT, S., LE, T. C., VILLEGAS, I., KAPLAN, B. S., APPEL, G. B. & POLLAK, M. R. 2005. Mutational and Biological Analysis of α-Actinin-4 in Focal Segmental Glomerulosclerosis. *Journal of the American Society of Nephrology,* 16**,** 3694-3701.

WEISS, P. & TAYLOR, A. C. 1960. Reconstitution of Complete Organs from Single-Cell Suspensions of Chick Embryos in Advanced Stages of Differentiation. *Proc Natl Acad Sci U S A,* 46**,** 1177-85.

WELSCH, T., ENDLICH, N., KRIZ, W. & ENDLICH, K. 2001. CD2AP and p130Cas localize to different F-actin structures in podocytes. *Am J Physiol Renal Physiol,* 281**,** F769-77.

WELSH, G. I. & SALEEM, M. A. 2011. The podocyte cytoskeleton--key to a functioning glomerulus in health and disease. *Nat Rev Nephrol,* 8**,** 14-21.

WHEATLEY, D. N. 1995. Primary cilia in normal and pathological tissues. *Pathobiology,* 63**,** 222-38.

WICKS, S. R., DE VRIES, C. J., VAN LUENEN, H. G. & PLASTERK, R. H. 2000. CHE-3, a cytosolic dynein heavy chain, is required for sensory cilia structure and function in Caenorhabditis elegans. *Dev Biol,* 221**,** 295-307.

WIJGERDE, M., KARP, S., MCMAHON, J. & MCMAHON, A. P. 2005. Noggin antagonism of BMP4 signaling controls development of the axial skeleton in the mouse. *Dev Biol,* 286**,** 149-57.

WILLIAMS, S. S., COBO-STARK, P., JAMES, L. R., SOMLO, S. & IGARASHI, P. 2008. Kidney cysts, pancreatic cysts, and biliary disease in a mouse model of autosomal recessive polycystic kidney disease. *Pediatr Nephrol,* 23**,** 733-41.

WINN, M. P., CONLON, P. J., LYNN, K. L., FARRINGTON, M. K., CREAZZO, T., HAWKINS, A. F., DASKALAKIS, N., KWAN, S. Y., EBERSVILLER, S., BURCHETTE, J. L., PERICAK-VANCE, M. A., HOWELL, D. N., VANCE, J. M. & ROSENBERG, P. B. 2005. A mutation in the TRPC6 cation channel causes familial focal segmental glomerulosclerosis. *Science,* 308**,** 1801-4.

WINNIER, G., BLESSING, M., LABOSKY, P. A. & HOGAN, B. L. 1995. Bone morphogenetic protein-4 is required for mesoderm formation and patterning in the mouse. *Genes Dev,* 9**,** 2105-16.

WOLF, M. T. 2015. Nephronophthisis and related syndromes. *Curr Opin Pediatr,* 27**,** 201-11.

WOOLLARD, J. R., PUNYASHTITI, R., RICHARDSON, S., MASYUK, T. V., WHELAN, S., HUANG, B. Q., LAGER, D. J., VANDEURSEN, J., TORRES, V. E., GATTONE, V. H., LARUSSO, N. F., HARRIS, P. C. & WARD, C. J. 2007. A mouse model of autosomal recessive polycystic kidney disease with biliary duct and proximal tubule dilatation. *Kidney Int,* 72**,** 328-36.

WU, D. & SMYTH, G. K. 2012. Camera: a competitive gene set test accounting for inter-gene correlation. *Nucleic Acids Res,* 40**,** e133.

WU, F., WU, D., REN, Y., HUANG, Y., FENG, B., ZHAO, N., ZHANG, T., CHEN, X., CHEN, S. & XU, A. 2019a. Generation of hepatobiliary organoids from human induced pluripotent stem cells. *Journal of Hepatology,* 70**,** 1145-1158.

WU, G., TIAN, X., NISHIMURA, S., MARKOWITZ, G. S., D'AGATI, V., PARK, J. H., YAO, L., LI, L., GENG, L., ZHAO, H., EDELMANN, W. & SOMLO, S. 2002. Trans-heterozygous Pkd1 and Pkd2 mutations modify expression of polycystic kidney disease. *Hum Mol Genet,* 11**,** 1845-54.

WU, H., KIRITA, Y., DONNELLY, E. L. & HUMPHREYS, B. D. 2019b. Advantages of Single-Nucleus over Single-Cell RNA Sequencing of Adult Kidney: Rare Cell Types and Novel Cell States Revealed in Fibrosis. *Journal of the American Society of Nephrology,* 30**,** 23-32.

WU, H., MALONE, A. F., DONNELLY, E. L., KIRITA, Y., UCHIMURA, K., RAMAKRISHNAN, S. M., GAUT, J. P. & HUMPHREYS, B. D. 2018a. Single-Cell Transcriptomics of a Human Kidney Allograft Biopsy Specimen Defines a Diverse Inflammatory Response. *J Am Soc Nephrol,* 29**,** 2069-2080.

WU, H., UCHIMURA, K., DONNELLY, E. L., KIRITA, Y., MORRIS, S. A. & HUMPHREYS, B. D. 2018b. Comparative Analysis and Refinement of Human PSC-Derived Kidney Organoid Differentiation with Single-Cell Transcriptomics. *Cell Stem Cell,* 23**,** 869-881 e8.

WU, J., HE, Z., WANG, D. L. & SUN, F. L. 2016. Depletion of JMJD5 sensitizes tumor cells to microtubule-destabilizing agents by altering microtubule stability. *Cell Cycle,* 15**,** 2980-2991.

WYNN, T. A. & RAMALINGAM, T. R. 2012. Mechanisms of fibrosis: Therapeutic translation for fibrotic disease. *Nature Medicine,* 18**,** 1028-1040.

XIA, Y., NIVET, E., SANCHO-MARTINEZ, I., GALLEGOS, T., SUZUKI, K., OKAMURA, D., WU, M. Z., DUBOVA, I., ESTEBAN, C. R., MONTSERRAT, N., CAMPISTOL, J. M. & IZPISUA BELMONTE, J. C. 2013. Directed differentiation of human pluripotent cells to ureteric bud kidney progenitor-like cells. *Nat Cell Biol,* 15**,** 1507-15.

XU, C., ROSSETTI, S., JIANG, L., HARRIS, P. C., BROWN-GLABERMAN, U., WANDINGER-NESS, A., BACALLAO, R. & ALPER, S. L. 2007. Human ADPKD primary cyst epithelial cells with a

novel, single codon deletion in the PKD1 gene exhibit defective ciliary polycystin localization and loss of flow-induced Ca2+ signaling. *Am J Physiol Renal Physiol,* 292**,** F930-45.

XU, M., YANG, L., WANG, F., LI, H., WANG, X., WANG, W., GE, Z., WANG, K., ZHAO, L., LI, H., LI, Y., SUI, R. & CHEN, R. 2015. Mutations in human IFT140 cause non-syndromic retinal degeneration. *Hum Genet,* 134**,** 1069-78.

YAMAMOTO, M., SAIJOH, Y., PEREA-GOMEZ, A., SHAWLOT, W., BEHRINGER, R. R., ANG, S. L., HAMADA, H. & MENO, C. 2004. Nodal antagonists regulate formation of the anteroposterior axis of the mouse embryo. *Nature,* 428**,** 387-92.

YAMANAKA, T., HORIKOSHI, Y., SUZUKI, A., SUGIYAMA, Y., KITAMURA, K., MANIWA, R., NAGAI, Y., YAMASHITA, A., HIROSE, T., ISHIKAWA, H. & OHNO, S. 2001. PAR-6 regulates aPKC activity in a novel way and mediates cell-cell contact-induced formation of the epithelial junctional complex. *Genes Cells,* 6**,** 721-31.

YANG, C. T., MA, R., AXTON, R. A., JACKSON, M., TAYLOR, A. H., FIDANZA, A., MARENAH, L., FRAYNE, J., MOUNTFORD, J. C. & FORRESTER, L. M. 2017. Activation of KLF1 Enhances the Differentiation and Maturation of Red Blood Cells from Human Pluripotent Stem Cells. *Stem Cells,* 35**,** 886-897.

YASUNAGA, T., HOFF, S., SCHELL, C., HELMSTADTER, M., KRETZ, O., KUECHLIN, S., YAKULOV, T. A., ENGEL, C., MULLER, B., BENSCH, R., RONNEBERGER, O., HUBER, T. B., LIENKAMP, S. S. & WALZ, G. 2015. The polarity protein Inturned links NPHP4 to Daam1 to control the subapical actin network in multiciliated cells. *J Cell Biol,* 211**,** 963-73.

YE, X., ZENG, H., NING, G., REITER, J. F. & LIU, A. 2014. C2cd3 is critical for centriolar distal appendage assembly and ciliary vesicle docking in mammals. *Proc Natl Acad Sci U S A,* 111**,** 2164-9.

YORIFUJI, T., KAWAI, M., MOMOI, T., SASAKI, H., FURUSHO, K., MUROI, J., SHIMIZU, K., TAKAHASHI, Y., MATSUMURA, M., NAMBU, M. & OKUNO, T. 1996. Nephropathy and growth hormone deficiency in a patient with mitochondrial tRNA(Leu(UUR)) mutation. *Journal of Medical Genetics,* 33**,** 621-622.

YOSHIKAWA, N., NAKANISHI, K., SAKO, M., OBA, M. S., MORI, R., OTA, E., ISHIKURA, K., HATAYA, H., HONDA, M., ITO, S., SHIMA, Y., KAITO, H., NOZU, K., NAKAMURA, H., IGARASHI, T., OHASHI, Y., IIJIMA, K. & JAPANESE STUDY GROUP OF KIDNEY DISEASE IN, C. 2015. A multicenter randomized trial indicates initial prednisolone treatment for childhood nephrotic syndrome for two months is not inferior to six-month treatment. *Kidney Int,* 87**,** 225-32.

YOUN, M. Y., YOKOYAMA, A., FUJIYAMA-NAKAMURA, S., OHTAKE, F., MINEHATA, K., YASUDA, H., SUZUKI, T., KATO, S. & IMAI, Y. 2012. JMJD5, a Jumonji C (JmjC) domain-containing protein, negatively regulates osteoclastogenesis by facilitating NFATc1 protein degradation. *J Biol Chem,* 287**,** 12994-3004.

YUAN, X. & YANG, S. 2015. Cilia/Ift protein and motor -related bone diseases and mouse models. *Front Biosci (Landmark Ed),* 20**,** 515-55.

ZACHARIAS, D. G., NELSON, T. J., MUELLER, P. S. & HOOK, C. C. 2011. The science and ethics of induced pluripotency: what will become of embryonic stem cells? *Mayo Clinic proceedings,* 86**,** 634-640.

ZENKER, M., AIGNER, T., WENDLER, O., TRALAU, T., MUNTEFERING, H., FENSKI, R., PITZ, S., SCHUMACHER, V., ROYER-POKORA, B., WUHL, E., COCHAT, P., BOUVIER, R., KRAUS, C., MARK, K., MADLON, H., DOTSCH, J., RASCHER, W., MARUNIAK-CHUDEK, I., LENNERT, T., NEUMANN, L. M. & REIS, A. 2004. Human laminin beta2 deficiency causes congenital nephrosis with mesangial sclerosis and distinct eye abnormalities. *Hum Mol Genet,* 13**,** 2625-32.

ZHAI, X.-Y., THOMSEN, J. S., BIRN, H., KRISTOFFERSEN, I. B., ANDREASEN, A. & CHRISTENSEN, E. I. 2006. Three-Dimensional Reconstruction of the Mouse Nephron. *Journal of the American Society of Nephrology,* 17**,** 77-88.

ZHANG, P., LI, J., TAN, Z., WANG, C., LIU, T., CHEN, L., YONG, J., JIANG, W., SUN, X., DU, L., DING, M. & DENG, H. 2008. Short-term BMP-4 treatment initiates mesoderm induction in human embryonic stem cells. *Blood,* 111**,** 1933-41.

ZHANG, P., ZHUO, L., ZOU, Y., LI, G. & PENG, K. 2019. COL4A5 mutation causes Alport syndrome with focal segmental glomerulosclerosis lesion: Case report and literature review. *Clin Nephrol,* 92**,** 98-102.

ZHANG, S. Z., LI, H. F., MA, L. X., QIAN, W. J., WANG, Z. F. & WU, Z. Y. 2015. Urine-derived induced pluripotent stem cells as a modeling tool for paroxysmal kinesigenic dyskinesia. *Biol Open,* 4**,** 1744-52.

ZHANG, X. B. 2013. Cellular reprogramming of human peripheral blood cells. *Genomics Proteomics Bioinformatics,* 11**,** 264-74.

ZHAO, C., OMORI, Y., BRODOWSKA, K., KOVACH, P. & MALICKI, J. 2012. Kinesin-2 family in vertebrate ciliogenesis. *Proc Natl Acad Sci U S A,* 109**,** 2388-93.

ZHAO, J., BRUCK, S., CEMERSKI, S., ZHANG, L., BUTLER, B., DANI, A., COOPER, J. A. & SHAW, A. S. 2013. CD2AP links cortactin and capping protein at the cell periphery to facilitate formation of lamellipodia. *Mol Cell Biol,* 33**,** 38-47.

ZHENG, Y. L. 2016. Some Ethical Concerns About Human Induced Pluripotent Stem Cells. *Sci Eng Ethics,* 22**,** 1277-1284.

ZHOU, T., BENDA, C., DUNZINGER, S., HUANG, Y., HO, J. C., YANG, J., WANG, Y., ZHANG, Y., ZHUANG, Q., LI, Y., BAO, X., TSE, H.-F., GRILLARI, J., GRILLARI-VOGLAUER, R., PEI, D. & ESTEBAN, M. A. 2012. Generation of human induced pluripotent stem cells from urine samples. *Nature Protocols,* 7**,** 2080.

ZHOU, Y., CASTONGUAY, P., SIDHOM, E.-H., CLARK, A. R., DVELA-LEVITT, M., KIM, S., SIEBER, J., WIEDER, N., JUNG, J. Y., ANDREEVA, S., REICHARDT, J., DUBOIS, F., HOFFMANN, S. C., BASGEN, J. M., MONTESINOS, M. S., WEINS, A., JOHNSON, A. C., LANDER, E. S., GARRETT, M. R., HOPKINS, C. R. & GREKA, A. 2017. A small-molecule inhibitor of TRPC5 ion channels suppresses progressive kidney disease in animal models. *Science,* 358**,** 1332-1336.

ZHU, F., LI, W., LI, Z., ZHU, H. & XIONG, J. 2018. Identification of a Novel COL4A4 Variant in Compound-Heterozygous State in a Patient With Alport Syndrome and Histological Findings Similar to Focal Segmental Glomerulosclerosis (FSGS). *Front Genet,* 9**,** 748.

ZHU, L., TAO, T., ZHANG, D., LIU, X., KE, K. & SHEN, A. 2015. NOS1AP O-GlcNAc Modification Involved in Neuron Apoptosis Induced by Excitotoxicity. *International Journal of Molecular Sciences,* 16**,** 16560-16575.

ZOU, L., YANG, S., CHAMPATTANACHAI, V., HU, S., CHAUDRY, I. H., MARCHASE, R. B. & CHATHAM, J. C. 2009. Glucosamine improves cardiac function following trauma-hemorrhage by increased protein O-GlcNAcylation and attenuation of NF-{kappa}B signaling. *Am J Physiol Heart Circ Physiol,* 296**,** H515-23.

Chapter 8 Appendices

8.1 Appendix 1: Oligonucleotide Primers used for Real Time PCR

Gene	Forward Primer (5' to 3')	Reverse Primer (5' to 3')
MARVELD2	ACAACAGGAGTGTGAAATGGC	TCGGGCATCACGATAGGTTTAG
MARVELD3	ATTACCAGTCAGAGGCGGAAGG	CCAGGATCAGCAAGTTCAGGAG
CLDN6	AATTTCCCTTATCTCCTTCGC	GACTCCCAGGATCTGCATTC
SORBS1	CCCACCACCTTAAACCACTG	ATCCATGTCTTTGTCTTGCC
CGN	AGAAGCGTTTGCTGGACAGG	GCAGGGCTTGCTTAGAGTCC
COBL	CTGTGCAAGACAAGGCATCG	TTATCCTCAGTGCGGTTGGG
DMTN	GACCGGACACCCTTCCATAC	CCCTGATGGGCTGAACTCTG
EGF	TCCTGAAGGCTCAGTGCTTG	GGGCTAAGAGGAACGCAGAG
EGFR	GGTGCAGGAGAGGAGAACTG	ACTGGTTGTGGCAGCAGTC
CRB1	CTACAATGGAGGCAACTGCAC	GAGTAAGTCCTGGCACAGACC
LIN7A	GGCAACAGCAAAGGTATTCTCG	TGGGAGTGGCCTTCACTAGC
PATJ	TAGAGATGAGGCACACTACCG	CTCCGCTTCCATTTCGTTTC
CDC42	CTGAAGGCTGTCAAGTATGTGG	GGCTCTTCTTCGGTTCTGGAG
DNAAF1	ACAGGCAAATCTCTGGAAGACC	GCACAGGGAGTGACGTGTAG
CCDC114	ACAGCTGGAGAAGCTCAAGG	CTGGTCTTGACCCCAAGGAG
ZMYND10	GCCTCGATATGGGAGACCTG	GGATGGCTTGCATGTTCAGC
DNAI1	AGTCTGGCAAGCACTCAGAC	ATCCTGCCGTCAGATGACAC
DNAH1	GGAACCCTGTGAAGATCCG	TCGTGTTTCGGCTATGGAC
IFT140	CCGACTTCTTCATCGAGCACAG	ACGGTCATCTTTTCCGCCATC

DNAH5	AAGTCCATGCTCGGAAGCTC	GAGGCGGAACGCATCATGTA
KDM8	AGGGAACCATCTCCCCACTA	CGTCAACCTGGCTCGTGTTA
RCCD1	GTTGCAGGGCCTAGTCATGG	CAGCTGCCCTGATTCATTCC
NFATC1	GCGGGAAGAAGATGGTCCTG	CGGGATCTCAACCACCAGAG
CCNA1	TCATCTCTCCTCTCCCAGTCTG	GCTGCTTCTTCATGTAGTGTGC
CDKN1A	ACTCTCAGGGTCGAAAACGG	ATGTAGAGCGGGCCTTTGAG
NOS1AP	CCTAGCAAAACCAAGTACAACC	CACGTCCAGGCTTCCTAC

8.2 Appendix 2: List of Primary and Secondary Antibodies

Primary antibodies

NPHS1 (Bioscientific, AF4263, 1:300)
biotinylated *Lotus tetragonolobus* lectin (Vector Laboratories, B-1325, 1:300)
CDH1/ECAD (BD Biosciences, 610181, 1:300)
CDH1/ECAD (Cell Signalling Technologies, 3195S, 1:300)
GATA3 (R&D Systems, AF2605, 1:300)
acetylated tubulin (Sigma Aldrich, T6793, 1:500)
IFT140 (Proteintech, 17460-1-AP, 1:100)
WDR19 (Proteintech, 13647-1-AP, 1:100)
IFT88 (Proteintech, 13967-1-AP, 1:100)
EpCAM-AF488 (Biolegend, 324210, 1:300)
ZO1 (Life Technologies, 40-2300, 1:200)
beta catenin (Sigma Alrdich, C2206, 1:200)
Phalloidin-FITC (Sigma-Aldrich, P5282, 1:1000)
PAX2 (Zymed Laboratories, 71-600, 1;:300)
LAMA5 (Abcam, AB77175, 1:300)
HNF4A (Life Technologies, MA1-199, 1:500)
CASP3 (Cell Signalling Technology, 9661, 1:200)
podocin (Sigma Aldrich, P0372, 1:600)
synaptopodin (Santa Cruz, SC21537, 1:300)
aPKC (Santa Crus, SC216, 1:300)
PAR3 (Merck 07-330, 1:300, 1:300)
NOS1AP (Novus Biologicals, NBP2-38758, 1:200)

Secondary antibodies

Streptavidin Alexa Fluor 405 conjugate (Life Technologies, S32351, 1:400)
Alexa Fluor 488 Donkey anti-mouse IgG (H+L) (Invitrogen, A21202, 1:400)
Alexa Fluor 488 Donkey anti-rabbit IgG (H+L) (Invitrogen, A21206, 1:400)
Alexa Fluor 568 Donkey anti-mouse IgG (H+L) (Invitrogen, A10037, 1:400)
Alexa Fluor 568 Donkey anti-rabbit IgG (H+L) (Invitrogen, A10042, 1:400)
Alexa Fluor 568 Donkey anti-goat IgG (H+L) (Invitrogen, AB175704, 1:400)
Alexa Fluor 647 Donkey anti-sheep IgG (H+L) (Invitrogen, A21448, 1:400)
Alexa Fluor 647 Donkey anti-goat IgG (H+L) (Invitrogen, A21447, 1:400)
Alexa Fluor 647 Donkey anti-mouse IgG (H+L) (Invitrogen, A31571, 1:400)
Alexa Fluor 647 Donkey anti-rabbit IgG (H+L) (Invitrogen, AB150075, 1:400)